UNIVERSITY OF CALIFORNIA,
IRVINE

Identifying genetic trends in neurodegenerative disease and determining the impact of genetic diversity in Alzheimer's disease pathology

DISSERTATION

submitted in partial satisfaction of the
requirements for the degree of

DOCTOR OF PHILOSOPHY

in

Mathematical, Computational, and Systems Biology

by

Neelakshi Soni

Dissertation Committee:
Professor Kim Green, Chair
Professor Ali Mortazavi
Assistant Professor Vivek Swarup

2023

DEDICATION

To

my parents,

for their constant love and support

throughout my life,

my sister,

for always being there for me

and my friends,

for keeping me sane through it

all.

"Still the voices of your critics. Listen intently to your own voice, to the person who knows you best. Then answer these questions: Do you think you should move ahead? How will you feel if you quit pursuing this thing you want to do? And what does your best self-advise? What you hear may change your life."
Steve Goodier

"Don't be satisfied with stories, how things have gone with others. Unfold your own myth."
Rumi, The Essential Rumi

TABLE OF CONTENTS

LIST OF FIGURES

LIST OF ABBREVIATIONS

Aβ	Amyloid beta
AD	Alzheimer's disease
ALS	Amyotrophic lateral sclerosis
ALSP	Adult-onset leukoencephalopathy with axonal spheroids and pigmented Glia
CC	Collaborative cross
CSF1R	Colony-stimulating factor-1 receptor
CSF1Ri	Colony-stimulating factor-1 receptor inhibition
CNS	Central nervous system
DAM	Disease-associated microglia
DEGs	Differentially expressed genes
ECM	Extracellular Matrix
EMASE	Expectation-Maximization for Allele Specific Expression
FDR	False Discovery Rate
GFAP	Glial fibrillary acidic protein
GO	Gene Ontology
HD	Huntington's disease
IFN	Interferon
IHC	Immunohistochemistry
IL	Interleukin
IPA	Ingenuity Pathway Analysis
ITAMs	Immunoreceptor tyrosine-based activation motifs
LPS	Lipopolysaccharide
MMP	Metalloproteinase
MS	Multiple sclerosis
NO	Nitric oxide
NPC	Neural precursor cells
NT	Non-transgenic
OPC	Oligodendrocyte precursor cell
PBS	Phosphate-buffered saline
PD	Parkinson's disease
PMD	Postmortem delay
PNNs	Perineuronal nets
PV	Parvalbumin
RI	Recombinant inbred
RIX	Recombinant inbred intercross
RNA-seq	RNA sequencing
ROS	Reactive oxygen species
TGF-β	Transforming growth factor beta
TNF-α	Tumor necrosis factor alpha
TREM2	Triggering receptor expressed on myeloid cells 2
WFA	Wisteria floribunda agglutinin
WGCNA	Weighted gene co-expression analysis
WT	Wild-type

ACKNOWLEDGEMENTS

My gratitude goes to Dr. Kim Green, my mentor and guide, who provided invaluable support and direction during my tenure as his student in the laboratory. Without his supervision, I would not have evolved into the scientist I am today, and I am grateful for his influence in every way. Dr. Green played a vital role in the success of the projects I have contributed to, propelling scientific progress with his wisdom and encouragement.

My heartfelt appreciation goes out to the Green lab team, whose support and camaraderie have been indispensable throughout the years. We were fortunate to have collaborated in such a way, as not all graduate students have the privilege of working with such a remarkable group. Although it was not always smooth sailing, we all gained measurable and immeasurable benefits from one another. I would like to extend special thanks to Joshua Crapser, Miguel Arreola, Lindsay Hohsfield and Caden Henningfield, who contributed significantly to my research across every project I undertook and were steadfast friends during what is typically a taxing experience for all involved.

Furthermore, I wish to express my gratitude to Dr. Swarup, my co-mentor at the University of California, Irvine. I sincerely believe that I would not be pursuing my current trajectory were it not for his exceptional mentorship and prescience regarding what a young scientist must possess to be most valuable to their laboratory. He motivated me to explore the computational aspects of research and collaborated on creating a course curriculum to optimally support this concept, even though no formal curriculum existed at that time.

I am immensely grateful to my family, whose contribution to my life cannot be adequately expressed in mere words. I have always regarded myself as extremely fortunate to have parents who tirelessly nurtured a passion for learning and reading in my sister and me during our formative years. It is this zeal for discovery that I believe has propelled me to make the choices I have made concerning my education and career and will continue to guide me in the future. My sister Ashima has also been a significant influence on me, consistently making time to listen, provide advice, and offer essential grounding when I need it the most. For this, I am truly thankful.

I also thank Oxford Academic for permission to include part material for portion of Chapter One of my thesis, which was originally published in *BRAIN*. I thank Science for permission to include material for portion of Chapter One of my thesis, which was originally published in *Science Advances*. I thank eLife for permission to include material for portion of Collaborations of my thesis, which was originally published *in eLife Neuroscience*. Finally, I thank Wiley Online Library for permission to include material for portion of Collaborations of my thesis, originally published in *GLIA*. Financial support was provided by the University of California, Irvine.

VITA

Neelakshi Soni

EDUCATION:

Ph.D. - Mathematical, Computational, and Systems Biology 2017-2023
University of California, Irvine

B.Tech. - Biotechnology 2013-2017
Vellore Institute of Technology, Vellore

RESEARCH EXPERIENCE:

Ph.D. Graduate Student Researcher, Green Lab, UCI 2018-Present
Understanding the role of perineuronal nets and microglia in neurodegeneration through multi-omic integration

PUBLICATIONS:

1. Henningfield CM, Arreola MA, **Soni N**, Spangenberg EE, Green KN. Microglia-specific ApoE knock-out does not alter Alzheimer's disease plaque pathogenesis or gene expression. Glia. 2022 Feb;70(2):287-302. doi: 10.1002/glia.24105. Epub 2021 Oct 13. PMID: 34643971; PMCID: PMC9308171.
2. Hohsfield LA, Najafi AR, Ghorbanian Y,**Soni N**, Crapser J, Figueroa Velez DX, Jiang S, Royer SE, Kim SJ, Henningfield CM, Anderson A, Gandhi SP, Mortazavi A, Inlay MA, Green KN. Subventricular zone/white matter microglia reconstitute the empty adult microglial niche in a dynamic wave. Elife. 2021 Aug 23;10:e66738. doi: 10.7554/eLife.66738. PMID: 34423781; PMCID: PMC8425950.
3. Arreola MA, **Soni N**, Crapser JD, Hohsfield LA, Elmore MRP, Matheos DP, Wood MA, Swarup V, Mortazavi A, Green KN. Microglial dyshomeostasis drives perineuronal net and synaptic loss in a CSF1R+/- mouse model of ALSP, which can be rescued via CSF1R inhibitors. Sci Adv. 2021 Aug 25;7(35):eabg1601. doi: 10.1126/sciadv.abg1601. PMID: 34433559; PMCID: PMC8386924.
4. Crapser JD, Ochaba J, **Soni N**, Reidling JC, Thompson LM, Green KN. Microglial depletion prevents extracellular matrix changes and striatal volume reduction in a model of Huntington's disease. Brain. 2020 Jan 1;143(1):266-288. doi: 10.1093/brain/awz363. Erratum in: Brain. 2020 Mar 1;143(3):e24. PMID: 31848580; PMCID: PMC6935750.
5. Hohsfield LA, Najafi AR, Ghorbanian Y,**Soni N**, Hingco EE, Kim SJ, Jue AD, Swarup V, Inlay MA, Green KN. Effects of long-term and brain-wide colonization of peripheral bone marrow-derived myeloid cells in the CNS. J Neuroinflammation. 2020 Sep 20;17(1):279. doi: 10.1186/s12974-020-01931-0. PMID: 32951604; PMCID: PMC7504855

Under review:

1. **Soni N**, Kawauchi S, Cunha C, Milinkeviciute G, Tran K, Swarup V, Mortazavi A, MacGregor G, and Green KN. GreenExploring genetic diversity in the 5xFAD mouse model to identify resilience and susceptibility. In preparation
2. Henningfield CM, **Soni N**, Sharma R, Cleland JL, Green KN. Selective targeting and treatment of plaque-associated microglia via systemic dendrimer administration in an Alzheimer's disease mouse model. In preparation.

CONFERENCES AND WORKSHOPS:

Next Generation Sequencing Data Analysis *2019*
University of California, Irvine

Center for Cell Circuits Computational Genomics Workshop *2021*
Broad Institute, MA

TEACHING:

Single Cell RNA-seq Analysis Computational Lab *2019 and 2022*
Cancer Systems Biology Short Course

- Organized and TA'ed 4-hour workshop introducing single cell RNA-seq data, technical challenges, and analysis considerations and workflow

Getting Started with Single Cell RNA-seq *2021*
Bioinformatics Support Group, UCI

- Presented recommendations for preliminary single cell RNA-seq analysis for first time users and new datasets

Mathematical, Computational and Systems Biology Bootcamp *2019 and 2021*
Crash Core Course, UCI

- Tutored mentees for their final presentation
- TA'ed Mathematica and MATLAB sections

ABSTRACT OF THE DISSERTATION

Identifying genetic trends in neurodegenerative disease and determining the impact of genetic diversity in Alzheimer's disease pathology

by

Neelakshi Soni

Doctor of Philosophy in Mathematical, Computational and Systems Biology

University of California, Irvine, 2023

Professor Kim Green, Chair

Alzheimer's disease (AD) is a complex neurodegenerative disorder with a multifactorial etiology, including genetic factors that play a significant role in disease susceptibility. However, in preclinical studies, the role of an individual's genetic makeup has been largely overlooked. To address this gap, we aimed to investigate the impact of genetic diversity in mouse models of AD on translational potential. In this study, we utilized a well-established AD mouse model and combined it with a complex genetically diverse reference panel to generate a novel AD mouse population. These mice carried identical high-risk human mutations for AD, but differed in the rest of their genome, allowing us to examine the effects of genetic variation on AD-related phenotypes. Our results demonstrated that genetic variation had analogous impact on pathological phenotypes associated with AD mutations. Mice with different genetic backgrounds exhibited consistent degrees of pathological changes, highlighting the importance of genetic diversity in AD research. Furthermore, we validated this complex AD model by demonstrating high degrees of genetic, transcriptomic, and phenotypic overlap with human AD, supporting its translational relevance. The findings of our study have

significant implications for AD research. By incorporating genetic diversity into mouse models of AD, we have created an innovative and reproducible resource for studying the mechanisms underlying AD. Our results suggest that preclinical models that incorporate genetic diversity may better reflect the complex nature of human AD, potentially leading to improved translation of findings from mouse models to human disease. In conclusion, our study highlights the importance of considering an individual's genetic makeup in the context of AD research. Incorporating genetic diversity in mouse models of AD can provide a more comprehensive understanding of the disease and improve translational potential, offering new opportunities for investigating AD mechanisms and developing effective therapeutic interventions.

BACKGROUND

Neurodegenerative disorders: Pathology and Features

Neurodegenerative conditions can be categorized based on their clinical manifestations, with the most prevalent being extrapyramidal and pyramidal movement abnormalities, as well as cognitive or behavioral disturbances. However, it is rare for patients to exhibit purely one type of symptom, as most individuals present with a combination of clinical features. Currently, the definitive diagnosis is determined through neuropathological examination during autopsy, which serves as the gold standard in diagnostics. Neurodegenerative diseases are characterized by the accumulation of specific proteins and vulnerability of certain anatomical regions. However, these diseases share common underlying processes that contribute to progressive dysfunction and death of neurons. These processes include proteotoxic stress, which affects the ubiquitin-proteasomal and autophagosomal/lysosomal systems, oxidative stress, programmed cell death, and neuroinflammation. It's important to note that protein abnormalities associated with neurodegenerative diseases can be present even before clinical symptoms manifest and more than one neurodegenerative disease process can be found in an individual (Milenkovic & Kovacs, 2013), (Schmitt et al., 2000), (Gibb & Lees, 1988), (Dugger et al., 2014). Currently, diagnostic biomarkers are limited in availability, with only rare cases where a causative genetic mutation can be definitively linked to a disorder (Ghasemi & Brown, 2018), (Hinz & Geschwind, 2017), (Ghasemi & Brown, 2018). As a result, there is a pressing need for specific in vivo biomarkers, such as those found in biofluids and molecular imaging markers (Tcw & Goate, 2017), (Seeley, 2017), to be a focal point of research in this field. The neuropathology of Alzheimer's disease (AD) involves a complex mixture of protein abnormalities. This includes the presence of both amyloid-beta (Aβ) deposits in the brain tissue, referred to as amyloid or senile plaques, as well as tau protein inclusions within neurons, known as

neurofibrillary tangles (NFTs). Additionally, many cases of AD also exhibit amyloid angiopathy, which is the deposition of Aβ in blood vessels within the brain. It is believed that the earliest form of Aβ deposits are diffuse and non-compact, often referred to as "pre-amyloid" deposits due to their weak staining with traditional amyloid dyes (Tagliavini et al., 1988). These deposits may be found in various brain regions, and depending on the location, they can have dense cores. Dense deposits are commonly observed in the primary motor and visual cortices. Amyloid plaques are composed of different cellular components, including neuronal processes called "dystrophic neurites," as well as astroglial processes and microglia, with microglia being particularly abundant in association with dense deposits (Fukumoto et al., 1996). One of the most clinically significant types of plaques in AD are neuritic plaques, which are characterized by the presence of tau-immunoreactive dystrophic neurites (Dickson, 1997). Determining the density of neuritic plaques and the distribution of NFTs in specific brain regions is crucial for the neuropathological diagnosis of AD (Hyman & Trojanowski, 1997). Neuritic plaques are often assessed using a semiquantitative method proposed by the Consortium to Establish a Registry for Alzheimer's Disease (CERAD) (Mirra et al., 1991), while the topographic distribution of amyloid deposits is evaluated using a staging scheme which categorizes amyloid "phases" based on their location in the neocortex, hippocampus, striatum, brainstem, and cerebellum (Thal et al., 2002). These criteria were further revised to include an assessment of the topographic distribution of amyloid deposits rather than their density (Montine et al., 2012).

Inflammatory response to the pathology

Microglia during homeostatic condition i.e healthy brains

Microglia, the primary brain resident macrophages, play essential functions in the central nervous system (CNS) including immune defense/response, tissue repair, and tissue maintenance/homeostasis. Studies have shown that colony-stimulating factor 1 receptor

(*CSF1R*) and interleukin *IL-34,* as well as transcription factors such as interferon regulatory factor 8 (*IRF8*) are required for microglial survival and maintenance (Masuda et al., 2014). The ongoing survival and maintenance of microglia population relies on the sustained activation of the *CSF1R*, a crucial factor in microglia and macrophage development (Erblich et al., 2011; Ginhoux et al., 2010). *CSF1R* is activated by endogenous ligands, such as *CSF-1* and interleukin-34 (*IL-34*), which are produced in the central nervous system (CNS) and must be continuously released, as blocking *CSF1R* pharmacologically results in rapid depletion of microglia (Greter et al., 2012).

Under homeostatic conditions, microglia act as the first line of defense in the brain. In this surveillance and immune response capacity, they detect insults/injury/pathogens via antigen receptor recognition, migrate to the site of interest as well as signal other cells to migrate to resolve injury, proliferate and phagocytose pathogens and associated tissue/cell damage. These processes occur via the secretion of chemokines, cytokines, and reactive oxygen species (ROS) as well as through a classical complement cascade (Schafer & Stevens, 2015). Microglia also play an important role in tissue repair by releasing anti-inflammatory cytokines, such as transforming growth factor beta (*TGFβ)* and interleukin *IL-10* (Norden et al., 2014). Microglia signaling through soluble/membrane-bound microglial factors (glutamate, reactive oxygen species, *TNF-α* as mentioned above) can induce programmed cell death prior to microglial phagocytosis of debris, reported phagocytosis of live cells ("phagoptosis"), and secretion of pro-survival factors (*IFG-1*) (Labandeira-Garcia et al., 2017). Increased activation of complement C1q and C3 pathways leads to synaptic loss and phagocytosis, and studies have shown that microglial depletion can rescue or restore these synapses, and prevent neuronal loss (Presumey et al., 2017), (Cho, 2019).

In addition to their roles in tissue surveillance, defense and repair, microglia have been shown to regulate other glial cell types in the brain. Microglia exhibit a bidirectional and temporal

communication with astrocytes, an interaction that is critically involved in the CNS immune response. For example, a recent study has shown that microglia regulate astrocyte activation (Rothhammer et al., 2018), (Palpagama et al., 2019). Microglia have also been shown to play a role in oligodendrocyte precursor cell (OPC) maturation and consequent myelinogenesis in the postnatal and adult brain (Hagemeyer et al., 2017), (Fernandez-Castaneda & Gaultier, 2016).

Research studies suggest that microglia have functions outside of their role as the primary immune cell of the brain, or non-immune-related functions. These functions serve to support neuronal health through synaptic pruning, promoting normal brain connectivity and development, and through the release of neurotrophic factors (Ferreira & Paganoni, 2002), (Palay, 1956). *CX3CL1,* expressed on neurons, and its receptor, *CX3CR1*, found primarily on microglia, regulate synaptic connectivity, and any inefficiencies in the CX3CL1/CX3CR1 axis can lead to dysfunctional brain circuitry observed as excessive dendritic spines and immature synapses (Meucci et al., 2000), (Zhang et al., 2018), (Fuhrmann et al., 2010). Using a diphtheria toxin-A mouse model and *CSF1R* inhibitor microglial elimination paradigm, a previous study in our lab demonstrated that microglia are involved in altering synaptic PSD95 and synaptophysin expression, as well as modulating dendritic spine densities following hippocampal lesion (MacDonald et al., 2005), (Son et al., 2020). During lesioning, it was shown that microglia play a protective role in diminishing neuronal loss (Rice et al., 2015). In addition to their role in modulating synaptic components, microglia also aid in the regulation of neural precursor cells (NPCs) by phagocytosing any aberrant NPCs (Matarredona et al., 2018), (Mosher et al., 2012).

Microglia-neuron interactions occur in developing and adult brains through contact-mediated cues and the secretion of soluble factors required for CNS activity. Changes in these cell-to-cell contacts have been hypothesized to initiate a local signaling cascade responsible for the

downregulation of neuronal activity (Szepesi et al., 2018). Among glial cells, astrocytes are the most abundant and play a significant role in synapse formation, maintenance, and elimination, thereby regulating the overall structure and activity of neuronal circuits. Astrocytes establish direct contacts with both pre- and postsynaptic neurons and release soluble factors to modulate synaptic transmission of excitatory and inhibitory synapses. This concept of the "tripartite synapse" considers astrocytes as an integrated functional unit along with two neurons (Nistico et al., 2017), (Farhy-Tselnicker & Allen, 2018). Microglia, on the other hand, are attracted to areas of synapse activity and serve as an additional component of the tripartite synapse, acting as a point of communication between neurons and glial cells. In a healthy brain, microglia exhibit a "surveying" phenotype that is actively repressed and relies on dynamic crosstalk with neurons (Kettenmann et al., 2011), (Biber et al., 2007), (Kierdorf & Prinz, 2017). However, the removal of inhibitory control from neurons is proposed to be a danger signal for microglia, indicating impaired neuronal function and resulting in changes in microglial morphology and function. This reciprocal communication between neurons and microglia involves various soluble factors, extracellular vesicles (EVs), and contact-dependent mechanisms, and is crucial for adaptive neuroplasticity and learning (Posfai et al., 2019).

Recent RNA-seq analysis studies of microglia in a healthy adult mouse brain have identified microglial-specific markers: *Hexb*, *P2ry12*, *S100A8*, *S100A9*, *Tmem119*, *Gpr34*, *Siglech*, *Trem2*, *Olfml3*, *Cx3cr1*, *Itgam*, *Aif1*, and *Adgre1*, aiding in the ability to distinguish microglia from other myeloid cell populations (Li et al., 2019). In addition, reports have identified ~100 genes (e.g., *P2yr12*, *Axl*, and *Mertk)* that are associated with the ability of microglia to sense changes in their microenvironment, referred to as the microglial sensome (Hickman et al., 2013).

Microglia during neurodegenerative disease

In recent years, microglial cells have come under the spotlight for playing an important role in disease (Gomez-Nicola & Perry, 2015). There have been extensive studies linking the progression of neuropathology in neurodegenerative disorders to neuroinflammation mediated by activated microglia (Harry & Kraft, 2008). Increased microglial cell density has been associated with pathology and disease progression in several neurodegenerative disorders, including multiple sclerosis, amyotrophic lateral sclerosis, Huntington's disease (HD), and Alzheimer's disease (AD) (Subhramanyam et al., 2019). Synaptic and neuronal loss are common features of neurodegeneration and recent studies indicate critical involvement of microglia. Furthermore, increases in microglial numbers have been correlated with white matter pathology, the primary readout of axonal damage in neurodegeneration (Friese et al., 2014), (Raff et al., 2002). Apart from cell numbers, microglia, which are typically in a resting state, can be activated by various pathological stimuli in the central nervous system (CNS) such as infection, brain trauma, stroke, and neurodegeneration (Kreutzberg, 1996). Upon activation, microglia undergo a transformation from ramified cells to reactive amoeboid cells. However, based on cellular experiments, preclinical models, and clinical investigations, chronic microglial activation has been suggested to have detrimental effects on the survival and normal functioning of neurons, as well as on neurodegeneration through stem cells (Banati et al., 1993).

It has been hypothesized that the dysfunctional states of microglia result in a chronic inflammatory environment and failed immune response as seen in various neurodegenerative disorders such as AD and HD (Stephenson et al., 2018). Recent studies have identified the reactive counterpart to the homeostatic microglia found in neurodegenerative brains, termed disease-associated microglia (DAM). These cells exhibit an increased expression of markers for macrophage activation with a concomitant downregulation of homeostatic microglial genes. The signature gene expression profiles for DAM are: *Axl*, *Clec7a*, *Cst7*, *Itgax*, *MHCII*,

CD14, *CD86* and *PD1L1*, *CSF1* (Butovsky & Weiner, 2018). Gene ontology and pathway analysis studies have identified that many of these genes are known to effect pathways involved in interferon response (*Ifitm3*, *Irf7*), lysosomal and phagosome function, lipid metabolism and viral defense (*Oas1a*, *Rsad2*, *Zbp1*) (Keren-Shaul et al., 2017), (Olah et al., 2020). Additionally, an increased expression of the orthologous interferon-related genes in human microglia, specifically *Isg15*, *Oasl*, *Ifitm3*, *Irf7*, and *Ifi30*, correlated significantly and robustly with age (Kawanokuchi et al., 2006), (Rock et al., 2005).

Astrocytes during homeostatic conditions

Astrocytes play crucial roles in maintaining the viability and function of the central nervous system (CNS), as evidenced by their involvement in synapse formation, maintenance, and elimination (Chung & Barres, 2012). Notably, astrocytes express a plethora of genes implicated in phagocytosis, arranged into three interconnected pathways that jointly activate this cellular process (Cahoy et al., 2008), (Mallat et al., 2005). The first pathway involves key proteins such as *CrKII*, *DOCK180*, *Rac1*, and *ELMO*, which govern the reorganization of the actin cytoskeleton necessary for encapsulating cellular debris (Kinchen et al., 2005). Additionally, recent research has revealed *Bai1* as a phagocytic receptor expressed in astrocytes that operates upstream of these components (Park et al., 2007). The second pathway encompasses the c-Mer tyrosine kinase receptor (*MerTK*), working in tandem with the Integrin pathway to regulate the *CrKII*/*DOCK180*/*Rac1* modules (Wu et al., 2005), (D'Cruz et al., 2000). The final pathway encompasses *MEGF10*, *GULP*, and *ABCA1*, which play a role in the recognition and engulfment of cellular debris (Yu et al., 2008). These findings raise the possibility that astrocytes could potentially participate in the elimination of synapses in coordination with specialized phagocytes, such as microglia, in the central nervous system.

The modulation of cerebral blood flow in response to neuronal energy demand through the release of vasoactive substances, including prostanoids, by astrocytes, along with the supply of essential metabolites such as lactate to neurons, is a critical physiological process (Allaman et al., 2011). Additional homeostatic functions of astrocytes include buffering potassium ions, water, and glutamate and regulating neurotransmitters in the synaptic clefts as well as tissue repair which is crucial in maintaining optimal neuronal function and intracellular signaling cascades in the brain (Stevens, 2008), (Bélanger & Magistretti, 2009), (Perea et al., 2009), (Sofroniew & Vinters, 2010). They have been shown to remove various neurotransmitters, including glutamate, *GABA*, dopamine, norepinephrine, serotonin, and acetylcholine, from the extracellular space through specific uptake and inactivation pathways. Astrocytes also convert these neurotransmitters into different substances, which are either utilized for alternative functions or secreted harmlessly into the extracellular space. Furthermore, astrocytes are involved in the regulation and production of various growth factors, such as *EGF*, *FGF*, *NGF*, and *CNTF*, which are essential for neurite outgrowth, synapse formation, and proper migration. As such, astrocytes serve as vital regulators of neurotransmission and growth factor production in the brain, playing a critical role in the induction and maintenance of neuronal processes (Ransom & Sontheimer, 1995). Astrocytes play a crucial role in maintaining brain homeostasis by contributing to glycogen storage and the formation of the blood-brain barrier (BBB), making them important subjects of research in neurobiology. Glycogen, stored predominantly in astrocytes, serves as a reserve energy source that can be broken down into glucose in situations where glucose availability is limited compared to glucose expenditure. This glucose can then be utilized for glycolysis to generate lactate. Lactate is subsequently exported from astrocytes and taken up by surrounding neurons, a process that has been highlighted in previous studies (Ransom & Sontheimer, 1995). Additionally, the BBB, which is primarily formed by endothelial cells lining the walls of blood vessels in the brain, tightly regulates the entry of

molecules from the blood into the brain. Emerging evidence suggests that astrocytes, through their complex interactions with endothelial cells, play a critical role in the proper formation and maintenance of a functional BBB, thus emphasizing their significance in brain health (Ransom & Sontheimer, 1995). The blood-brain barrier (BBB) prevents peripheral immune cells, such as T cells and B cells, from entering the brain, leaving resident glial cells (astrocytes and microglia) responsible for immune functions within the brain. Astrocytes have been demonstrated to produce major histocompatibility complex (*MHC*) class I and II molecules, as well as intracellular adhesion molecules (*ICAMs*), indicating their capacity to function as antigen-presenting cells. Astrocytes can directly affect endothelial cells, leading to increased BBB permeability to activated and circulating T cells. Once in the brain, these T cells may influence the immune response and modulate brain homeostasis by secreting various pro- and anti-inflammatory cytokines. Astrocytes themselves are capable of producing numerous cytokines, including interleukins (*IL*), tumor necrosis factor (*TNF*), and interferons (*IFN*), which can have multiple effects depending on the cell type encountered (Aschner, 1998). For example, IL-6 has been shown to promote neurite extension and increase the number of voltage-dependent sodium channels in neurons, as well as stimulate the secretion of nerve growth factor (*NGF*) by astrocytes (Sredni-Kenigsbuch, 2002). Similarly, IL-1 has been shown to alter the rate of neuronal signaling, and stimulate lipid peroxidation and reactive oxygen species production by astrocytes and microglia (Rothwell & Luheshi, 2000). Astrocytes play a crucial role in providing the brain with Apolipoprotein E (*ApoE*), a multifunctional signaling molecule that is vital for various brain functions. *ApoE* is a widely distributed 34 kD glycosylated protein that primarily functions as a transporter of cholesterol and phospholipids. In humans, there are three known isoforms of *ApoE*, namely *ApoE2*, *ApoE3*, and *ApoE4*. Among these isoforms, *ApoE3* is the most abundant, characterized by a cysteine residue at position 112 and an arginine residue at position 158. In contrast, *ApoE2* contains cysteine at

both residues, and *ApoE4* possesses arginine in both positions. These isoform-specific variations in *ApoE* protein structure have been found to impact its interactions with lipids, receptors, and other proteins, thus influencing its functional properties (Cedazo-Mínguez & Cowburn, 2001). The role of *ApoE* in the brain goes beyond its traditional function as a lipid transport molecule, as recent research suggests that it plays additional roles in regulating astrocyte and neuronal function (Misra et al., 2001). Studies have shown that *ApoE* may regulate calcium homeostasis, impact neuronal regulation of ion-dependent receptors, modulate neurotransmitter release/sequestration, enhance the effects of growth factors, promote neuron survival and sprouting, and protect against oxidative stress (Cedazo-Mínguez & Cowburn, 2001), (Lee et al., 2004). *ApoE* also plays a role in regulating innate and adaptive immune responses in the brain, inhibiting neutrophil and lymphocyte proliferation, and reducing inflammatory signaling in astrocytes and microglia (Bouchareychas & Raffai, 2018). These findings highlight the complex and diverse functions of *ApoE* in the brain, which may have implications for neurodegenerative diseases and other neurological conditions. Although the precise mechanism by which astrocytes recognize and degrade Aβ remains unknown, studies have proposed that apolipoprotein E (ApoE), which is predominantly expressed in astrocytes, may be responsible for this cellular action (Koistinaho et al., 2004). ApoE has been shown to be essential for astrocytes to attract, internalize, and degrade Aβ deposits in vitro, indicating its crucial role in astrocyte-mediated plaque degradation.

Reactive astrocytes, known for their distinct responses, have traditionally been categorized as A1 (pro-inflammatory and neurotoxic) or A2 (anti-inflammatory and pro-regenerative) based on previous studies (Liddelow et al., 2017); (Zamanian et al., 2012). However, recent research has challenged this simplified A1/A2 nomenclature, suggesting that astrocyte inflammatory profiles actually transition along a spectrum in response to stimulatory cues in their microenvironment (Al-Dalahmah et al., 2020); (Escartin et al., 2021); (Wheeler et al., 2020).

In support of this view, studies have shown that reactive astrocytes isolated from human Grade III/IV HD patients or MS patients and EAE mice exhibit diverse gene expression patterns, leading to the identification of several distinct "states" (Al-Dalahmah et al., 2020); (Wheeler et al., 2020). Using single-cell RNA sequencing, Al-Dalahmah and colleagues categorized human HD patient-derived astrocytes into quiescent and various reactive states based on their relative expression of GFAP, solute carrier family-1 member-2, metallothionein, fibroblast growth factor receptor-3, and glutamate-ammonia ligase (Al-Dalahmah et al., 2020). Similarly, Wheeler and colleagues identified a specific population of pro-inflammatory and neurotoxic astrocytes (MAFG+/NRF2−) that were most prevalent in pathological tissues of EAE and MS patients compared to healthy samples, indicating the diverse nature of reactive astrocytes (Wheeler et al., 2020).

Astrocytes during neurodegenerative diseases

While microglial cells have been implicated in the formation of Aβ plaques, recent research has highlighted the crucial role of astrocytes in plaque degradation and inhibition of microglial activation, suggesting their importance in AD pathology and providing evidence from ultrastructural studies and cellular mechanisms to elucidate the protective role of astrocytes in AD. Ultrastructural studies using three-dimensional reconstructions of human classical plaques at different stages of development have revealed that astrocytes play a pivotal role in plaque degradation (Wegiel et al., 2000). However, the failure of astrocytes to properly degrade Aβ results in the accumulation of Aβ-containing neuronal debris in astrocytes and the formation of astrocytic plaques (Nagele et al., 2003). Furthermore, accumulated Aβ activates astrocytes to produce inflammatory mediators, such as interleukin 1β (*IL-1β*) and tumor necrosis factor-α (*TNF-α*), which can induce neuronal injury (Johnstone et al., 1999). Aβ-induced TNF-α increases calcium-dependent glutamate release, leading to excitotoxicity and neuronal death in AD (Rossi et al., 2005). Oxidative stress, triggered by Aβ, has also been implicated in Aβ

toxicity as it stimulates the production of reactive oxygen species (*ROS*) and reduces glutathione (*GSH*) levels in astrocytes (Abramov et al., 2004); (Canevari et al., 2004). Additionally, Aβ disrupts glucose metabolism in astrocytes, impairing neuronal viability (Allaman et al., 2010). Impairment of glutamatergic neurotransmission associated with excitotoxicity has been implicated in the progression of AD. The major mediator of glutamate clearance in humans, glutamate transporter *GLT1*, is preferentially localized in astrocytes. Loss of *GLT1* has been reported in the brains of AD patients (Tian et al., 2010). This effect may be partially mediated by oxidative stress and the complex balance between the *MAP* kinase signaling pathways (Matos et al., 2008).Astrocyte dysfunction in AD leads to impaired Aβ clearance, neuroinflammation, oxidative stress, and glutamatergic neurotransmission dysfunction, which contribute to the pathogenesis of AD. Apart from the characteristic hypertrophic astrocytes commonly found at neuritic plaques, there was also evidence of astroglial atrophy in different brain regions away from the plaques in a transgenic mouse model of Alzheimer's disease (Olabarria et al., 2010).

Transcriptionally a significant portion of the astrocyte genes associated with reactive responses have been extensively studied in the context of injury and wound healing in peripheral tissues. Reactive astrocytes play a critical role as a prominent source of pro-inflammatory cytokines (such as tumor necrosis factor-α (TNF-α), IL-1β, IL-6), chemokines (such as CXCL1/10, CCL2/3/5), and ATP, which amplify microglial activation and infiltration of blood-borne leukocytes (Bianco et al., 2005); (Choi et al., 2014). These inflammatory factors can also be transported systemically via membrane-bound exosomes, inducing cytokine release in the liver and recruiting inflammatory cells to the central nervous system (CNS) (Dickens et al., 2017). In human-derived samples from various CNS pathologies, including Alzheimer's disease (AD), Huntington's disease (HD), Parkinson's disease (PD), and multiple sclerosis (MS), pro-inflammatory and neurotoxic astrocytes have been identified (Liddelow et al., 2017).

Therefore, it is believed that reactive astrogliosis serves as a major driving force behind inflammation in neurodegenerative diseases. Studies in human AD patients have shown a significant increase in circulating exosomes derived from astrocytes, which are enriched with pro-inflammatory cytokines and complement factor complexes, suggesting their potential contribution to progressive inflammation and neurodegeneration (Goetzl et al., 2018). Recent research has further supported this notion, revealing that knockout of astrocytic STAT3 expression in AD mice attenuates both reactive astrogliosis and overall TNF-α and IL-1β expression in the brain, resulting in fewer dystrophic neurons, reduced Aβ plaque load, and improved cognitive function (Reichenbach et al., 2019). Taken together, a wealth of evidence highlights the crucial role of astrocytes in driving neuroinflammation in pathological conditions of the CNS. Neurotrophic cytokines and growth factors are genes that undergo rapid downregulation. On the other hand, pro-inflammatory cytokines are genes that show persistent elevation (Bauer et al., 2007). Additionally, the chemokine *CCL2*, which is a potent chemoattractant for macrophages, is rapidly induced initially and then subsequently downregulated. The acute phase protein, *Lcn2*, and the proteinase inhibitor, Serpina3n, have been identified as common markers of reactive astrocytes induced by both MCAO (middle cerebral artery occlusion) and LPS exposure in a recent genomic study (Zamanian et al., 2012). Previous studies have shown that their expression is induced in response to various injuries, including inflammation, excitotoxicity (Chia et al., 2011), nerve injury (Gesase & Kiyama, 2007), and amyotrophic lateral sclerosis (Fukada et al., 2007). *Lcn2* may be a marker of the early phase of reactive astrogliosis, as its expression is rapidly downregulated after initial induction. Interestingly, deficiency of *LCN2* has been associated with a stronger inflammatory response in mice with experimental autoimmune encephalomyelitis (EAE), a model of multiple sclerosis (MS) (Berard et al., 2012). These findings suggest that the effects of *LCN2* on astrocytic inflammation may vary depending on the context. In addition to *LCN2*, reactive

astrocytes also secrete lactosylceramide (LacCer), which acts as an autocrine signal to activate the *NF-κB* pathway and induce the expression of pro-inflammatory proteins like *IL-1β* and *CCL2* (Mayo et al., 2014). Modulating reactive astrogliosis has been shown to attenuate chronic inflammation and neurodegeneration in mice with EAE by several studies (Guo et al., 2014), (Mayo et al., 2014), (Moreno et al., 2014). On the other hand, *Serpina3n* may serve as a useful marker of the more persistent reactive gliosis response, as its expression remains elevated for at least a week. These two markers, due to their expression in response to diverse injuries, hold potential as universal markers for reactive astrocytes. In addition to *Lcn2* and *Serpina3n*, *Ptx3*, *Tgm1*, and *Cd109* are also potential markers of reactive astrocytes. Similar to *Serpina3n*, the expression of these genes is specific to astrocytes in our expression profile dataset. While they show low induced expression in LPS reactive astrocytes, they are highly induced in MCAO reactive astrocytes, suggesting that they may serve as markers for this specific subtype of reactive astrocytes. Drawing an analogy from the immune system, previous research has revealed gene profiles that suggest reactive astrocytes can exhibit either a protective or destructive orientation. Gene profiles indicate that reactive astrocytes in the context of MCAO are more likely to be protective (Sofroniew, 2009). These astrocytes show heightened expression of neurotrophic factors and cytokines, such as *CLCF1*, *LIF*, and *IL6*, as well as thrombospondins, which are known to play a role in repairing and rebuilding lost synapses (Christopherson et al., 2005), (Eroglu et al., 2009). On the other hand, astrocytes that react to lipopolysaccharides (LPS reactive astrocytes) exhibit a more robust upregulation of the early components of the classical complement cascade (C1r, C1s, C3, and C4), which play a role in synapse pruning during development (Stevens et al., 2007). It is postulated that this upregulation may contribute to the loss of synapses, ultimately leading to neuronal loss in neurodegenerative diseases (Stevens et al., 2007), (Stephan et al., 2012). Reactive astrocytes are often found at the margins of active demyelinating lesions in MS, where they engulf

inhibitory myelin debris by upregulating certain proteins like *ABCA1*, *MEGF10*, and *GULP1* (Morizawa et al., 2017). Myelin internalization induces a reactive and pro-inflammatory phenotype in cultured astrocytes through a *NF-κB*-dependent mechanism (Ponath et al., 2017). Furthermore, reactive astrocytes can act as antigen-presenting cells and stimulate the activation of naïve *CD4* and *CD8* T cells (Cornet et al., 2000), establishing a positive feedback mechanism between reactive astrocytes and immune cells in perpetuating chronic inflammation in MS. Similar positive feedback mechanisms between reactive astrocytes and immune cells have also been elucidated in human T-lymphotropic virus type 1-associated myelopathy/tropical spastic paraparesis (HAM/TSP), a chronic inflammatory condition (Ando et al., 2013), (Yamano & Coler-Reilly, 2017). Additionally, chronic inflammation is commonly associated with mechanosensory hypersensitivity and neuropathic pain after SCI, and positive feedback between distressed neurons and reactive astrocytes via chemokine signaling has been implicated in mechanosensory hypersensitivity and neuropathic pain. Cortical astrocytes have also been implicated in chronic pain after peripheral nerve injury by secreting *TSP-1*, which affects neural circuitry in the cortex (Kim et al., 2016). Reactive astrocytes play a role in resolving neuroinflammation by releasing anti-inflammatory and neuroprotective factors such as *TGFβ* (Norden et al., 2014), *IL-10* (Bsibsi et al., 2006), (Ledeboer et al., 2002), *IL-17* (Hu et al., 2014), insulin-like growth factor-I (*IGF-I*) (Garcia-Estrada et al., 1992), and glial-derived neurotrophic factor (*GDNF*) (Rocha et al., 2012). The mechanisms underlying the phenotypic shift in astrocytes require further investigation, but evidence suggests that *NF-κB* and *IGF-I* signaling pathways are involved in regulating the transition from a pro-inflammatory to an anti-inflammatory profile in reactive astrocytes (Fernandez et al., 2007). *NF-κB* and *IGF-I* appear to have opposing effects, with *NF-κB* promoting pro-inflammatory mediator expression through the recruitment of forkhead box O3 (*Foxo3*), a pro-inflammatory transcription factor, and calcineurin, while *IGF-I* signaling promotes an anti-inflammatory and neuroprotective

phenotype by recruiting calcineurin and peroxisome proliferator-activated receptor-γ (*PPARγ*) to inhibit Foxo3 activation (Fernandez et al., 2012), (Choi et al., 2014). Recent studies have also shown that inhibiting astrocytic glycolysis with non-metabolizable 2-deoxyglucose can attenuate pro-inflammatory response induced by lipopolysaccharide (LPS) in mouse astrocytes, suggesting that targeting astrocytic glycolysis could be a potential strategy for limiting *NF-κB*-mediated inflammation in CNS pathologies (Robb et al., 2020). Overall, astrocytes have emerged as promising targets for modulating neuroinflammation in the CNS due to their crucial role in driving the innate immune response.

Tools available to study the mechanisms behind this inflammatory response (focusing on AD)

Transgenic mouse models

Alzheimer's disease (AD), the primary cause of dementia, is typically characterized by progressive memory loss in the early stages, followed by impairments in executive functions and other behavioral disturbances such as agitation and paranoia. AD is distinguished by three key pathological features: senile plaques, neurofibrillary tangles, and neurodegeneration in the hippocampus and cortex (Holtzman et al., 2011), (Jack et al., 2016). Senile plaques, composed of fibrillar aggregates of Aβ, are unique to AD, while neurofibrillary tangles, consisting of hyperphosphorylated, fibrillar forms of tau proteins, are found in various neurodegenerative conditions including FTD linked to chromosome 17 (FTD-MAPT) (Holtzman et al., 2016). Mutations in genes such as amyloid precursor protein (APP), presenilin 1 (PSEN1), and presenilin 2 (PSEN2) are the main causes of autosomal dominant early-onset AD, whereas the APOEε4 allele is a significant risk factor for late-onset AD (Carmona et al., 2018). In addition to these, there are over 25 other loci and rare coding variants associated with AD risk (Lambert

et al., 2013), with some genetic associations implicating the immune system in the disease's development (Tansey et al., 2018).

Amyloid pathology models: Transgenic rodents have been engineered to develop amyloid deposition in senile plaques, similar to what is observed in Alzheimer's disease (AD). These rodent models carry human mutations in APP, PSEN1, and PSEN2 genes associated with AD, and they exhibit similar pathology to humans (Ashe & Zahs, 2010), (Price et al., 1998), (Sasaguri et al., 2017), (LaFerla & Green, 2012). Mutations in APP result in increased production of Aβ, particularly the more aggregation-prone Aβ42 form (Golde et al., 2011). Mutations in PSEN1/2 affect the processing of mouse APP, but do not lead to amyloid deposition. However, co-expression of PSEN1/2 mutants with an APP transgene accelerates the development of amyloid pathology (Haass & De Strooper, 1999). These transgenic rodents also exhibit other features of AD, such as abnormal dystrophic neurites, astrocytosis, microgliosis, and molecular changes in immune activation (Spires & Hyman, 2004). Interestingly, behavioral alterations in these transgenic rodent models do not always correlate well with the accumulation of visible Aβ aggregates, and the behavioral deficits usually do not progress (Ashe & Zahs, 2010), (LaFerla & Green, 2012). Mouse models that drive Aβ production and deposition without overexpressing APP, including knock-in models, may show little or subtle behavioral abnormalities that better coincide with the development of amyloid pathology (J. Kim et al., 2013), (McGowan et al., 2005), (Saito et al., 2014). However, these models do not fully recapitulate the cognitive and behavioral dysfunction observed in AD, as they lack prominent tau accumulation, robust neurodegeneration, and neurotransmitter abnormalities that accompany the symptomatic phases of human AD. Therefore, while transgenic rodents engineered to accumulate Aβ aggregates are useful for studying Aβ pathology, they are not comprehensive models of AD cognitive and behavioral dysfunction, but rather models of Aβ aggregate pathology (Dawson et al., 2018).

Tau pathology models: Transgenic mice that exhibit robust neuronal tau inclusion pathology (tauopathy) are primarily generated through overexpression of mutations associated with frontotemporal dementia (FTD) caused by MAPT mutations (FTD-MAPT) (LaFerla & Green, 2012), (Goedert et al., 2017), (McGowan et al., 2006), unlike models of amyloid-beta (Aβ) which do not show significant neurodegenerative changes. However, there are concerns about the relevance of these FTD-MAPT tauopathy models to tauopathy in Alzheimer's disease (AD). In fact, the tau inclusions in mice often resemble Pick bodies more than the classic neurofibrillary tangle pathology seen in AD. Moreover, commonly used tau transgenic mice are based on specific mutations (P301L or P301S) linked to FTD, but it is unclear if these mutations accurately represent tau dysfunction in all forms of FTD-MAPT (Strang et al., 2018). An alternative transgenic mouse model called the human bacterial artificial chromosome (BAC) hTau mouse, which expresses all human tau isoforms (wild-type) in a mouse MAPT-knockout background, shows limited tau pathology and subtle age-dependent neurodegenerative changes that may be more relevant to AD tauopathy (Andorfer et al., 2005). Expression of the mutant tau transgene at high levels in the spinal cord leads to a motor phenotype (Lewis et al., 2000), while more localized expression in specific brain regions such as the forebrain, hippocampus, or entorhinal cortex results in tau pathology and neurodegeneration in those regions (de Calignon et al., 2012), (Fu et al., 2017), (Santacruz et al., 2005). This suggests that tau aggregation can induce neurodegeneration in various types of neurons. However, the reason why different neuronal populations are affected in AD and FTD, despite widespread expression of tau in the central nervous system (CNS), remains unclear. The mechanisms underlying tau-induced neurodegeneration are still not fully understood, and there is no consensus or comprehensive understanding of how tau dysfunction and aggregation drive neurodegeneration (Goedert et al., 2017). Some studies suggest that co-expression of mutant human tau protein and mutant amyloid precursor protein (APP) accelerates tau

pathology, as well as injection of aggregated Aβ into tau transgenic models (Bolmont et al., 2007), (Götz et al., 2001), (Lewis et al., 2001), (Oddo et al., 2003). However, other reports do not find such synergistic interaction between Aβ or APP and tau pathology. The utility of animal models that contain both human mutant tau, mutant APP, and in some cases mutant PSEN1/2, remains uncertain, as there is ongoing controversy regarding whether these models exhibit synergistic interactions between the two pathologies. Ongoing studies with more rigorous controls, such as those supported by MODEL-AD (https://model-ad.org/), may help to resolve these controversies and refine our current models.

Genetic etiology

In a recent meta-analysis, a substantial and novel case-control study was integrated with existing GWASs (Bellenguez et al., 2022). Through this comprehensive approach, a total of 75 distinct loci associated with ADD were uncovered, with 33 of them having been previously reported, while 42 were newly identified signals at the time of the analysis. The pathway enrichment analyses clarified the involvement of tau-binding proteins and APP/Aβ peptide metabolism in late-onset AD processes to a much greater extent than previously described (Kunkle et al., 2019). The study identified *ADAM17*, a gene known to carry α-secretase activity similar to *ADAM10* (Deuss et al., 2008), suggesting potential deregulation of the non-amyloidogenic pathway for APP metabolism in AD. Additionally, six other highly plausible genes were identified (*ICA1L, DGKQ, ICA1, DOC2A, WDR81,* and *LIME1*) that may modulate APP metabolism as tier 1 genes. The pathway enrichment analyses further corroborated the involvement of innate immunity and microglial activation in Alzheimer's disease (ADD) and the ingle-cell expression enrichment analysis also revealed the expression of microglia-related genes. Notably, three of our top-prioritized (tier 1) genes (*RHOH, BLNK,* and *SIGLEC11*) and two of our tier 2 genes (*LILRB2* and *RASGE1FC*) were predominantly expressed in microglia (>90% of total expression across cell types. Of significance, *SIGLEC11* and *LILRB2* have

previously been implicated in Aβ peptides/amyloid plaques (T. Kim et al., 2013), (Salminen & Kaarniranta, 2009). LUBAC is recognized as a critical factor for the activation of *NLRP3* inflammasome, making it a crucial regulator of innate immunity which also was seen to be involved (Rodgers et al., 2014),(Iwai, 2021). The *NLRP3* inflammasome, in turn, plays a vital role in the development and progression of Aβ pathology in mice (Venegas et al., 2017), and may also contribute to tau pathology through Aβ-induced microglial activation (Ising et al., 2019). Additionally, LUBAC has been implicated in autophagy, with suggestions that linear ubiquitin chain modifications of TDP-43-positive neuronal cytoplasmic inclusions could potentially stimulate autophagic clearance (Nakayama et al., 2020). Lastly, LUBAC has been investigated for its role in regulating *TNF-α* signaling, particularly in *TNF-α* related pathways (Spit et al., 2019). ADAM17, also known as TNF-α-converting enzyme, plays a crucial role in activating TNF-α signaling (Black et al., 1997). *TNIP1*, the gene product of TNF-α-induced protein 3-interacting protein 1, is involved in inhibiting the TNF-α signaling pathway and nuclear factor κB activation/translocation (Verstrepen et al., 2009). Another signal associated with TNF-α is found at SPPL2A, one of the confirmed loci. The protein encoded by SPPL2A is implicated in noncanonical shedding of TNF-α, while PGRN has been identified as a TNF receptor ligand and antagonist of TNF-α signaling (Spitz et al., 2020), (Tang et al., 2011). Multiple lines of evidence have linked inhibition of TNF-α signaling with reduction of both Aβ and tau pathologies in vivo (He et al., 2007), (Shi et al., 2011). Although TNF-α has been suggested to have potential inflammatory connections through NLRP3 inflammasome activation, it is also involved in various brain physiological functions, such as synaptic plasticity in neurons, and pathophysiological processes, including synapse loss in the brain (Bezbradica et al., 2017), (De Strooper & Karran, 2016). Furthermore, the TNF-α signaling pathway and the LUBAC may play important roles in cell types other than microglia in the context of AD. It is noteworthy that six of the prioritized (tier 1) genes, namely *ICA1L*, *EGFR*,

RITA1, *MYO15A*, *LIME1*, and *APP*, are expressed at low levels in microglia (<10% relative to total expression across cell types), highlighting the complex crosstalk between different cell types in the brain in the development of AD (Dourlen et al., 2019). Additionally, the EGFR pathway is known to interact with the TNF-α signaling pathway, suggesting potential interplay between the two pathways in the pathogenesis of AD (Gong et al., 2018). A deeper understanding of the root causes of Attention Deficit Disorder (ADD) could potentially be gained by noting that the same genetic variants in GRN and TMEM106B are associated with both ADD and frontotemporal dementia. It is possible that this association is influenced by misdiagnosis of Alzheimer's disease (AD) and inclusion of proxy-ADD cases in the UK Biobank. However, *GRN* and *TMEM106B* have also been implicated in brain health and other neurodegenerative conditions. For example, they have been identified as potential genetic risk factors for age-related differences in the cerebral cortex (Rhinn & Abeliovich, 2017), cognitive impairment in amyotrophic lateral sclerosis (Vass et al., 2011), and Parkinson's disease (Baizabal-Carvallo & Jankovic, 2016), (Tropea et al., 2019). Moreover, both *GRN* and *TMEM106B* have been linked to neuropathological features of AD. Collectively, these findings suggest a potential continuum between neurodegenerative diseases, wherein common pathological mechanisms involving *GRN* and *TMEM106B* may be at play (Mendsaikhan et al., 2019), (Li et al., 2020), (Yang et al., 2020). Notably, both *GRN* and *TMEM106B* are implicated in defective endosome/lysosome trafficking and function, a defect also observed in AD (Paushter et al., 2018), (Feng et al., 2021). A recent study has estimated that fewer than 100 common genetic variants may account for the entire risk of Alzheimer's disease (AD) (Zhang et al., 2020). If this estimate is accurate, our study may have already identified a significant portion of these common variants. However, there are compelling reasons to continue efforts to fully understand the genetic component of AD. Firstly, there may be additional, unknown genetic locations that contain common variants that modulate the risk of AD. Secondly,

identifying rare variants with very low frequencies is challenging due to the limited sample sizes of available data for sequencing in AD research. It is worth noting that many genes associated with rare variants linked to AD risk also have common variants associated with AD risk. These genes include *TREM2*, *SORL1*, *ABCA7*, *ABCA1*, *PLCγ2*, and *ADAM10* (Holstege et al., 2020). Thirdly, gene-gene and gene-environment interactions have not been extensively studied yet. Therefore, increasing the sample size of genome-wide association studies (GWAS) and improving imputation panels, as well as utilizing more complex analyses, will likely enhance the statistical power and enable the characterization of associations with rare or structural variants. Lastly, GWAS conducted on populations with diverse ancestries will be crucial in identifying potential new genetic risk factors, refining fine-mapping approaches, and developing specific genetic risk scores (GRS) that are more effective for populations of non-European ancestries.

Caveats of using congenic mice to study pleotropic disease

The primary objective of developing animal models for neurodegeneration is to identify crucial points in the disease process that can serve as potential therapeutic targets. However, clinical trials based on successful outcomes in animal models for neurodegenerative diseases such as Alzheimer's disease (AD), Amyotrophic lateral sclerosis (ALS), Frontotemporal dementia (FTD), and Parkinson's disease (PD) have largely failed. This lack of success can be attributed to various factors in both preclinical and clinical studies, including inadequate preclinical study designs, limitations in animal models, overly optimistic interpretations of preclinical data, lack of target engagement in humans, and challenges in conducting clinical trials without informative biomarkers (Berry et al., 2014). In the field of Alzheimer's disease (AD) research, despite successful outcomes in mouse models, the translation of these findings to clinical trials has been disappointing (Pistollato et al., 2016); (Zeiss, 2015). This issue came to a head in 2012 with the failure of trials involving two promising anti-amyloid β antibodies, bapineuzumab and

solanezumab, leading to questions about the central role of the amyloid hypothesis in AD, as well as the reliability of mouse models (Selkoe & Hardy, 2016). Despite adhering to target-driven research methodology, efforts to develop AD therapies have faced challenges. A recent report sheds light on how past setbacks may have arisen due to an evolving understanding of the relationship between amyloid fibrillogenesis, pharmacokinetics and pharmacodynamics of different anti-amyloid antibodies, and the accuracy of amyloid imaging modalities in reflecting cognitive decline in humans (Sevigny et al., 2016). The study utilized amyloid β transgenic (Tg2576) mice to establish a connection between the binding properties of the antibody (for oligomeric and fibrillar forms) with dose-dependent clearance of histopathologic plaques, which in turn correlated with dose-dependent reduction in plaque burden and reduced clinical decline in patients. In the field of behavioral neuroscience, it has been proposed that introducing heterogeneity in the environment and testing procedures can improve reproducibility by increasing variation within experiments compared to between experiments (Richter et al., 2010). Despite being crucial for our understanding of Alzheimer's disease (AD), traditional transgenic mouse models have several limitations. These include potential mis- or over-expression of transgenic proteins compared to endogenous proteins, compensatory mechanisms in response to knocked-out or over-expressed genes during development, and unintended disruption of endogenous genes by the transgenic construct. Moreover, most transgenic lines are generated on standard genetic backgrounds that may not accurately reflect disease phenotypes. Importantly, the timing of transgenic promoter-driven expression may not mimic disease onset, limiting the ability to study disease mechanisms in a realistic context. Additionally, legal restrictions on availability and use, particularly for therapy development projects by for-profit companies, further limit the utility of these models for the research community (Bubela & Cook-Deegan, 2015). The majority of mouse models used in Alzheimer's disease (AD) research are limited to a single or very few genetic backgrounds.

Previous studies have demonstrated that modifying the genetic background of mice can have a substantial influence on AD-related traits (Onos et al., 2016). However, there has been a lack of comprehensive evaluation of AD mutations using genetically diverse mouse strains, including wild-derived strains like CAST/EiJ. Furthermore, using quantitative trait loci (QTL) mapping to identify specific genetic variations that affect the phenotype has limitations in terms of statistical power, often resulting in the identification of large genetic intervals instead of pinpointing specific variations. This encompasses individuals with mixed genetic backgrounds, which can complicate the interpretation of research findings. Previous studies in mice have shown that the genetic background can strongly influence levels of amyloid-beta (Ab) protein, with mapping studies identifying genomic regions that impact amyloid burden (Ryman et al., 2008), (Sebastiani et al., 2006). However, these studies have not thoroughly examined how genetic background affects cognitive performance (Jackson et al., 2015), (Sipe et al., 1993)) Studies have shown that genetics play a significant role in cognitive decline in human populations, so its been hypothesized that genetic background also plays a crucial role in modifying cognitive decline in animal models of Alzheimer's disease (AD) (Gatz et al., 1997). Including genetic diversity in AD mouse models would likely enhance the translational validity of the findings.

Using Genetic diversity in mouse models to recapitulate human population in disease

A crucial obstacle in genomic medicine is determining the causal relationship between human genetic variants and disease. To address this challenge, it is essential to establish a comprehensive catalogue of mammalian gene function, which serves as a foundational platform for deciphering gene-disease associations. However, refining current approaches is necessary to gain a more nuanced understanding of the intricate relationship between specific

human variants and disease. Rare diseases and Mendelian disorders pose a particularly daunting task, as there are numerous variants of uncertain significance in both known and unknown disease genes (Ramoni et al., 2017). To tackle this issue, the mouse model emerges as a critical tool for attributing a specific gene or variant to a disease (Wangler et al., 2017), (Lloyd et al., 2020). Mouse genetics centers worldwide have already established CRISPR pipelines for generating mice carrying human disease-associated coding variants. These initiatives, such as the Rare Disease Models and Mechanisms programs, are being implemented globally (Boycott et al., 2020) (https://j-rdmm.org; http://solve-rd.eu/rdmmeurope/). Through phenotyping of these mutant mice, the validity of the variant in question can be tested. Furthermore, comprehensive phenotyping of these mutants can unveil pleiotropy, expanding our understanding of co-morbidities, enhancing diagnosis, and potentially improving treatment options. Additionally, these pipelines provide invaluable models for pre-clinical testing and therapeutic development. Expanding existing pipelines to analyze genetic variants associated with non-coding sequences, which are increasingly recognized as significant contributors to human disease, poses a formidable challenge due to the potentially vast array of variants in non-coding elements (CNEs). However, a promising starting point could be to initially focus on conserved CNEs. Mouse pan-genome functional data, particularly from null mutations, are already making a considerable impact in deciphering the significance of human variants. Integrating data and developing ontologies across mouse and human, along with appropriate software tools, is critical (Smedley & Robinson, 2015), (Robinson et al., 2014). Automated variant prioritization tools like Exomiser, which compare clinical phenotypes with those observed in mice, are proving invaluable, and the inclusion of mouse and fish model phenotype data in Exomiser has been shown to increase the validation rate of variants in the National Institutes of Health Undiagnosed Disease Programme by 10-20% (Gall et al., 2017). The interactions between genetic context (G × G interactions) and environmental context (G × E

interactions, including ageing) play a significant role in shaping gene-phenotype and gene-disease relationships. While genome-wide mutation resources are valuable for understanding gene function and disease at a fundamental level, they may not fully capture the phenotypic consequences of genetic background. However, environmental impacts can be taken into account in phenotype platforms. To better understand the complexities of genetic context, mouse genetics offers a range of resources that utilize diverse inbred mouse lines, including wild-derived inbred lines (Li & Auwerx, 2020), (Nadeau & Auwerx, 2019). In addition to the mouse inbred lines, there are two types of tools that are commonly used in research. The first type is recombinant inbred (RI) lines, which are genetically identical and include panels such as the BXD recombinant inbred panel (Ashbrook et al., 2021) and the Collaborative Cross (CC) lines (Churchill et al., 2004). The BXD lines are valuable for mapping quantitative trait loci (QTLs) with high resolution, as they encompass millions of common sequence variants, surpassing the genetic diversity of many human populations. These lines have been extensively phenotyped for a wide range of traits, including omics datasets and classic phenotypes, making them a valuable resource for research. Recently, the number of BXD strains has been expanded, providing even more power and resolution for mapping studies (Ashbrook et al., 2021). Additionally, crossing BXD lines to generate a diallel cross (DAX) of BXD F1 lines allows for studying epistasis and evaluating complex genetic models, as well as studying dominance effects. Moreover, BXDs can be crossed with single gene models to map modifiers of disease traits. For example, Neuner et al. demonstrated the use of isogenic F1s generated by crossing the 5XFAD Alzheimer's disease (AD) model with 27 BXD lines, revealing wide variability in cognitive phenotypes among the F1 strains, reflecting the genetic diversity observed in human populations. By computing genetic risk scores based on human genes associated with AD risk, they showed that allele dosage at these loci was significantly associated with cognitive outcomes across the 27 lines, indicating that the modifying effects of genetic background in

BXDs recapitulate the effects of genetic context in humans. Expanding the number of lines used in these studies will allow researchers to identify additional loci, refine mapping efforts, and identify underlying genetic factors that modify AD risk, including those that contribute to resilience. Importantly, incorporating genetic diversity into model systems not only increases the complexity of genetic pathways and their interactions, but also provides an improved platform for pre-clinical testing of personalized therapeutic interventions. The CC lines have been extensively researched for various disease phenotypes, and they offer high-resolution mapping capabilities, which have been utilized to investigate the genetic basis of different traits (Shusterman et al., 2013). Additionally, the Hybrid Mouse Diversity Panel, which combines inbred and RI strains, has been used to localize diverse traits (Bennett et al., 2010), (Patterson et al., 2017).

Another class of mouse tools for QTL analyses involves the generation of outbred populations using pseudo-random breeding schemes. These populations include Heterogeneous Stocks (HS) (Solberg et al., 2006) and Diversity Outbred (DO) Populations (Churchill et al., 2012). HS mice are created by intercrossing inbred or recombinant inbred lines followed by mating schemes that minimize inbreeding. The DO population, a type of HS, is generated by random mating of partially inbred CC lines. Both types of outbred populations have been employed to map disease traits (Valdar et al., 2006), (Svenson et al., 2012). Moreover, commercially available outbred populations have been used to map specific disease traits, and when coupled with high-throughput phenotyping pipelines, they have been used at scale to discover and map a wide range of disease loci (Nicod et al., 2016). The integration of diversity resources in mouse research, along with large-scale efforts to develop and characterize null mutant (and other monogenic alleles) resources such as IMPC, will be crucial to fully capitalize on these advancements. Phenotypic characterization of comprehensively studied single gene mutants is essential in transitioning from identifying trait loci to identifying causal genes, providing

important validation and biological insights. These single gene mutants serve as a critical foundation for combining resources, such as BXDs with disease models, to systematically investigate modifier effects on a gene-by-gene basis, as demonstrated above. These modifier loci would then become targets for further rounds of analysis, where null mutants at the modifier genes would be subjected to additional BXD/G analysis. Through this iterative process, common modifier loci between BXD/G crosses would begin to reveal genetic networks, and these common modifiers would themselves become priority targets for further BXD/G analysis. In conjunction with F1s generated from diallel crosses of BXD (Ashbrook et al., 2021), this approach would unveil numerous networks related to pleiotropy and disease mechanisms. The magnitude of this undertaking would necessitate significant investment and a global effort, but it would be a decisive step towards unraveling the genetic networks underlying diseases and supporting genomic and precision medicine. In 2003, Zambrowicz and Sands published a groundbreaking paper that conducted a retrospective review of mouse knock-out models for the top 100 best-selling drugs, revealing a strong correlation between phenotypic effects and known drug efficacy (Zambrowicz & Sands, 2003). This highlighted the value of mice as a powerful tool for target discovery and disease modeling. Recent analysis of gene-disease associations has further supported the predictive power of animal model disease-phenotype data for identifying novel therapeutic targets (Ferrero et al., 2017). However, there has been frustration with the lack of translation from pre-clinical studies to human therapies (Justice & Dhillon, 2016). To address this challenge, the biomedical sciences community has recognized the importance of validity and reproducibility in mouse models, including model characterization, variation control, and appropriate statistical analysis. It's crucial to understand that mouse models can play critical roles at different stages of the translational process, from mechanistic studies to pre-clinical studies to therapeutic

development. The strict notion of "predictive validity" in drug responses of model organisms should be reconsidered in this context.

CHAPTER 1. Identification of conserved trends in health and neurodegenerative disease with microglial depletion

Portions of Chapter 1 of this thesis/dissertation is a reprint of the material as it appears in (Crapser, Ochaba, et al., 2020), used with permission from Joshua Crapser. Portions of Chapter 1 of this thesis/dissertation is a reprint of the material as it appears in (Arreola et al., 2021), used with permission from Miguel Arreola.

Background

Microglia facilitate loss of PNNs in the Huntington's disease brains

Huntington's disease (HD), an autosomal dominant neurological disorder, is caused by an abnormal expansion of CAG triplet repeats in exon 1 of the huntingtin (HTT) gene, resulting in an elongated polyglutamine (Q) tract in the mutant huntingtin protein (mHTT) ("A novel gene containing a trinucleotide repeat that is expanded and unstable on Huntington's disease chromosomes. The Huntington's Disease Collaborative Research Group," 1993), (Lobanov et al., 2022). While unaffected individuals typically have 16-20 triplet repeats, affected patients have ≥40 CAGs, and the age of symptom onset generally correlates inversely with repeat length (Duyao et al., 1993), (Labbadia & Morimoto, 2013). The disease is characterized by progressive movement abnormalities (chorea, dystonia) and cognitive-behavioral impairments, accompanied by selective death of medium spiny neurons in the striatum and cortical atrophy (Ross & Tabrizi, 2011). Pathologically, mHTT accumulates in various cell types and forms, partly due to failures in protein quality control networks, as evidenced by accumulation of ubiquitin and other post-translationally-modified proteins, as well as disruptions in autophagy (Ochaba et al., 2016), (Kurosawa et al., 2015). Despite its monogenic origin, the specific contributions of different cell types in the brain to HD are still being elucidated. Microglia, which are resident myeloid phagocytes comprising about 12% of brain cells, actively survey

the brain parenchyma for deviations from homeostasis every 24 hours (Nimmerjahn et al., 2005). It is now well established that microglia play critical roles in neurodegeneration and injury (Li & Barres, 2018), and ongoing research continues to uncover the full functional spectrum and unique characteristics of microglia among immune cells in development, aging, and disease (Bennett et al., 2018), (Mrdjen et al., 2018). Previously, a pharmacological method was developed to selectively eliminate nearly all (~99%) microglia from the mouse brain for extended periods of time by inhibiting the colony-stimulating factor 1 receptor (CSF1R) signaling, which is essential for microglial survival (Elmore et al., 2014), (Dagher et al., 2015). This approach, using CSF1R inhibitors formulated in chow, allows for non-invasive and uninterrupted drug delivery to achieve long-term elimination of microglia during treatment (Asai et al., 2015), (Rice et al., 2015), (Acharya et al., 2016), (Feng et al., 2016), (Spangenberg et al., 2016), (Stafford et al., 2016), (Szalay et al., 2016), (Li et al., 2017). In HD, activation of microglia, a type of immune cell in the brain, is detected years before clinical symptoms appear and is correlated with dysfunction of neurons in the striatum, both in early and advanced stages of the disease (Tai et al., 2007), (Pavese et al., 2006), (Politis et al., 2011). Post-mortem analysis of brains from individuals with HD shows increased microglial activity in regions where neurons are lost, and this phenomenon is also observed in mouse models of the disease (Sapp et al., 2001), (Simmons et al., 2007). Unlike their conventional role in responding to stress signals and toxins in neurodegeneration, microglia in HD are altered by the presence of mutated huntingtin protein (mHTT) alone, resulting in changes in gene expression and increased production of inflammatory molecules (Benraiss et al., 2016). Furthermore, engraftment of human glial progenitor cells expressing mHTT in mice leads to hyperexcitability of neurons in the striatum and motor impairments (Osipovitch et al., 2019). To further investigate the role of microglia in HD, we used a CSF1R inhibitor (CSF1Ri), a drug that depletes microglia, in a mouse model of the disease called R6/2 mice. These mice express a mutated form of human

huntingtin protein and exhibit motor and behavioral deficits. We found that treatment with CSF1Ri resulted in improved grip strength and memory, reduced accumulation of mHTT, and restored protein clearance system pathway function in the R6/2 mice. At the molecular level, we observed impaired neuronal development pathways and an interferon signature, which is also seen in human HD, in the striatum of R6/2 mice, and these changes were diminished after microglial depletion. Additionally, despite a reduction in the volume of the caudoputamen, a region of the brain affected in HD, we observed increased densities of neuronal and neurite cytoskeletal elements in the R6/2 mice after CSF1Ri treatment at 11 weeks. This was accompanied by astrogliosis and increased deposition of extracellular matrix chondroitin sulphate proteoglycans (CSPGs), which are components of glial scars and inhibit axon growth (Hsu et al., 2008), (Ohtake et al., 2016). Interestingly, we also observed increased PNN densities, specialized structures associated with interneurons, in the brains of non-transgenic littermates after microglial depletion, suggesting that microglia play a role in regulating PNN formation in both health and disease (Fawcett et al., 2019). Overall, our findings highlight the critical role of microglia in the pathogenesis of HD and provide evidence that targeting microglial activation and function may have therapeutic potential for this devastating neurodegenerative disorder.

Microglia facilitate loss of perineuronal nets in the Adult-onset leukoencephalopathy with axonal spheroids and pigmented glia diseased brains

ALSP, also known as hereditary diffuse leukoencephalopathy with spheroids, is a rare autosomal dominant neurodegenerative disease affecting the white matter of the brain. It is characterized by the presence of patchy lesions in the frontal and parietal white matter, leading to thinning of the corpus callosum and subsequent cortical atrophy (Kondo et al., 2020). Genetic studies have identified mutations in the tyrosine kinase domain of the colony-stimulating factor 1 receptor (CSF1R) as the underlying cause of ALSP (Konno et al., 2018).

CSF1R is primarily expressed in microglia, and mutations in CSF1R have been shown to impair its kinase activity (Rademakers et al., 2011). However, the exact cellular mechanisms by which these mutations lead to ALSP are still unclear, with some studies suggesting a dominant-negative effect and others suggesting haploinsufficiency (Hoffmann et al., 2014), (Adams et al., 2018). Recent findings have shown that haploinsufficiency of CSF1R alone can cause ALSP in clinical populations, leading to the development of CSF1R+/− mice as a disease model (Konno et al., 2014). These mice exhibit similar behavioral and histopathological deficits as patients with ALSP, including depression, seizures, cognitive deficits, abnormal myelination, and neurodegeneration (Chitu et al., 2015). Mutations in other genes highly expressed in microglia, such as Trem2 and Tyrobp, have also been implicated in other leukodystrophies and neurodegenerative disorders, collectively termed microgliopathies (Guerreiro et al., 2013), (Meuwissen et al., 2016). The aim of the study was to investigate the impact of loss of one allele of the Csf1r gene on microglial and parenchymal homeostasis. Our findings revealed that deletion of one copy of Csf1r specifically in myeloid cells in adult mice resulted in a disruption of microglial homeostasis, as evidenced by the loss of P2RY12 expression, a marker of microglial function. This microglial dyshomeostasis was accompanied by a decrease in synaptic markers and dysregulation of extracellular matrix (ECM) components, particularly a loss of perineuronal nets (PNNs), indicating that these downstream effects are originating from adult microglia. We observed similar microglial phenotypes, including loss of P2RY12 expression and hyper-ramification, in a mouse model of adult-onset leukoencephalopathy with axonal spheroids and pigmented glia (ALSP) that carries a constitutive heterozygous mutation in Csf1r (CSF1R+/−). In CSF1R+/− mice, we also observed impaired behavioral performance in novel object recognition (NOR) and novel place recognition (NPR) tasks, along with decreased synaptic markers and PNNs. Notably, complete elimination of microglia from adult CSF1R+/− mice reversed the deficits in PNNs and synaptic

markers. Furthermore, we compared the genetic monoallelic loss of Csf1r with low-grade chronic CSF1R inhibition and found significant overlap in gene expression changes, indicating that partial disruptions to CSF1R signaling, whether through pharmacological or genetic means, result in similar downstream signaling abnormalities. Surprisingly, low-grade CSF1R inhibition in CSF1R+/− mice was able to reverse microglial dyshomeostasis, restore cognition, and prevent the loss of synaptic markers and PNNs, rather than exacerbating these alterations. Additionally, analysis of aged CSF1R+/− mice revealed significant loss of myelin basic protein (MBP) staining in the corpus callosum (cc) and ECM structures in the somatosensory cortex (SS Ctx), with PNNs being rescued when treated with low-grade CSF1R inhibition. These findings suggest that CSF1R signaling plays a crucial role in maintaining microglial homeostasis, specifically regulating microglial effects on synapses and the ECM where synaptic connections are embedded, and may serve as a potential target for modulating microglial phenotype (Arreola et al., 2021).

Microglia and the regulation of perineuronal nets

In the adult brain, the space (~20% of the total volume) between neurons and glial cells is occupied by the ECM. This matrix is composed of a network of proteins and polysaccharides (e.g., glyocosaminoglycans, proteoglycans, glycoproteins, and fibrous proteins) and acts as a physical barrier and regulator of many neural processes in the CNS, including neurite outgrowth, synaptogenesis, synaptic stabilization and plasticity (Lam et al., 2019). Metalloproteinases (*MMPs*) and serine proteases are involved in modulating both cognitive and neurodegenerative processes through ECM proteolysis (Ziemianska et al., 2012).

Microglia have been implicated to play a pivotal role in extracellular matrix (ECM) remodeling in various neurological disorders. During an ischemic stroke, loss of hippocampal neuronal *IL-33* or microglial *IL-33* receptors lead to impaired spine plasticity, dysregulation of impaired ECM engulfment and a concomitant accumulation of ECM proteins in contact with synapse—

all of which regulate memory consolidation (Nguyen et al., 2020). Numerous substrates, both secreted by microglia or already present like metalloproteinases (*MMP*), *neuromelanin, α-synuclein, TLRs,* known to degrade the ECM have been studied as potential/candidate targets for intermediation of neuronal damage and microglial activation (Kim & Joh, 2006), (Konnecke & Bechmann, 2013).

Perineuronal nets (PNNs) are condensed ECM structures that provide scaffolding for neuronal synapses, and studies have shown that these structures are directly involved in neuronal plasticity and memory as they are present throughout the brain, especially around fast-spiking parvalbumin interneurons (Carulli et al., 2020). After the developmental stage is completed, PNNs form around parvalbumin (PV)+ GABAergic interneurons to provide synaptic stability by "locking" synapses in place (Wen et al., 2018). There are studies analyzing PNN structure in the both healthy and diseased brain using WFA-immunolabelling. All levels of the entorhinal cortex show that WFA is more loosely distributed in the diseased cortex, suggesting presence of degraded PNNs (Pantazopoulos & Berretta, 2016).

Synaptic structure and function are regulated by four key elements: pre- and post-synaptic compartments, glial cells, and the ECM, including critical components such as CSPGs/PNNs. Interestingly, most synaptic abnormalities are usually accompanied by PNN impairments as observed in various psychiatric and neurodegenerative disorders (Pantazopoulos & Berretta, 2016), (Baig et al., 2005), (Colton et al., 2006). Analysis of in vivo PNNs in the hippocampus of quadruple knockout mouse deficient for the ECM molecules *tenascin-C (TnC), tenascin-R (TnR), neurocan* and *brevican* revealed a reduction of PNN size and complexity in the CA2 region along with a significant increase in the ratio of excitatory synapses to inhibitory synapses. The gene expression analysis revealed alteration in the genes *Gpc3, Gabrq, Gad2, Wnt7, Syt9, Sod3, Dnm3, Cript, Sema4c, Calr, Cplx3, Col4a3, Col27a1, Adamts13, Grin2d, Col1a2, Spon2* and *Rapsn* (Gottschling et al., 2019). The broad objective of my thesis is to

explore the role of microglia in regulating PNNs and other aspects of the ECM under both homeostatic and disease states, and to identify any potential mechanisms by employing RNA-seq with mouse genetics and histology.

CSF1R signaling and microglial depletion using CSF1R inhibitors

CSF1R is a receptor critical for the survival and maintenance of microglia, including cell proliferation, survival, and differentiation. Studies have shown that CSF1R is required during development for survival; mice devoid of this receptor are born without microglia and only survive to week 6 of the postnatal period (Erblich et al., 2011), (Spangenberg et al., 2019)]. Developing microglia upregulate this receptor in two phases: (1) during chromatin remodeling of the macrophage promoter with the help of transcriptional factors *PU.1, Runx1, and C/EBP,* and (2) when macrophage genes are upregulated, and transcriptional neutrophil genes are downregulated following assembly of the transcription factors *Egr1* and *Egr2*. This mechanism prevents multipotent cells that require growth factors such as IL-3 from expressing CSF1R (Spooner et al., 2009). CSF1R is also required for macrophage proliferation as it induces CSF1 dose-dependent amplification of protein synthesis. Activation of the receptor leads to a signaling cascade involving phosphorylation of the *ITAM* cytoplasmic domains of *DAP12,* eventually ending with activation of cell cycle genes and nuclear translocation of *β-catenin* (Hamerman et al., 2009). *Akt/PI3K* pathways are known to modulate macrophage survival with the help of CSF1. Loss of *PI3K* results in reduced macrophage numbers without any effects on cell proliferation (Linton et al., 2019), (Yu & Cui, 2016).

Several studies by our lab and others have provided extensive evidence on the critical importance of CSF1R function to microglial survival (Spangenberg et al., 2019). Pharmacological inhibition of the CSF1R receptor results in rapid elimination of nearly all microglia in the CNS (Wesolowski et al., 2019). There are several CSF1R inhibitors (PLX3397, PLX5622) that can cross the blood-brain barrier, and when orally administered can

result in the depletion of up to ~99% of microglia (Ali et al., 2020); the extent of depletion is dependent on dose, and microglia remain depleted for the duration of treatment (Elmore et al., 2014). In these studies, conducted on adult mice, despite overt microglial loss, we observe no cognitive deficits or peripheral cell infiltration, even with a treatment duration of 6 months (Spangenberg et al., 2019). Thus, the use of CSF1R inhibitors has emerged as an effective tool to ablate the microglial compartment and gain further understanding of microglial function in the healthy and diseased brain. A study conducted by our lab revealed that the elimination of microglia in 5xFAD mice led to a reduction in brain-wide inflammatory signaling, as evidenced by RNA analysis of several inflammation-related genes (Spangenberg et al., 2016). Specifically, we observed decreases in transcripts associated with microglia reactivity, such as *C1q*, *Tlr2*, *Tlr3*, *Tlr4*, *Tlr7*, *Ccl3*, *Nlrp3*, and *Pdcd1*, as well as reductions in anti-inflammatory/phagocytic markers, including *Tgfb1*, *Tgfbr1*, *Tgfbr2*, *Mrc1*, and *Itgb2*. Moreover, our results demonstrated that the elimination of microglia had a positive impact on hippocampal-dependent cognitive tasks. These findings are consistent with previous studies that have shown that modulating microglial function in Alzheimer's disease models can restore or improve memory (Kiyota et al., 2010), (Parachikova et al., 2010), (Gabbita et al., 2012), (Yamanaka et al., 2012).

Data

During disease or injury, microglia alter their morphology and phenotype to adopt an activated state. Preclinical disease models show that disease progression can be exacerbated by inflammation, indicating crosstalk can happen between systemic inflammation and microglia in the CNS (Perry et al., 2010). To further understand the mechanism between this interaction, we chose to examine microglia in two neurological disorders characterized by activated microglia: Huntington's and Adult-Onset Leukoencephalopathy with Axonal Spheroids and

Pigmented Glia (ALSP) in both healthy and diseased brains (Kempthorne et al., 2020a), (Yang et al., 2017). Notably, as detailed below, we find a common pathological feature of both diseased brains; microglia mediated loss of PNN's that are not associated with typical inflammatory states of microglia.

Chapter 1.1. Identifying the novel role of microglia in PNN regulation in the homeostatic and HD mouse brain.

Mutations in the huntingtin gene (mHTT) lead to an expansion of the trinucleotide CAG region (Aziz et al., 2011), and this polyglutamine stretch in the protein HTT causes HD. Since microglial activation has been shown to correlate with neuronal dysfunction and HD severity (Palpagama et al., 2019), we were interested in investigating the role of microglia in a mouse model of HD utilizing CSF1R inhibitors to deplete the microglial tissue. Joshua Crapser performed the following experiments and collected the data. I executed the transcriptional analyses.

This study used transgenic R6/2 mice, a common mouse model of HD. These mice express the human *huntingtin* gene with ~150 CAG repeats, which results in 75% of the endogenous huntingtin transgene expression level. The R6/2 line is a rapidly progressing disease model that displays severe motor and behavioral deficits by 8-12 weeks of age, with initial signs of disease appearing as early as 3 weeks (Carter et al., 1999), (Luesse et al., 2001). To eliminate microglia, 6-week-old R6/2 mice or non-transgenic (NT) littermate controls were treated with the CSF1R inhibitor, PLX3397 (*Pexidartinib*) (Cannarile et al., 2017), (Elmore et al., 2014), and either placed on a diet containing 275 mg/kg chow PLX3397 or in the vehicle (n=6/group) until sacrifice at 11 weeks (**Figure 1A**). Immunohistochemistry with ionized calcium binding adaptor molecule 1 (*IBA1*), a common myeloid cell marker, was used to access microglial densities. We observed elevated microglial densities in the striatum and cortex of the R6/2

brain (**Figure 1B-C**). Although microglial densities were elevated, the microglia were negative for *IB4* marker, a marker for cell activation, and we detected no differences in microglial morphology, indicating that microglia in the HD brain are not classically activated (data not shown). CSF1Ri leads to a significant reduction in the number of the microglia in both genotypes across all regions of the tissue (**Figure 1B-C**). Following microglial elimination, we observed several rescues of disease-associated alterations including: grip strength, object recognition deficits, *mHTT* accumulation, astrogliosis, and striatal volume loss (Crapser, Ochaba, et al., 2020); data not shown).

Although this analysis will not be discussed in detail in this advancement, we observed a significant loss of striatal volume in R6/2 (**Figure 1D-E**), which we hypothesized could be a result of ECM degradation in HD; thus, we next expanded our analysis to the ECM. To investigate the ECM, we performed immunohistochemical analysis on PNNs, proteoglycans associated with the ECM. These reticular dendrosomatic structures can encase largely parvalbumin (PV)-expressing interneurons (Miyata et al., 2012), (Yutsudo & Kitagawa, 2015)

and are thought to "lock" synapses in place

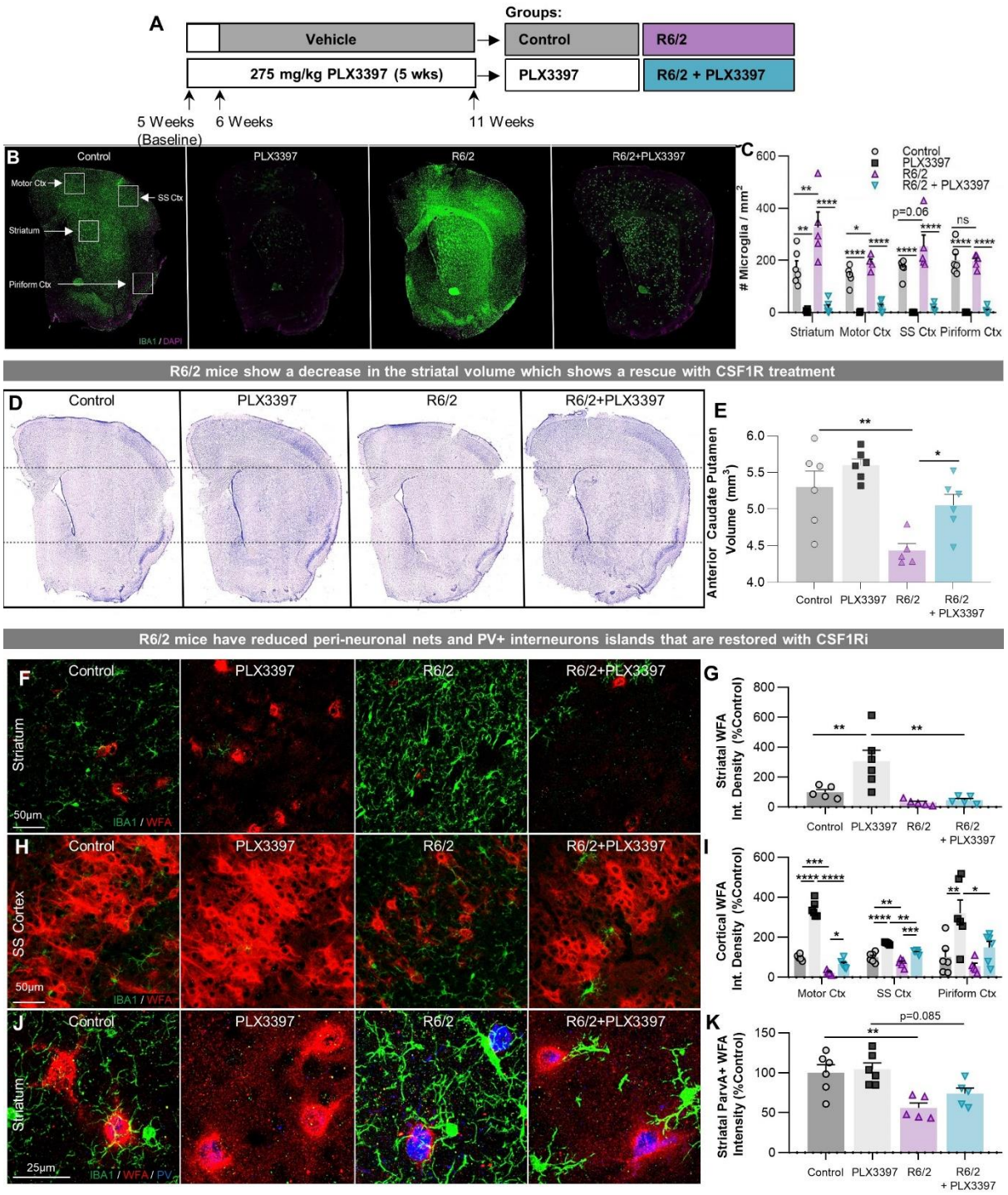

***Figure 1**: (**A**) Experimental design (n = 5–6/group) following baseline measurements, 6-week-old non-transgenic or R6/2 mice were treated with vehicle (Control, R6/2) or 275 mg/kg PLX3397 (PLX3397, R6/2+PLX3397) for 5 weeks to attain microglial depletion through CSF1Ri. (**B**) Representative IBA1$^+$ whole-brain images (×20) from non-transgenic and R6/2 mice treated with vehicle or PLX3397 confirmed R6/2 microgliosis and microglial depletion (n = 5–6/group). (**C**) Quantification of IBA1$^+$ microglia revealed significant increases in the R6/2 striatum ($P < 0.01$) and motor cortex ($P < 0.05$), with a trending increase in the somatosensory cortex ($P = 0.06$) but no change in the piriform cortex compared to control. PLX3397 significantly depleted microglia in both genotypes and in all regions (two-way ANOVAs with Tukey's post hoc test; n = 4–6/group). (**D**) Representative*

*images of cresyl-violet stained coronal sections used for stereological assessment of striatal volume (n = 5–6/group, six sections/mouse separated by 240-μm intervals, spanning the anterior caudoputamen). (**E**) Quantification of stereological analysis reveals a significant reduction in R6/2 striatal volume versus control (P < 0.01) that is prevented with PLX3397 (P < 0.01) (two-way ANOVA with Tukey's post hoc test; n = 5–6/group). (**F-I**) Striatal and cortical images (×20) of WFA$^+$ PNN staining (with IBA1$^+$, **F** and **H**) quantified as integrated density (**G** and **I**) revealed significant reductions in the motor (P < 0.001) and somatosensory (P < 0.01) cortices, which were restored by microglial depletion with PLX3397 (P < 0.05, P < 0.001) (two-way ANOVAs with Tukey's post hoc test; n = 5–6/group). Surprisingly, PLX3397 in healthy non-transgenic controls significantly increased WFA$^+$ PNN density in every region examined: striatum (P < 0.01), motor cortex (P < 0.0001), somatosensory cortex (P < 0.0001), and piriform cortex (P < 0.01) (two-way ANOVAs with Tukey's post hoc test; n = 5–6/group). Quantification of mean WFA$^+$ intensity co-localizing with striatal parvalbumin-expressing GABAergic interneurons (×63; **J** and **K**) revealed significant (P < 0.01) and trending (P = 0.085) reductions in R6/2 and R6/2+PLX3397 mice respectively, indicating loss of interneuron-associated PNN integrity (two-way ANOVA with Tukey's post hoc test; n = 5–6/group**). This data was collected and analysed by Joshua Crapser.***

during development (Wen et al., 2018). Of note, reports have shown that there is a ~75% decrease in PV interneurons in HD brains (Reiner et al., 2013). Here, we used the lectin marker *Wisteria floribunda agglutinin* (WFA) to immunolabel PNNs. Interestingly, microglial elimination in control littermates resulted in brain-wide increases (specifically, the striatum, somatosensory cortex, and motor cortex) in PNN density (**Figure 1F-G**), suggesting that microglia play an important role in mediating PNNs in the healthy brain. R6/2 somatosensory and motor cortex showed a loss in the PNN counts compared to the control mouse brain (**Figure 1H-I**). PV-expressing interneurons in HD striatum showed a deficit in WFA staining intensity, suggesting a loss of encapsulating PNNs (**Figure 1J-K**). Depleting microglia showed a rescue in the deficits seen above, including disease-associated striatal volume loss (**Figure 1D-K**), underscoring their role as coordinators of brain ECM remodeling which appears to contribute to neurodegeneration in HD. These results, for the first time, demonstrate that 1) microglia regulate basal levels of PNNs in the homeostatic brain, and 2) microglia in R6/2 mice are responsible for the pathological degradation of the PNNs. However, the exploration of the aforementioned behavioral and molecular rescues is out of the scope of this advancement.

Here, I will focus on my contribution to the project, which set out to 1) identify microglial signatures that affect PNNs in both the homeostatic and R6/2 mouse diseased brain, and 2) define the gene expression changes that accompany the pathogenesis of the disease and how

these are impacted by the elimination of microglia in order to identify microglia's involvement in HD.

To understand the role microglia play in this disease at the transcriptional level, I analyzed raw RNA-seq reads generated using Illumina on bulk striatal tissue (**Figure 2A,H**). After a series of quality control steps that involved discarding low-quality reads, trimming adaptor sequences using TRIMMOMATIC (Bolger et al., 2014) and BBMAP (Bushnell et al., 2017), sorting for rRNA contamination with SORTMERNA (Kopylova et al., 2012) and elimination of poor-quality bases, I aligned the raw reads to the reference mm10 genome using STAR (Dobin et al., 2013) to produce featureCounts. Downstream differential gene expression of RPKMs revealed effects of CSF1Ri on R6/2 mice including dysregulation of excitatory/inhibitory balance (*GAD1, GAD2* (Consortium, 2017), *Scn4b* (Miyazaki et al., 2014), (Oyama et al., 2006), *Slc7a11*) (**Figure 2G,K**). We also observed CSF1Ri rescued disease-associated suppression of *Isl1* and *Cacna2d2* (**Figure 2G,K**). *Isl1* is a gene involved in motor neuron development (Liang et al., 2011), and a previous study has shown that the conditional knock-out of this gene using Six3-cre transgene leads to striatal cholinergic interneuron loss (Elshatory & Gan, 2008). Interestingly, mutations in *Cacna2d2* decrease Ca^{2+} channel subunit expression, which are implicated as important regulators of synapse formation (Geisler et al., 2015), (Pippucci et al., 2013). Aligning with the histological data we found no evidence of overt inflammation in R6/2 striatal tissue compared to WT; statistically significant changes (FDR< 0.1) were not observed in cytokine transcript levels (*Il6, Il1β, Ifnγ, Tnfα*) or other glial inflammatory readouts, such as astrocyte marker (*S100β, C3*) transcript expression, during differentially expressed gene (DEG) analysis using edgeR (McCarthy et al., 2012), (Robinson et al., 2010). However, we did find a conserved downregulation of the adenosine A2a receptor (*Adora2a*) (Blum et al., 2018) along with a dysregulated interferon (IFN) signature in R6/2 compared to WT mice (altered T-cells and interferon signaling: ↑ *Twist1, Ebi3, Tal1, Ccl19,*

Irf7, Irf4, Bst2, Ifit3, Psmb8; ↓ CD4, Alcam, Tcf7, Mcam, Ccl25, Il18; (**Figure 2J)**). These alterations have been reported in human HD and murine models of HD, respectively

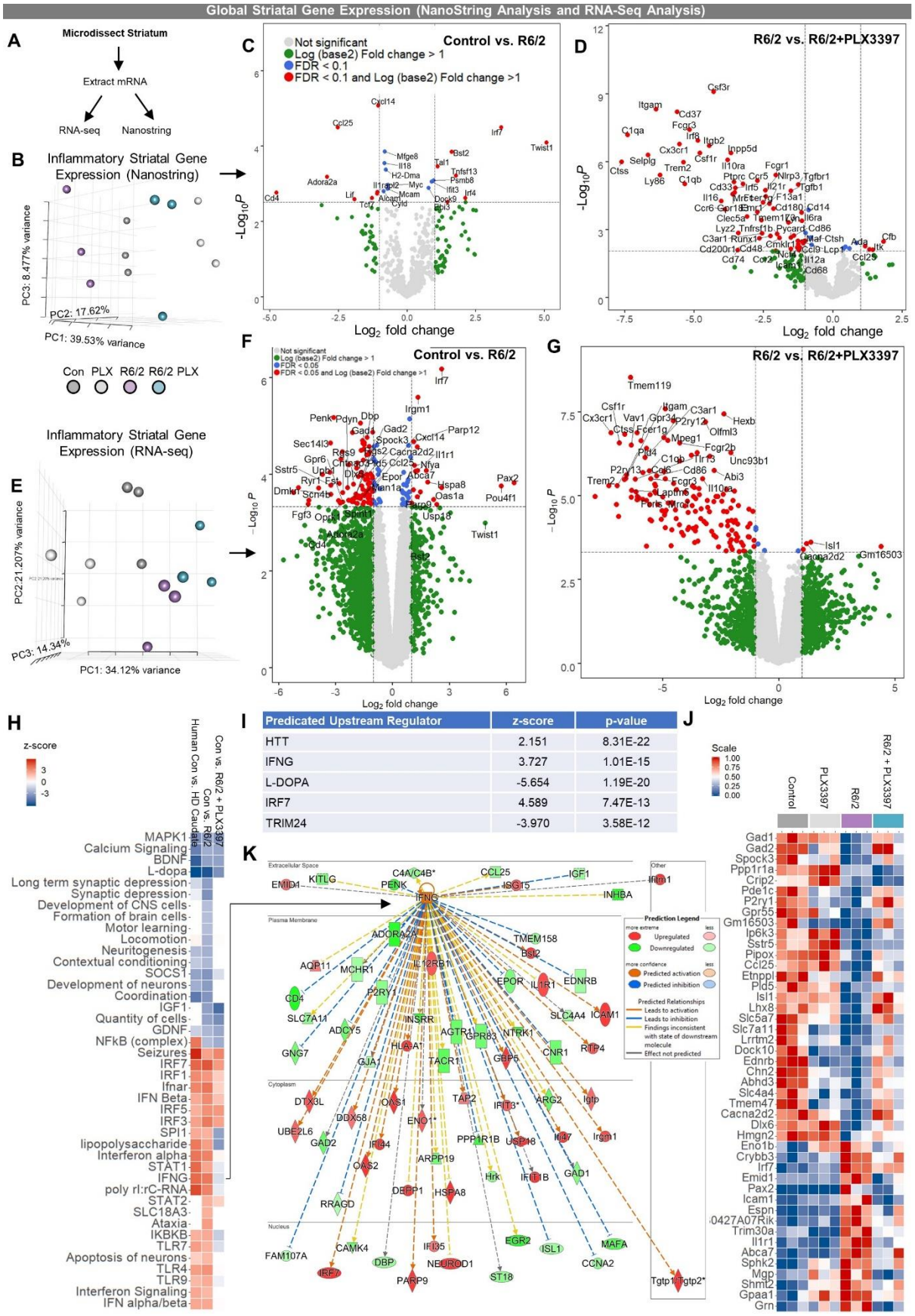

Predicated Upstream Regulator	z-score	p-value
HTT	2.151	8.31E-22
IFNG	3.727	1.01E-15
L-DOPA	-5.654	1.19E-20
IRF7	4.589	7.47E-13
TRIM24	-3.970	3.58E-12

***Figure 2**: (**A**)Schematic design for mRNA extraction and RNA-seq data analysis (**B**) Striatal inflammatory gene expression assessed with a NanoString immune panel revealed non-overlapping clustering of samples in each group by principal component analysis (PCA; n = 3/group). (**C** and **D**) Volcano plots of differentially expressed genes (DEGs) in R6/2 versus control striatum (**C**) indicated a lack of inflammatory transcription at an FDR of < 0.1, but (**D**) confirmed loss of the microglial gene signature with PLX3397 in R6/2 striatum (n = 3/group). Statistical significance is denoted by *P < 0.05, **P < 0.01, ***P < 0.001, ****P < 0.0001, ns = not significant. Error bars indicate SEM. (**E**) PCA of striatal gene expression as determined by mRNA-seq confirmed similar non-overlapping clustering of control and R6/2 samples but a divergent effect of PLX3397 (n = 3/group). (**F** and **G**) Volcano plots of control versus R6/2 DEGs (**F**) confirmed an absence of inflammatory transcript upregulation in the R6/2 striatum and (**G**) a loss of microglial gene expression with PLX3397 (FDR ≤ 0.05; n = 3/group). (**H**) Pathway analysis (IPA) of 860 control versus R6/2 DEGs and 1380 control versus R6/2+PLX3397 DEGs (FDR ≤ 0.1; n = 3/group) revealed a distinct interferon signature and suppressed neuronal development and neuritogenesis pathways in the R6/2 striatum that closely resembled the human Huntington's disease caudate, and which were partially resolved following PLX3397. (**I**) Top significant predicted upstream regulators included HTT, IFNγ, l-DOPA, IRF7, and TRIM24, with associated activation z-scores of 2.151 ($P < 8.31 \times 10^{-22}$), 3.727 ($P < 1.01 \times 10^{-15}$), −5.654 ($P < 1.19 \times 10^{-20}$), 4.589 ($P < 7.47 \times 10^{-13}$), and −3.970 ($P < 3.58 \times 10^{-12}$), respectively. (**J**) A heat map of control versus R6/2 DEGs (FDR < 0.1) that were reversed with treatment by unadjusted P-value (P < 0.05) to indicate potential mediators of beneficial PLX3397 effects (n = 3/group). (**K**) IPA predicted IFNγ as the major cytokine upstream regulator in the R6/2 striatum, signalling that, along with IFNα, is no longer enriched in R6/2+PLX3397 striatum. All RPKM values can be searched and visualized at http://rnaseq.mind.uci.edu/green/R62_PLX/gene_search.php.*

(S. W. Lee et al., 2018). Of note, changes in T-cell transcripts (*Tal1, Ccl25)* showed a partial rescue when the R6/2 mice were treated with CSF1Ri, along with decreased accumulation of several pathologic *mHTT* species (**Figure 2J**). Although microglia rarely contain nuclear *mHTT* themselves (Jansen et al., 2017), these findings suggest they may play a role in driving HD progression. To validate the absence of the specific inflammatory signal mentioned before, we used a NanoString inflammatory panel consisting of ~700 preselected genes examining bulk striatal tissue collected from 3 mice per group at the 11-week timepoint (**Figure 2B-D**).

To gain insight on the alterations of the IFN signature we observe in the R6/2 mouse model of HD—alterations which have also been reported in both AD-like neurodegeneration as well as aging human (Mathys et al., 2017), (Galatro et al., 2017)—we next explored the correlations between common pathways in human and mouse HD. To accomplish this, we compared the activation z-score of pathways in human control vs. HD caudate (z-score overall = 41.23; gene expression data from (Hodges et al., 2006) and control vs. R6/2 striatal tissue (**Figure 2H**). Here, we observed similarities between the human disease and mouse model of HD, notably the presence of a dysregulated IFN signature (**Figure 2H**). This gene signature was partially rescued when microglial loss driven by CSF1Ri resolved *IFNα* and *IFNγ,* but not *IFNβ,* in

control vs. R6/2 microglial depleted samples (**Figure 2H**). IFN-involved toll-like receptor signaling (*TLR4, 7, 9*) and downstream IFN effector pathways (*STAT1*) were also downregulated (**Figure 2H**). *HTT*, *IFNγ, L-dopa*, the type I IFN regulator *IRF7* and *TRIM24* were identified as the top enriched pathways (**Figure 2I**). Given these, pathway analysis using Ingenuity Pathway Analysis (IPA) predicted IFNγ, known as a potent microglial activation stimulator (Monteiro et al., 2017), as the primary cytokine regulator of disease DEGs (**Figure 2J**). However, with an upregulation of a microglial activation inhibitor known to block IFN-induced transcription (Goldmann et al., 2015), *USP18* (**Figure 2G,J**), we believe there are some compensatory mechanisms involved as well. Since the pro-inflammatory *NFκβ* pathway was upregulated in the human HD caudate but not R6/2 striatal tissue (**Figure 2H**), and the *IL6* and *IL1B* transcripts were not detected, we believe the R6/2 mouse model may not fully recapitulate the neuroinflammation observed in the end stages of human HD (Yang et al., 2017), (Crotti & Glass, 2015). A comparison of WT vs. R6/2 (FDR<0.1) and R6/2 vs. R6/2 + PLX3397 ($p<0.05$) mice using IPA revealed potential molecular targets of microglial depletion-related rescue of R6/2 mice including *TGF-β1* (**Figure 2G, J**). *TGF-β1* is known to upregulate astrocytic CSPG, a component of the ECM, production stimulating neural stem cell survival via neuritogenesis (Tham et al., 2010).

Chapter 1.2. Microglial dysfunction caused by CSF1R haploinsufficiency drive PNN loss in mouse model of ALSP.

After discovering a novel role for microglia in regulating PNNs in the healthy adult brain and showing that disease states could induce further microglia mediated PNN loss, we next turned to a second model of neurodegeneration: one that stems from loss of function mutations arising from microglia. In the adult brain, CSF1R is expressed primarily by microglia, and genome-wide linkage analyses have identified mutations in CSF1R that lead to Adult-Onset

Leukoencephalopathy with Axonal Spheroids and Pigmented Glia (ALSP), also known as Hereditary Diffuse Leukoencephalopathy with Spheroids (HDLS). This rare autosomal dominant disorder is a neurodegenerative disease characterized by extensive white matter loss. ALSP is one example of how disruption in microglial-specific genes can lead to CNS disorders resulting in neurodegeneration, implicating microglia in brain disease and providing tools for us to investigate and understand how microglia drive disease. Miguel Arreola performed the following experiments and collected the data. I ran the transcriptional analyses.

Here, we employed both genetic and pharmacological approaches to manipulate CSF1R to identify and explore the role of partially disrupted CSF1R signaling on microglial homeostasis and CNS function. For our genetic approach, we used *Csf1r* haploinsufficient ($CSF1R^{+/-}$) mice. These mice exhibit executive dysfunction, psychosis and progressive memory decline mimicking ALSP patients (Sundal & Wszolek, 1993) with reports of cognitive deficits beginning as early as 7 months of age (Chitu et al., 2020), (Chitu et al., 2015). For our pharmacological approach, we used CSF1R inhibition (CSF1Ri), which is highly dynamic and can be administered in a dose-dependent manner; low levels of inhibition can modulate microglial activity/function, while high levels of inhibition can deplete the brain of almost all microglia. 6-month-old WT and CSF1R+/- mice were treated with the CSF1R inhibitor, PLX5622 (150ppm in chow), and sacrificed at eight months old (**Figure 3A**).

In this study, after validating the effects of PLX5622 chow through quantification of CSF1R expression (**Figure 3B**), we observed a significant increase in microglial densities throughout the $CSF1R^{+/-}$ mouse brain (**Figure 3C**). Morphological changes were also observed in $CSF1R^{+/-}$ mice., These include increased complexity of microglial process branching and reduced P2RY12 protein expression (**Figure 3D-F**), a characteristic seen in microglial cells under conditions of non-homeostasis or murine disease (Keren-Shaul et al., 2017), (Krasemann et al., 2017). Additionally, these morphological changes have been reported in affected white

matter brain regions of human patients with *Csf1r* mutations (Kempthorne et al., 2020b). Microglia in CSF1R$^{+/-}$ mice also lacked amoeboid morphology and CD68 immunopositivity (data not shown), indicating a lack of classic activation.

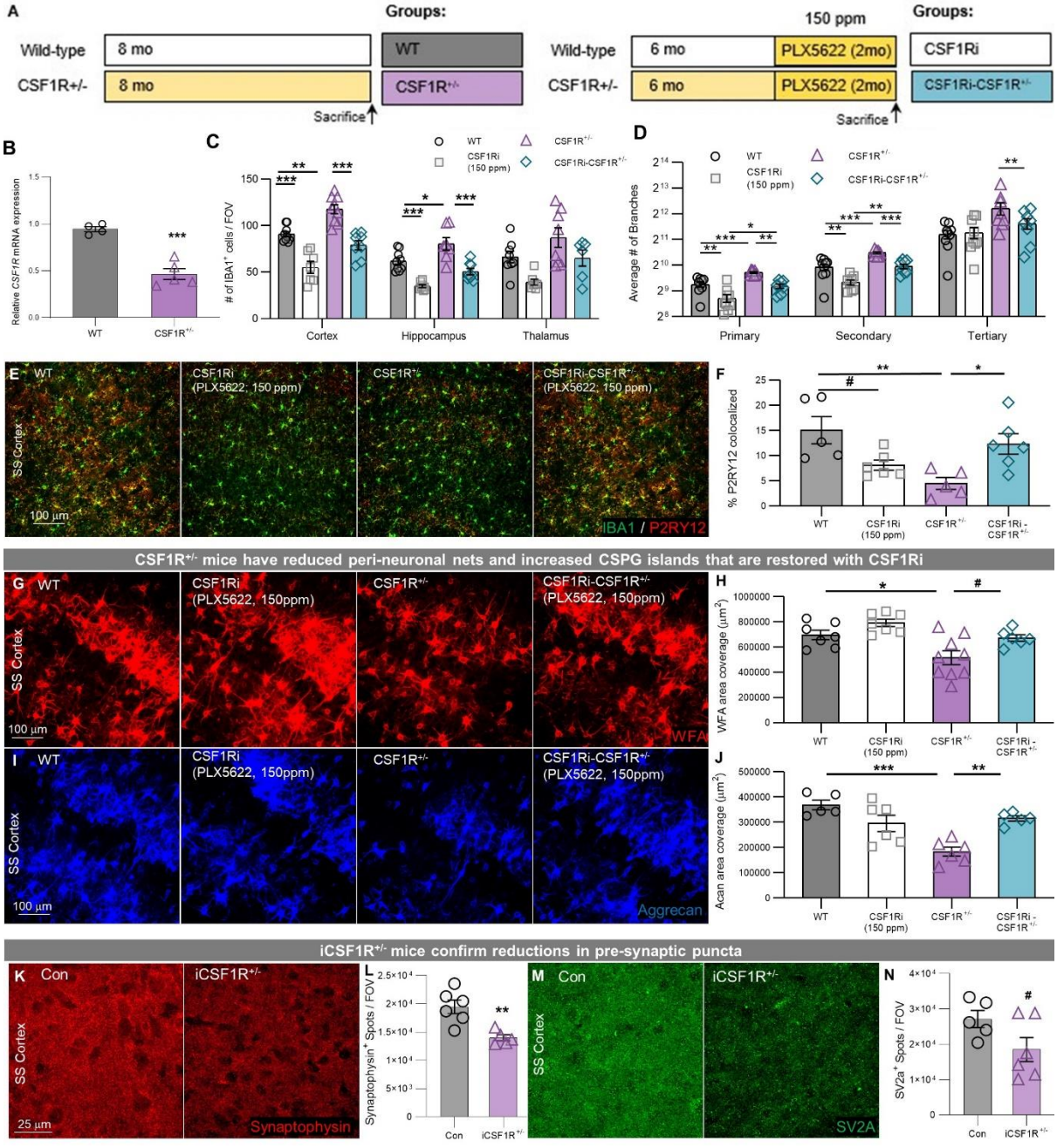

***Figure 3**: (**A**) Experimental design (n=8-10/group) following baseline measurements WT and CSF1R +/- mice were treated with 150 ppm PLX5622 for two months beginning at 6 months of age. Mice were sacrificed at 8 months of age. (**B**) Relative expression levels of CSF1R normalized to GAPDH via qPCR. Expression levels of CSF1R in CSF1R$^{+/-}$ was reduced ~50% compared to WT mice ($p < 0.0001$). Statistical analysis used two-tailed t-test. (**C**)Quantification of IBA1^{+} cells / FOV in Cortex, Hippocampus, and Thalamus. 25-30% increase in IBA1^{+} cells were found in Somatosensory Cortex, Hippocampus, and Thalamus. Treatment with 150 ppm PLX5622 reduced IBA1^{+} cells by 25% in both WT and CSF1R$^{+/-}$ mice. (**D**)Morphological analysis of branch patterns revealed decreased number of primary and secondary branches in CSF1RI microglia compared to*

*WT. CSF1R$^{+/-}$ microglia had increased numbers of primary, secondary, and tertiary branching which were reduced to WT levels by CSF1Ri. (**E, F**) Representative 20x image of the Somatosensory cortex reveals a marked decrease in microglial P2RY12 immunopositivity in CSF1Ri and CSF1R$^{+/-}$ mice. CSF1Ri of CSF1R$^{+/-}$ mice revealed an increased expression of P2RY12 expression. Statistical analysis used a two-way ANOVA with Sidak multiple comparisons correction. Significance * p< 0.05; ** p < 0.01, *** p < 0.001, # 0.05 < p < 0.1. (**G**) Representative 20x images of Somatosensory Cortex from WT, CSF1Ri, CSF1R$^{+/-}$, and CSF1Ri-CSF1R$^{+/-}$ mice immunostained for WFA. (**H**) Quantification of WFA area coverage revealed significant decrease in WFA coverage in CSF1R$^{+/-}$ Somatosensory cortex and a trending recovery in the CSF1Ri-CSF1R$^{+/-}$ group. (**I**) Representative 20x confocal images of aggrecan immunostaining, another component ECM perineuronal nets quantification of which (**J**) revealed similar significant decreases in are coverage in CSF1R$^{+/-}$ group and significant recovery in CSF1Ri-CSF1R$^{+/-}$ group. Representative 20x image of somatosensory cortex revealed significant decrease in Synaptophysin (**K,L**), SV2A (**M,N**) in myeloid-specific CSF1R knockout mice.* ***This data was collected and analysed by Miguel Arreola.***

As discussed previously, non-classically activated microglia in HD are associated with loss of PNNs in the ECM; thus, we wanted to examine if such changes occur in CSF1R$^{+/-}$ mice. We found significant reductions in cortical PNNs, as seen by WFA (**Figure 3G,H**) and Aggrecan (**Figure 6I,J**) staining in CSF1R$^{+/-}$ mice compared to their WT counterparts, suggesting a similarity in microglial phenotype across diseases with similar downstream effects on the ECM compartment (directly or indirectly effected by microglia) and the synapse. Although not explored in detail here, it is important to note that cognitive deficits in CSF1R$^{+/-}$ mice (i.e., lifelong loss of CSF1R) can be rescued with low dose CSF1Ri (PLX5622 – 150 ppm; data not shown), suggesting microglial involvement. Surprisingly, low dose CSF1R signaling inhibition also led to the recovery and normalization of microglial phenotypes (densities, morphologies, P2RY12 expression; **Figure 3D-F**), PNNs (**Figure 3G-J**) and presynaptic puncta (**Figure 3K-N**).

To explore microglial homeostasis at the transcriptional level, I performed RNA-seq data analysis on micro-dissected cortices of each mouse group: wildtype (WT), CSF1Ri, CSF1R$^{+/-}$, and CSF1Ri-CSF1R$^{+/-}$. For quantification, I generated Fragments Per Kilobase of transcript per Million mapped reads (FPKM) for each gene. I then used an FDR value of 0.05 to filter and compare the data. Differentially expressed genes (DEGs) were then identified between the various groups to help identify the molecular underpinnings of a given treatment or genotype. Comparing DEGs between the WT and CSF1Ri mice (**Figure 4B**) and WT and CSF1R$^{+/-}$ mice (**Figure 4C**), we observed a 34% (412 genes) overlap (**Figure 4A**). We also

observed a downregulation in expression levels of myeloid-expressed genes in WT vs. CSF1Ri (**Figure 4B**) and CSF1R$^{+/-}$ (**Figure 4C**) mice vs. CSF1Ri-CSF1R$^{+/-}$ (**Figure 4D**) mice, consistent with the ~20% microglial depletion seen with CSF1Ri. In line with immunohistochemical analysis, RNA-seq revealed that classic activation markers for microglia were not enriched in CSF1R$^{+/-}$, supported by a lack of changes in inflammatory gene transcripts (e.g., *Cst7*, *Axl, Clec4a1*, *Tnf, Ifitm3* or *Ldl* were previously reported in damage-associated microglia (DAM)) (Keren-Shaul et al., 2017) (data not shown).

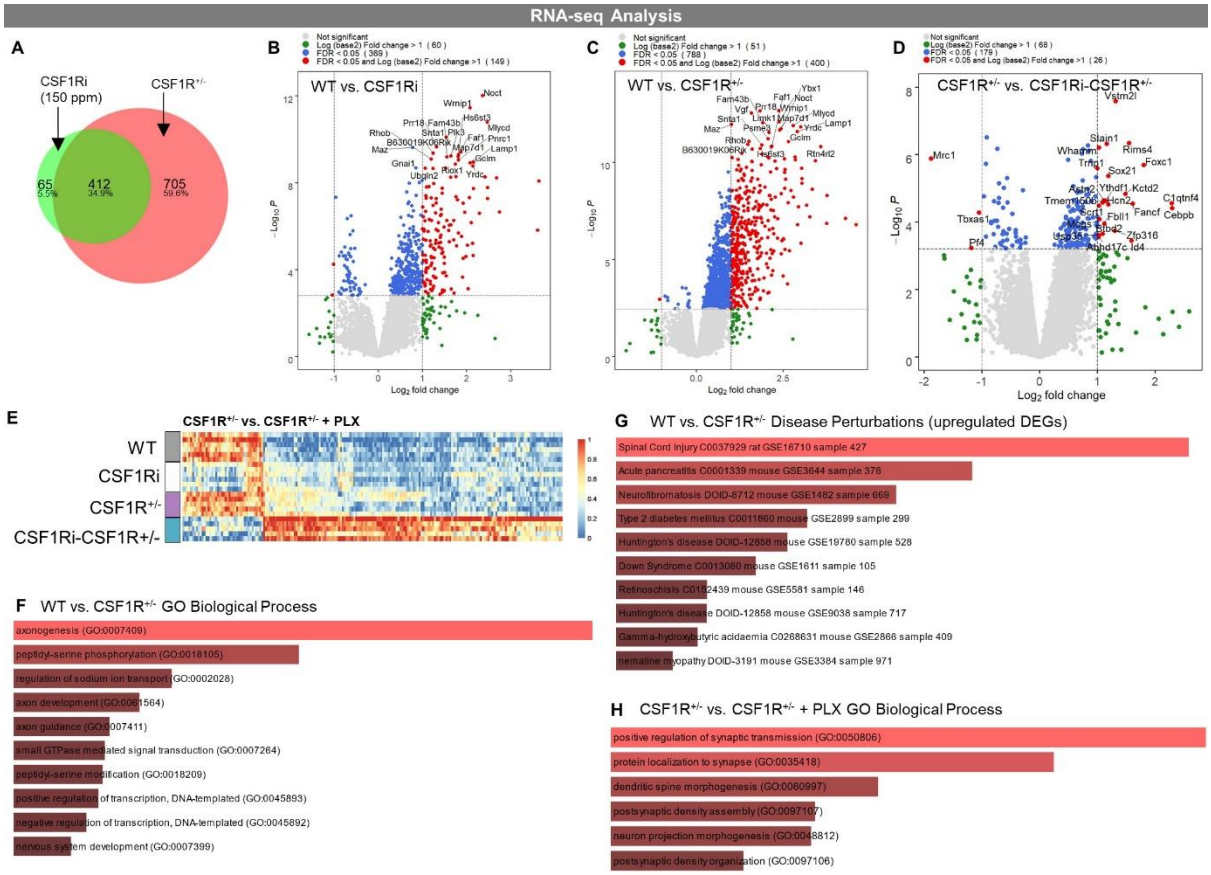

***Figure 4**: (**A**) Venn diagram displaying the number of differentially expressed genes (DEGs, numbers provided) generated in transcriptional comparisons between CSF1Ri mice and CSF1R$^{+/-}$ mice in comparison with WT mice. (**B-D**) Volcano plots displaying the fold change of genes (log2 scale) and their p-values (-log10 scale) between WT vs CSF1Ri mice (**B**), WT vs CSF1R$^{+/-}$ mice (**C**) and CSF1R$^{+/-}$ vs CSF1Ri-CSF1R$^{+/-}$ (**D**). (**E**) Heatmap of DEGs between CSF1R$^{+/-}$ and CSF1Ri-CSF1R$^{+/-}$ mice. (**F**) GO terms for biological processes and (**G**) GO Terms for Disease Pathways for genes differentially expressed in WT vs CSF1R$^{+/-}$ mice.(**H**) Top biological processes gene ontology (GO) term enrichment for upregulated genes from the heatmap (**E**).*

WT vs. CSF1R$^{+/-}$ comparison revealed top DEGs including the circadian rhythm-associated gene *NOCT*, as well as *LAMP1*, *FAM43b*, *Prr18*, and *Wrnip1* (**Figure 4C**). Gene

ontology (GO) analysis of DEGs of WT vs. CSF1R$^{+/-}$ mice shows enrichment in the following Biological Processes: *axonogenesis*, *axon development*, *axon guidance*, and *nervous system development*, and Disease Perturbations: *Spinal Cord Injury*, *Down Syndrome*, and *Huntington's disease* (**Figure 4F-G**). These enrichments indicate that loss of functional CSF1R signaling is associated with alterations in axon-associated processes and neurological disorders. Furthermore, RNA-seq data analysis highlighted dramatic increases in neuronal- and synaptic-associated genes (*Syn2, Begain, Rims3)* with CSF1Ri in CSF1R$^{+/-}$ cortices (**Figure 4D**). CSF1Ri-treated CSF1R$^{+/-}$ mice compared to CSF1R$^{+/-}$ mice exhibited a significant upregulation of DEGs associated with synaptic function and morphology, such as *regulation of synaptic transmission*, *dendritic spine morphogenesis*, *postsynaptic density assembly*, and *neuron projection morphogenesis* (**Figure 4H**). In line with this, we performed immunohistochemical analysis on synaptic components to validate the findings of the RNA-seq analysis and observed a downregulation of presynaptic markers (Synaptophysin, Sv2a) with disease (**Figure 6A-D**). These findings implicate that CSF1R or microglia have a role in modulating synaptic elements (Terry et al., 1991), which could be the cause of cognitive decline in CSF1R$^{+/-}$ mice.

To better interpret and explore the relationships behind gene expression changes, we next performed weighted gene co-expression network analysis (WGCNA) (Zhang & Horvath, 2005), (Langfelder & Horvath, 2008) and identified 16 independent modules (**Figure 5A)**. These modules divided genes into groups depending on their correlation to either genotype (i.e. CSF1R$^{+/-}$), as seen in the *brown* module (**Figure 5B, E**), or treatment (i.e. CSF1Ri), as seen in the *dark grey* module (**Figure 5C, F**), or in some cases, their differential expression between both genotype changes and treatment effects, as seen in the *midnight blue* module (note:

correlation scores >0.5; shown as red dotted lines)

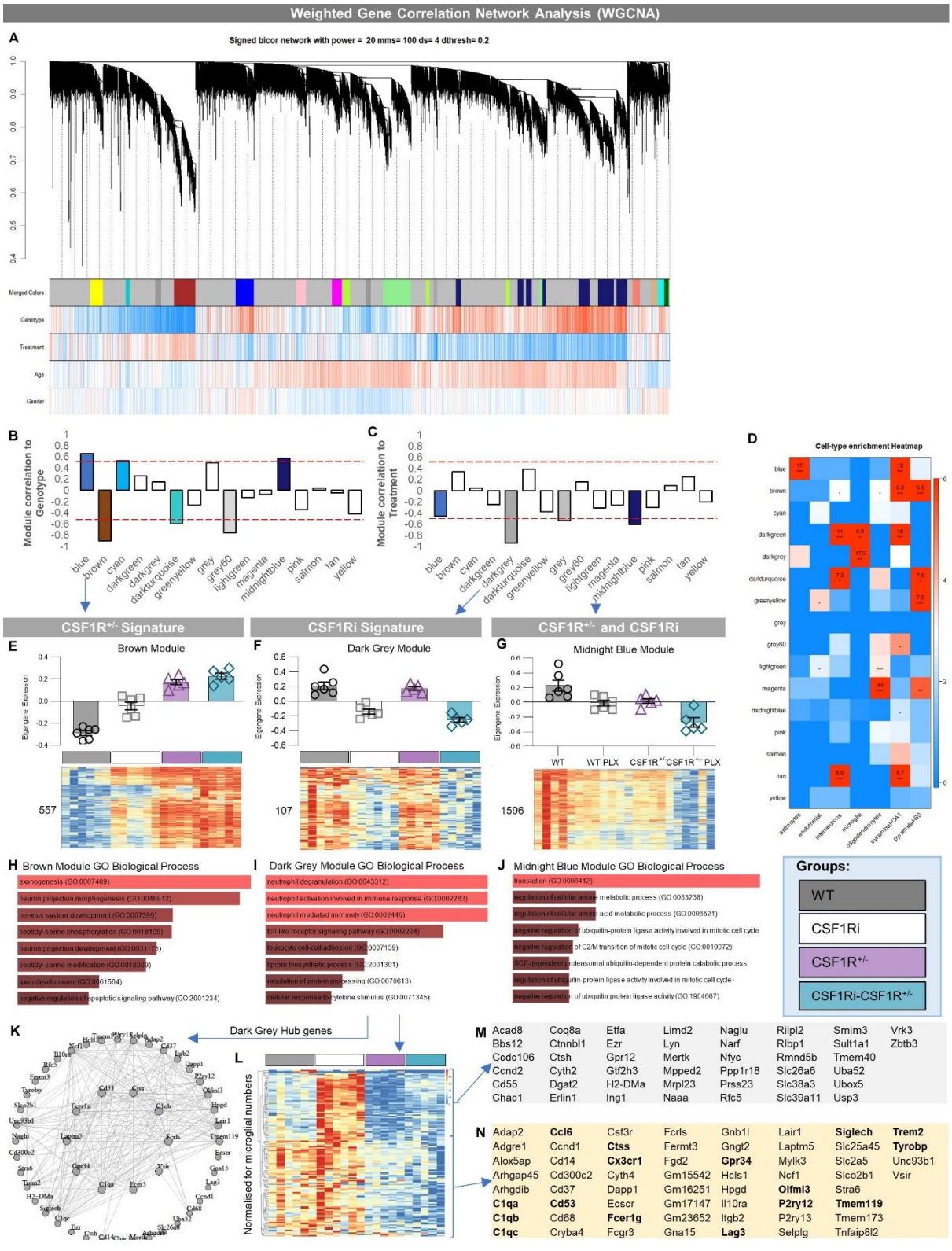

***Figure 5**: (**A**) Signed bicor network shows the effects of genotype, treatment, age and gender which are separated into distinct colored modules. (**B**) Correlation of modules generated by weighted gene correlation network analysis (WGCNA) to the genotype (Z-score cut-off: +/-0.5). (**C**) Correlation of modules generated by WGCNA to the treatment (Z-score cut-off: +/-0.5) (**D**) Cell-type enrichment heatmap displays genes associated with specific cell types within a given color module. Values provided indicate the number of genes within the net work*

*associated with that a specific cell type. *** = 6+ genes. ** = 3+ genes. (**E,H**) CSF1R$^{+/-}$ signature: Module eigengene trajectory and heatmap of gene expression value in brown (**E**), as well as gene ontology (GO) term enrichment for brown (**H**). (**F,I**) CSF1Ri signature: Module eigengene trajectory and heatmap of gene expression value in dark grey (**F**), as well as gene ontology (GO) term enrichment for dark grey (**I**). (**G,J**) CSF1Ri signature: Module eigengene trajectory and heatmap of gene expression value in midnight blue (**G**), as well as gene ontology (GO) term enrichment for midnight blue (**J**). (**K**) Interactive plot between hub genes extracted from the dark grey module showing a distinct CSF1Ri signature. (**L**) Heatmap of genes found in the dark grey module normalized to the average microglial numbers found within a group. (**M**) List of genes displaying increased expression mice that are upregulated CSF1Ri-CSF1R$^{+/-}$ compared to CSF1R$^{+/-}$ mice. (**N**) List of downregulated genes between WT and CSF1R$^{+/-}$ mice normalized for number of microglia.*

(**Figure 5C, G**). Calculating and plotting the eigengene values as well as performing GO analysis of the modules revealed the following, respectively: the *brown* module (associated with the CSF1R$^{+/-}$ genotype) was enriched with genes that are expressed in pyramidal neurons (**Figure 5D**) and associated with *axonogenesis*, *neuron projection morphogenesis*, and *nervous system development* pathways (**Figure 5H**); the *midnight blue* module (associated with both CSF1R$^{+/-}$ genotype and CSF1Ri treatment) was not associated with any specific cell type (**Figure 5D**), however, it was strongly enriched for genes associated with *translation* pathways (**Figure 5J**). The *dark grey* module (associated with CSF1Ri treatment) contained microglial-associated genes (**Figure 5D**) including *C1qa*, *C1qb*, *Cd53*, *Ctss*, *Gpr34*, *P2ry12*, *Tmem119*, and *Siglech* as well as other immune genes (**Figure 5I,K-N**). Upon normalizing the gene expression levels to microglial densities of corresponding mice, we saw a downregulation of microglial genes, which could account for the non-homeostasis in CSF1R$^{+/-}$ mice (**Figure 5L-N**). These findings along with our immunohistochemical data suggest that the phenotypic state of microglia observed in CSF1R$^{+/-}$ mice is due to a loss of microglial homeostatic signature, rather than a reactive or activated signature.

Given the loss of PNNs in CSF1R+/- mice, we sought to identify microglial expressed genes that could account for the loss of PNNs in CSF1R+/- mice. Loss of PNNs by microglia is likely mediated either by the release of enzymes that degrade PNN components, direct phagocytosis, or both. I identified genes implicated in potential degradation or phagocytic machinery that were upregulated in CSF1R+/- mice including *MMP14*, *Ctss*, *C1qa*, *C1qb*, *C1qc*, *Trem2*,

MerTK, MEGF10, APOE, TM2D3, LRRK2, CD200, CCRL2, LRP1, CD68, CD14, mTOR, TLR4.

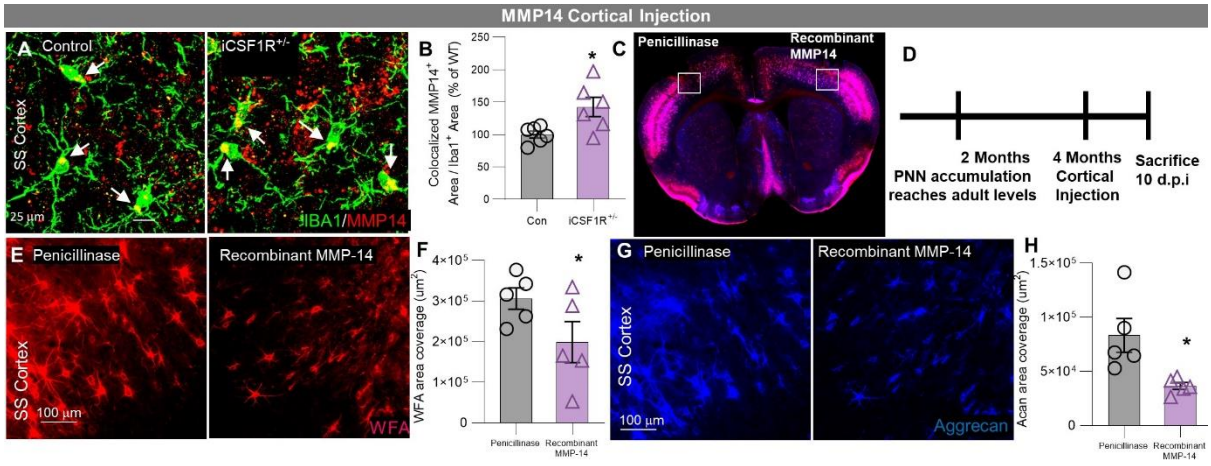

Figure 6**: (**A**) Representative 63x immunofluorescent images of MMP-14^{+} and IBA1^{+} in Control and iCSF1R$^{+/-}$ somatosensory cortex. (**B**) Quantification of colocalized area displayed increased area of colocalized MMP-14 in iCSF1R$^{+/-}$ microglia. (**C,D**) WT mice were aged to 4 months at which point they received injection of recombinant MMP-14 and Penicillinase in contralateral cortices. 10 days post injection (d.p.i.) mice were sacrificed and brains were harvested. (**E**) Representative 20x confocal immunofluorescent staining of WFA or (**G**) Aggrecan in the respective injection area. (**F**) Quantification of WFA^{+} area and (**H**) Aggrecan^{+} area revealed significant decreases in MMP-14 injection site compared to Penicillinase injection site. Statistical analysis used a two-way ANOVA with Sidak multiple comparisons correction or Two-Tailed T-Test. Statistical analysis used a two-tailed paired T-Test for MMP-14 injection comparisons. Significance * $p < 0.05$; ** $p < 0.01$; *** $p < 0.001$. **This data was collected and analysed by Miguel Arreola.

We focused on *MMP-14*, a key enzyme involved in the degradation of ECM components that has recently been implicated in microglial-mediated ECM changes (Langfelder & Horvath, 2008). An immunofluorescent analysis in CSF1R$^{+/-}$ mice presented elevated *MMP-14* expression (**Figure 6A,B**). Thus, we then sought to investigate *MMP-14* involvement further. To accomplish this, recombinant *MMP-14* was injected into one cortical hemisphere of 4-month-old (mo) WT mice and sacrificed 10 days post injection (**Figure 6C,D)**. Penicillinase was injected to serve as a control. Of note, we found that injection of recombinant *MMP-14* was sufficient to induce PNN degradation as seen by a significant decrease in immunofluorescent staining of two key components of PNNs: WFA (**Figure 6E,F**) and Aggrecan (**Figure 6G,H**). We postulate that increased *MMP-14* levels could initiate a cascade of aberrant MMP activity by cleaving inactive forms of other MMPs and thus perpetuate ECM breakdown by microglia in the CNS of CSF1R$^{+/-}$ mice.

Conclusions

Our results clearly demonstrate that 1) microglia regulate PNN levels under homeostatic conditions, and 2) microglia facilitate PNN loss across multiple disease states, suggesting that microglial-mediated PNN loss and ECM remodeling could be a universal feature of neurodegenerative diseases, and an important facet of the pathogenesis. In the healthy brain PNNs are important for a number of processes in the CNS, including regulation of GABAergic cell function, protection of neurons from oxidative stress, and closure of developmental critical period plasticity windows (Wen et al., 2018). Microglia have been implicated in learning and memory in the adult brain. Thus, the regulation of PNNs by microglia provides an important mechanism that can drive disease progression in neurodegenerative and neurodevelopmental disorders, both of which can be linked to downstream cognitive and behavioral deficits. My work has highlighted that a non-classical activation state of microglia appears to be responsible for PNN loss in disease, and are associated with a lack of microglial homeostasis rather than a pro-inflammatory phenotype. Furthermore, I identified microglial *MMP14* as a potential PNN degrading candidate, which was confirmed via direct infusion of the enzyme into the adult mouse brain. However, it is likely that microglia possess multiple mechanisms to regulate PNNs in the healthy adult brain (where *MMP14* is not expressed), along with other degrading and phagocytic proteins/enzymes that could contribute to PNN loss in different disease states. The remainder of my thesis will utilize diverse genetic backgrounds combined with AD pathology to identify if this conserved pathology we see across different neurodegenerative disorders can be replicated and find the putative mechanisms involved if so.

CHAPTER 2. Utilizing genetic diversity to discern its effect on healthy and diseased brains in the 5xFAD Mouse Model of Amyloidosis

Background

Alzheimer's disease (AD) is one of the most common causes of dementia, affecting more than 6.5 million Americans and 32 million globally ("2022 Alzheimer's disease facts and figures," 2022), (Gustavsson et al., 2023). AD is characterized by neuropathological lesions, which consist of amyloid-beta (Aβ) plaques followed by tau neurofibrillary tangles (Selkoe, 1991). Other changes associated with this neurodegenerative disorder include cerebral atrophy, neuroinflammation, neuronal cell loss, and cognitive dysfunction (Hardy & Higgins, 1992). Although age is the biggest risk factor for developing AD, previous studies have alluded that an individual's genetic makeup can play a large role in AD susceptibility (Neuner et al., 2019). Heritability of AD is estimated to be around 50-80% and does not differ by sex as confirmed by a population-based twin study of dementia (Gatz et al., 2006). Age of onset separates the two primary types of AD and various genetic risk variants have been identified for each. Rare mutations or pathological variants in amyloid precursor protein (APP), presenilin 1 (PSEN1) and presenilin 2 (PSEN2) have been identified as the cause of autosomal dominant or, familial AD (Lanoiselée et al., 2017) that only comprise of 1-6% of all dementia causing AD cases in comparison to the more common sporadic/late-onset AD (LOAD) (Drummond & Wisniewski, 2017). Moreover, common variants in these genes unfortunately do not have a strong impact on susceptibility for LOAD (Gerrish et al., 2012). There is a complex causative genetic architecture in play for LOAD and early genome-wide association studies (GWAS) have identified several single nucleotide polymorphisms that alter the risk of developing sporadic AD; including protein apolipoprotein E (APOE), a well-established genetic risk variant for LOAD, estimated to have ~6% of total phenotypic variance (Ridge et al., 2013)). The modern

era of GWAS has helped in identifying novel significant associations of 40 single-nucleotide polymorphisms (SNPs) mapped to 21 risk genes including *ABCA7*, *ADAM10*, bridging integrator 1 (*BIN1*), *CD33*, clusterin (*CLU*), complement receptor 1 (*CRI*), *CTSB*, *CTSD*, ephrin type-A receptor 1 (*EPHA1*), *GAB2*, *HLA-A*, *INPP5D*, *ITGAX*, *MAPT*, membrane-spanning 4-domains, subfamily A (*MS4A*), *LILRB2*, *LIPC*, *TREM2*, and phosphatidylinositol binding clathrin assembly protein (*PICALM*) loci (Misra et al., 2018), (Marioni et al., 2018), (Nazarian et al., 2019), (Jansen et al., 2019), (Kunkle et al., 2019), http://dx.doi.org/10.1007/s13273-021-00130-z) which individually are believed to have smaller effect sizes. Like other common genetic diseases and disorders, AD is now believed to be polygenic in nature and Polygenic Risk Scores (PRS) for AD offer unique possibilities for reliable identification of individuals at high and low risk of AD (Escott-Price et al., 2015), (Chouraki et al., 2016), (Desikan et al., 2017), (Escott-Price et al., 2017). PRS can reduce large numbers of potentially contributing SNPs to one variable assessing disease risk prior to onset and it's hoped that eventually these would indicate shared etiology between SNPs leading to AD (Baker & Escott-Price, 2020), (Clark et al., 2022). Variation in an individual's genome can introduce minor fluctuations in any-or-all individual level risk scores which may influence the stability or confidence of population studies estimates (Chen et al., 2020). Considering humans are genetically diverse, understanding the role of diversity in disease onset and progression could play a critical role in understanding disease process. Notably, individuals with different genetic dispositions could have different impact on certain pathways of potential therapeutic interventions. To complement human studies, genetic diversity should be an important consideration in optimizing the development of mouse models for AD. Heritability of the disease is believed to be dependent on inherited DNA variants which were identified by a two-stage meta-analysis of genome-wide association studies (GWAS) eleven new Alzheimer's associated susceptible loci, including HLA-DRB5–DRB1, INPP5D, and MEF2C that have

been implicated in immune response and inflammation pathways (Lambert et al., 2013). Standardized animal models of diseases used in the past by researchers to study the biological impacts of pathology in the brains of plaque and tangle laden brains are now being used to evaluate the impact introduction of GWAS identified risk variants has on aged brains during disease progression. However, current transgenic AD mouse models have largely ignored this component, with most preclinical models deriving from a single or few genetic backgrounds, leading to a lack of allelic heterogeneity and hybrid vigor. One of the most common genetic backgrounds that AD models have been backcrossed to is the C57BL6/J background (Onos et al., 2016). C57BL6/J is a Jackson (JAX) laboratory-generated inbred lab strain that has been the most widely used since the early 1950s due to its high reproducibility. Additionally, C57BL6/J is also the most cited and well-characterized laboratory strain used in biomedical research and hence was selected by the Mouse Genome Sequencing Consortium (MGSC) as the reference mouse genome in 1999 (Waterston et al., 2002). The potential of incorporating genetic variation in AD mouse models is immense since the influence genetic diversity has on disease is unknown and researchers have started taking advantage of the level of naturally occurring genetic variation in the form of genetically distinct wild-derived strains specifically to quantify plaque-associated myeloid responses, elevating the demand and underscoring the importance of genetically diverse models (Onos et al., 2019). With raised standards for genetic mapping of complex traits along with expectations for high mapping resolution for genetic variant identification, various new mouse model are being developed (Churchill et al., 2012). The first transgenic mouse reference panel was developed in hopes of determining the genes resulting in resilience to AD termed the AD-BXDs where the resulting fully isogenic F1 hybrids were used to monitor the phenotypic outcomes as a result of orthologous human high-risk FAD mutations with different genomes. This study showed a significant overlap between the AD-BXD reference panel and the human AD at phenotypic, genomic, and transcriptional

levels as observed by the conserved variations between the mice and human patients, the influence of allelic distribution across a set of 21 sporadic LOAD associated loci on cognitive function as well as the upregulated inflammatory pathways and downregulated neuronal signatures respectively (Neuner et al., 2019). Given the impact that the introduction of genetic diversity in the form of these bi-parental crossed BXD mice (Peirce et al., 2004), (Taylor et al., 1999) has on the translatability of human AD in mice, we hypothesized that more complex multi-parent families such as the CC mice would mimic a human population better in terms of heterogeneity and would hence lead to an improved translational model of human AD. Furthermore, to control for the environmental heterogeneity, population structure, and rare alleles while keeping the sample size and power during studies, heterozygous stocks like the Diversity Outbred (DO) mice were designed using a Recombinant Inbred (RI) panels which has the same eight founder strains known as the Collaborative Cross (CC) inbred strains (Svenson et al., 2012), (Churchill et al., 2012). These RI panels (i.e, BXDs and CCs) as well as the resulting heterozygous stocks (i.e, DO) mice have since been utilized to study various disease processes in the context of genetically diverse strains. Hence to test this hypothesis and to better understand and recapitulate the contribution of genetic diversity to human AD while utilizing mouse disease models, we crossed the well-established 5xFAD transgenic AD mouse model with five different CC lines. These CC mouse lines are the products of an eight-way funnel breeding design involving the JAX mouse founder strains: A/J, C57BL/6J, 129S1/SvImJ, NOD/ShiLtJ, NZO/HiLtJ, CAST/EiJ, PWK/PhJ, and WSB/EiJ (Threadgill et al., 2011). In this breeding scheme, each founder strain equally contributes to the autosomal genomes of these CC lines resulting in independent recombination accumulated during breeding. This F1 hybrid panel is a novel resource raised in controlled environments with different allelic contributions across the genome except all the F1 progenies carry an identical high-risk FAD mutation in the human APP and PSEN1 transgenes. To accomplish this, we

developed a mouse reference genome panel that combines two resources: (1) the 5xFAD transgenic line on an otherwise fully inbred C57BL/6J (B6) genetic background (Oakley et al., 2006) and (2) the collaborative cross (CC) genetic reference panel (Threadgill et al., 2011). This panel allowed us to explore the ability of these models to recapitulate genetic diversity and the human AD signature, as well as identify genetic modules that contribute to AD susceptibility and/or resilience as the CC panel segregates for around 52 million sequence variants including high-risk AD genes. Here, we wanted to test the validity of these AD-CCs as a systemic resource for testing AD susceptibility and the genetic variants responsible for it. This study provides an in-depth transcriptional, immunohistochemical, and biochemical analysis of the effect of genetic diversity on AD pathogenesis. We found that inclusion of diversity resulted in changes in the development of plaque pathology. Accompanying this we observed, altered glial and reactive astrocytic response along with differences in gene expression across the different CC lines. Notably, the highest tissue damage in response to plaques was seen in C57BL6/J as confirmed by brain and plasma neurofilament light chain (N*f*L) levels.

Alzheimer's disease brain

Neuroinflammation along with amyloid-β plaque and tau neurofibrillary tangle deposition are well-known hallmarks of AD pathology. Presence of reactive astrocytes and activated microglia surrounding amyloid plaques have been used as identifying characteristics of inflammation, indicating that inflammation and microglia, the primary immune cells of the brain, may play an important role in disease progression (Mandrekar-Colucci & Landreth, 2010). Several studies have implicated microglia in AD; however, the mechanism by which this occurs remains largely unknown (Jawhar et al., 2012), (Buskila et al., 2013). Our lab recently identified a novel role in the homeostatic and HD brain, in which microglia modulate PNNs, ECM structures that help stabilize synapses (Crapser, Spangenberg, et al., 2020). Since

synaptic loss is observed in AD, we were interested in investigating whether PNN loss is present in mouse models of AD and human AD post-mortem tissue, and whether loss of microglia results in any PNN changes.

To explore the role of microglia in modulating PNNs, we utilized CSF1Ri to deplete microglia in the 5xFAD mouse model. As previously shown, PNN loss was apparent in vehicle-treated 5xFAD mice compared to vehicle-treated WT at 4 mo. However, CSF1Ri-treated 5xFAD mice exhibited dramatically reduced PNNs compared to vehicle-treated 5xFAD mice, while PNN levels in CSF1Ri-treated 5xFAD were comparable to vehicle-treated WT levels (data not shown).

Immunolabelling of postmortem cortical tissue from clinically and neuropathologically diagnosed AD and non-demented control human brains was performed for ACAN+ PNNs (aggrecan 7D4), dense-core plaques (Thio-S), and microglia (IBA1+). Aggrecan was chosen rather than WFA because prolonged postmortem delay (PMD) of tissue collection/fixation after death (which can occur in human specimens) can lead to decreased reactivity of WFA lectin but not for aggrecan (Morawski et al., 2012), (Virgintino et al., 2009). Data in the AD postmortem brains corroborated our previous murine 5xFAD findings showing a similar brain-region dependent relationship between PNNs and plaques (data not shown). Aggrecan was present inside the plaque core and around the microglia, and a close spatial association was observed in the nearby intact PNNs (data not shown).

Genome-wide association studies have provided strong indications of microglial involvement in AD. Several variants that increase AD risk have been identified, and several of these variants are microglial-associated genes: Trem2, CR1, HLA–DRB1, CD33, MS4A6A, and BIN1 (Kim, 2018). is the transmembrane protein CR1(CD35), was found to be over-expressed in cerebrospinal fluids of AD patients (Daborg et al., 2012) and implicated in regulating the complement cascade activation through binding with the complement factors C3b and C4b

(Brouwers et al., 2012). Activated microglia show an increased CR1 expression and evidence of its detrimental effects on neurons has been provided (Crehan et al., 2013). Complement factor C3 can induce pathogenic phagocytosis by interacting with Mac-1, a microglial receptor overexpressed in AD individuals (Strohmeyer et al., 2002). CD33, a risk factor gene for AD is over-expressed in microglia and positively correlated with plaque burden in diseased brains, which once inactivated can mitigate Aβ pathology (Griciuc et al., 2013), (Jiang et al., 2014), (Butler et al., 2021). Membrane spanning four-domain subfamily A members 4A and 6A (MS4A4A, MS4A6A) have recently been associated with altered sTrem2 (proteolytically cleaved TREM2) levels in patient CSF and an increased plaque score in AD patients (Karch et al., 2012), (Proitsi et al., 2014), (Allen et al., 2012), (Ramirez et al., 2016). BIN1 remains one of the earliest genes to be linked to AD across multiple backgrounds in both genome-wide associated studies (Harold et al., 2009), (Seshadri et al., 2010) and epigenome-wide association studies (Chibnik et al., 2015), (Yu et al., 2015), (De Jager et al., 2014). Although the underlying mechanisms behind BIN1's contribution to AD remains unknown, BIN1 is correlated to amyloid plaque and neurofibrillary tangle pathologies and involved in the regulation of neuronal activity (Voskobiynyk et al., 2020), (Beecham et al., 2014).

Microglia have been linked to neuronal loss in AD where the studies have showed a deficit in the classical complement system C1q (Perry & O'Connor, 2008) and C3 (Ricklin et al., 2010), which can be associated to synaptic refinement and plasticity. C3-dependent microglial phagocytosis (Schafer et al., 2012)] for synapse pruning through complement localization happens during development (Stevens et al., 2007), normal ageing (Stephan et al., 2013) and neurodegeneration (Howell et al., 2011), (Rosen & Stevens, 2010) The normative immune pathway involves the upregulation of microglial-localized C1q to act as a recognition molecule and trigger activation of downstream C3, which is associated with neuropathological alterations and demyelination in AD patients (Michailidou et al., 2015).

Data

Immunohistochemical and biochemical characterization of the collaborative cross (CC) lines of the 5xFAD mouse model.

To study and improve translation validity of AD mouse models, we decided to explore the role of genetic diversity as a variable for influencing disease-associated outcomes in 5xFAD mice, a model that recapitulates the human disease in terms of $A\beta_{42}$ accumulation, cognitive decline, and neuronal deficits (Illouz et al., 2017), (Oakley et al., 2006), (Youmans et al., 2012). This was accomplished by using the F1 progeny of six different transgenic lines to cross: (1) fully inbred C57BL6/JJ (B6) background (WT and 5xFAD transgenes) with (2) a Collaborative cross (CC) genetic panel, which combines the genomes of eight genetically diverse founder strains: A/J, C57BL6/JJ, 129S1/SvImJ, NOD/LtJ, NZO/HlLtJ, CAST/EiJ, PWK/PhJ, and WSB/EiJ (**Figure 7A,B**). Breeding was facilitated by the Transgenic Mouse Facility at UCI, in combination with MODEL-AD. Compared to AXB/BXA and BXD (the most commonly used inbred mouse panels), that accounts for only 13% of variance, the CC panel is known to capture ~ 90% of the known variation present in laboratory mice. Moreover, the CC panel uses over 1,000,000 potential 'outbred,' but completely reproducible, genomes to create a series of 1,000 "engineered" inbred (RI) mice strains utilizing the generation of recombinant inbred intercrosses (RIX) (Chesler et al., 2008). In this study, UNC/Jax generated more than 70 new recombinant inbred mouse lines using a funnel breeding scheme. This genetic variation provides significant power in assigning causality to genetic variation seen in human populations, which we postulated to help us better understand the intricacies of the biological networks underlying human AD.

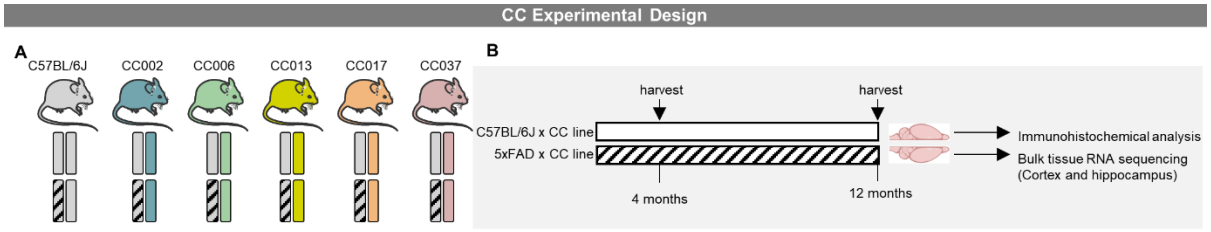

***Figure 7**: (**A**) Allelic representation of the mice generated using a breeding scheme where the C57BL6/J female mice heterozygous for the dominant 5xFAD transgene were bred to males from five different Collaborative cross strains (CC002, CC006, CC013, CC017, CC037) to generate genetically diverse F1 offspring with homozygous C57BL6/J as controls. (**B**) Experimental paradigm where the mice were sacrificed at the 4-month and 12-month time points, and the tissue harvested was used for both immunohistochemical analysis and bulk RNA sequencing*

for Cortex and Hippocampus and just Hippocampus, respectively.

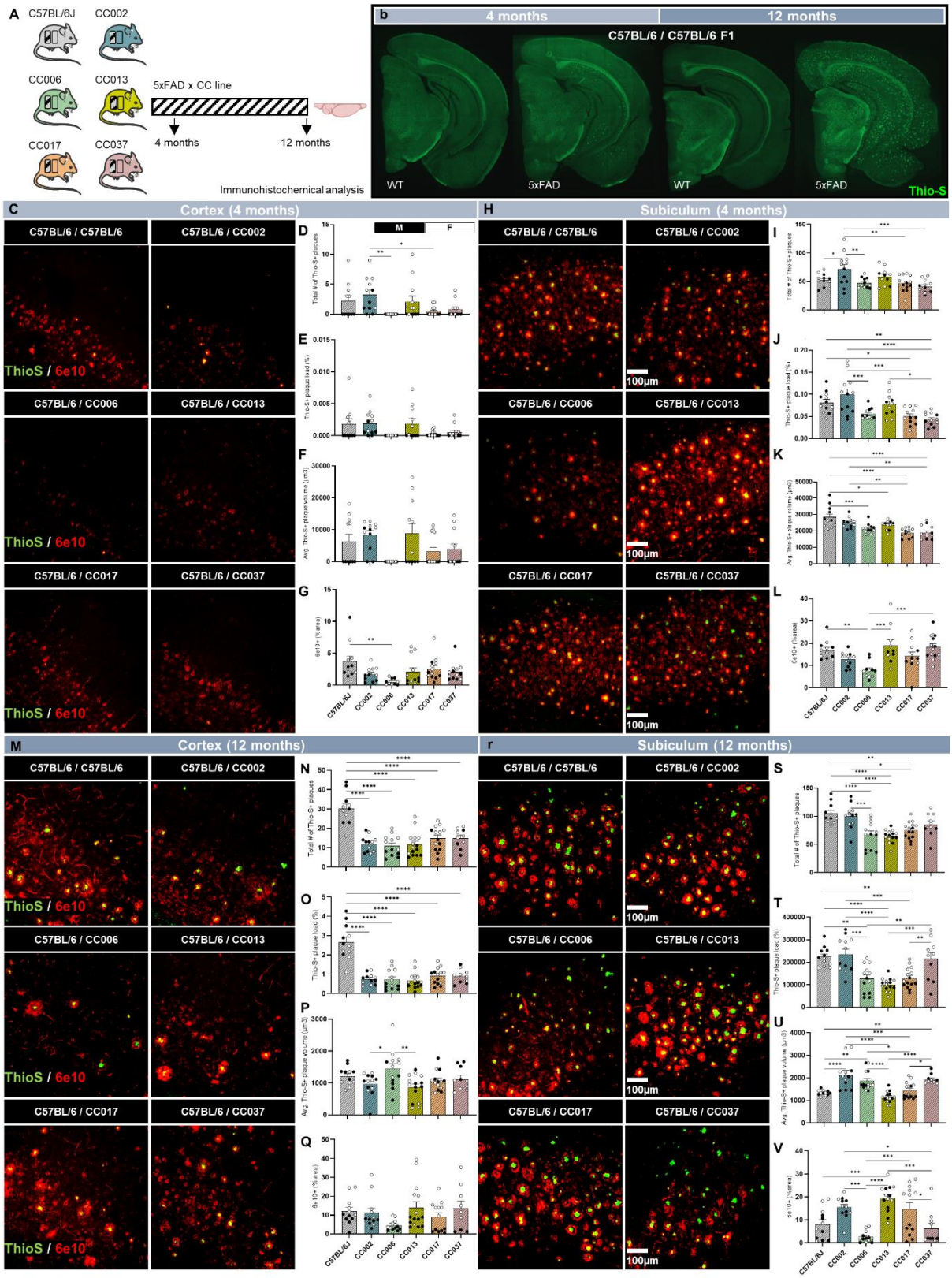

Figure 8**: (**A-B**) Schematic representation of Immunohistochemical analysis performed on F1 progeny of collaborative cross lines (CC002, CC006, CC013, CC017, CC037) with the 5xFAD transgene dominant C57BL6/J allele. The mice were sacrificed at the 4-month and 12-month timepoints, and half of the brains harvested were used for the staining. b. Representative whole brain images of 4-month and 12-month wild-type and 5xFAD transgene carrying C57BL6/J mice stained for dense-core plaques using Thioflavin-S (green). **C.

Representative somatosensory cortex 20X confocal images of 4-month 5xFAD transgene carrying F1 progeny of collaborative cross mice (CC002, CC006, CC013, CC017, CC037) for Thioflavin-S (Thio-S, green) and immunolabeled with 6E10 for diffused plaque (6e10, red). Scale bar = 100µm. ***D****. At 4-months in cortex, quantification of Thio-S+ plaques revealed a slight increase in CC002 X 5xFAD line compared to CC006 X 5xFAD and CC017 X 5xFAD. However, Thio-S+ plaque load (****e****) and average plaque volume (****f****) saw no significant differences across the lines.* ***G****. Quantification of 6e10+ area (%) revealed that 5xFAD transgenic C57BL6/J mice had more diffused plaque coverage compared to CC006 X 5xFAD.* ***H****. Representative subiculum 20X confocal images of 4-month 5xFAD transgene carrying F1 progeny of collaborative cross mice (CC002, CC006, CC013, CC017, CC037) for Thioflavin-S (Thio-S, green) and immunolabeled with 6E10 for diffused plaque (6e10, red). Scale bar = 100µm.* ***I****. At 4-months in subiculum like cortex, quantification of Thio-S+ plaques revealed a significant increase in CC002 X 5xFAD line compared to all the other lines except CC013 X 5xFAD.* ***J****. Quantification of Thio-S+ plaque load percentage revealed that 5xFAD and CC002 X 5xFAD were significantly more than CC017 X 5xFAD and CC037 X 5xFAD and CC006 X 5xFAD was also significantly lower than CC002 X 5xFAD.* ***K****. The average Thio-S+ plaque volume in 5xFAD was seen to be significantly increased compared to all the other lines except CC002 X 5xFAD, a line that was also significantly more than CC017 X 5xFAD and CC037 X 5xFAD* ***L****. 6e10+ area (%) showed a significant reduction in the CC006 X 5xFAD line compared to 5xFAD and CC013 X 5xFAD and CC037 X 5xFAD.* ***M****. Representative somatosensory cortex 20X confocal images of 12-month 5xFAD transgene carrying F1 progeny of collaborative cross mice (CC002, CC006, CC013, CC017, CC037) for Thioflavin-S (Thio-S, green) and immunolabeled with 6E10 for diffused plaque (6e10, red). Scale bar = 100µm. Quantification of Thio-S+ plaques (****N****) and Thio-S+ plaque load (****O****) revealed that 5xFAD is significantly more susceptible to plaque formation compared to the other F1 progenies of collaborative cross lines.* ***P****. CC006 X 5xFAD had significantly increased average Thio-S+ plaque volume compared to CC002 X 5xFAD and CC013 X 5xFAD.* ***Q****. However, 6e10+ area was consistent across all the lines at 12-month time point in the cortex.* ***R****. Representative subiculum 20X confocal images of 12-month 5xFAD transgene carrying F1 progeny of collaborative cross mice (CC002, CC006, CC013, CC017, CC037) for Thioflavin-S (Thio-S, green) and immunolabeled with 6E10 for diffused plaque (6e10, red). Scale bar = 100µm.* ***S****. Quantification of Thio-S+ plaque number showed that 5xFAD and CC002 X 5xFAD were significantly more plaque su sceptible than CC006 X 5xFAD, CC013 X 5xFAD and CC017 X 5xFAD. t. Similarly, plaque load for 5xFAD, CC002 X 5xFAD and CC037 X 5xFAD were significantly more plaque susceptible than CC006 X 5xFAD, CC013 X 5xFAD and CC017 X 5xFAD.* ***U****. The subiculum average plaque volume at the 12-month timepoint showed CC002 X 5xFAD, CC013 X 5xFAD and CC037 X 5xFAD are significantly higher than 5xFAD.* ***V****. The 6e10+ area at 12-month timepoint in subiculum showed that CC013 X 5xFAD has significantly more diffused plaques compared to 5xFAD, CC006 X 5xFAD and CC037 X 5xFAD. No significant changes were seen between males and females across all the comparisons made. Data are represented as mean ± SEM. Statistical significance is denoted by * p<0.05, ** p<0.01, ***p<0.001, ****p<0.0001 via two-way ANOVA tests for all quantifications.*

To investigate the impact of genetic diversity on plaque development, we stained diffuse and dense core plaques in CC X 5xFAD transgene carrying lines at both the 4-month and 12-month timepoints (**Figure 8A**). As expected, there is an increase in pathology, especially in the dense core plaques once age and genotype are factored in across all the lines. Representative stains for the homozygous C57BL6/J line are shown at 4-month and 12-month timepoints (**Figure 8B**). I observe that at both ages there is consistent plaque burden across all CC x 5xFAD lines (**Figure 8C-J**), indicating stable transgene expression in all CC lines which I validated using Thy1 expression data. Amyloid plaques exhibit features that could be broadly characterized as dense core or diffuse, which can be readily detected using Thio-S (labels the beta sheets in the fibrillar Aβ aggregates) or 6e10 (binds to the amino acid residues of Aβ and APP), respectively.

Quantifications in the cortex at 4-month timepoint (**Figure 8C-G**) reveal that the CC002 X 5xFAD line has the highest amount of dense core plaques, especially when compared to the CC006 X 5xFAD line, which has the lowest. (**Figure 8D**). However, there are no significant changes in the plaque load (**Figure 8E**) or average volume (**Figure 8F**) of dense core plaques. Consistent with dense core plaque data, CC006 X 5xFAD has the least number of diffuse plaques in comparison to 5xFAD at this timepoint (**Figure 8G**). Previous studies have reported a spatially and temporally defined pattern of plaque formation in specific neocortical and hippocampal regions henceforth hippocampus has a higher plaque load in comparison to the cortex (Reilly et al., 2003). In concordance, the hippocampus at 4-month timepoints (**Figure 8H-L**) shows a significant increase in plaque pathology in CC002 X 5xFAD line compared to all the other lines (**Figure 8I**). 5xFAD has the second highest plaque load after CC002 X 5xFAD, while CC037 X 5xFAD has the lowest (**Figure 8J**). Congenic C57BL6/J 5xFAD has the highest average plaque volume while CC017 X 5xFAD and CC037 X 5xFAD have the least (**Figure 8K**). CC006 X 5xFAD mice have reduced diffuse plaque volume compared to 5xFAD while CC013 X 5xFAD and CC037 X 5xFAD have the most (**Figure 8L**). Similarly, staining at the 12-month timepoint in the cortex reveals that 5xFAD show the most pathology with respect to dense core plaque number and load (**Figure 8M-O**). Average plaque volume is highest in CC006 X 5xFAD (**Figure 8P**) but there are no significant changes in diffuse plaques during this timepoint in the cortex (**Figure 8Q**). Stain quantifications in the hippocampus of 12-month-old mice reveals CC006 X 5xFAD, CC013 X 5xFAD and CC017 X 5xFAD are significantly more resistant to plaque formation than 5xFAD (**Figure 8R-S**). A similar pattem of plaque susceptibility is seen in 5xFAD when compared to the other mice for plaque load (**Figure 8T**). CC002 X 5xFAD have a higher average plaque volume than 5xFAD (**Figure 8u**), while diffuse plaques appear higher in CC013 X 5xFAD compared to CC006 X 5xFAD (**Figure 8v**). From this, we conclude that congenic C57BL6/J 5xFAD has a tendency to form

more plaques compared to the other tested lines, and identified CC006 X 5xFAD and CC013 X 5xFAD as lines that may be more resistant to plaque formation.

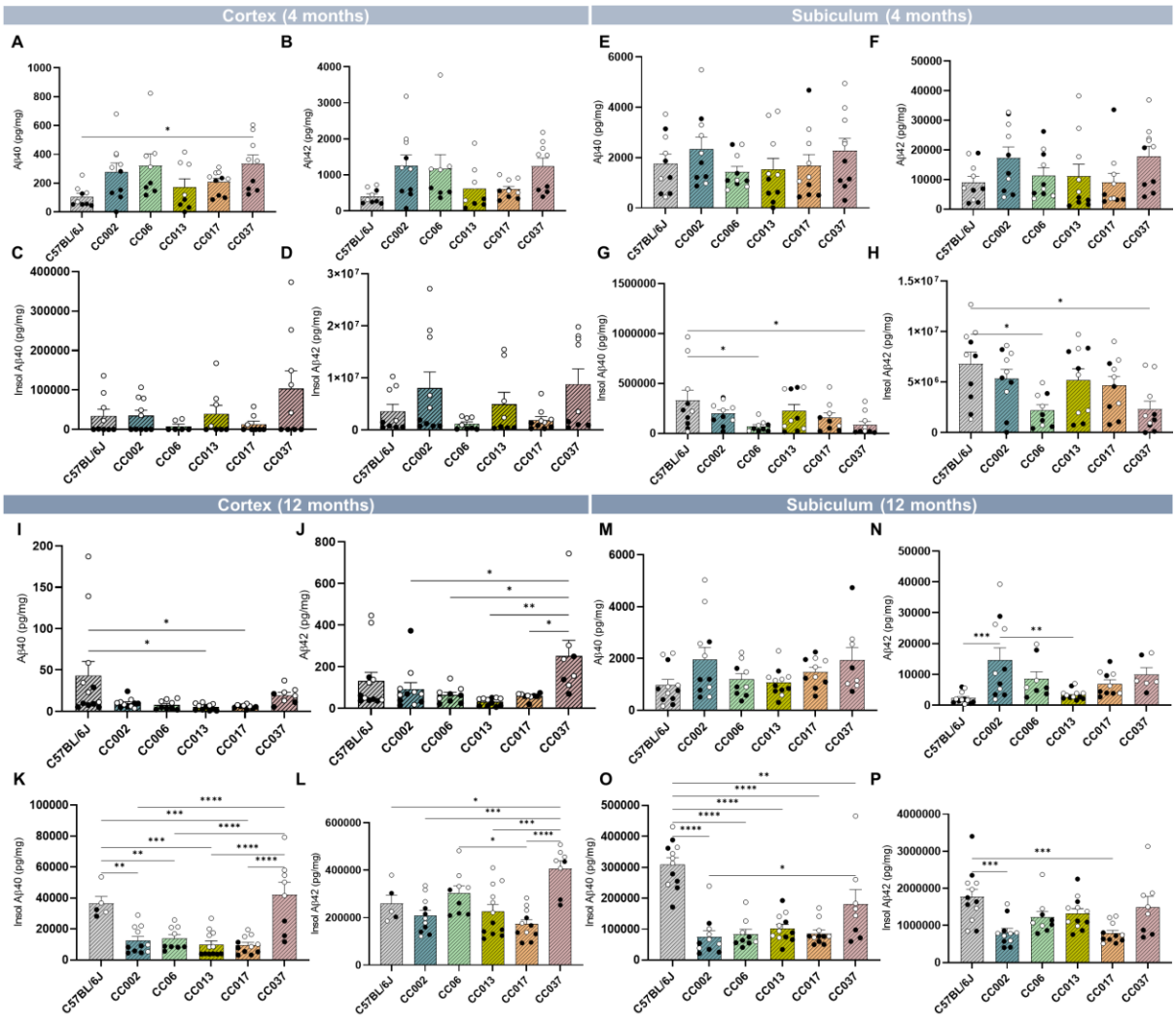

***Figure 9**: **(A-D)** Cortical soluble fraction quantification at 4-month revealed a slight increase in Aβ40 of CC037 X 5xFADmice in comparison to 5xFAD. No significant changes were seen in insoluble Aβ40 (**C**) and soluble (**B**) and insoluble (**D**) Aβ42 in cortex at this time point. Soluble fraction quantification at 4-month in subiculum showed no change in Aβ40 (**E**) and Aβ42 (**F**) but insoluble fraction quantification in 5xFAD for Aβ40 (**G**) and Aβ42 (**H**) showed an increase compared to some of the other collaborative cross lines (CC006 X 5xFAD and CC037 X 5xFAD). **I.** At 12-month soluble fraction quantification in the cortex showed that 5xFAD had more Aβ40 compared to CC013 X 5xFAD and CC017 X 5xFAD whereas CC037 X 5xFAD had more soluble Aβ42 fraction compared to all the other lines except 5xFAD (**J**). **K.** 5xFAD and CC037 X 5xFADalso had the most insoluble Aβ40 fraction at 12-month in cortex compared to all the other lines, but only CC037 X 5xFAD had the most insoluble Aβ42 fraction except when compared to CC013 X 5xFAD (**L**). **M.** There were no significant differences in the subiculum Aβ40 soluble fraction quantification at the 12-month timepoint. **N.** At the 12-month timepoint, CC002 X 5xFAD had significantly more soluble Aβ42 fraction in subiculum compared to its 5xFAD and CC013 X 5xFAD counterparts. However, 5xFAD seem to have the most insoluble Aβ40 (**O**) and Aβ42 (only in comparison to CC002 X 5xFAD and CC017 X 5xFAD) (**P**) fraction in the subiculum at 12-months. No significant changes were seen between males and females across all the*

*comparisons made. Data are represented as mean ± SEM. Statistical significance is denoted by * p<0.05, ** p<0.01, ***p<0.001, ****p<0.0001 via two-way ANOVA tests for all quantifications.*

To explore the effect genetic diversity has on overall Aβ levels we assayed detergent soluble and insoluble fractions of Aβ40 and Aβ42 from micro-dissected cortices and hippocampi. At the 4-month timepoint, CC037 X 5xFAD produces more Aβ40 than 5xFAD (**Figure 9A**). However, there are no differences at this timepoint in the cortices for insoluble Aβ40 and soluble/insoluble Aβ42, as well as soluble Aβ40 and Aβ42 in the subiculum (**Figure 9C-F**). We observe elevated insoluble Aβ40 and Aβ42 levels in 5xFAD relative to CC006 X 5xFAD and CC037 X 5xFAD (**Figure 9G-H**). In the cortex at the 12-month timepoint, 5xFAD mice have higher levels of soluble Aβ40 than CC013 X 5xFAD and CC017 X 5xFAD, and higher levels of Aβ42 than all the other lines (**Figure 9I-J**). 5xFAD and CC037 X 5xFAD have elevated insoluble Aβ40 levels in comparison to all the other lines whereas, CC013 X 5xFAD has the lowest insoluble Aβ42 fraction level with respect to CC037 X 5xFAD in the cortex at the 12-month timepoint (**Figure 9K-L**). No differences are detected in the 12-month-old hippocampal Aβ40 soluble fraction (**Figure 9M**). In the subiculum at the 12-month timepoint, we observe a decrease in 5xFAD and CC013 X 5xFAD soluble Aβ42 fraction; however, insoluble Aβ40 and Aβ42 levels are higher in 5xFAD compared to CC002 X 5xFAD and CC017 X 5xFAD (**Figure 9N-P**). We notice conserved trends in the plaque quantification through Aβ quantification where 5xFAD and CC037 X 5xFAD are the most susceptible to plaque formation, and CC006 X 5xFAD and CC013 X 5xFAD are the most plaque resistant lines. To determine the correlation between plaque load and microglial as well as astrocytic counts, I quantified the

IBA1+ microglia (**Figure 10**) along with S100b+ and GFAP+ astrocytes (**Figure 11**) at both time points across the two regions compared to their WT counterparts.

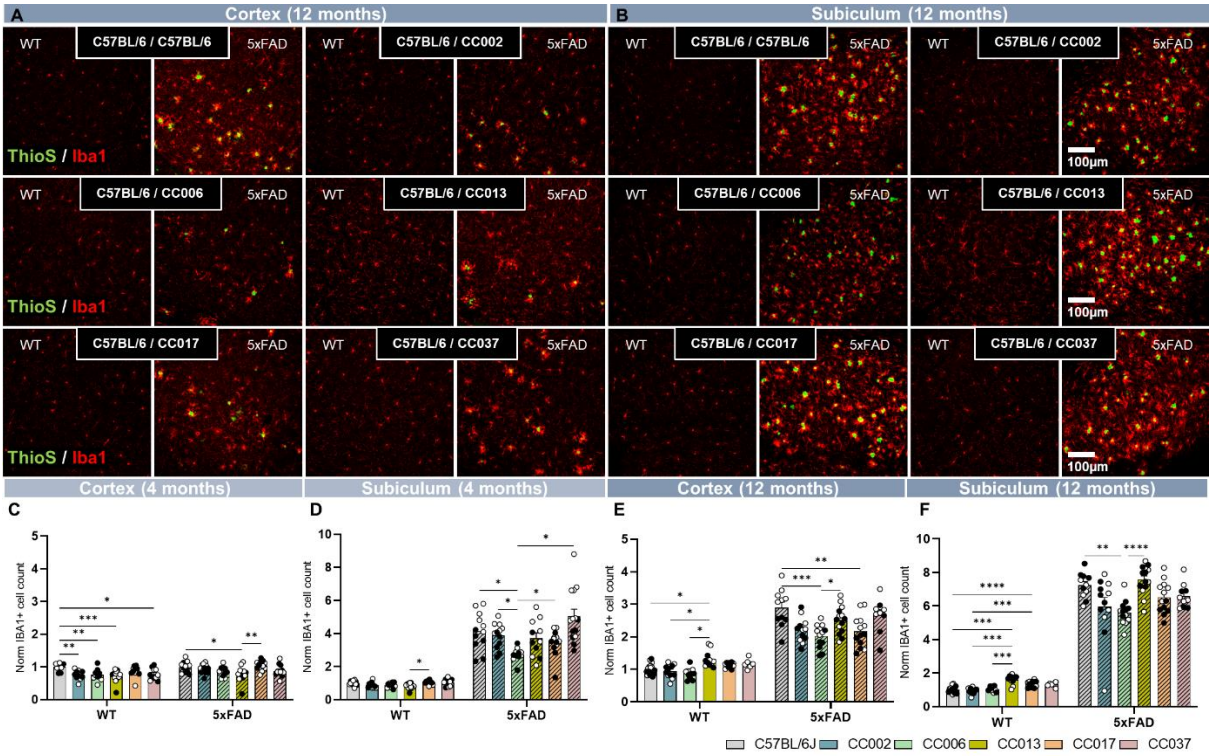

***Figure 10**: Representative somatosensory cortex (**A**) and subiculum (**B**) 20X confocal images of 12-month wild-type and 5xFAD transgene carrying F1 progeny of collaborative cross mice (CC002, CC006, CC013, CC017, CC037) for dense-core plaques using Thioflavin-S (Thio-S, green) and immunolabeled microglia (IBA1, red). Scale bar = 100µm. **C-F.** Quantification of number of microglial cells normalized to the wild-type C57BL6/J at the 4-month timepoint **C.** Wild-type had the most microglia in Cortex at the 4-month timepoint when compared to the other lines except CC017 X C57BL6/J whereas CC013 X 5xFAD had lower microglia compared to 5xFAD and CC017 X 5xFAD **D.** CC013 X C57BL6/J had significantly lower microglial cells at 4months in the subiculum when compared to CC017 X C57BL6/J, however all the lines except CC013 X 5xFAD had more microglia than CC006 X 5xFAD. **E.** In cortex at 12-months CC013 X C57BL6/J had more microglial cells in comparison to CC006 X C57BL6/J, CC002 X C57BL6/J and C57BL6/J. 5xFAD was found to have significantly more microglia than CC017 X 5xFAD and CC006 X 5xFAD, which is a line that was also significantly lower than CC013 X 5xFAD. **F**. In subiculum at the 12-month timepoint CC013 X C57BL6/J was found to have significantly more microglial cells than CC006 X C57BL6/J and CC002 X C57BL6/J and C57BL6/J. CC017 X C57BL6/J was also significantly higher in the microglial cell count than CC002 X C57BL6/J and C57BL6/J. 5xFAD and CC013 x 5xFAD were the two lines that had higher microglial counts than CC006 x 5xFAD. No significant changes were seen between males and females across all the comparisons made. Data are represented as mean ± SEM. Statistical significance is denoted by * $p<0.05$, ** $p<0.01$, *** $p<0.001$, **** $p<0.0001$ via two-way ANOVA tests for all quantifications.*

Mounting evidence has implicated glial cells in the modulation of neurons as well as synaptic elements in both the healthy and diseased brain, which in turn may affect learning and memory (Paolicelli et al., 2011), (Rice et al., 2015), (Elmore et al., 2014), (Elmore et al., 2018). It's been hypothesized that once in close proximity to plaques, microglia

become activated or undergo morphological changes and surround plaques, releasing cytokines and chemokines which cause inflammation hence contributing to disease progression (Bandyopadhyay, 2021), (Dzamba et al., 2016), (Nordengen et al., 2019). This implicates microglia as a key component in Alzheimer's disease, hence we explored microglial densities in both the wildtype and 5xFAD progenies to characterize any strain related effects (**Figure 10A-B**). To get an accurate measure of relative change, we normalized the quantifications across all lines with respect to average microglial density of C57BL6/J (**Figure 10C-F**), which is higher at 4-month timepoint in cortex in comparison to all the other groups in WTs. CC013 X 5xFAD mice show a slight reduction in comparison to 5xFAD, and CC017 X 5xFAD has the highest normalized microglial density (**Figure 10C**). In the subiculum, CC013 X C57BL6/J has the lowest normalized microglial density, while CC006 X 5xFAD and CC013 X 5xFAD were the lines with the lowest microglial densities when compared to other 5xFAD lines (**Figure 10D**). In conclusion we observe a strong positive correlation between the microglial quantifications and plaque pathology quantifications, as C57BL6/J and 5xFAD show higher levels of microglial densities and CC006 X C57BL6/J and CC013 X C57BL6/J as well as CC006 X 5xFAD and CC013 X 5xFAD have lower normalized microglial density quants at the 4-month timepoint.

At the 12-month timepoint in the cortex CC013 X C57BL6/J mice have higher normalized microglial densities in comparison to C57BL6/J mice. Also, CC006 X 5xFAD and CC017 X 5xFAD groups have lower normalized microglial densities compared to 5xFAD (**Figure 10E**). The hippocampus shows that CC013 X C57BL6/J has the highest normalized microglia density compared to C57BL6/J, whereas CC006 X C57BL6/J has the lowest. Additionally, CC006 x 5xFAD mice exhibit lower normalized microglial counts compared to 5xFAD, which are the highest of all groups (**Figure 10F**). Altogether at the 12-month

timepoint, C57BL6/J and 5xFAD show higher levels of microglial densities and CC006 X C57BL6/J as well as CC006 X 5xFAD and CC013 X 5xFAD have lower normalized microglial density quants.

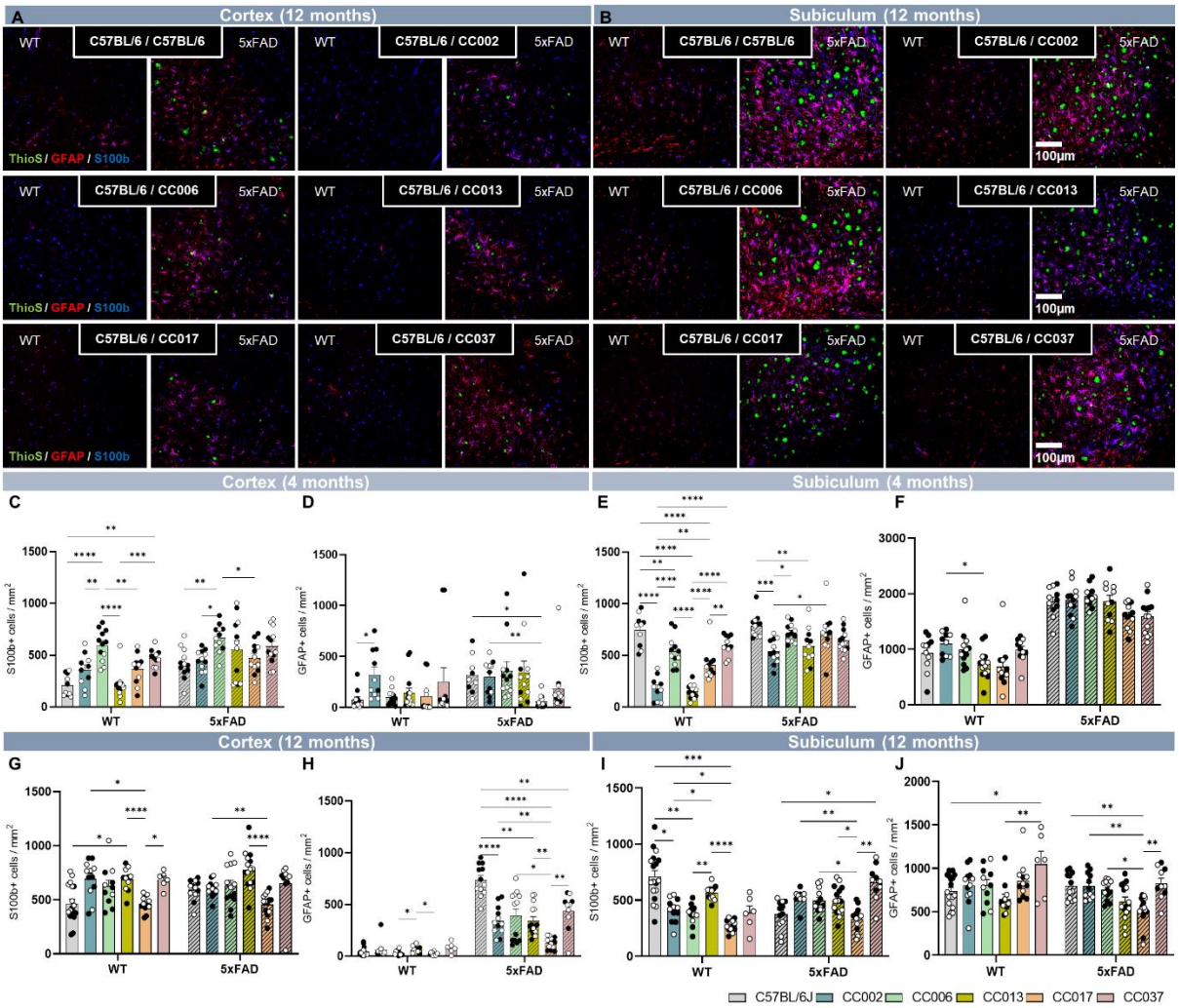

***Figure 11**: **A-B.** Representative somatosensory cortex (**A**) and subiculum (**B**) 20X confocal images of 12-month wild-type and 5xFAD transgene carrying F1 progeny of collaborative cross mice (CC002, CC006, CC013, CC017, CC037) for dense-core plaques using Thioflavin-S (Thio-S, green) and immunolabeled reactive astrocytes (GFAP in red and s100β in blue). Scale bar = 100µm. **C.** At the 4-month timepoint in cortex, the s100β$^+$ cell density quantification showed that CC013 X C57BL6/J had more reactive astrocytic cells than all the other lines except CC037 X C57BL6/J and that CC037 X C57BL6/J also had significantly more reactive astrocytic cells than C57BL6/J and CC013 X C57BL6/J. It also revealed than CC013 X 5xFAD had more reactive astrocytic cells than 5xFAD, CC002 X 5xFAD and CC017 X 5xFAD. **D.** Quantification of GFAP$^+$ cell density in cortex at 4-months was significantly more in CC002 X C57BL6/J compared to C57BL6/J and that CC017 X 5xFAD had significantly lower GFAP+ cell density in comparison to 5xFAD and CC002 X 5xFAD. **E.** In the subiculum at the 4-month time point the quantification of s100β$^+$ cell density showed that C57BL6/J had significantly more reactive cells in comparison to all the other lines except CC037 X C57BL6/J. CC013 X C57BL6/J had the lowest amount of s100β$^+$ cell density compared to all the other lines. CC002 X 5xFAD had significantly lower reactive astrocytic cells in comparison to CC0017 X 5xFAD, CC006 X 5xFAD and 5xFAD, which was a line found to also be significantly more compared to CC013 X 5xFAD. **F.** Quantification of GFAP$^+$ cell density revealed than CC002 X C57BL6/J had more reactive astrocytic cells than CC013 X C57BL6/J. However, no significant changes were seen in lines carrying the 5xFAD transgene. **G.** When s100β$^+$ cell density was quantified in the cortex at the 12-month timepoint, CC017*

X C57BL6/J seemed to have lower reactive astrocytic cell count compared to CC037 X C57BL6/J, CC002 X C57BL6/J and CC013 X C57BL6/J, which is also a line having significantly more cell density quantification in comparison to C57BL6/J. CC017 X 5xFAD also showed a significant reduction in the reactive astrocytic cell density in comparison to CC013 X 5xFAD and CC002 X 5xFAD. ***H.*** *Quantification of GFAP$^+$ cell density in cortex at the 12-month timepoint revealed that CC013 X C57BL6/J had more cell density in comparison to CC006 X C57BL6/J and CC017 X C57BL6/J. 5xFAD controls were found to have the most reactive astrocytic cell density except when compared to CC006 X 5xFAD and CC017 X 5xFAD had the least amount of GFAP$^+$ cell density compared to all the other lines.* ***I.*** *At the 12-month timepoint in the subiculum quantification of s100β$^+$ cell density revealed that C57BL6/J and CC013 X C57BL6/J had more reactive astrocytic cells in comparison to CC002 X C57BL6/J, CC006 X C57BL6/J and CC017 X C57BL6/J. CC017 X 5xFAD was found to have the lower reactive astrocytic cells when compared to all the other lines except in comparison to 5xFAD, a line that had significantly lower s100β$^+$ cell density to CC037 X 5xFAD.* ***J.*** *Quantification of GFAP$^+$ cell density at the 12-month timepoint in subiculum revealed that CC037 X C57BL6/J had significantly more reactive astrocytic cells in comparison to CC013 X C57BL6/J and C57BL6/J. CC017 X 5xFAD was found to have the least reactive astrocytic cell density in comparison to all the other lines except in comparison to CC013 X 5xFAD. No significant changes were seen between males and females across all the comparisons made. Data are represented as mean ± SEM. Statistical significance is denoted by * p<0.05, ** p<0.01, ***p<0.001, ****p<0.0001 via two-way ANOVA tests for all quantifications.*

To characterize the effect of genetics on the densities of astrocytes, we stained for astrocytic markers at both the 4-month and 12-month timepoints in the cortex and hippocampus using s100β; a biomarker expressed by most astrocytes and GFAP; a biomarker that's expressed by only reactive cortical and all hippocampal astrocytes (**Figure 11A-B**). The cortex at the 4-month timepoint shows an increase in s100β+ cell density for CC006 X C57BL6/J and CC037 X C57BL6/J in comparison to C57BL6/J and CC013 X C57BL6/J. Interestingly, CC006 X 5xFAD has higher s100β+ cell density than 5xFAD (**Figure 11C**). Staining for GFAP+ cell density in the cortex at 4-months reveals highest astrocytic density in CC002 X C57BL6/J. Additionally, the lowest GFAP+ cell density in CC017 X 5xFAD is seen when compared to 5xFAD (**Figure 11D**). In the subiculum, C57BL6/J has the highest s100β+ cell density in comparison to all the other lines, while CC013 X C57BL6/J has the lowest. Similarly, 5xFAD has the highest s100β+ cell density in comparison to CC013 X 5xFAD, however, CC002 X 5xFAD has the lowest density overall (**Figure 11E**). CC013 X C57BL6/J was found to have the lowest GFAP+ in WT mice, and no significant differences are observed between 5xFAD transgenic lines (**Figure 11F**).

Similar labelling at the 12- month timepoint revealed that CC013 X C57BL6/J has the highest s100β+ cell density in the cortex while C57BL6/J and CC017 X C57BL6/J have

the lowest in WT groups. CC017 X 5xFAD has lowest s100β+ cell density and CC013 X 5xFAD the highest (**Figure 11G**) in the 5xFAD groups. CC013 X C57BL6/J has the highest GFAP+ cell density in cortex at the 12-month timepoint across WT groups. In 5xFAD groups, CC017 X 5xFAD has the lowest GFAP+ cell density in comparison to all the other lines, suggesting a markedly altered astrocytic response to plaques, and 5xFAD the highest (**Figure 11H**). In the subiculum, the s100β+ cell density is higher in C57BL6/J compared to other WT groups. In 5xFAD groups s100β+ cell density highest in CC037 X 5xFAD mice, and lowest in CC017 X 5xFAD mice (**Figure 11I**). GFAP+ cells in the subiculum at 12 months do not vary greatly between groups, other than a reduced density in CC017 X 5xFAD mice in comparison to all the other lines (**Figure 11J**). From the astrocytic staining I discovered that CC017 consistently had lower cell density compared to all the other cell lines for both WTs and AD-CC groups, revealing a profoundly altered astrocytic response to plaques.

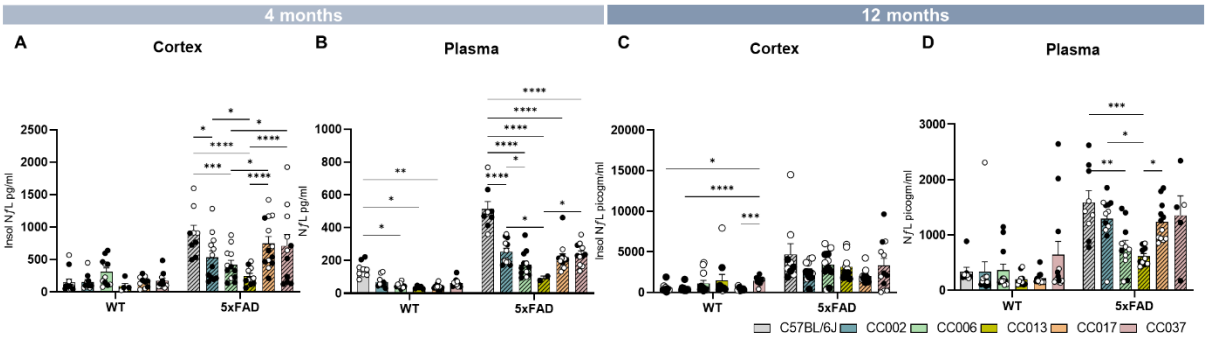

Figure 12: A-D*. Measurement of NfL in cortical insoluble fraction (**A**) via Meso Scale Discovery technology revealed significant changes only in the 5xFAD transgene carrying samples at the 4-month timepoint. CC013 had lower NfL in comparison to all the other lines except CC006 X 5xFAD, a line that is also found to have lower NfL than 5xFAD, CC017 X 5xFAD and CC037 X 5xFAD. Plasma NfL (**B**) level was significantly more in C57BL6/J compared to CC006 X C57BL6/J, CC013 X C57BL6/J and CC017 X C57BL6/J. 5xfAD also had the highest NfL levels across the lines with CC013 X 5xFAD having the least in comparison to others except in comparison to CC006 X 5xFAD. Surprisingly the NfL levels in cortical insoluble fraction (**C**) at the 12-month timepoint revealed the opposite with significant changes only seen in the non-5xfAD transgene carrying samples. CC037 X C57BL6/J had significantly more NfL levels in comparison to C57BL6/J, CC002 X C57BL6/J and CC017 X C57BL6/J. Significant changes in the plasma NfL levels (**D**) were only seen in 5xFAD transgene carrying samples with CC013 X 5xFAD having the lower NfL levels in comparison to CC017 X 5xFAD, CC002 X 5xFAD and 5xFAD. 5xFAD also had higher NfL levels than CC006 X 5xFAD in the plasma. No significant changes were seen between males and females across all the comparisons made.*

*Data are represented as mean ± SEM. Statistical significance is denoted by * p<0.05, ** p<0.01, ***p<0.001, ****p<0.0001 via two-way ANOVA tests for all quantifications.*

Recently, certain clinical blood-based biomarkers have emerged that can help track cognitive decline and neuro-damage in mouse models of AD. One such biomarker is Neurofilament light chain (N*f*L), which has also been implicated as a strong measure for the determination of plaque load and risk of developing dementia (Benedet et al., 2019), (E. H. Lee et al., 2022). To gain insight into the brain damage caused by age and the 5xFAD transgene on these strains we measured N*f*L levels in both the plasma and insoluble fraction of the cortex of 4- and 12-month-old mice. No differences are observed in cortex N*f*L levels of WT groups at 4 months of age, but increased N*f*L levels are found in 5xFAD groups, consistent with the presence of plaques increasing N*f*L (**Figure 12a**). Of the 5xFAD groups, 5xFAD on the C57BL6/J background has the highest N*f*L levels, and CC013 X 5xFAD the lowest. Plasma N*f*L at this 4-month timepoint mirrored the cortical N*f*L levels, with levels being robustly increased in most 5xFAD groups compared to WT (**Figure 12b**). 5xFAD also has the highest plasma N*f*L levels across all the lines with CC006 X 5xFAD and CC013 X 5xFAD having the least (**Figure 12b**).

By the 12-month timepoint, N*f*L levels in the cortical insoluble fraction no longer differ between 5xFAD groups (**Figure 12c**). Notably, plasma N*f*L levels mirror the effects seen at the 4-month timepoint, with the most plasma N*f*L in 5xFAD mice, and the least in CC006 X 5xFAD and CC013 X 5xFAD (**Figure 12d**). Overall, the N*f*L levels correlate well with the plaque load seen in Figure 2; where 5xFAD and CC037 have the highest levels and

CC006 and CC013 have the lowest levels for both plaques and plasma N*f*L.

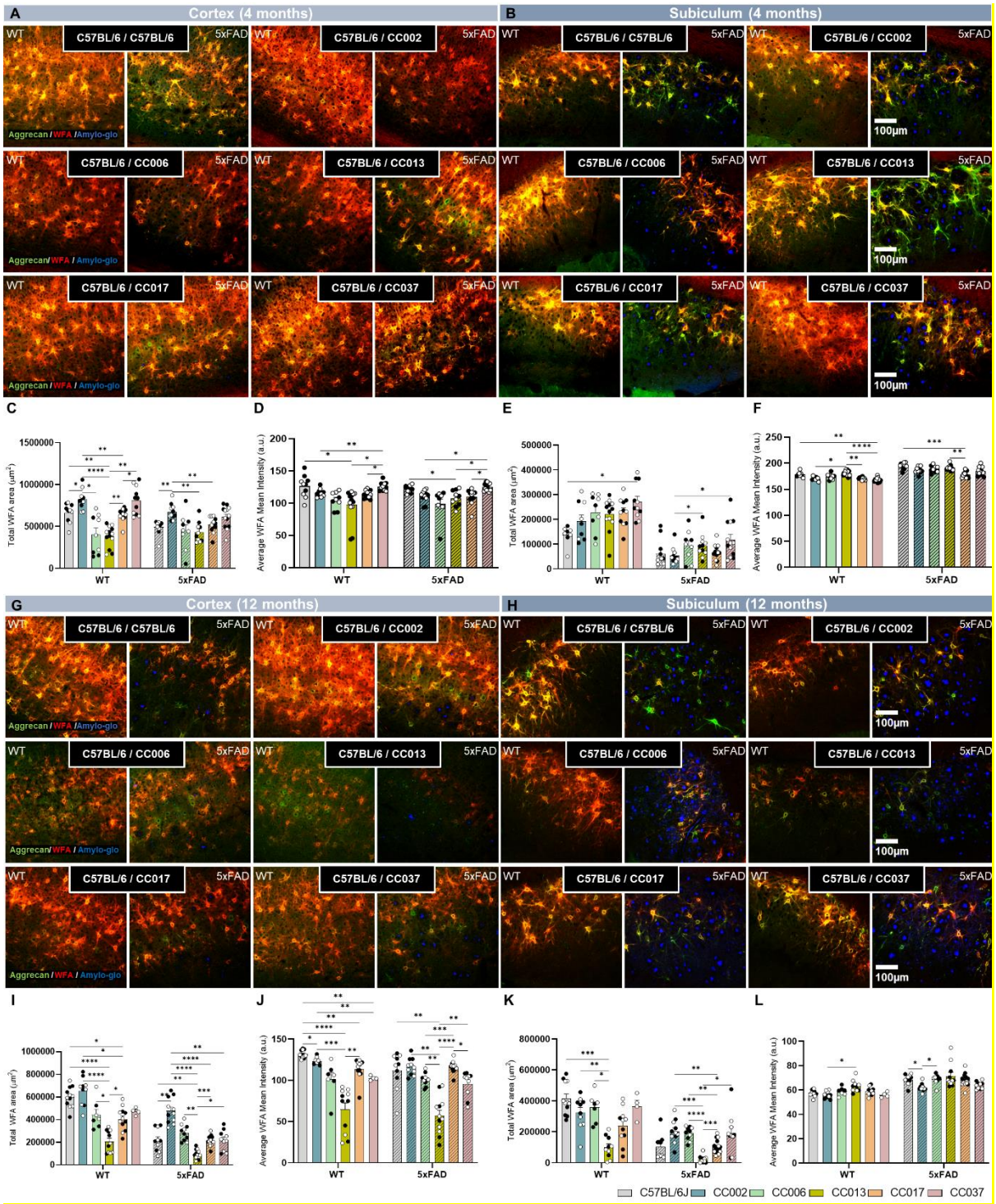

Figure 13: *Representative somatosensory cortex (**A**) and subiculum (**B**) 20X confocal images of 4-month wild-type and 5xFAD transgene carrying F1 progeny of collaborative cross mice (CC002, CC006, CC013, CC017, CC037) for dense-core plaques using Amylo-glo (Amylo-glo, blue) and immunolabeled perineuronal nets (WFA in red and Aggrecan in green). Scale bar = 100µm.* ***C.*** *In cortex, the total WFA area quantifications were the least in CC006 X C57BL6/J and CC013 X C57BL6/J than all the other lines. It also revealed than CC002 X 5xFAD had more total WFA area in comparison to 5xFAD, CC013 X 5xFAD and CC017 X 5xFAD.* ***D.*** *Quantification of average WFA mean intensity in cortex was significantly more in C57BL6/J and CC037 X C57BL6/J compared to CC013 X C57BL6/J and that CC037 X 5xFAD had significantly higher average WFA mean intensity in comparison to CC002 X 5xFAD, CC013 X 5xFAD and*

CC017 X 5xFAD. ***E.*** *In the subiculum the quantification of total WFA area in CC037 X C57BL6/J was significantly more in comparison to C57BL6/J. CC002 X 5xFAD had significantly lower total WFA area in comparison to CC0013 X 5xFAD, CC037 X 5xFAD.* ***F.*** *Quantification of average WFA mean intensity in subiculum revealed than CC013 X C57BL6/J had more intensity compared to CC002 X C57BL6/J, CC017 X C57BL6/J and CC037 X C57BL6/J which is also lower in intensity in comparison to C57BL6/J. CC017 X 5xFAD had the least average WFA mean intensity in comparison to 5xFAD and CC013 X 5xFAD. Representative somatosensory cortex (**G**) and subiculum (**H**) 20X confocal images of 12-month wild-type and 5xFAD transgene carrying F1 progeny of collaborative cross mice (CC002, CC006, CC013, CC017, CC037) for dense-core plaques using Amylo-glo (Amylo-glo, blue) and immunolabeled perineuronal nets (WFA in red and Aggrecan in green). Scale bar = 100µm.* ***I.*** *In cortex, the total WFA area quantifications were the least in CC013 X C57BL6/J than all the other lines expect CC037 X C57BL6/J. CC017 X C57BL6/J was also found to have lower area in comparison to C57BL6/J and CC02 X C57BL6/J. It also revealed that CC013 X 5xFAD had the least total WFA area in comparison to all the other lines. CC002 X 5xFAD was higher in total WFA area in comparison to 5xFAD, CC017 X 5xFAD and CC037 X 5xFAD.* ***J.*** *Quantification of average WFA mean intensity in cortex was significantly more in C57BL6/J compared to all the other lines. CC013 X C57BL6/J and CC037 X C57BL6/J were also lower in average WFA mean intensity in comparison to CC002 X C57BL6/J. CC013 X 5xFAD had the least average WFA mean intensity across all the lines. CC017 X 5xFAD had more average WFA mean intensity in comparison to CC006 X 5xFAD and CC037 X 5xFAD.* ***K.*** *In the subiculum the quantification of total WFA area in CC013 X C57BL6/J was significantly lower in comparison to C57BL6/J, CC002 X C57BL6/J and CC006 X C57BL6/J. CC013 X 5xFAD had significantly lower total WFA area in comparison to all lines except 5xFAD. CC0017 X 5xFAD was also lower in area in comparison to CC002 X 5xFAD and CC006 X 5xFAD.* ***L.*** *Quantification of average WFA mean intensity in subiculum revealed that CC013 X C57BL6/J had more intensity compared to CC002 X C57BL6/J. CC002 X 5xFAD had the lower average WFA mean intensity in comparison to 5xFAD and CC006 X 5xFAD. No significant changes were seen between males and females across all the comparisons made. Data are represented as mean ± SEM. Statistical significance is denoted by * p<0.05, ** p<0.01, ***p<0.001, ****p<0.0001 via two-way ANOVA tests for all quantifications.*

To evaluate ECM damage, we stained for perineuronal nets markers at both the 4-month and 12-month timepoints in the cortex and hippocampus using WFA; lectin protein that binds specifically to certain sugars in the extracellular matrix of PNNs and Aggrecan; proteoglycan molecule that is a major component of PNNs used to visualize the overall structure of PNNs (**Figure 13A,B,G,H**). The cortex at the 4-month timepoint shows an increase in total WFA area for CC002 X C57BL6/J and CC037 X C57BL6/J in comparison to CC006 X C57BL6/J and CC013 X C57BL6/J. Interestingly, CC006 X 5xFAD and CC013 X 5xFAD also have lower total WFA area in comparison to 5xFAD and CC002 X 5xFAD (**Figure 13C**). Staining for average WFA mean intensity in the cortex at 4-months reveals higher intensity in C57BL6/J and CC037 X C57BL6/J and lower in CC006 X C57BL6/J and CC013 X C57BL6/J. Additionally, the lowest average WFA mean intensity is also seen in CC006 X 5xFAD and CC013 X 5xFAD in comparison to 5xFAD and CC037 X 5xFAD (**Figure 13D**). In the subiculum, CC037 X C57BL6/J has the highest total WFA area in comparison to all the other lines, while C57BL6/J has the lowest. Similarly, 5xFAD

has the lowest total WFA area in comparison to CC013 X 5xFAD and CC037 X 5xFAD which are the highest (**Figure 13E**). CC013 X C57BL6/J is found to have the highest average WFA mean intensity and CC037 X C57BL6/J the lowest among subiculum of WT mice, and CC017 X 5xFAD was the lowest among the 5xFAD transgenic lines (**Figure 13F**).

Similarly labelling in the cortex at the 12- month timepoint reveals CC013 X C57BL6/J as the line with the lowest total WFA area in comparison to C57BL6/J and CC002 X C57BL6/J having the highest among the WT groups. Similarly, 5xFAD and CC013 X 5xFAD have the lower total WFA area and CC002 X 5xFAD the highest (**Figure 13I**) in the 5xFAD groups. CC013 X C57BL6/J has the lowest average WFA mean intensity in cortex at the 12-month timepoint across WT groups in comparison to C57BL6/J which is the highest. Similarly, in 5xFAD groups CC013 X 5xFAD has the lowest average WFA mean intensity in comparison to all the other lines, suggesting a markedly altered ECM structure with respect to perineuronal nets response to plaques, and 5xFAD the highest (**Figure 13J**). In the subiculum, the total WFA area is higher in C57BL6/J compared to other WT groups and CC013 X C57BL6/J has the lowest. In 5xFAD groups total WFA area is the highest in CC002 X 5xFAD mice, and lowest in 5xfAD and CC013 X 5xFAD mice (**Figure 13K**). Average WFA mean intensity in the subiculum at 12 months do not vary hugely between groups, other than a reduced density in CC002 X C57BL6/J and CC002 X 5xFAD mice in comparison to their matched counterparts (**Figure 13L**). From the PNN staining we discovered that CC006 and CC013 even though started with comparable quants at the 4-month timepoint showed a stark reduction by the 12-month timepoint compared to all the other cell lines for both WTs and AD-CC groups, revealing a profoundly strain dependent ECM alteration.

Chapter 2.2. Identify the transcriptional changes associated with PNN alterations in CC and CC x 5xFAD mouse lines.

To complement and validate the biochemical experimental data, as well as to provide critical evidence to support whether microglia could be major regulators of PNNs, I performed transcriptional analyses to computationally link this phenotypic variance to founder strains.

Generating Custom Transcriptome: To accomplish this, I have been analyzing bulk mRNA collected from both WT and 5xFAD CCXC57BL6/J mouse lines to determine the underlying relationship between PNN loss and microglial dysfunction on a transcriptional level. Having no reference genomes available for the CC lines, I first tried aligning the sample FASTQ files to the genomes of the founder strain pooled together. This resulted in >50% transcript dropout due to the presence of the excessive transcripts from the eight founder strains, making it impossible to get any significant statistics after downstream processing. I then reconstructed genomes using GBRS, a suite of tools that uses the multiparent populations RNA-seq data directly and simultaneously reconstructs the individual diploid genome and quantifies the total and allele-specific expression. However, due to limitations of the software and the extensiveness of the background strain, the genome created showed only ~80% likeness when compared to the actual haplotype information provided by JAX (**Figure 14A**), which again would have led to loss of data. To make the constructed genome more robust and decrease loss of data, instead of changing the custom genome using GBRS, I decided to use the aforementioned haplotype file for each of the CC lines we were interested in and manually picked the region of interest from the Founder strains based on the chromosome number and location provided. I then used that data to select the transcripts we would be interested in. This

custom transcriptome for all the required CC lines was then used to align our samples to.

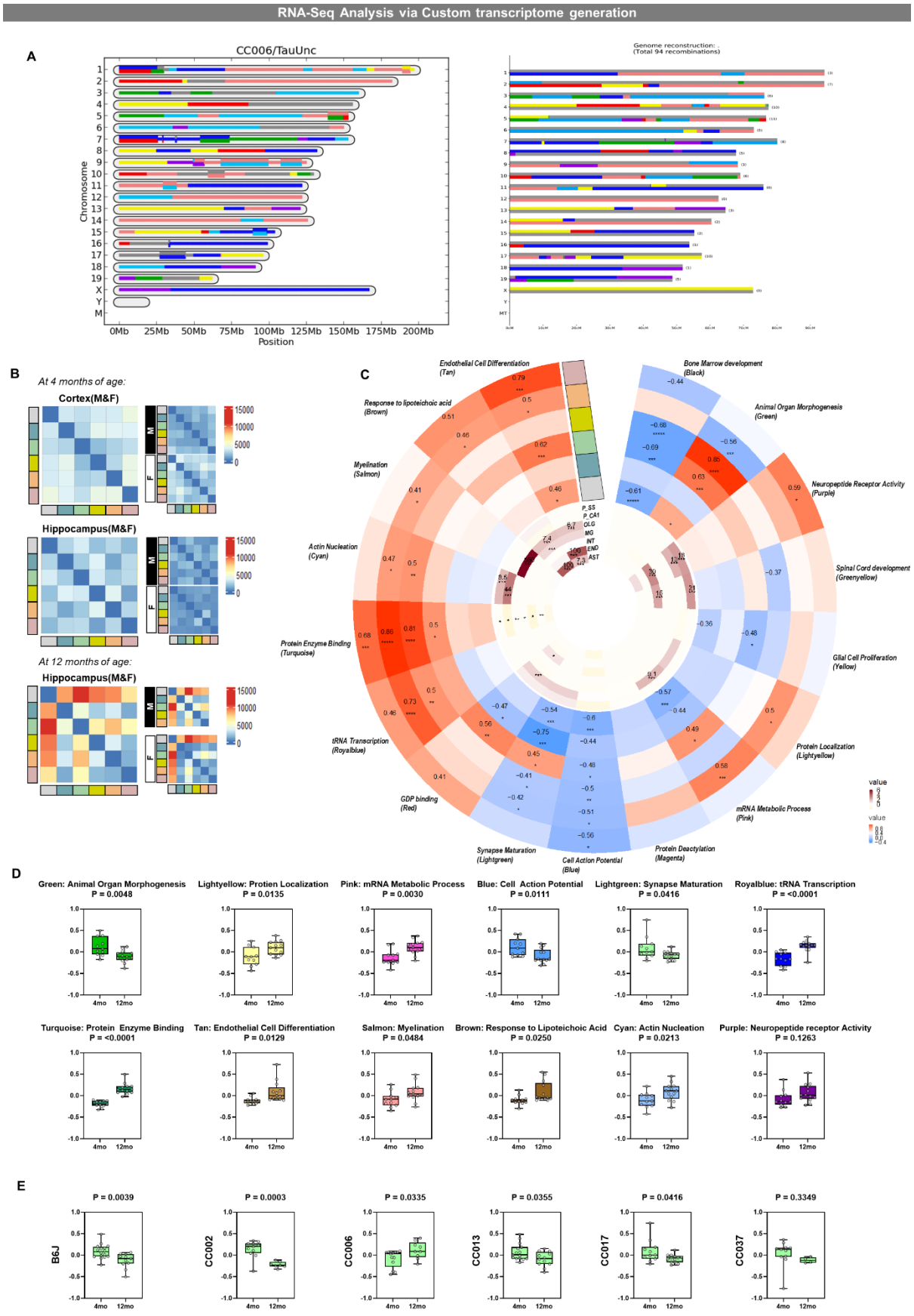

***Figure 14**: (**A**) Comparison between haplotype mosaic of the sequenced representative provided by JAX and generated by GBRS using the sample fastq files, showing only an 80% overlap. (**B**) Example of volcano plots generated for CC06 versus C57BL6/J mice (as proof of principal) for both males and females resulting in ~7000 DEGs (FDR ≤ 0.05; n = 6-8/group). Heatmaps of genetic changes in form of the number of differential genes between the F1 progeny of the collaborative cross and wild-type C57BL6/J mice in the cortex at the 4-month timepoint and hippocampus at the 4-month as well as the 12-month timepoint. Insets of samples separated by sex attached where the color shows the total number of differential genes between the comparisons. C. Circular heatmap depicting module-trait relationships generated to explore relationships between age as a variable from WGCNA (red represents positive correlation and blue represents negative correlation) and the cell type enrichment analysis (dark maroon symbolizes high enrichment and pale-yellow shows no enrichment) along with the GO-Elite pathway analysis (pathways with the highest combined score for each module selected. **D.** Module eigengene plots with the most significant differences are selected when comparing 4-month and 12- month timepoint for the F1 progeny of CC017 and wild-type C57BL6/J mice. The bar plot colors are associated to the module colors. E. Module eigengene plot for the LightGreen module shown across the lines to understand effects of directionality pertaining to the positive and negative correlation. The analysis only includes the non-transgenic mice i.e.no 5xFAD samples were included. Statistical significance is denoted by * p<0.05, ** p<0.01, ***p<0.001, ****p<0.0001.*

Statistical expression analysis: Once the custom transcriptome for the CC lines (CC06 shown as prelim data) was constructed with the required incorporated transgene and indexed, I used EMASE (Expectation-Maximization for Allele Specific Expression) (Raghupathy et al., 2018) and aligned our samples to their corresponding references to quantify allele specific expression at the gene and isoform levels. This would have generated not only the Total TPM (Transcripts per million) but contributions of the founder strains to the allele expression. However, the power due to the excessive number of strains led to allelic bias in the data. To ascertain the non-transgenic genetic changes between the different WT F1 progenies, we visualized total number of differential genes with heatmaps for the CC X C57BL6/J mice in the cortex at the 4-month timepoint and the hippocampus at the 4-month and 12-month timepoint. We normalized the scales across the three comparisons to visualize the relative changes across the brain regions and timepoints which reveal that in the hippocampus at 12-months, the homozygous C57BL6/J mice were genetically the most divergent from the other CC X C57BL6/J mice. To further investigate whether the changes observed were sex driven or not, we re-analyzed the sex-differentiated cohort of mice, and comparisons were plotted as heatmaps (**Figure 14B**). We explored the relationships of these genes' expression through changes seen in the network built using consensus weighted gene co-expression network analysis (cWGCNA) on the different non-transgenic heterozygous CC X C57BL6/J lines

(WT). The resulting network consisted of seventeen independent modules or communities of genes related to one another by their co-expression across 4-month and 12-month of age. We determined functional pathways represented by each consensus network module using gene ontology analysis (GO-Elite) on the genes comprised and based on the highest z-score we assigned primary ontology to each of the modules. Additionally, we assessed the cell-type nature of each module by determining if certain cell-type-specific protein markers were enriched within. Having a highly powered network with a significant correlation 0.1 and -0.1 being observed at FDR < 0.05 for most lines; we discerned a significant correlation of specific modules with certain cell-types/traits with the highest enrichment threshold assigned at 0.6. This revealed both lines and modules that are of unique interest, including the Myelination (Salmon) module that is enriched for oligodendrocytes (OLG) and the Neuropeptide Receptor Activity (Purple) module enriched for interneurons (INT) as well as CA1 (P_CA1) and somatosensory cortex pyramidal neurons (P_SS) (**Figure 14C**). Strikingly, a large fraction of the seventeen modules are significantly correlated to CC017 X C57BL6/J. Wanting to distinguish alterations caused by ageing, all module eigengenes were compared and plotted across the two different time points; 4- and 12-month; in the hippocampus. Based on their trajectories, these modules are classified as down-regulated (Green: Animal Organ Morphogenesis, Blue: Cell Action Potential, LightGreen: Synapse Maturation); up-regulated (LightYellow: Protein Localization, Pink: mRNA Metabolic Process, RoyalBlue: tRNA Transcription, Turquoise: Protein Enzyme Binding, Tan: Endothelial Cell Differentiation, Salmon: Myelination, Brown: Response to lipoteichoic acid, Cyan: Actin Nucleation, Purple: Neuropeptide receptor activity) and non-significant (Black, GreenYellow, Yellow, Magenta, Red) (**Figure 14D**). Interestingly, the synapse maturation module (LightGreen) is significantly regulated with respect to age and across the lines (**Figure 14E**). In summary, the analysis of WT (CC X C57BL6/J) F1 progeny of more than 400 brain tissues allows us to quantify gene

differences and construct a highly powered robust gene co-expression network, showing a replicated pattern of alterations correlated to age across lines; none of which are sex driven.

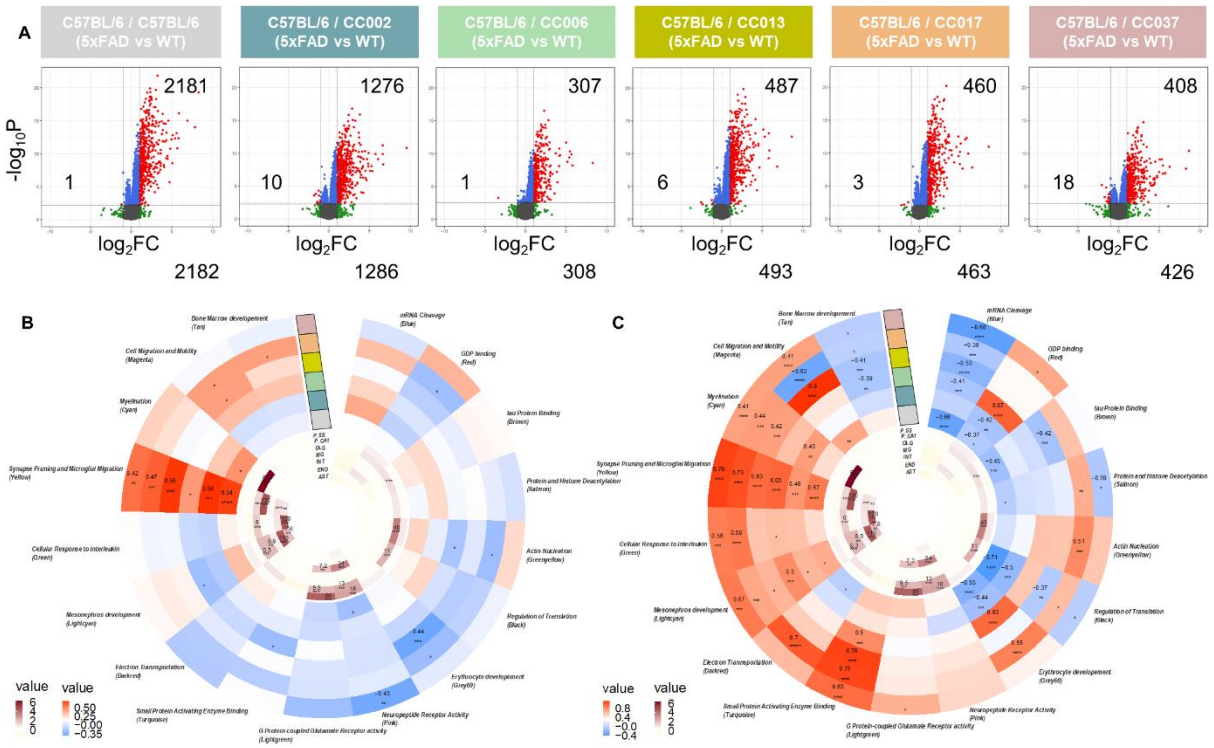

Figure 15: A. *Volcano plot of DEGs, displaying fold change of gene expression (log_2 scale) and P values ($-log_{10}$ scale) at 12-month timepoint in hippocampal tissue between wild-type vs 5xFAD. B. Circular heatmap depicting module-trait relationships generated to explore relationships between genotype (wild-type vs 5xFAD) as a variable from WGCNA (red represents positive correlation and blue represents negative correlation) and the cell type enrichment analysis (dark maroon symbolizes high enrichment and pale-yellow shows no enrichment) along with the GO-Elite pathway analysis (pathways with the highest combined score for each module selected). C. Circular heatmap depicting module-trait relationships generated to explore relationships between age (4-month vs 12-month) as a variable from WGCNA (red represents positive correlation and blue represents negative correlation) and the cell type enrichment analysis (dark maroon symbolizes high enrichment and pale-yellow shows no enrichment) along with the GO-Elite pathway analysis (pathways with the highest combined score for each module selected). The analysis includes all groups including wild-types and 5xFAD transgene carrying samples. Statistical significance is denoted by * p<0.05, ** p<0.01, ***p<0.001, ****p<0.0001.*

Assessing the genotypic impact of 5xFAD transgene on genetically diverse strains is fundamental in understanding the link between dysregulated biological processes and AD susceptibility of a strain. To characterize gene expression differences induced by the transgene between lines, RNA-seq analysis was performed comparing CC X C57BL6/J (WT) and CC X 5xFAD (AD-CCs) mice. Differentially expressed genes for 12-month-old hippocampal tissue comparing transgenic mice and their wild-type counterparts were visualized using volcano plots (grey: non-significant; green: |log2FoldChange| >1; red: FDR < 0.05 and blue:

|log2FoldChange| >1 & FDR < 0.05) (**Figure 15A**). To further explore the gene expression changes as a function of the genotype (presence and absence of 5xFAD), age (4- and 12-month-old), and gender (males and females), cWGCNA was performed; consistent to the WT datasets. We further discerned whether functional networks of these correlated genes are enriched for specific cell-types (with the highest enrichment threshold assigned at 0.6) and gene-ontology pathways (GO-Elite). The investigation of module-trait relationships resulted in seventeen different modules containing genes related to one another by their co-expression across genotype (**Figure 15B**) and age (**Figure 15C**), where the significant correlation 0.1 and -0.1 is observed at FDR < 0.05 for most lines. This unveiled modules of interest, one of which is Synapse pruning, and microglial migration (Yellow); the only module significantly up regulated as a result of genotype and enriched for microglial markers. Comparing the two networks, we find that most of the modules are significantly correlated to age, as opposed to the strain. Inferring that changes induced by pathology are largely conserved across diverse

backgrounds.

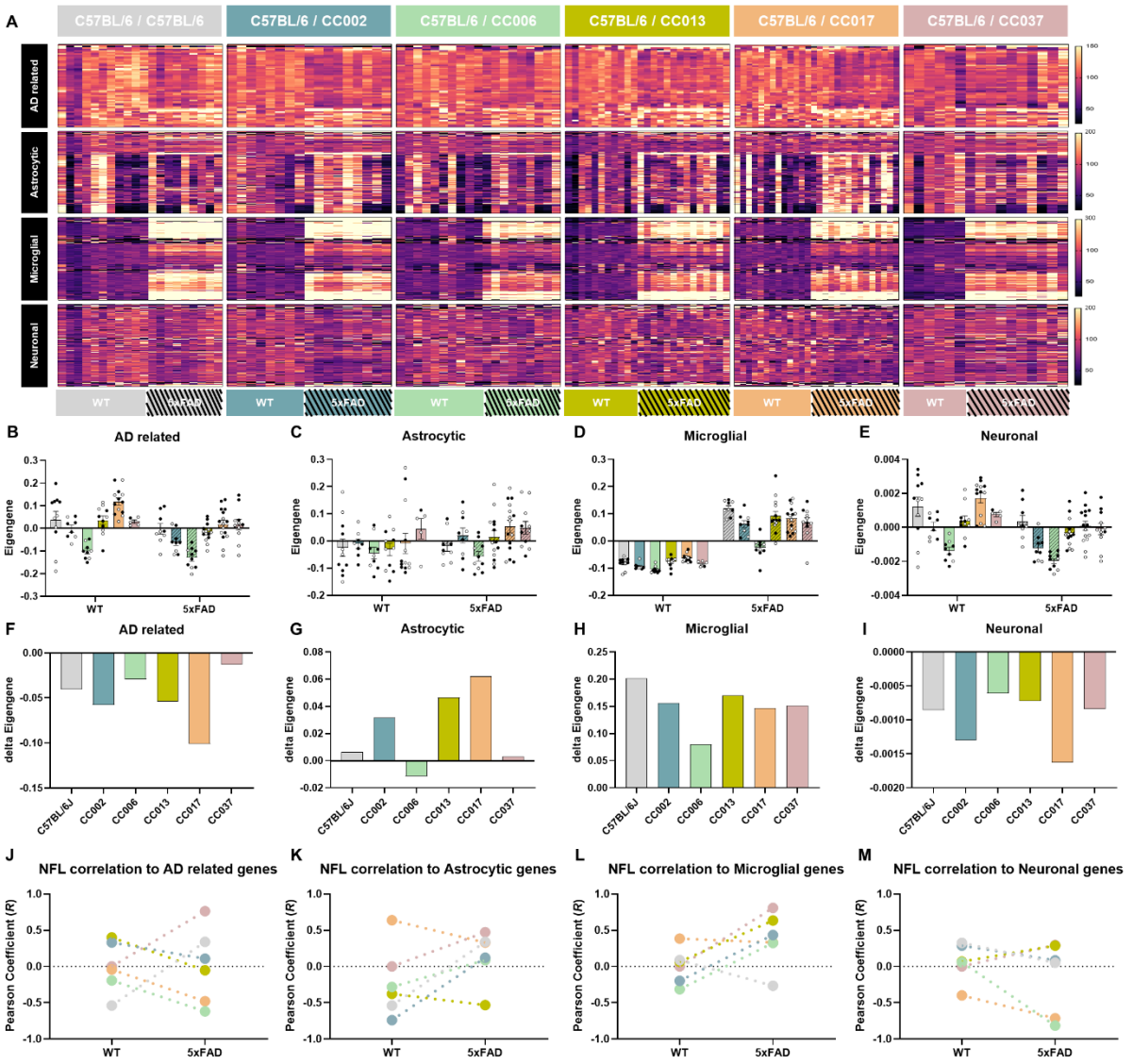

***Figure 16: A**. Heatmaps generated using curated gene lists (genes were included based on association of previous work) for all samples (wild-type and 5xFAD transgene carrying) across all lines. **B-E**. PC1 calculated from the heatmap generated for a. was used for bar eigengene plots across AD-related (**B**), astrocytic (**C**), microglial (**D**) and neuronal (**E**) gene lists for wild-type and 5xFAD transgenic collaborative cross lines. **F-I**. delta eigengene plots as bar plots across AD-related (**F**), astrocytic (**G**), microglial (**H**) and neuronal (**I**) gene lists for wild-type and 5xFAD transgenic collaborative cross lines. **J-M**. Dot plot of Pearson coefficients for correlation between plasma NfL levels in 12d. and AD-related (**J**), astrocytic (**K**), microglial (**L**) and neuronal (**M**) gene lists for wild-type and 5xFAD transgenic collaborative cross lines.*

Having looked at certain pathological and histological markers through IHC and assays, we decided to further investigate their transcriptional associations. Accordingly, four separate custom gene lists were curated using genetic databases distinguished by their AD-related, astrocytic, microglial or neuronal functions. We generated heatmaps using these curated lists across all the lines comprised of CC X C57BL6/J (WT) and CC X 5xFAD (AD-CCs) groups

(**Figure 16A**). These lists were utilized in calculating the eigengene value (PC1) for each of the sample using the principal component analysis which we then visualized using bar plots for all the groups (**Figure 16B-E**). Wanting to explore the correlation between these trends due to 5xFAD transgene overexpression, we computed delta eigengene values (5xFAD – WT) using wild-types as the basal values (**Figure 18F-I**). The AD-related eigengene values indicate that CC006 X C57BL6/J is the lowest, while CC017 X C57BL6/J is the highest. We observe a conserved trend among the transgenic groups, with CC006 X 5xFAD exhibiting the lowest AD-related eigengene value, while the remaining lines had similar levels (**Figure 16B**). The AD-related gene deltas are negative, indicating a genetic downregulation, with CC017 showing the greatest reduction and CC037 the least. (**Figure 16F**). The eigengene values of astrocytic genes are lowest in CC006 and highest in CC037, for both the wild type and AD-CC groups. This is supported by the downregulation of the astrocytic eigengene delta in CC006, whereas CC017 shows the highest upregulation (**Figure 16C,G**). Microglial eigengene shows a stark genotypic bias with WTs having negative PC values and all the AD-CCs having positive which is to be expected since the genes included were upregulated in the transgenic lines across all strains, due to the profound microglial response to plaques. Again, the lowest eigengene levels are seen in CC006 X C57BL6/J and CC006 X 5xFAD while the highest are observed in 5xFAD, validated by upregulation in the microglial gene deltas with CC006 being the least and C57BL6/J being the highest (**Figure 16D,H**). Lastly, the neuronal eigengene levels are the lowest for CC006 X C57BL6/J and CC006 X 5xFAD and the highest in C57BL6/J as well as CC017 X C57BL6/J (**Figure 16E**). The neuronal gene deltas show a downregulation across all lines with CC017 being the largest and CC006 and CC013 being the least (**Figure 16I**). Finally, we correlated the plasma N*f*L levels at the 12-month timepoint to the eigengene values to see trends that could have been overlooked. We visualized Pearson coefficients for correlation between plasma N*f*L levels using dot plots linking the wild-types to their 5xFAD transgenic

counterparts for AD-related, astrocytic, microglial and neuronal gene lists. C57BL6/J and CC037 show a positive correlation between the AD-related genes and the plasma N*f*L levels. The negative correlation observed in CC017 between astrocytic eigengene values and plasma N*f*L levels indicates that the upregulation of certain genes may be responsible for the reduced astrocytic response. C57BL6/J has a negative correlation between the plasma N*f*L levels and the microglial eigengene values. Similarly, CC006 has the largest negative correlation with respect to the neuronal eigengene values and plasma N*f*L levels (**Figure 16J-M**). Collectively, this data shows a strong correlation between the pathology seen and the transcriptional analysis conducted, where the lines C57BL6/J and CC037 seem to be plaque susceptible and CC006 and CC013 more plaque resistant.

Chapter 2.3. Mapping novel neuropathological-associated genetic loci to human Alzheimer's disease cases.

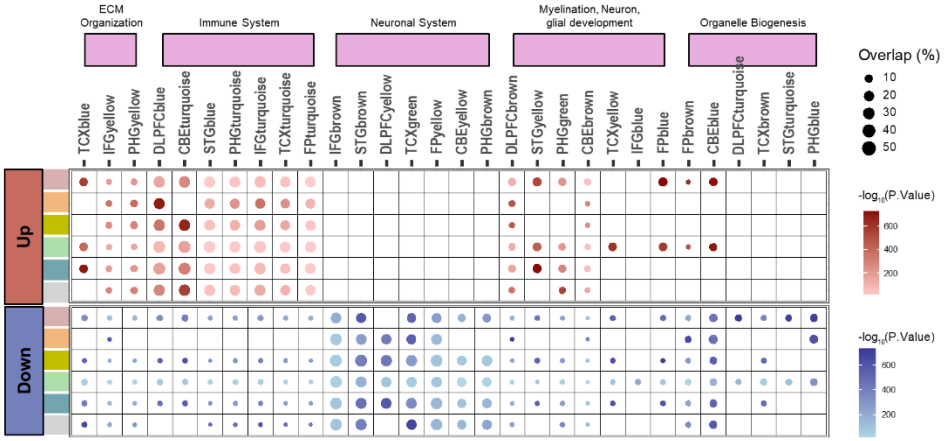

Figure 17: *Heatmap generated from DEG lists showcased in the volcano plots (**16A**) separated based on fold change of gene expression (log_2 scale) i.e., up and down regulation to display the overlap (%) to human amp-AD modules. The size and color of the color depends on the number and directionality of genes overlapping between the lists. The analysis includes all groups including wild-types and 5xFAD transgene carrying samples. Statistical significance is denoted by * p<0.05, ** p<0.01, ***p<0.001, ****p<0.0001.*

Homozygous C57BL6/J strain has the greatest number of differentially expressed up-regulated genes (2181) in comparison to the other lines. Notably, a large overlap is seen between the up- and down-regulated genes across the strains suggesting a conserved trend. We extended our

analysis to identify directional coherence by determining significant overlap between the 30 modules from the Accelerating Medicines Partnership Program for Alzheimer's Disease (AMP-AD) to our separated up- or down-regulated differential gene lists. Using Fisher test, correlation was computed (P.Value) and the extent of overlap was dependent on the percentage of genes overlapping. Both up- and down-regulated gene lists for the CC006 and CC037 showed significant overlap with the AMP-AD modules, especially with Myelination, Neuron, glial development (Cluster 4) as well as Organelle Biogenesis (Cluster 5) insinuating greater transcriptional similarities between the lines (CC006, CC037) and human AD (**Figure 17**).

Conclusions

AD is influenced by multiple genetic and environmental factors which are known to play a role in the development of AD, however, no single gene has been identified as the sole cause of the disease. These causative genetic variants may interact with each other and with environmental factors to increase the risk of developing the disease (Dunn et al., 2019). While researchers have made significant progress in identifying genetic risk factors for the disease, there is still much to learn about the complex interplay of genetic and environmental factors that contribute to the development of AD (Rojas-Rueda et al., 2021). To determine the mutual influence among variables (genetic and age) we introduced a genetically diverse population of mice – the AD-CCs - that have been generated by crossing eight genetically diverse founder strains, followed by inbreeding to create a panel of over 100 recombinant inbred strains to mimic the complex genetic makeup of human Alzheimer's disease (AD). Specifically, the genetic variation that was observed in the AD-CC exhibited a preserved epidemiological pattern that is also seen in human FAD patients (Prince et al., 2012), (Eratne et al., 2018), (Gao et al., 1998), (Livingston et al., 2017). Additionally, the transcriptional alterations across the AD-CCs compared to the WTs, especially at advanced stages of aging, exhibit a significant degree of

similarity with transcriptional changes seen in human patients with AD compared to age-matched controls. This overlap is observed in terms of the upregulation of inflammatory pathways (cellular response to interleukin) and the downregulation of neuronal signatures (dysregulation of mRNA cleavage), indicating the presence of shared molecular mechanisms between mice and humans. The findings of this study highlight the significant influence of genetic background in determining an individual's vulnerability to disease. Moreover, given the limited success in translating research using previous AD mouse models into effective treatments, the AD-CC panel presents itself as a valuable resource for identifying modifier genes that may have more relevance to human patients. Like the AD-BXD model (Neuner et al., 2019) our panel aims to provide valuable insights into not only the genetic basis of AD, but also its molecular and pathological phenotypes, as well as the response to interventions. Our hypothesis was that enhanced genetic background diversity could have a substantial impact on the development of complex pathological traits, thereby improving the translational relevance of animal models to human diseases and providing valuable insights into the pathways that regulate disease pathogenesis.

This diverse genetic panel enables us to investigate the relationship between phenotypic traits and genetic pathways and mechanisms that overlap between normal ageing and disease. Comparing the genetic mapping results across different lines would reveal the specific genotypes that contribute to modifying a phenotype, regardless of disease status. Moreover, it could identify AD-specific modifiers that exhibit allelic interactions with the 5xFAD transgene. With this goal in mind, our results surprisingly demonstrate concurrences as a result of diversity despite robust transcriptional alterations due to plaque formation. In particular, the lines appear to have analogous total soluble and insoluble Aβ40 and Aβ42 levels across brain regions and ages. In addition, single-cell transcriptome analysis of human datasets has been invaluable in establishing the correlation between genomic signals and immune-specific microglial gene

modules (Luquez et al., 2022). Genetic and molecular data indicate that microglia play a crucial role in Aβ accumulation, and recent research has also implicated an association with an astrocytic gene module (Fakhoury, 2018), (Rostami et al., 2021). Similarly, we observed parallels in glial responses, gene expression and N*f*L levels in cortex and plasma.

Additionally, with respect to the neuropathological diagnosis of AD, no differences were observed between sexes in terms of the plaque quantities across different ages and brain regions within the lines. Remarkably, plaque load was highest in 5xFAD congenic on C57BL6/J mice, with CC006 X 5xFAD and CC013 X 5xFAD being resistant to plaque production. Although its yet to be determined whether microglia are causal, contributory, or consequential to plaque formation (Stalder et al., 1999), (Zhao et al., 2017), (Casali et al., 2020), (Bolmont et al., 2008), CC006 X C57BL6/J was found to have the lowest microglial density across brain regions and age, suggesting a potential link between microglial density and AD-like pathology.

Another significant factor of the glial response was the alterations observed in reactive astrocytes due to plaques, with CC017 demonstrating the most substantial reduction in S100β and GFAP astrocytes across genotype and age. Despite this, there was an unexpected increase in the expression of astrocytic genes, while genes associated with AD and neurons were significantly downregulated. This suggests that the presence of plaques triggered an immune response and a process to remove toxic substances, but this response may not be sufficient to prevent damage or clear the plaques, leading to a decrease in the number of astrocytes. There are several possible explanations for this, including direct toxicity of plaques on astrocytes, the disease process itself leading to astrocyte loss, or a decrease in the brain's ability to repair and regenerate due to the loss of astrocytes, as has been suggested in prior research (Yshii et al., 2022), (Liddelow et al., 2017), (Robel et al., 2015).

Genetic diversity may also influence the brain's susceptibility to damage caused by plaque pathology (Shulman et al., 2013). As previously noted, there is evidence of varying levels of initial dysregulation of neuronal processes induced by plaques across different lines, providing support for this idea. Our findings suggest that cortex and plasma N*f*L can serve as a reliable biomarker of brain injury, which is closely associated with cortical thinning and cognitive decline in AD populations even in the presence of plaques (Bacioglu et al., 2016), (de Wolf et al., 2020), (S. Lee et al., 2022). We observed a strong correlation between plaque load and N*f*L levels, as evidenced by the brain insoluble fraction's N*f*L levels correlating with those in the plasma. Notably, CC006 X 5xFAD and CC013 X 5xFAD exhibited the lowest N*f*L levels across age, indicating a strong association between N*f*L levels and plaque load. Furthermore, this data also revealed a link to plaque resistance and glial response as CC017 X 5xFAD was shown to have the least astrocytic activation but higher N*f*L damage. Collectively, these results highlight how plaques can induce variation in damage on clinically relevant endpoints.

Ultimately, these results evidentiate C57BL/6 as an appropriate genetic background model for simulating AD, as it allows for the permissive development of plaques, along with suitable glial and gene expression changes in response to these plaques. Additionally, this background generates the highest level of plasma N*f*L per plaque, which is indicative of damage. In contrast to previous data (Neuner et al., 2019), our findings suggest that the introduction of eight different founder strains had a modulatory effect, unlike when crossing the DBA/2J strain with C57BL/6J, which appeared to produce mice with greater pathogenic diversity. However, regardless of this compensatory adjustment we saw some significant variation in the glial response and functions across genotypes. A previous study compared the C57BL6/J mouse strain with three wild-derived mouse strains (CAST/EiJ, WSB/EiJ, and PWK/PhJ), and the results of the Weighted Gene Co-expression Network Analysis (WGCNA) indicated significant differences in the transcriptomic profile and functional diversity of microglia

subtypes. These differences suggest that natural genetic variation may impact the microglia's initial response, response efficiency, and return to surveillance state, which is supported by our study's findings. (Yang et al., 2021). Nevertheless, there is evidence indicating that there is a consistent presence of plaque accumulation among these genotypes, which suggests that the C57BL6/J strain is resilient to neurodegeneration. (Onos et al., 2019).

An alternative explanation for the incongruity may be hybrid vigor and a potential solution could involve introducing the transgene into homozygous CC lines. While this approach may provide more insight into the disparity in the results, it is known to be experimentally challenging. In addition, a heterozygous population may be more representative of the human population.

COLLABORATIONS

Portions of Chapter Collaborations of this thesis/dissertation is a reprint of the material as it appears in (Hohsfield et al., 2020),(Hohsfield et al., 2021) , used with permission from Lindsay Hohsfield. Portions of Chapter Collaborations of this thesis/dissertation is a reprint of the material as it appears in (Henningfield et al., 2022), used with permission from Caden Henningfield.

Effects of long-term and brain-wide colonization of peripheral bone marrow-derived myeloid cells in the CNS *(Hohsfield et al., 2020)*

Data

Our investigation detected changes in myeloid cell expression, where we studied the impact of long-term peripheral myeloid cell engraftment at the transcriptional level. Previous studies have shown that microglial heterogeneity is region-specific and can be detected through RNA sequencing of bulk tissue in distinct brain regions. Therefore, we performed RNA sequencing analysis on three brain regions: cortex, hippocampus, and thalamus/striatum. The gene expression results can be found at http://rnaseq.mind.uci.edu/green/long-term_monocytes/.

To identify gene expression changes due to irradiation and the brain-wide presence of monocytes, we compared the transcriptomes of GFP-BM REPOP mice to controls (WT CON), which revealed 2695 differentially expressed genes (DEGs) across all brain regions. The effects were most prominent in the thalamus (2401 DEGs), followed by the hippocampus (370 DEGs), with few DEGs detected in the cortex (36 DEGs; **Figure C1:A**). We further analyzed transcriptional changes due to irradiation alone (WT-CON vs. GFP-BM CON) and the presence of monocytes (GFP-BM CON vs. GFP-BM REPOP; **Figure C1:A**) and presented the results as volcano plots (**Figure C1:B-D**). Our observations showed that the hippocampus and thalamus were more susceptible to irradiation-induced gene changes compared to the cortex,

which remained relatively unchanged. Additionally, the most significant transcriptional changes due to monocyte infiltration occurred exclusively in the hippocampus. Therefore, our findings demonstrate that different brain regions exhibit selective vulnerabilities to irradiation and the infiltration of monocytes. Finally, we were able to develop a unique long-term monocyte-related signature using the DEGs identified in the transcriptional comparison between WT CON vs. GFP-BM REPOP mice across all three brain regions. Among the genes most prominently upregulated in monocyte-engrafted mice were Apobec1, the chemokine receptor Ccr1, the C-type lectin Mrc1, and several members of the Ms4a cluster (Ms4a6b, Ms4a6c, and Ms4a7). To gain a more comprehensive understanding of the transcriptional changes associated with microglial-monocyte replacement and irradiation in three different brain regions, we conducted a weighted gene co-expression network analysis (WGCNA). We identified 22 distinct modules, each given a color-based name (**Figure C1:4F**) and analyzed their correlations with one another (Fig. S2B). We focused on modules that showed the highest correlation with monocyte presence in the brain and identified the darkgreen module (**Figure C1:G–I**), which consistently increased in GFP-BM REPOP mice across all three brain regions. Cell-type enrichment analysis demonstrated that darkgreen genes are myeloid-enriched and include peripheral myeloid-related genes. Pathway analyses showed that darkgreen genes are involved in response to other organisms, defense response to protozoa, response to external stimuli, defense response, and positive regulation of cytokine production. The functional protein-protein interaction network of genes in the darkgreen module highlighted those involved in defense response (**Figure C1:I**). We also identified several modules associated with irradiation across all three brain regions, including the salmon module (**Figure C1:J–K**), which is significantly enriched with interneuron genes and involved in cellular processes, gene expression, metabolism of RNA, processing of capped intron-containing pre-mRNA, mRNA splicing, and RNA polymerase II transcription. Our findings are consistent with the known

effects of irradiation on DNA damage and repair, with recent studies showing that splicing factors are recruited to sites of DNA damage. Several modules suggest that monocyte engraftment leads to a partial recovery of irradiation-induced effects, particularly in the hippocampus. We identified the brown module (**Figure C1:L–N**), which is highly enriched for astrocyte-expressed genes and involved in cilium organization, plasma membrane bounded cell projection assembly, cilium assembly, and cell projection organization. The functional protein-protein interaction network of genes in the brown module highlighted those involved in cilium organization. Analysis of cell enrichment showed that the brown module had a high concentration of genes expressed in astrocytes (astro) (**Figure C1:O**). The most significant Gene Ontology (GO) terms found in this module were related to the organization of cilia, the assembly of cell projections bounded by the plasma membrane, and the organization of cell projections. The genes in the brown module were mapped onto a protein-protein interaction network to highlight those involved in cilium organization (shown in red) (**Figure C1:N**). Our results indicate that irradiation and the presence of repopulating monocytes alter astrocyte and neuronal-related genes in the brain and exhibit distinct effects in different brain regions, including the cortex and hippocampus.

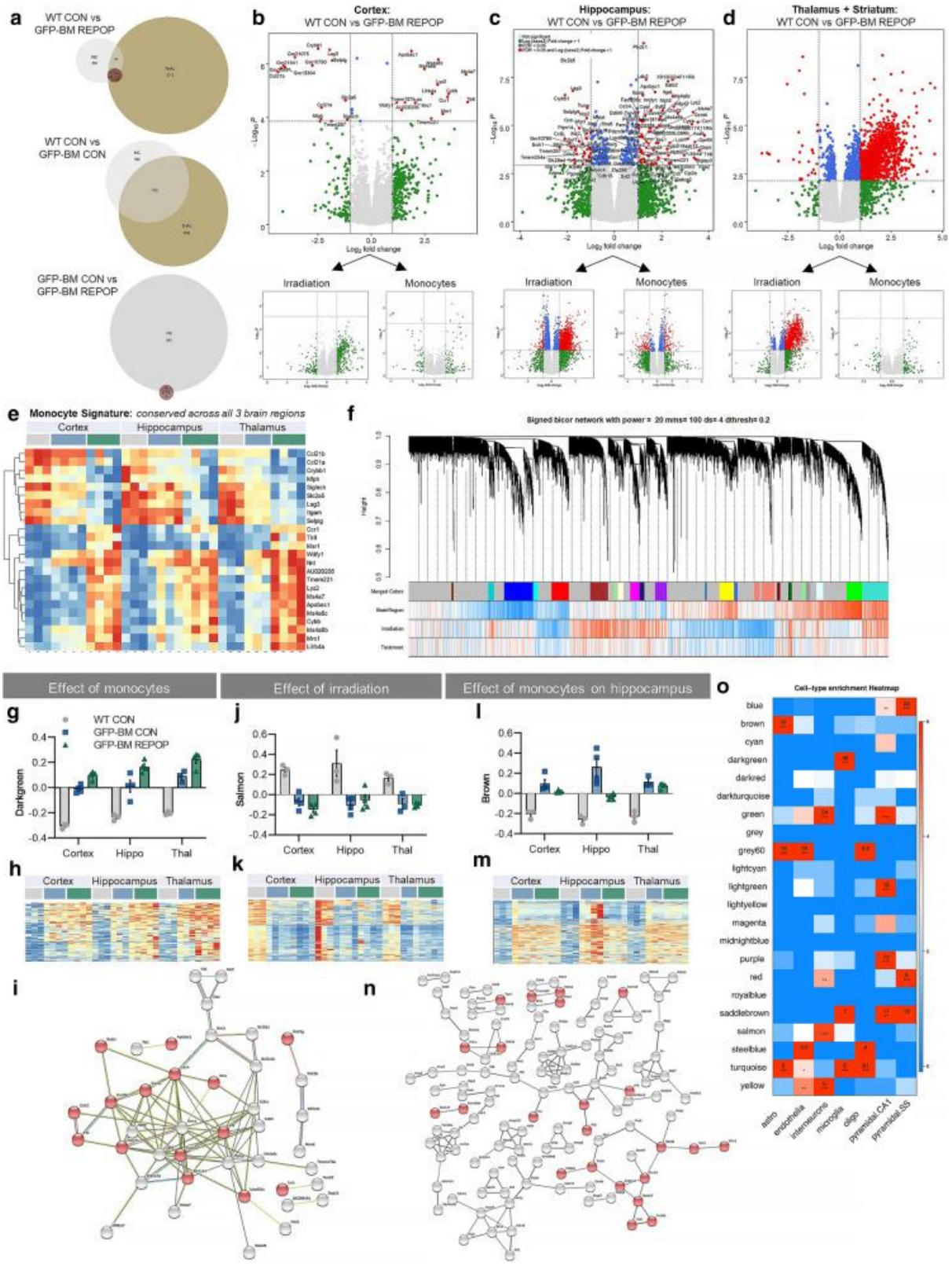

Figure C1: a *Venn diagrams displaying the number of differentially expressed genes (DEGs, numbers provided) generated in transcriptional comparisons between mice (control, WT CON; irradiated, GFP-BM CON; monocyte-engrafted, GFP-BM REPOP) in the hippocampus (HC, gray), cortex (CTX, red), and thalamus + striatum (THAL, tan).* ***b–d*** *Volcano plots displaying the fold change of genes (log2 scale) and their p values (−log10 scale) between WT CON vs GFP-BM REPOP in the cortex (**b**), hippocampus (**c**), and thalamus + striatum (**d**). Plots are further separated by the effect of irradiation and presence of monocytes alone.* ***e*** *Heatmap of the*

monocyte signature (selected DEGs conserved in all three brain regions in monocyte-engrafted mice). ***f*** *Signed bicor network shows the effects of brain region (BrainRegion), irradiation, and treatment, which are separated into distinct colored modules.* ***g***–***i*** *Monocyte signature: Module eigengene trajectory of darkgreen (****g****), heatmap of gene expression value in darkgreen (****h****), and a STRING interaction map of darkgreen (****i****). Red nodes indicate genes enriched in the gene ontology (GO) term defense response. (****j****–****k****) Irradiation: Module eigengene trajectory of salmon (****j****) and heatmap of gene expression value in salmon (K).* ***l***–***n*** *Effects of monocytes specific to the hippocampus: Module eigengene trajectory of red (****l****), heatmap of gene expression value in red (****m****), and a STRING interaction map of red (****n****). Red nodes indicate genes enriched in the GO term cilium organization. o Cell-type enrichment heatmap displays genes associated with specific cell types within a given color module. Values provided indicate the number of genes within the network associated with that a specific cell type. *** = 6+ genes. ** = 3+ genes.*

Conclusion

Monocytes are myeloid cells that can differentiate into tissue-specific macrophages in various organs, including the central nervous system (CNS). Their role in the CNS and their long-term effects on the brain are not well understood. A study developed a paradigm to achieve near-complete and long-term engraftment of peripheral-derived myeloid cells (monocytes) in the brain. The study found that monocytes can outcompete endogenous microglia under specific conditions and can fill the microglial niche in the brain. However, monocytes remain phenotypically, transcriptionally, epigenetically, and functionally distinct from their microglial counterparts, and this difference can have long-term consequences on the brain (Cronk et al., 2018), (Bennett et al., 2018), (Lund et al., 2018), (Shemer et al., 2018). The study evaluated mice for transcriptional, cellular, and behavioral changes six months following monocyte engraftment into the CNS. The vulnerable brain regions to irradiation were determined through transcriptional analysis, revealing the thalamus and hippocampus as the most affected. Further analysis showed that only the hippocampus experienced significant translational changes in response to monocyte infiltration. WGCNA analysis identified several modules that reversed the effects of irradiation after monocyte engraftment, exclusively in the hippocampus. Pathway analysis revealed mechanisms involving cilium organization and assembly. A recent study using granulocyte colony-stimulating factor (GCSF) receptor knockout mice and BM transplant showed that BM cells responding to G-CSF promoted brain repair and neural progenitor cell proliferation in the irradiated brain (Dietrich et al., 2018). Engrafted monocytes

exhibited a distinct gene signature compared to microglia following 6 months of recovery from CSF1Ri administration and 10 months after irradiation. The monocyte signature included upregulation in *Ccr1*, *Ms4a6b*, *Ms4a6c*, *Ms4a7*, *AU020206*, *Apobec1*, *Lyz2*, *Mrc1*, *Tmem221*, *Tlr8*, *Lilrb4a*, *Msr1*, *Nnt*, and *Wdfy1*, coinciding with downregulation of *Siglech*, *Itgam*, *Selpig*, *Lag3*, *Slc2a5*, *Mlph*, *Crybb1*, *Ccl21a*, and *Ccl21b*. *Tlr8*, predominantly expressed on peripheral blood leukocytes, was the only gene that overlapped between brain-extracted monocytes and engrafted monocytes (Cronk et al., 2018). This finding highlights the critical role that extraction techniques and time in the brain play in monocyte gene expression. The study found that irradiation reduced astrocyte and *MAP2* numbers, which are important for neural plasticity and normal neuronal cytoskeletal structure, while monocyte engraftment elevated astrocyte numbers past control levels in both the cortex and hippocampus (Sterpka & Chen, 2018), (Yuan & Sun, 2013). The study also found alterations in synaptic markers, with brain region-specific vulnerability to irradiation and monocyte engraftment. The study showed that irradiation caused alterations in behavior, specifically in locomotive activity and working memory, and that monocyte engraftment did not significantly alter cognitive function (Cronk et al., 2018). Overall, the study suggests that monocyte-astrocyte crosstalk could be possible and that replacing microglia with monocytes may help facilitate primary cilia integrity lost due to irradiation (Chen et al., 2017). However, further work is needed to explore these long-term engrafted monocyte-synapse interactions.

Subventricular zone/white matter microglia reconstitute the empty adult microglial niche in a dynamic wave *(Hohsfield et al., 2021)*

Data

We analyzed the mRNA transcript levels of whole brain hemispheres from control, 14 day PLX3397-treated, 7 day recovery, and 28 day recovery samples using a Nanostring Immune

Profiling panel, which includes approximately 700 genes related to immunology (**Figure C2: J**), in order to gain insight into the transcriptional profile of WM repopulating cells. By comparing the gene expression profile of the initial repopulating cells in 14 day PLX3397-treated brains (which lack microglia) to 7 day recovery brains, we found that the most upregulated genes in the latter are related to myeloid cell activation/priming, pathogen sensing, and monocyte-macrophage signaling, such as *Mrc1*, *C3ar1*, *Ccl12*, *Clec7a*, *Ccr2*/*Ccl2*, *Cybb*, and *Ccl9*, instead of homeostatic microglia signature genes (**Figure C2:K**). Furthermore, comparing 28 day recovery brains to controls, we detected increased expression of several genes associated with myeloid cell signaling (*Ccl8*, *Cmah*, *Ly9*, *Lyz2*, *Tlr8*, *C4b*), especially major histocompatibility complex I (*H2-D1*) and II (*H2-Aa*, *H2-Ab1*, *Cd74*) components and microglial priming (*Clec7a*, *Cybb*) (**Figure C2:L**).

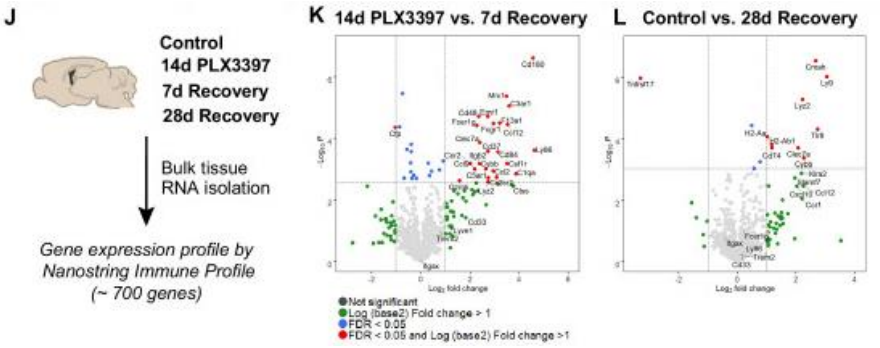

Figure C2: *(**J**) Control, 14 day PLX3397, 7 day recovery, and 28 day recovery mouse hemispheres were collected and analyzed for bulk-tissue gene expression changes using Nanostring Immune Profile. (**K**–**L**) Volcano plots displaying the fold change of genes (log2 scale) and their significance (y axis, -log10 scale) between 14 day PLX3397 depleted vs. 7 day recovery mice (**K**) and control vs 28 day recovery (**L**). Data are represented as mean ± SEM (n=3–5). *p < 0.05, ** p < 0.01, *** p < 0.001; significance symbols represent comparisons between groups: control *, 0d #, 3d ◊, 7d Δ, 14d Φ. CC, corpus callosum; CP, caudoputamen; CTX, cortex; HC, hippocampus; LV, lateral ventricle; SVZ, subventricular zone; WM, white matter.*

In order to investigate the changes in gene expression that occur in the SVZ during the early stages of WM repopulation, we dissected the SVZ from control, 14 day PLX3397-treated, and 5 day recovery mice and conducted RNA-seq analyses on bulk tissue gene expression (**Figure C3:A**). The gene expression data is available for exploration at http://rnaseq.mind.uci.edu/green/alt_repop_svz/gene_search.php. A comparison of control vs.

5 day recovery mice revealed 227 differentially expressed genes (DEGs) (FDR < 0.05) between the two groups, with the majority of DEGs being downregulated microglia-enriched/related genes, reflecting the reduced pool of myeloid cells in the CNS during the early stages of repopulation (**Figure C3:B**). On the other hand, upregulated non-myeloid enriched DEGs in depleted vs. 5 day recovery mice (Figure 6B) consisted of genes involved in cell cycle regulation, DNA transcription/recombination/repair/expression, cell adhesion/migration/proliferation, and development. Gene ontology (GO) analysis of DEGs between control and 5 day recovery SVZ tissue identified the following top four enriched pathways: myeloid cell differentiation, leukocyte immunity, leukocyte activation, and leukocyte chemotaxis and phagocytosis (**Figure C3:C**). Specifically, focusing on myeloid genes, we found that *P2ry12*, *Siglech*, *Trem2*, *Cd33*, and *Cx3cr1* were least enriched during initial repopulation, whereas *Ccl12*, *Cd52*, *Lyz2*, *Itgb2*, and *Cd84* were highly enriched **(Figure C3:D**). To further investigate the biological significance of these findings and the impact of the loss of one of these critical genes/signals on early repopulation dynamics, we administered an antibody against *CCL12*, the most highly upregulated gene during early WM repopulation (**Figure C3:E**). Our results demonstrate that neutralization of *CCL12* leads to a significant reduction in repopulating cell numbers at 7 day recovery, but not total distance of cell spreading (**Figure C3:F–H**), indicating that this chemokine may play an important role in early repopulating cell proliferation or survival. Overall, these findings shed light on the crucial role of the SVZ and signaling during the early stages of WM repopulation.

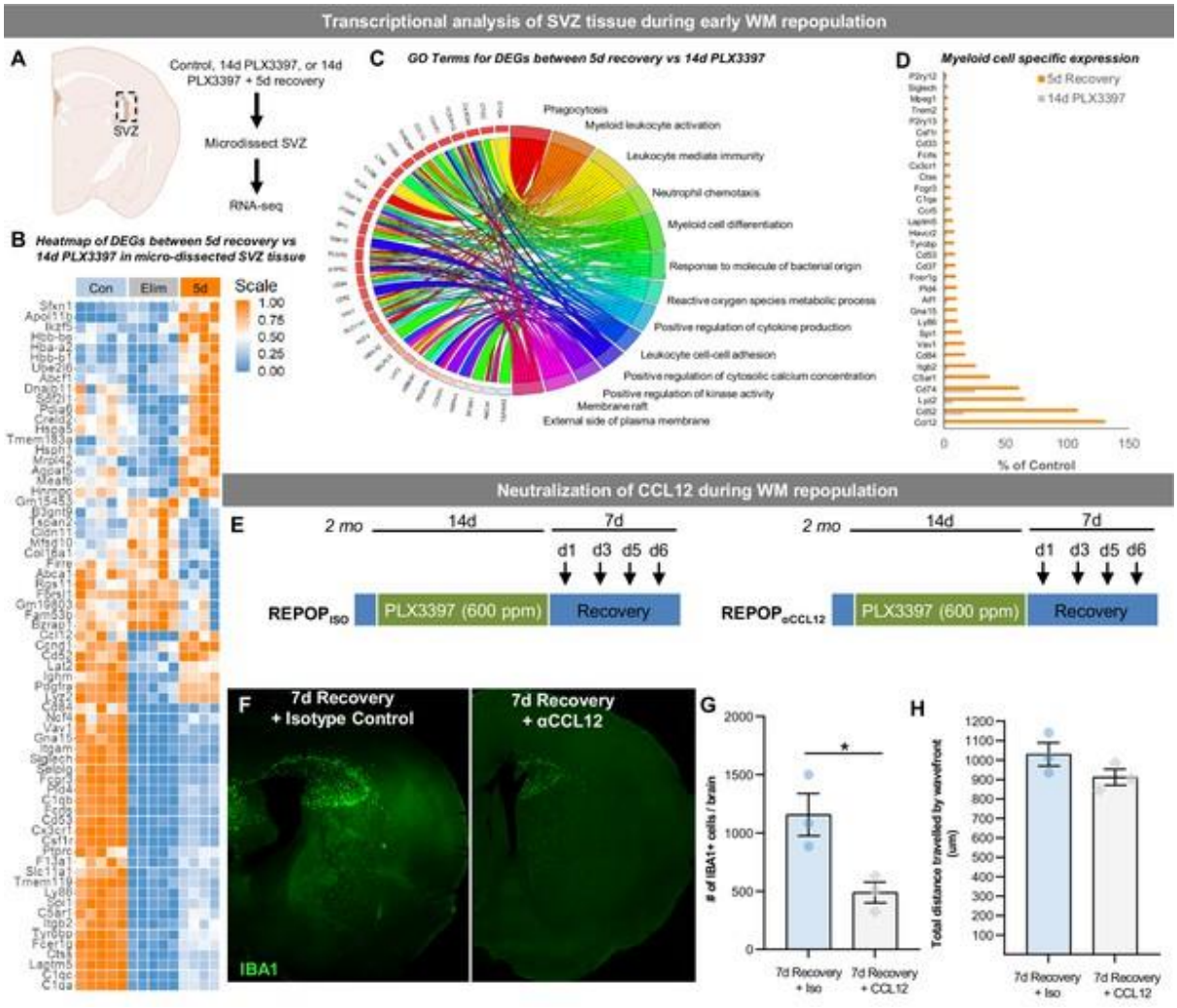

Figure C3: *(A–D) Transcriptional analysis of SVZ tissue during early WM repopulation. (A) Bulk tissue RNA-seq analysis was performed on micro-dissected SVZ tissue from control, 14 day PLX3397, and 5 day recovery brains (n=5).* ***(B)*** *Heatmap of DEGs between 14 day PLX3397 (Elim) and 5 day recovery SVZ tissue. Gene expression data can be explored at http://rnaseq.mind.uci.edu/green/alt_repop_svz/gene_search.php.* ***(C)*** *Gene ontology chord plot of DEGs between control and 5 day SVZ tissue.* ***(D)*** *Plot highlighting expression (% of control) changes in myeloid-associated genes in depleted (14d PLX3397) and repopulated (5d recovery) SVZ tissue.* ***(E–H)*** *Neutralization of CCL12 during WM repopulation.* ***(E)*** *Experiment schematic of CCL12 neutralization study: 2-month-old WT mice were treated for 14 days with PLX3397 (600 ppm) and then placed on control diet for 7 days allowing for WM repopulation. Four i.p. injections were administered of anti-CCL12 antibody or goat IgG (Isotype control) at 1 day recovery, 3 day recovery, 5 day recovery, and 6 day recovery.* ***(F)*** *Representative whole brain images of IBA1+ cell (green) deposition following treatment.* ***(G–H)*** *Quantification of number of total IBA1+ cells and total distance traveled by IBA1+ wavefront in* ***(F)****. Total distance was calculated by measuring the length from the ventricular edge of SVZ to the leading edge of the IBA1+ cell wavefront.*

Our next objective was to gain understanding of the transcriptional profile of WM repopulating cells once they have taken residence in the brain. Additionally, we explored whether any phenotypic and transcriptional alterations in these cells had functional consequences by examining their response to immune challenge through LPS administration (**Figure C4:A**). To

achieve this, we conducted RNA sequencing (RNAseq) on FACS-sorted CD11b+CD45int cells from control and 28-day recovery mice at 6 and 24 hours after LPS-induced immune challenge. RNA-seq analysis was conducted on FACS-sorted CD11b+CD45int cells to establish a high-resolution transcriptome profile in the presence and absence of LPS. Gene expression data is available at http://rnaseq.mind.uci.edu/green/alt_repop_lps/gene_search.php. Unlike the GLOBAL repopulation, where there are few transcriptional differences between control and repopulating cells (25 DEGs in GLOBAL vs. control), we identified 69 DEGs in WM repopulated myeloid cells compared to control microglia in the absence of LPS (logFC > 1, FDR > 0.05; **Figure C4:B**). The top five enriched pathways in DEGs between control and 28 day repopulated cells were regulation of cellular component size, negative regulator of chemotaxis, ameboidal-type cell migration, negative regulation of response to external stimulus, and wound healing (**Figure C4:C**). To compare the gene expression profile of these cells with other myeloid cell subsets, we used previously established myeloid cell signatures, including homeostatic microglia, HSC/BM-derived myeloid cells, BAMs/CAMs, DAMs/MGnD/ARMs, PAMs/ATMs, and WAMs. Repopulating cells showed robust enrichment of DAM and WAM-associated genes, including *Clec7a*, *Axl*, *Apoe*, *Cst7*, *Ctsd*, and *Ly9* (**Figure C4:D**). *AXL* and *CLEC7A*, recently identified as WAM markers, were immunostained in repopulating myeloid cells, particularly in the early stages of repopulation and in cells located at the wavefront, but were not detected in microglia from control brains (**Figure C4:E–F**). In addition, *Sall1*, a transcription factor unique to microglia, showed a reduction in expression in repopulating compared to homeostatic microglia. After observing distinctive differences in transcriptomes between control and 28-day recovery isolated microglia at 0 hr LPS (in the absence of LPS), we proceeded to examine their gene expression patterns at 6 hr and 24 hr following LPS challenge. Principal component analysis demonstrated strong correlations between biological replicates, with samples

clustering into six distinct groups (**Figure C4:G**). Using K-means clustering, we identified nine gene clusters (**Figure C4:H**) and found that Cluster 3 contained genes that were significantly different between control and repopulating cells across all time points, including genes associated with clearance, cell growth/differentiation, stress, inflammation, and senescence. Clusters 2, 5, 7, and 8 showed differential responses to LPS at the 24 hr timepoint between control and repopulating cells (**Figure C4:I**). GO term analysis of Cluster 3 showed enrichment in phagopore assembly site membrane, extrinsic component of membrane, and endosome pathways. Cluster 8 showed enrichment in negative regulation of glucocorticoid secretion, negative regulation of interleukin-1 mediated signaling pathway, and connective tissue replacement involved in inflammatory response wound healing pathways. These findings suggest that WM repopulating cells are transcriptionally and functionally distinct from adult homeostatic microglia and share similarities with a subset of WAMs, which are absent in the adult mouse brain but constitute 20% of microglia in the aged mouse brain. Further investigations are required to determine if these WM repopulating cells exist in the naïve brain as WAMs or if CSF1Ri treatment induces this phenotype. Additionally, more research is necessary to explore the contributions and potential cross talk with astrocytes and other cell types during repopulation.

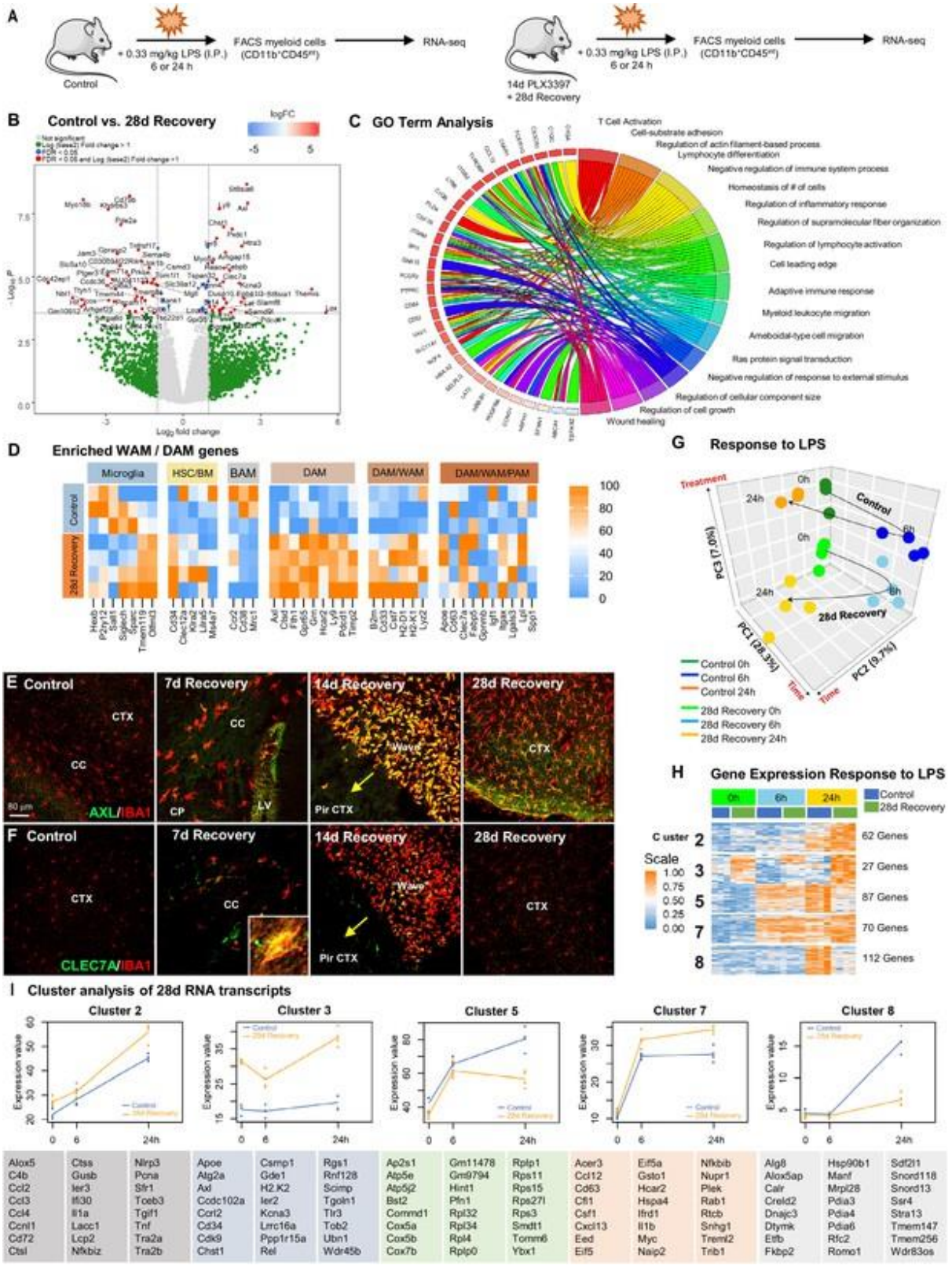

Figure C4: *(**A**) Two-month-old WT control or 28 day recovery mice were given intraperitoneal injections of either PBS or LPS (0.33 mg/kg) and then collected at 6 or 24 hr post injection. Controls, which were mice that did not receive LPS, are referred to as 0 hr post LPS. Myeloid cells were extracted from whole brain hemispheres, isolated using FACS gating for CD11b+CD45int and processed for RNA-seq. (**B**) Volcano plots displaying the fold change of genes (log2 scale) and their significance (y axis, -log10 scale) between control vs. 28 day recovery mice. (**C**) Gene ontology chord plot of DEGs between control and 28 day recovery myeloid cells. (**D**) Heatmap showing*

*expression of genes enriched in DAM, HSC/BM-derived cells, canonical microglia, BAM, PAM, and WAM signatures in control and 28 day repopulating myeloid cells. (**E**–**F**) Representative immunofluorescence 20x images of IBA1+ (red) and AXL+ (green, **I**) or CLEC7A+ (green, **J**) cells shown in areas with high repopulating cell deposition in control, 7, 14, and 28 day recovery mice. (**G**) Principal component analysis plot of extracted control and 28 day recovery cells, across time (0 hr, 6 hr, 24 hr) and treatment (+/- LPS), depicting the separation of groups into six clusters. (**H**) Heatmap of selected time-series cluster analysis of control and 28 day recovery cells. Provided number indicates number of genes per cluster. (**I**) Time-series cluster analysis of control vs. 28 day recovery myeloid cell response (during WM repopulation) to LPS challenge following 14 day PLX3397 (600 ppm in chow; from **H**). Clusters showing distinct responses to LPS between control and 28 day WM repopulated cells, across time, were plotted as eigengene values, along with the top represented genes within each cluster. Data are represented as mean ± SEM (n=3–5). *p < 0.05, ** p < 0.01, *** p < 0.001. CP, caudoputamen; CC, corpus callosum; CTX, cortex; LV, lateral ventricle; PirCTX, piriform cortex. Gene expression data can be explored at http://rnaseq.mind.uci.edu/green/alt_repop_lps/gene_search.php.*

In order to discern whether the phenotypic and transcriptional variances observed in WM repopulating microglia are due to a delayed recovery of the microglial phenotype (temporary) or sustained changes after a longer period of recovery (indicative of a distinct cell subtype), we subjected 2-month-old wild-type mice to treatment with PLX3397 for 14 days followed by 3 months of recovery (**Figure C5:A-B**). Our morphological analysis of IBA1+ cells revealed that WM repopulating cells maintain reduced cell density (**Figure C5:C**) and amoeboid-like cell features, including larger cell body size (**Figure C5:D**), reduced number of processes (*Figure C5:E*), and reduced process length (**Figure C5:F**). Furthermore, our bulk tissue RNAseq analysis (**Figure C5:H**) demonstrated that transcriptional differences persist in the brain even three months after CSF1Ri withdrawal (**Figure C5:I**). Similar to previous WM repopulation timepoints, differential expression gene (DEG) analysis revealed a downregulation of the homeostatic-associated microglial gene *P2ry12* and upregulation of the DAM/WAM-associated genes *Clec7a* (**Figure C5:I-J**). Gene ontology (GO) term analysis indicated that upregulated DEGs are involved in neuron projection development, axon guidance, synaptic transmission, and synaptic potential, which provides evidence that WM repopulating cells may play a vital role in axonal homeostasis. Taken together, our findings suggest that WM repopulating microglia constitute a distinct population of myeloid cells rather than a delayed recovery of the microglial phenotype.

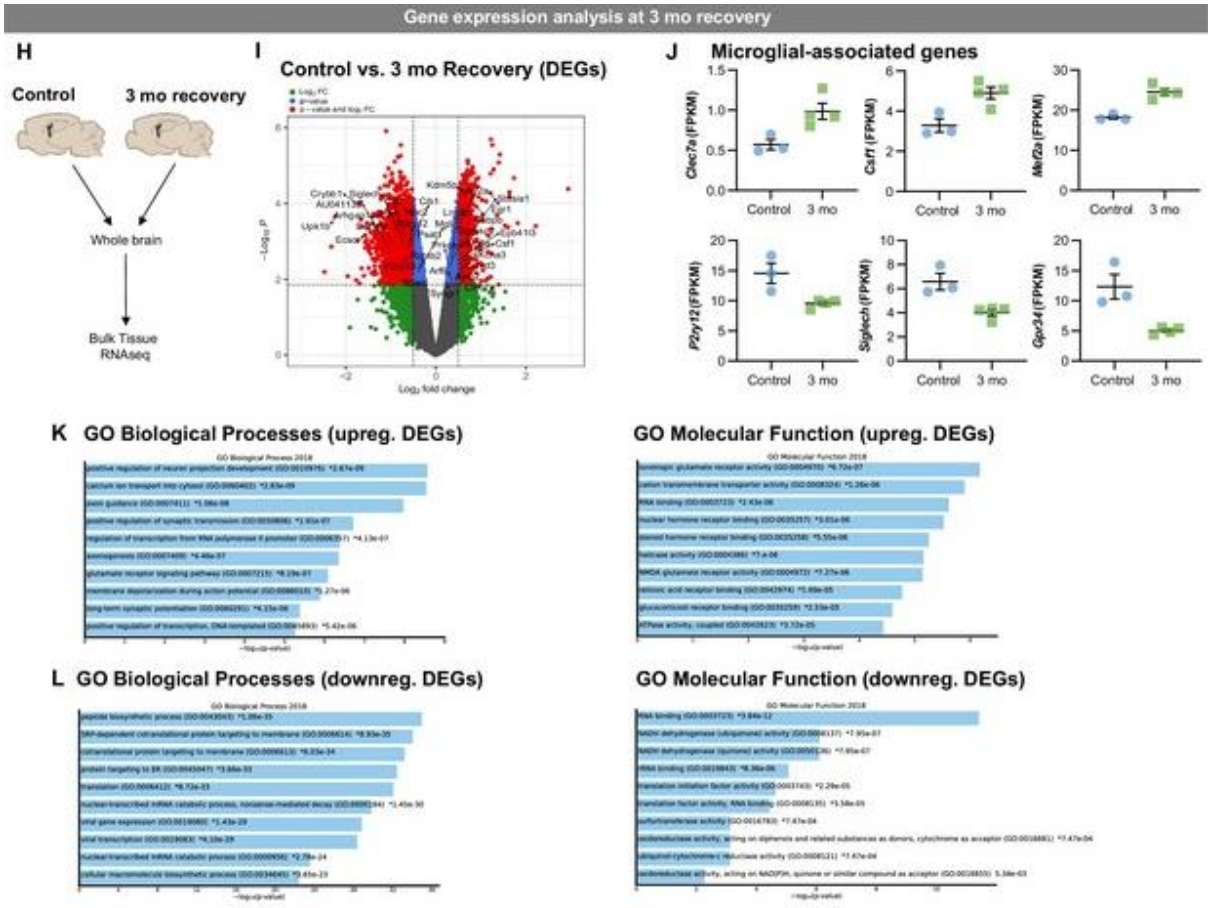

Figure C5: *Two-month-old WT mice treated with vehicle or PLX3397 (600 ppm in chow) for 14 days. Chow was then withdrawn, and animals were allowed to recover on control diet for three months, assessing the long-term effects of filling the brain with WM repopulated myeloid cells.* ***(H-L)*** *Transcriptional analysis of 3-month recovery WM repopulation brain tissue.* ***(A)*** *Bulk tissue RNA-seq analysis was performed on whole brain hemispheres from control and 3-month recovery brains.* ***(I)*** *Volcano plot displaying the fold change of DEGs (log2 scale) and their significance (y axis, -log10 scale) between control vs. 3 month recovery.* ***(J)*** *Quantification of relative expression (FPKM, fragments per kilobase of transcript per million) for microglial-associated genes in control and 3 month recovery brain tissue.* ***(K-L)*** *Gene ontology analysis of upregulated* ***(K)*** *and downregulated* ***(L)*** *DEGs between control and 3 month recovery mice. Data are represented as mean ± SEM (n=3-4). * $p < 0.05$, ** $p < 0.01$. DG, dentate gyrus; SS CTX, somatosensory cortex; Pir CTX, piriform cortex.*

Conclusion

Microglia are important cells in the central nervous system (CNS) and their origins were once controversial. It is now known that microglia come from yolk sac-derived erythromyeloid progenitors (Ginhoux & Prinz, 2015). Adult microglia require CSF1R signaling for survival, and when *CSF1R* inhibitors are used to eliminate microglia, subsequent withdrawal of the inhibitors results in rapid microglial repopulation from surviving microglia (Elmore et al., 2014), (Zhan et al., 2019), (Najafi et al., 2018). This makes it difficult to study the contribution of specific myeloid cell subtypes to the adult CNS, so a paradigm without notable surviving

microglia was developed (Elmore et al., 2018). Researchers have achieved 99.98% microglial depletion in the brain using sustained high-dose CSF1Ri administration, leading to the identification of a CNS myeloid cell subset that repopulates the brain parenchyma from SVZ/WM areas without contributions from the periphery. This type of repopulation is called WM repopulation and involves specific spatiotemporal patterns and a dynamic migratory wave of proliferating cells. Previous attempts to achieve an empty microglial niche have fallen short, and incomplete microglial elimination leads to repopulation from surviving microglia, including cortical microglia. Peripheral BM-derived myeloid cells do not contribute to CNS myeloid cell repopulation in the absence of toxin, irradiation, or injury (Lund et al., 2018), (Bruttger et al., 2015). Cells that repopulate the brain after damage initially appear in specific neuroanatomical niches, starting in the SVZ, before spreading throughout the brain via WM tracts. The caudoputamen is closely associated with these niches, which may explain why certain areas see more repopulating cell deposition. This distribution pattern is similar to the colonization and distribution of microglia during development, with microglia entering the brain via ventricular routes and remaining restricted in WM zones before migrating out to the rest of the brain (Tay et al., 2017), (Ueno et al., 2013), (Verney et al., 2010), (Ginhoux et al., 2013). These findings highlight important anatomical structures that facilitate cell migration in an empty microglial niche, which play a role in both development and adult brain function. However, the repopulating cells are not believed to be microglial precursors. We used a microglial depletion and repopulation method to identify a unique subset of myeloid cells in the SVZ/WM area that serve as the source for WM repopulating cells. Our novel paradigm replaces microglia with Cx3cr1+ myeloid cells originating from the SVZ and associated WM areas, allowing us to study their biology and adaptation to extrinsic environmental cues from grey matter. SVZ/WM myeloid cells are initially resistant to CSF1R inhibition due to unique properties of the SVZ environment, but once WM repopulating cells take up residence in other

areas, they become susceptible to CSF1Ri treatment (Lavin et al., 2014), (Lavin et al., 2014). The local niche or microenvironment plays a role in establishing macrophage identity, and a combination of factors may contribute to the uniqueness of SVZ/WM microglia and their enhanced survival (Easley-Neal et al., 2019), (Zheng et al., 2017). It remains unclear if PLX3397 concentration levels are lower in specific brain regions. Previous research suggests that while CSF1 and CSF1R are critical for macrophage survival, other factors like GM-CSF and IL-3 may also play a role (Rojo et al., 2019), (Pixley & Stanley, 2004). Recent studies on mice and zebrafish indicate that certain microglia populations may be partially resistant to CSF1R and rely on alternative survival factors. A recent study found a CSF1R-resistant microglial population, but its contribution to repopulation is unclear, as the overall repopulation dynamics were like the control group (Zhan et al., 2020). Therefore, this identified population is unlikely to significantly contribute to WM repopulation. Recent studies have shown the existence of unique microglial cells in brain-specific regions, such as the SVZ/WM, with distinct identities and properties (Zhan et al., 2020), (Li et al., 2019), (Stratoulias et al., 2019), (Tan et al., 2020). These cells maintain altered phenotypes and responses to LPS, suggesting that they are highly distinct from other microglia. SVZ microglia are less branched, express surface markers associated with an alternatively active phenotype, and exhibit unique gene expression patterns. In humans, microglia in the SVZ exhibit a more activated phenotype compared to other brain regions. WM microglia have also been reported to display unique properties, including an amoeboid morphology and enriched expression of genes related to microglial priming, phagocytosis, and migration (Ribeiro Xavier et al., 2015), (Staszewski & Hagemeyer, 2019). Therefore, it appears that WM repopulating myeloid cells share many characteristics with SVZ/WM microglia. After being established in the brain, the gene expression profile of white matter (WM) repopulating cells displays a higher enrichment for DAM genes such as *Clec7a*, *Axl*, *Ly9*, *Apoe*, and *Itgax*. Recently, a single-cell RNAseq analysis

uncovered a microglia-specific cluster in the WM, specifically a group of microglia associated with the WM (WAMs) that rely on *TREM2* signaling (Safaiyan et al., 2021). The similarities between WAMs and WM repopulating cells are notable. WAMs demonstrate a downregulation in homeostatic microglial genes (*P2ry12*, *Hexb*) and an upregulation in DAM-associated genes (*Apoe*, *B2m*, *Lyz2*, and *Clec7a*), cathepsins, and major histocompatibility complex (MHC) class II-related genes (*H2-D1*, *H2-K1*), which are also observed in WM repopulating cells. These cells are found in the corpus callosum, a WM region near the subventricular zone (SVZ), according to droplet-based single-cell RNAseq analysis. The WAM signature genes include *Lpl* and *Itgax*, which are also elevated in 28-day WM repopulating cells. Additionally, WM repopulating cells and WAMs express markers connected with phagocytic activity, such as *CLEC7A* and *AXL* (Safaiyan et al., 2021). Researchers have identified an early postnatal phagocytic subset of microglia located in the WM, referred to as PAMs, which also share a gene signature with DAMs (Li et al., 2019). WM repopulating cells seem to closely resemble WAMs, although PAMs/ATMs may represent the developmental equivalent of this cell population. These findings reinforce the identification and presence of a unique microglia population in the WM. However, further research is necessary to investigate whether surviving SVZ/WM microglia exist in their naive state as WAMs or whether CSF1Ri treatment induces this WAM-like phenotype. The study found a subtype of myeloid cells that originate from the SVZ and are resistant to CSF1Ri, which repopulate the microglial-depleted brain with distinct properties compared to homeostatic microglia. These cells have similar phenotypic and transcriptional profiles to DAMs and WAMs, suggesting the complexity and diversity of myeloid cells in the adult brain. This model system provides new insights into myeloid cell homeostasis and dynamics in the brain, which could aid in understanding aging and age-related disorders (Sirkis et al., 2021). Manipulating or enhancing WM microglial function may be therapeutically beneficial, especially in microglial-related diseases.

Microglia-specific ApoE knock-out does not alter Alzheimer's disease plaque pathogenesis or gene expression *(Henningfield et al., 2022)*

Data

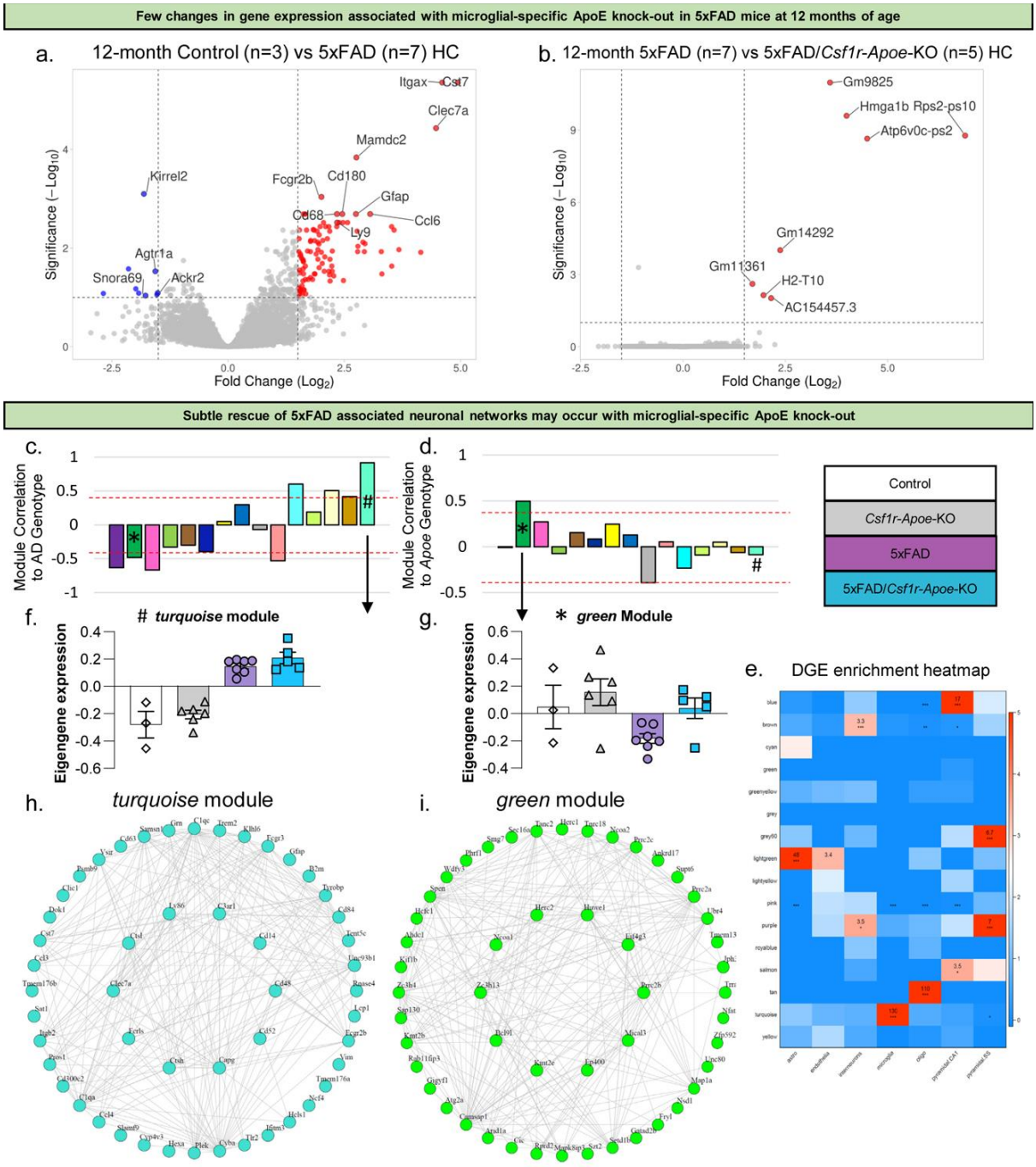

Figure C6: *Few RNA changes associated with microglial-specific ApoE knock-out. Volcano plot showing higher expression of inflammatory and other AD associated genes in the hippocampus of 5xFAD mice (n = 7) compared to control mice (n = 3) at 12 months of age (a). Volcano plot showing very few changes in gene expression between 5xFAD (n = 7) and 5xFAD/Csf1r-Apoe-KO (n = 5) mice at 12 months of age (b). Correlation of modules generated by weighted gene correlation network analysis (WGCNA) to the AD genotype (Z-score cut-off: ±0.4; **

*= green module; # = turquoise module) (c). Correlation of modules generated by WGCNA to Apoe genotype (Z-score cut-off: ±0.4) (d). Cell-type enrichment heatmap displays genes associated with specific cell types within a given color module (e). Values provided indicate the number of genes within the network associated with that of a specific cell type. *** = 6+ genes. ** = 3+ genes. Module eigengene trajectory of gene expression value in turquoise (f) and green (g) modules. Interactive plot between hub genes extracted from the turquoise module showing a distinct AD signature (h). Interactive plot between hub genes extracted from the green module showing a distinct signature associated with Apoe knockout (i)*

In order to investigate the effect of microglial-specific ApoE knock-out on overall gene expression in 5xFAD mice, bulk-tissue RNA sequencing of the mouse hippocampus was conducted. Consistent with expectations, inflammatory genes were found to be upregulated in 5xFAD mice compared to Control mice at 4 and 12 months of age, including disease-associated microglia (DAM) genes such as *Cst7*, *Clec7a*, and *Itgax* (**Figure C6:a**). However, knocking out microglial-specific ApoE in 5xFAD mice did not result in significant changes in gene expression at the bulk-tissue level at 4 and 12 months of age (**Figure C6:b**). Weighted gene co-expression network analysis (WGCNA) was employed to explore changes in network gene expression, revealing 15 independent modules. Correlation analysis showed that the turquoise module was highly correlated with AD genotype (**Figure C6:c,f**) , consisting of 1398 genes, while the green module was highly correlated with both AD and Apoe KO genotypes, consisting of 392 genes(**Figure C6:d,g**). The turquoise module displayed gene network changes associated with microglia and was strongly upregulated in both 5xFAD and 5xFAD/Csf1r-Apoe-KO mice, while the green module was only downregulated in 5xFAD mice and consisted of genes associated with axonogenesis, microtubule bundle formation, and chromatin remodeling (**Figure C6:e**). Hub microglial genes such as *Clec7a*, *Ctsl*, and *Ctsh* with pathway analyses identified GO terms such as viral gene expression and viral transcription for turquoise module (**Figure C6:h**). Hub genes of the green module included *Eif4g3*, *Ncoa1*, and *Huwe1* (**Figure C6:i**).

Conclusion

In this study, we aimed to investigate the role of microglial-expressed ApoE in AD by using a mouse model that specifically eliminates microglial-Apoe expression. Previous studies on ApoE's role in AD used global ApoE knock-out mouse models, which did not differentiate the role of microglial-expressed ApoE from astrocytic-expressed ApoE (Bales et al., 1999), (Krasemann et al., 2017), (Meilandt et al., 2020). Differentiating these roles is essential because astrocytes have the ability to interact with Aβ plaques in an ApoE-dependent way and internalize Aβ peptides (Koistinaho et al., 2004), (Matsunaga et al., 2003). To create the mouse model, we crossed Csf1r-cre mice with a 5xFAD mouse model and Apoefl/fl mice, resulting in progeny with Apoe expression knocked-out of microglia. Previous research has demonstrated that global knock-out of Trem2 or Apoe reduces plaque-associated microgliosis in various mouse models of AD (Bales et al., 1999), (Krasemann et al., 2017), (Meilandt et al., 2020), but this effect was not observed in the model utilized in this study. Furthermore, the dysfunctional transcriptional phenotype of microglia in AD is driven by the interaction between TREM2 and ApoE (Krasemann et al., 2017). In Alzheimer's disease (AD), the association between ApoE and Aβ has been extensively studied (Spangenberg et al., 2019). Studies have shown that eliminating ApoE globally or specifically in microglia reduces the number of Aβ plaques, but does not change plaque or cerebral amyloid angiopathy (CAA) load or the levels of soluble and insoluble Aβ1–40 and Aβ1–42 (Ulrich et al., 2018), (Holtzman et al., 2000). Interestingly, microglial-expressed ApoE appears to be necessary for microglial interaction with Aβ plaques, which may be important for plaque compaction. Additionally, reducing ApoE signaling prior to plaque deposition was shown to prevent Aβ accumulation, while its reduction after the emergence of plaques resulted in an increase in average plaque size (Bolmont et al., 2008), (Condello et al., 2015). These findings are consistent with the results of microglia-specific ApoE knock-out (Huynh et al., 2017). To investigate whether this finding holds true in our knockout model, we conducted bulk-RNA sequencing on hippocampal tissue and found

minimal changes in gene expression between 5xFAD mice and 5xFAD mice with intact microglial-specific ApoE. This lack of change included genes known to be associated with DAM (*Cst7*, *Trem2*, *Ctss*, *Itgax*, etc.). In addition, we did not observe a decrease in Apoe mRNA with microglial-specific ApoE knock-out in 5xFAD mice. These findings suggest that ApoE produced by microglia may not be required for the transcriptional shift into a DAM state. However, it is important to note that bulk-tissue RNA sequencing has limitations as it reflects the average gene expression across various cell types in the hippocampus. It is worth mentioning that microglia may use ApoE produced by other brain cells, such as astrocytes, as we detected ApoE protein in plaque-associated microglia in 5xFAD/Csf1r-Apoe-KO mice. We utilized weighted gene co-expression analysis (WGCNA) to investigate potential causes for changes in plaque size and neuritic dystrophy. Our genetic network analysis identified 15 distinct modules, with the turquoise and green modules showing the most notable results. The turquoise module was significantly associated with the AD genotype (5xFAD vs. non-5xFAD), while the green module was strongly associated with both the AD and Apoe KO genotypes (microglial-ApoE intact vs. microglial ApoE KO). Interestingly, within the green module, we observed that the expression of genes associated with this network was downregulated in 5xFAD mice, but upregulated in mice with microglial-specific ApoE knock-out. Our analysis of gene ontology terms revealed that these genes are involved in neuronal processes such as axonogenesis, microtubule bundle formation, and chromatin remodeling. These findings suggest that microglial-specific ApoE may promote these neuronal functions (Lane-Donovan et al., 2016), potentially explaining the observed decrease in neuritic dystrophy in mice with this knock-out compared to 5xFAD controls. In mouse models of Alzheimer's disease, the absence of ApoE results in increased neuritic dystrophy and synaptic loss. However, reducing APOE signaling after initial plaque deposition in APOE*ε4 APP/PS1–21 mice can attenuate neuritic dystrophy, suggesting a time-specific role of ApoE in the disease (Huynh et al., 2017).

Microglial-specific knock-out of ApoE in 5xFAD mice showed a trend towards a decrease in the ratio of dystrophic neurites to plaque volume, indicating that microglial-expressed ApoE may contribute to neuronal damage in Alzheimer's disease. Through genetic network analysis, the turquoise and green modules were identified, with the green module being highly correlated with both Alzheimer's disease and Apoe KO genotypes. Genes associated with this network were downregulated in 5xFAD mice but upregulated with microglial-specific ApoE knock-out, suggesting that microglial-specific ApoE may promote neuronal functions such as axonogenesis, microtubule bundle formation, and chromatin remodeling, which could be a reason for the observed downward trend in neuritic dystrophy. In mice and human brain tissue with a genetic risk factor for Alzheimer's disease (APOE*ε4), there is a reduction in synaptic proteins. The same reduction was observed in microglial-specific ApoE knock-out mice and 5xFAD microglial-specific ApoE knock-out mice. This loss of synaptic markers was not exacerbated in the latter group. Additionally, staining of tissue with a homeostatic microglial marker revealed a loss in intensity associated with microglial-expressed ApoE knock-out, mirroring the synaptic protein findings (Liraz et al., 2013), (Love et al., 2006), (Yong et al., 2014). Dysregulation of microglial homeostasis through partial inhibition of Csf1r also results in a reduction in *P2ry12* expression and synaptic proteins (Arreola et al., 2021). Therefore, microglial-expressed ApoE knock-out may dysregulate microglial homeostasis, potentially leading to changes in synapse maintenance and development outside of AD. Our study suggests that microglial-expressed ApoE may not significantly affect the development of AD, particularly in regards to microglial reaction to plaques and disease-associated gene expression. However, it's important to note that targeting ApoE in mice may not have the same effects as targeting human APOE variants, and the role of microglial-expressed ApoE in tau pathology requires further investigation. Recent studies suggest that global ApoE knock-out and microglial depletion may have protective effects on brain atrophy induced by tau, and removing

APOE*ε4 from astrocytes may reduce tau pathology and neurodegeneration (Shi et al., 2019), (Shi et al., 2017). Therefore, it's crucial to explore the impact of microglial-specific knock-out of ApoE in tauopathy models.

Selective targeting and modulation of plaque associated microglia via systemic dendrimer administration in an Alzheimer's disease mouse model.

Data

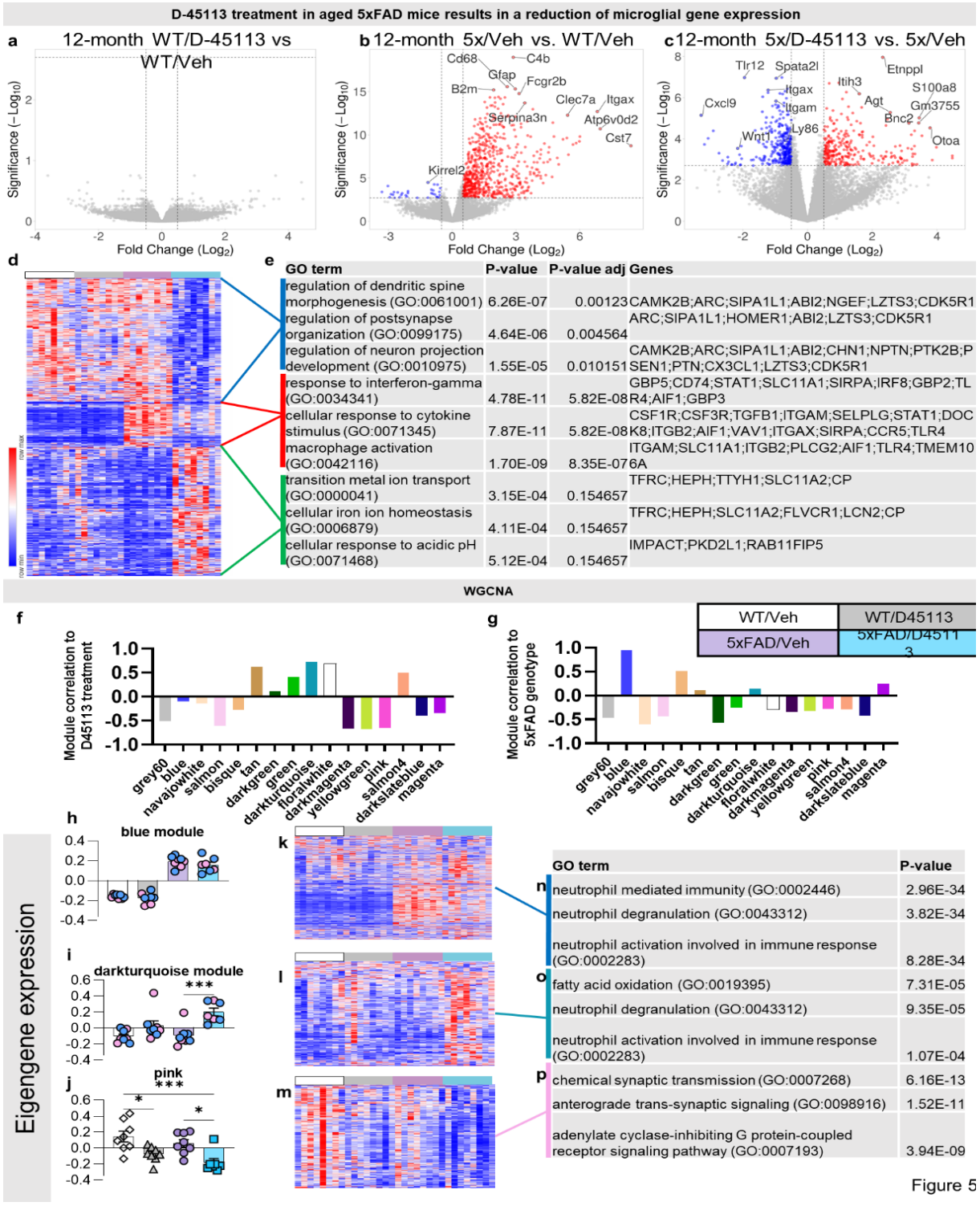

Figure C7: Volcano plot looking at differentially expressed genes (DEGs) between WT/D45113 and WT/Veh groups show no changes in gene expression between the groups ***(a)****. Volcano plot examining the DEGs between 12-month-old 5xFAD/Veh mice compared to WT/Veh mice reveals upregulation of classical AD inflammatory genes (Clec7a, Itgax, Cst7, etc.)* ***(b)****. Volcano plot examining the DEGs between 12-month-old 5xFAD/D45113 mice and 5xFAD/Veh mice reveals downregulation of microglial and inflammatory genes (Itgax, Itgam, Cxcl9, etc.)* ***(c)****. Heatmap of individual FPKM values of the DEGs between the 12-month-old 5xFAD/D45113 group and 5xFAD/Veh group for all mice analyzed via bulk RNA-seq* ***(D)****. Gene ontology analysis on three distinct populations of DEGs* ***(e)****. Sixteen weighted gene connectivity network analysis (WGCNA) modules graphed according to correlation to D45113 treatment* ***(f)*** *and 5xFAD genotype* ***(g)****. Module eigengene expression*

*trajectory of gene expression value in blue **(h)**, darkturquoise **(i)**, and pink **(j)**. Heatmap of genes within its respective module **(k-m)** and subsequent GO analysis terms and p-value for the blue **(n)**, darkturquoise **(o)**, and pink **(p)** modules. Statistical analysis for (h-j) used a one-way ANOVA with Tukey's multiple comparison test. Significance indicated as * $p < 0.05$; ** $p < 0.01$; *** $p < 0.001$.*

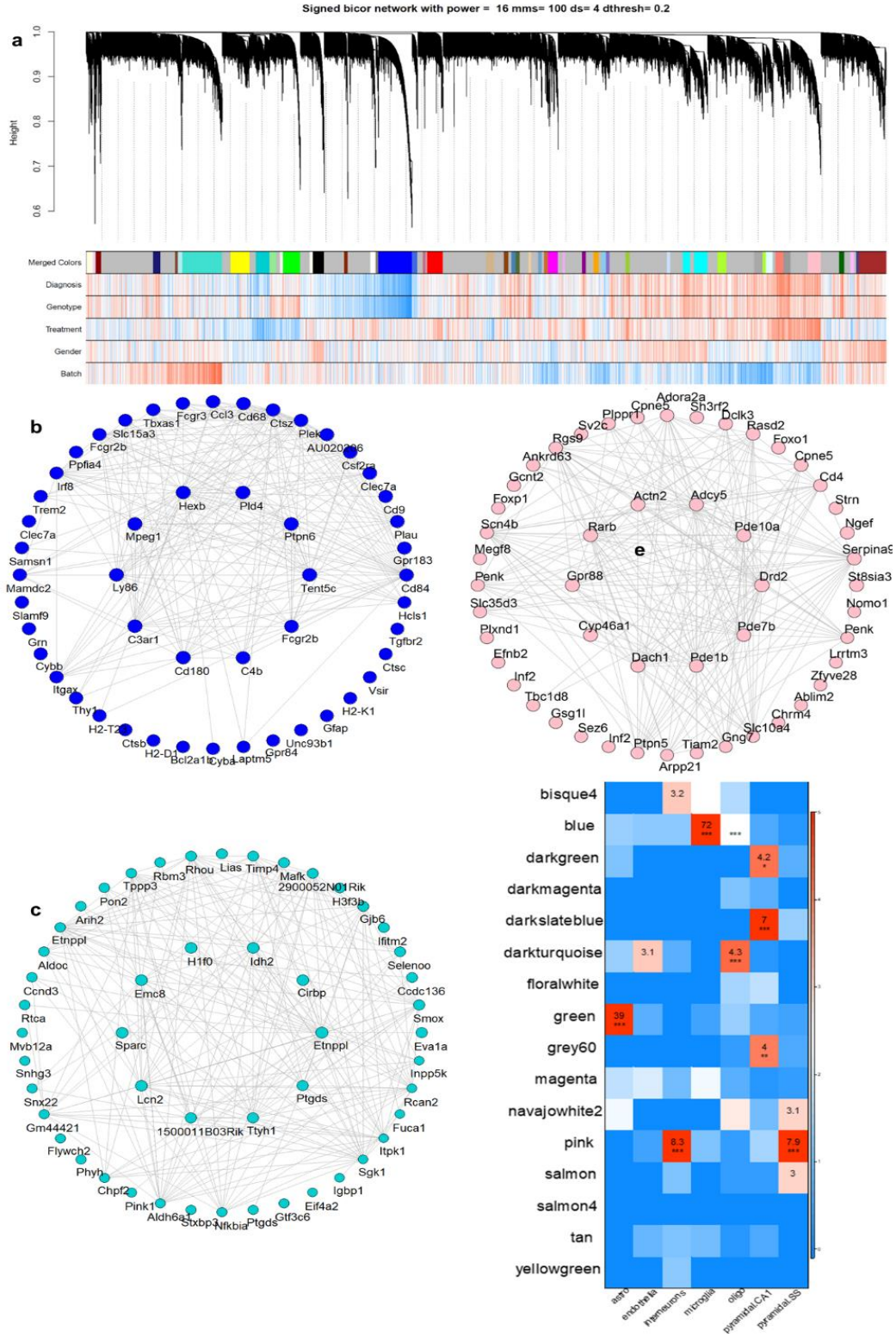

*Figure C8: WGCNA dendrogram highlighting 48 modules **(a)**. Interactive plot between hub genes extracted from the blue **(b)**, darkturquoise **(c)**, and pink **(d)** modules. Cell-type enrichment heatmap which displays gene network associations with different cell-types **(e)**.*

In order to verify the impact of D-45113 treatment on IHC changes, we conducted bulk RNA sequencing (RNA-seq) on microdissected hippocampi from WT/Veh, WT/D-45113, 5xFAD/Veh, and 5xFAD/D-45113 mice. The differentially expressed genes (DEGs) were compared between WT/D-45133 and WT/Veh, and no significant changes were found between the two groups, indicating that D-45113 does not affect hippocampal gene expression in the WT mice (**Figure C7:a**). Inflammatory genes were found to be upregulated in 5xFAD/Veh mice compared to WT/Veh, in line with previous research (Forner et al., 2021), with genes such as *Cst7*, *Itgax*, and *Clec7a* being highly upregulated (**Figure C7:b**). On the other hand, 5xFAD/D-45113 mice showed significant gene expression changes compared to 5xFAD/Veh mice, with marked downregulation of genes associated with microglia and inflammation such as Itgam, Itgax, and Cxcl9 (**Figure C7:c**). A clustered heatmap was generated for the 777 DEGs identified between 5xFAD/D-45113 and 5xFAD/Veh mice based on fragments per kilobase of exon per million mapped fragments (FPKM) values (**Figure C7:d**), and three gene clusters were identified based on the direction of expression changes: genes that are downregulated with D-45113 treatment, genes that are upregulated in 5xFAD/Veh mice but rescued in 5xFAD/D-45113 mice, and genes that are upregulated with D-45113 treatment. Gene ontology (GO) analysis was performed on the three gene clusters, and the associated GO terms, P-value, adjusted P-value, and genes were listed in a table (**Figure C7:e**). The GO terms for the group of genes that are downregulated with D-45113 treatment are linked to synapses and neurons, with the top GO term being related to the regulation of dendritic spine morphogenesis. The top GO terms for the second group of genes, which are upregulated in 5xFAD/Veh mice but downregulated in 5xFAD/D-45113, are related to inflammation, with response to interferon-gamma being the top GO term. The GO terms associated with the third group, which contains genes that are upregulated with dendrimer administration, are linked to ion transport and homeostasis, but the adjusted P-values of the top GO terms are not significant. Overall, it seems

that D-45113 treatment may affect inflammatory and dendritic and neuronal gene expression in the hippocampi of these mice. To investigate the impact of dendrimer treatment on gene networks, we conducted weighted gene co-expression network analysis (WGCNA) on the gene expression dataset and identified 48 independent modules (**Figure C8:a**). Correlations of each module to either D-45113 treatment (**Figure C7:f**) or 5xFAD genotype status (**Figure C7:g**) were calculated, and 16 modules were graphed. The blue module was highly correlated with the 5xFAD genotype, while the darkturquoise and pink modules were correlated with D-45113 treatment. Eigengene expression for the blue, darkturquoise, and pink modules was counted and plotted (**Figure C7:h.i.j**), and genes from each module were displayed as a heatmap (**Figure C7:k,l.m**). The blue module, which consists of 1294 genes, was highly upregulated in the 5xFAD/Veh and 5xFAD/D-45113 groups, and the GO terms associated with this module were related to inflammation (**Figure C7:n**). Furthermore, the blue module showed gene network changes associated with microglia (**Figure C8:b**). The module colored in darkturquoise contains a total of 520 genes and shows significant upregulation in 5xFAD/D-45113 mice. The gene ontology (GO) terms associated with this module are neutrophil activation and degranulation (**Figure C7:o**). On the other hand, the pink module is made up of 500 genes and exhibits downregulation in 5xFAD/D45113 mice. The GO terms related to this module are associated with synaptic transmission (**Figure C7:p**). These findings strengthen the possibility of a correlation between D-45113 treatment and alterations in neurons and synapses.

Conclusion

Dendrimers are dynamic nanomolecules used for drug delivery in cancer and brain when BBB is compromised (Santos et al., 2018). However, traditional PAMAM dendrimers face challenges in passing BBB (Zhu et al., 2019). Invasive methods like CSF, intracerebral, and intracerebralventricular injection are efficient but have limitations (Dong et al.,

2018),(Pardridge, 2022). Non-invasive methods like nasal drug administration, exosome delivery, and nanoparticle delivery are promising but have toxicity, dosing, and drug conjugation problems (Dong et al., 2018),(Heidarzadeh et al., 2021),(Ozsoy et al., 2009),(Saraiva et al., 2016). PAMAM hydroxyl-terminated dendrimers have potential to bypass partially impaired BBB and target PAMs. This study aims to investigate if these dendrimers can selectively target and treat PAMs in the context of AD. Targeting specific subsets of microglia, particularly PAMs, is crucial to understand the role of microglia in AD pathogenesis. TREM2 is a key regulator of microglial-plaque association in AD, and its downstream effectors have emphasized the role of TREM2 in promoting microglial association with plaques (Gratuze et al., 2021), (Gratuze et al., 2018), (Jay et al., 2017), (Jay et al., 2015), (C. Y. D. Lee et al., 2018),(Lee, Meilandt, et al., 2021),(Pardridge, 2022),(Wang et al., 2015). However, the impact of this association on the brain remains uncertain. Dendrimers targeting only the most phagocytic microglia in AD have potential to be very promising in this regard. These dendrimers may target microglia only when needed in disease, making them beneficial. In this study, we demonstrate that PAMAM hydroxyl dendrimers can be used to deliver a drug payload to PAMs in a mouse model of Alzheimer's disease (AD). They show that treatment with D-45113, a dendrimer conjugated with Dasatinib, leads to a rescue in behavioral deficits, a reduction in Aβ levels, and changes in microglial gene expression in 12-month-old 5xFAD mice (Zhang et al., 2019). We suggest that these findings suggest that microglia play an important role in controlling Aβ levels in AD and that dendrimers can be a valuable tool for delivering therapeutics to PAMs. Previous studies have successfully conjugated dendrimers with siRNAs, ASOs, and other drugs, making them essential for delivering therapeutics across the blood-brain barrier and directly to PAMs (Dong et al., 2018). They suggest that future studies employing dendrimers in plaque + tau mouse models will be crucial to understanding the interaction between microglia and the two primary histopathological hallmarks of AD.

Ultimately, the PAMAM hydroxyl dendrimers can selectively target a subset of microglia, providing a valuable screening tool for potential drug candidates that impact microglia and resulting in higher precision and personalized medicine for AD patients (Bemiller et al., 2017),(Gratuze & Holtzman, 2021), (Lee, Turpin, et al., 2021).

METHODS

RNA sequencing (RNA-Seq) is a high-throughput sequencing method that provides comprehensive insights into the transcriptome of a cell. RNA-Seq has advantages over previous methods, such as Sanger sequencing and microarrays, due to its higher coverage, greater resolution, and ability to detect novel transcripts and alternatively spliced genes. RNA-Seq can be used to investigate various RNA populations, including total RNA, pre-mRNA, noncoding RNA, and mRNA transcripts. Recent advances in RNA-Seq workflows have enabled researchers to better understand the functional complexity of transcription. High-throughput next-generation sequencing (NGS) technologies have revolutionized transcriptomics by eliminating challenges posed by hybridization-based microarrays and Sanger sequencing-based approaches (Tomita et al., 2004). RNA-Seq involves isolating RNA, converting it to cDNA, preparing the sequencing library, and sequencing it on an NGS platform. However, experimental details such as biological and technical replicates, sequencing depth, and desired coverage across the transcriptome should be considered before performing RNA-Seq to balance high-quality results and time and monetary investment. The first step in transcriptome sequencing is isolating RNA from a sample, and it must be of high quality for a successful RNA-Seq experiment (Thompson et al., 2007). The quality of RNA is measured by an RNA Integrity Number (RIN) based on the ratios of 28S to 18S ribosomal bands using gel electrophoresis. Low-quality RNA can negatively affect sequencing results and lead to incorrect biological conclusions. High-quality RNA is crucial for RNA-Seq experiments, but degraded RNA may be unavoidable in certain cases like autopsy or paraffin-embedded tissues. The effect of degraded RNA on sequencing results should be carefully considered (Rudloff et al., 2010). After RNA isolation, the next step in transcriptome sequencing is creating an RNA-Seq library, which can vary based on RNA species and NGS platforms. This involves isolating desired RNA, reverse-transcribing it to cDNA, fragmenting or amplifying cDNA, and ligating

sequencing adaptors. There are choices in library construction and experimental design that must be carefully made based on specific needs. The accuracy of detection for specific RNAs depends on library construction. Each stage can be manipulated to enhance the detection of certain transcripts while limiting the ability to detect others (Christodoulou et al., 2011). All RNA-Seq preparation methods involve converting RNA to cDNA as most sequencing technologies require DNA libraries. Traditional cDNA synthesis protocols generate libraries from each cDNA strand uniformly, which means that strand orientation information of the original RNA is lost (Parkhomchuk et al., 2009). This maximizes reverse transcription efficiency but is problematic for distinguishing overlapping transcripts on opposite strands. To address this issue, alternative library preparation protocols have been developed to yield strand-specific reads (Vivancos et al., 2010), (Mills et al., 2013). One such strategy involves ligating adapters in predetermined directions to single-stranded RNA or the first-strand of cDNA, but this approach is laborious and results in coverage bias. A preferred strategy is to incorporate a chemical label, such as deoxy-UTP (dUTP), during the synthesis of the second-strand cDNA, which can be enzymatically removed (Lister et al., 2008). This approach facilitates distinguishing the second-strand cDNA from the first strand and preserves strandedness. However, caution should be exercised when assessing antisense transcripts near highly expressed genes as a small proportion of reads (~1%) from the opposite strand may still be observed (Zeng & Mortazavi, 2012). To construct RNA-Seq libraries in a cost-effective manner, it is worth considering assaying multiple indexed samples in a single sequencing lane (Smith et al., 2010). With modern sequencing technology, a single run can generate a large number of reads, up to 750 million paired-end reads per lane on an Illumina HiSeq 2500. This makes it possible to analyze increasingly complex samples. However, oversampling can occur with minimal improvement in data quality for lower complexity samples when using high sequencing depths, which limits the cost-effectiveness of this approach. Therefore, a more

affordable and efficient solution is to use unique 6-bp indices, or "barcodes," to identify each RNA-Seq library and enable the pooling and sequencing of multiple samples in the same reaction. Depending on the application, coverage for 2-20 samples can be achieved (Consortium et al., 2007), (Blencowe et al., 2009). To accurately quantify gene expression of moderately to highly expressed transcripts, around 30-40 million reads are needed. For full-sequence diversity of complex transcript libraries, including rare and lowly-expressed transcripts, up to 500 million reads may be required (Fu et al., 2014). Thus, it is important to consider the required sequencing depth to answer experimental questions confidently and use NGS resources efficiently for any given study.

Sequencing Platforms for Transcriptomics

When conducting an RNA-Seq experiment, selecting the appropriate sequencing platform is critical and contingent on the specific research objectives. Several commercial next-generation sequencing (NGS) platforms are currently available, with other platforms under active development (Metzker, 2010). High-throughput sequencing platforms can be categorized as either ensemble-based, which sequence many identical copies of a DNA molecule, or single-molecule-based, which sequence a single DNA molecule. These sequencing techniques and platforms differ in various ways, potentially influencing downstream data analysis and interpretation.

Illumina dominates the sequencing industry, utilizing an ensemble-based sequencing-by-synthesis approach that provides relative RNA expression levels of genes (Bentley et al., 2008). Low sequencing error rates, less than 1%, are a significant benefit of ensemble-based platforms and are crucial when sequencing miRNAs, where high error rates can result in loss of reads or misalignment. Illumina's HiSeq platform is the most widely applied NGS technology for RNA-Seq, offering a standard for NGS sequencing. The recently released MiSeq, a desktop

sequencer with lower throughput, provides faster turnaround times for transcriptome sequencing on a smaller scale. Single-molecule-based platforms, such as PacBio, allow single-molecule real-time sequencing, which avoids amplification bias and yields long reads, with average lengths of 4200 to 8500 bp, allowing for the detection of novel transcript structures (Eid et al., 2009), (Au et al., 2013), (Sharon et al., 2013). However, the high error rate of ~5% presents a disadvantage, with misalignment and loss of sequencing reads being prevalent due to the difficulty of matching erroneous reads to the reference genome (Eid et al., 2009).

Another crucial factor to consider when selecting a sequencing platform is transcriptome assembly. Longer sequencing reads enable more accurate and unambiguous assembly of transcripts, which is necessary for detecting splicing isoforms. PacBio's extremely long reads are optimal for de novo transcriptome assembly, while Moleculo's technology can produce reads up to 8500 bp long (Carneiro et al., 2012). Although not widely adopted, it can aid transcriptome assembly. Illumina's MiSeq protocols can also produce slightly longer reads, up to 350 bp, which can improve both de novo and reference transcriptome assembly.

Transcriptome Analysis

RNA-Seq enables a high-resolution view of the global transcriptional landscape and presents new informatics challenges and applications as sequencing technologies and protocol methodologies continue to evolve. In addition to surveying gene expression levels, RNA-Seq can uncover novel gene structures, alternatively spliced isoforms, and allele-specific expression (ASE) (Montgomery et al., 2010), (Pickrell et al., 2010), (Battle et al., 2014), (Lappalainen et al., 2013). This section aims to introduce the analytical techniques used to gain a deeper understanding of the intricate complexity of transcriptomes. Single- and bulk-cell transcriptional profiling have been used to study microglia across development and disease (Srinivasan et al., 2020); (Tay et al., 2018); (Hammond et al., 2019).

Read Alignment: Compared to mapping DNA sequencing reads, mapping RNA-Seq reads to the genome poses a greater challenge due to the presence of splice junctions in many reads. Traditional read mapping algorithms like Bowtie (Langmead et al., 2009) and BWA (Li & Durbin, 2009) are not suitable for this purpose as they cannot handle spliced transcripts. To address this issue, one approach is to supplement the reference genome with sequences from exon-exon splice junctions obtained from known gene annotations (Mortazavi et al., 2008). An alternative and preferred strategy is to use a "splicing-aware" aligner, which can distinguish between a read aligning across an exon-intron boundary and one with a short insertion. Several splicing-aware mapping tools have been developed specifically for RNA-Seq data, including GSNAP (Wu & Nacu, 2010), MapSplice (K. Wang et al., 2010), RUM (Grant et al., 2011), STAR (Dobin et al., 2013), and TopHat (Trapnell et al., 2009), each with its own advantages in terms of performance, speed, and memory usage. Choosing the best aligner depends on these factors and the objectives of the RNA-Seq study. The performance of these aligners has been systematically evaluated by the RNA-Seq Genome Annotation Assessment Project (RGASP3), which has identified significant differences in alignment yield, basewise accuracy, mismatch and gap placement, and exon junction discovery (Engstrom et al., 2013).

Transcript Assembly and Quantification: Once RNA-Seq reads are aligned, the mapped reads can be assembled into transcripts using computational programs that infer transcript models from read alignments to the reference genome (Trapnell et al., 2010), (Li et al., 2011), (Roberts, Pimentel, et al., 2011), (Mezlini et al., 2013). Alternatively, de novo reconstruction can be used to assemble contiguous transcript sequences with the use of a reference genome or annotations (Robertson et al., 2010), (Grabherr et al., 2011), (Schulz et al., 2012). However, reconstructing transcripts from short-read data remains a major challenge, and there is no gold standard method for transcript assembly due to various factors that can affect assembly quality, including gene complexity, degree of polymorphisms, alternative splicing, dynamic range of

expression, sequencing errors, gene annotation, and inference of isoforms (Steijger et al., 2013).

Gene expression levels can be estimated using computational tools like Cufflinks (Trapnell et al., 2010), FluxCapacitor (Montgomery et al., 2010), (Griebel et al., 2012), and MISO (Katz et al., 2010), which quantify expression by counting the number of reads that map to full-length transcripts. Alternatively, tools like HTSeq can quantify expression without assembling transcripts by counting the number of reads that map to an exon (Anders et al., 2013), (Roberts, Trapnell, et al., 2011). However, to accurately estimate gene expression, read counts must be normalized to correct for systematic variability, such as library fragment size, sequence composition bias, and read depth (Oshlack & Wakefield, 2009). The RPKM metric normalizes a transcript's read count by both the gene length and the total number of mapped reads in the sample, while the FPKM metric accounts for the dependency between paired-end reads in the RPKM estimate for paired-end reads (Trapnell et al., 2010). Another technical challenge for transcript quantification is the mapping of reads to multiple transcripts resulting from genes with multiple isoforms or close paralogs. One solution is to exclude all reads that do not map uniquely, but this strategy is not ideal for genes lacking unique exons. Alternatively, tools like Cufflinks (Trapnell et al., 2012) and MISO (Katz et al., 2010) construct a likelihood function that models the sequencing experiment and estimates the maximum likelihood that a read maps to a particular isoform to correct for "read assignment uncertainty" (Griffith et al., 2010).

Quality Assessment and Technical Considerations: During the RNA-Seq analysis pipeline, it is crucial to carefully identify and correct various sources of bias that can occur throughout the experimental process. These biases can arise during RNA extraction, sample preparation, library construction, sequencing, and read mapping (Kleinman & Majewski, 2012), (Lin et al., 2012), (Pickrell et al., 2012), (t Hoen et al., 2013). To ensure high-quality reads, the quality of the raw sequence data in FASTQ-format files should be assessed using software tools such as

the FASTX-toolkit [http://hannonlab.cshl.edu/fastx_toolkit], FastQC [http://www.bioinformatics.babraham.ac.uk/projects/fastqc] software, and RobiNA (Lohse et al., 2012) package. Important parameters to evaluate include sequence diversity of reads, adaptor contamination, base qualities, nucleotide composition, and percentage of called bases. Technical artifacts can arise at the sequencing stage or during RNA-Seq library construction, such as higher error rates at the 5′ read end due to mispriming events introduced by random oligos (Lin et al., 2012). Corrective measures such as trimming the ends of reads should be taken whenever possible to improve the quality of read alignments.

After aligning the reads, additional parameters should be evaluated to account for biases that occur at the read mapping stage. These include the percentage of reads mapped to the transcriptome, the percentage of reads with a mapped mate pair, coverage bias at the 5′- and 3′-ends, and the chromosomal distribution of reads. Misalignment can occur when a read spans the splicing junction of an alternatively spliced gene, especially if the reference transcriptome contains an incomplete annotation of isoforms (Kleinman & Majewski, 2012), (Pickrell et al., 2012). To evaluate sample integrity, the correlation of single-nucleotide variants (SNVs) between the DNA and RNA reads (t Hoen et al., 2013) should be investigated if genotype information is available. Discordant variants would be observed between DNA and RNA sequencing data in the case of a swapped sample, whereas more significant patterns of allele-specific expression would be observed than expected for a single individual in the case of a mixture of samples.

Differential Gene Expression: The main goal of gene expression experiments is to identify transcripts that exhibit differential expression across various conditions. Statistical methods have been developed to test for differential expression using microarray data, where probe intensities can be approximated by a normal distribution (Cui & Churchill, 2003), (Smyth, 2004), (Grant et al., 2005). However, these methods cannot be directly applied to RNA-Seq

data, which is discrete and does not fit a normal distribution (Marioni et al., 2008). Initially, a Poisson distribution was used to model read count data, but this assumption resulted in high false-positive rates due to underestimation of sampling error (Anders & Huber, 2010), (Langmead et al., 2010), (Robinson & Oshlack, 2010). Negative binomial distribution models have been shown to best fit the distribution of read counts across biological replicates, accounting for overdispersion or extra-Poisson variation.

To handle sources of variability in RNA-Seq data, complex statistical models have been developed that model overdispersion across technical and biological replicates. One source of variability is differences in sequencing read depth, which can create artificial differences between samples. To correct for this, raw read count data is transformed into FPKM or RPKM values. However, highly expressed genes can significantly alter these values, so statistical models that use highly expressed genes as covariates have been proposed (Robinson & Oshlack, 2010). Another source of variability is unequal distribution of sequencing reads across genes, which can be corrected using a two-parameter generalized Poisson model (Srivastava & Chen, 2010).

Various statistical methods have been designed specifically for detecting differential expression in RNA-Seq data (Trapnell et al., 2013), such as Cuffdiff, baySeq (Hardcastle & Kelly, 2010), DESeq (Anders & Huber, 2010), DEGseq (L. Wang et al., 2010), and edgeR (Robinson et al., 2010). However, each model makes specific assumptions that may not hold true for the observed data, so careful interpretation of the results is necessary (Bullard et al., 2010). Replicates are crucial for measuring variability and improving model estimations, with biological replicates preferred over technical replicates (Auer & Doerge, 2010). Using multiplexed RNA-Seq libraries and ERCC spike-in controls can improve the accuracy of measurements of differential gene expression (Liu et al., 2014).

Weighted Gene Co-expression Network Analysis: Gene expression data can have diverse expression profiles, which can be identified through dimension reduction techniques such as principal component analysis (PCA) and clustering analysis. PCA identifies the dimensions with the highest variation, but it may not reflect true expression profiles. Cluster analysis groups genes with similar expression profiles and can be unsupervised or supervised. Supervised methods find genes that classify samples into known classes. Network analysis takes a global approach to study interconnectedness between genes, as biological functions arise from complex interactions between cell constituents. Gene networks provide potential to identify disease-causing genes for therapeutic interventions (Schadt et al., 2005), (Chen et al., 2008). Weighted Gene Co-expression Networks (Zhang & Horvath, 2005) is a primary method to infer gene networks.

The foundation of WGCNA is the concept of a scale-free network, which has been observed in numerous empirical studies, and is believed to be present in metabolic networks across all organisms (Carlson et al., 2006), (Dong & Horvath, 2007), (Gargalovic et al., 2006), (Zhang & Horvath, 2005), (Horvath et al., 2006). In a scale-free network, gene connectivity, represented by p(k), follows a power law distribution, $p(k) \sim k^{-\gamma}$ (Barabasi & Albert, 1999), (Ravasz et al., 2002). The existence of highly connected nodes, or hubs, is a critical characteristic of a scale-free network, as they participate in a large number of metabolic reactions and integrate all substrates into a single, interconnected web. Although scale-free networks are robust against random failures, they are vulnerable to coordinated (Albert et al., 2000). Therefore, identifying hub molecules involved in specific diseases could pave the way for developing new drugs that target those hubs (Barabasi & Bonabeau, 2003).

Consensus Network: From a gene-centric perspective, modules are clusters of highly interconnected genes that may form a biological pathway. However, from a systems biology standpoint, functional modules act as mediators between individual genes and emergent global

properties. These modules are fundamental system components, represented as nodes in a network, and described using network language to define their relationships. Co-expression modules can form a biologically meaningful meta-network that reveals a higher-order organization of the transcriptome. Meta-modules refer to modules in a meta-network of modules. Meta-network analysis is a dimension reduction technique that reduces a gene co-expression network involving thousands of genes to a smaller meta-network involving module representatives, where each module is represented by one eigengene (Ravasz et al., 2002). The resulting network is known as an eigengene network, and it captures far more information than a simple catalog of module memberships (individual genes) (Langfelder & Horvath, 2007).

Eigengene networks are useful in describing module relationships in a single data set (single eigengene network analysis) or comparing module relationships across different data sets (differential eigengene network analysis). To facilitate differential eigengene network analysis, methods have been proposed for finding consensus modules (Horvath et al., 2006), (Horvath & Dong, 2008). The approach for detecting consensus modules relies on a consensus dissimilarity measure that compares topological overlap matrices of different data sets. The consensus matrix can also be defined using the topological overlap matrix (TOM), which typically leads to more robust and larger modules (Oldham et al., 2006). Like the single network case, the consensus gene dissimilarity is defined as the 1 minus the consensus TOM (Li & Horvath, 2007), (Yip & Horvath, 2007).

The dissimilarity is used as input to average linkage hierarchical clustering. Based on the module memberships derived from the clustering analysis, further analysis of module preservation can be defined as scaled connectivity of preservation network at the gene level and module level. The preservation network's whole network preservation can also be defined as the scaled density of the preservation network at both the gene level and the module level.

MasigPro: A statistical method for identifying differentially expressed genes in microarray time-course experiments has highlighted the availability of various methods for identifying and clustering gene expression patterns, decoding gene regulatory networks, and detecting differentially expressed genes (Bar-Joseph, 2004). However, the latter task is challenging as only a few methodologies exist for finding statistical profile differences between experimental groups. A method proposed to identify differentially expressed genes between two cell-cycle microarray datasets using a difference measure between continuous representations of time-series expression data, which works best for long time series (Bar-Joseph et al., 2003). ANOVA-based models have also been suggested, but they are not appropriate for analyzing quantitative variables or experiments with unbalanced designs (Park et al., 2003). Regression approaches are a more flexible solution as they treat time as a quantitative variable, allowing for the detection of differentially expressed genes and changes in trends. Regression modeling to identify differential gene profiles in an inducible transgenic model, but their approach is tailored to specific properties of the data under study. To address this limitation, a general regression-based approach called maSigPro (microarray Significant Profiles) was proposed as a two-step regression strategy that allows for the adjustment of model parameters according to the specific interests of the researcher and the data under study (Xu et al., 2002). The method involves a two-step regression approach, where experimental groups are defined by dummy variables. The first regression fit adjusts a global model and identifies differentially expressed genes, while the second step applies a variable selection strategy to identify statistically significant profile differences between experimental groups. This approach provides a versatile procedure for studying specific pattern differences among experimental groups and genes (Harrell et al., 1984).

The two-regression steps approach is chosen because it is more appropriate than fitting a unique model in multicollinear scenarios. The goodness of fit criterion, high R-squared, is used for

gene selection, providing the possibility of selecting genes for which good models could be obtained. However, the researcher must decide on the R-squared threshold based on the research objectives (Harrell et al., 1984).

Validation of the models is essential because regression approaches rely on several assumptions such as independence of the observations, homoscedasticity, and normality. The maSigPro package is validated for the detection of profile differences, including heteroscedasticity and influential values present in the data (Bar-Joseph, 2004).

The proposed method can be applied to simple gene expression responses, a reduced number of time points, and experiments with larger numbers of time points. For experiments with larger numbers of time points, a piecewise regression or splines regression approach could be applied. The method detects significant profile differences without multiple pairwise comparisons, allowing for unbalanced designs and heterogeneous sampling times. The variable definition of the models enables the analysis of not only genes with temporal expression changes between experimental groups, but also the magnitude of these differences. The proposed method can be extended to include additional variables or reduced by removing variables.

NanoString: The NanoString nCounter system has gained popularity as a gene expression profiling method in various research fields (Veldman-Jones et al., 2015). This system enables direct measurement of gene expression without the need for cDNA preparation and polymerase chain reaction (PCR) analysis, allowing for more efficient sample preparation and expression profiling of up to 800 targets, such as in validation studies or when focusing on specific gene types (Geiss et al., 2008). However, data analysis remains a challenge, requiring proprietary software or an experienced data analyst for processing and normalization, as well as selecting and implementing appropriate differential expression analysis methods. While certain R libraries have addressed specific steps in the nCounter analysis pipeline, including quality

control, normalization, and differential expression analysis, an all-in-one open-source package is currently unavailable (Canouil et al., 2020), (Waggott et al., 2012), (Wang et al., 2016).

The NanoString nCounter system is a cost-effective and straightforward method for profiling specific nucleic acid molecules in complex mixtures. The system utilizes color-coded barcodes that can hybridize directly to target molecules, and the expression level of a target molecule is measured by counting the number of times the barcode for that molecule is detected by a digital analyzer. The system can detect low abundance molecules without the need for amplification and can quantify up to 800 different targets simultaneously, making it ideal for miRNA profiling and targeted mRNA expression analysis (Geiss et al., 2008). The NanoString nCounter system provides more accurate quantification of mRNA expression than polymerase chain reaction (PCR)-based methods and microarrays, particularly in formalin-fixed paraffin-embedded samples, where RNA degradation is common (Reis et al., 2011).

Identifying differential expression (DE) for mRNAs or miRNAs across experimental conditions is a fundamental task in molecule expression studies. Current methods for DE detection in nCounter data, such as NanoStringNorm (Waggott et al., 2012) and NanoStriDE (Brumbaugh et al., 2011), are based on t-tests, which are not the most appropriate method for analyzing count data produced by the nCounter Analyzer. To address this issue, a novel DE detection method, NanoStringDiff, has been developed, which utilizes a generalized linear model of the negative binomial family to characterize count data and allows for multi-factor design (Robinson & Smyth, 2008). The method incorporates size factors calculated from positive controls, housekeeping genes, and background levels obtained from negative controls in the model framework, enabling the full utilization of all normalization information provided by the nCounter Analyzer. The NanoStringDiff method provides more accurate and powerful results in DE detection compared to existing methods, as demonstrated by simulations and real data analysis (Robinson & Smyth, 2007).

REFERENCES

2022 Alzheimer's disease facts and figures. (2022). *Alzheimers Dement*, *18*(4), 700-789. https://doi.org/10.1002/alz.12638

Abramov, A. Y., Canevari, L., & Duchen, M. R. (2004). Calcium signals induced by amyloid beta peptide and their consequences in neurons and astrocytes in culture. *Biochim Biophys Acta*, *1742*(1-3), 81-87. https://doi.org/10.1016/j.bbamcr.2004.09.006

Acharya, M. M., Green, K. N., Allen, B. D., Najafi, A. R., Syage, A., Minasyan, H., Le, M. T., Kawashita, T., Giedzinski, E., Parihar, V. K., West, B. L., Baulch, J. E., & Limoli, C. L. (2016). Elimination of microglia improves cognitive function following cranial irradiation. *Sci Rep*, *6*, 31545. https://doi.org/10.1038/srep31545

Adams, S. J., Kirk, A., & Auer, R. N. (2018). Adult-onset leukoencephalopathy with axonal spheroids and pigmented glia (ALSP): Integrating the literature on hereditary diffuse leukoencephalopathy with spheroids (HDLS) and pigmentary orthochromatic leukodystrophy (POLD). *J Clin Neurosci*, *48*, 42-49. https://doi.org/10.1016/j.jocn.2017.10.060

Al-Dalahmah, O., Sosunov, A. A., Shaik, A., Ofori, K., Liu, Y., Vonsattel, J. P., Adorjan, I., Menon, V., & Goldman, J. E. (2020). Single-nucleus RNA-seq identifies Huntington disease astrocyte states. *Acta Neuropathol Commun*, *8*(1), 19. https://doi.org/10.1186/s40478-020-0880-6

Albert, R., Jeong, H., & Barabasi, A. L. (2000). Error and attack tolerance of complex networks. *Nature*, *406*(6794), 378-382. https://doi.org/10.1038/35019019

Ali, S., Mansour, A. G., Huang, W., Queen, N. J., Mo, X., Anderson, J. M., Hassan, Q. N., 2nd, Patel, R. S., Wilkins, R. K., Caligiuri, M. A., & Cao, L. (2020). CSF1R inhibitor PLX5622 and environmental enrichment additively improve metabolic outcomes in middle-aged female mice. *Aging (Albany NY)*, *12*(3), 2101-2122. https://doi.org/10.18632/aging.102724

Allaman, I., Bélanger, M., & Magistretti, P. J. (2011). Astrocyte-neuron metabolic relationships: for better and for worse. *Trends Neurosci*, *34*(2), 76-87. https://doi.org/10.1016/j.tins.2010.12.001

Allaman, I., Gavillet, M., Bélanger, M., Laroche, T., Viertl, D., Lashuel, H. A., & Magistretti, P. J. (2010). Amyloid-beta aggregates cause alterations of astrocytic metabolic phenotype: impact on neuronal viability. *J Neurosci*, *30*(9), 3326-3338. https://doi.org/10.1523/jneurosci.5098-09.2010

Allen, M., Zou, F., Chai, H. S., Younkin, C. S., Crook, J., Pankratz, V. S., Carrasquillo, M. M., Rowley, C. N., Nair, A. A., Middha, S., Maharjan, S., Nguyen, T., Ma, L., Malphrus, K. G., Palusak, R., Lincoln, S., Bisceglio, G., Georgescu, C., Schultz, D., . . . Woltjer, R. L. (2012). Novel late-onset Alzheimer disease loci variants associate with brain gene expression. *Neurology*, *79*(3), 221-228. https://doi.org/10.1212/WNL.0b013e3182605801

Anders, S., & Huber, W. (2010). Differential expression analysis for sequence count data. *Genome Biol*, *11*(10), R106. https://doi.org/10.1186/gb-2010-11-10-r106

Anders, S., McCarthy, D. J., Chen, Y., Okoniewski, M., Smyth, G. K., Huber, W., & Robinson, M. D. (2013). Count-based differential expression analysis of RNA sequencing data using R and Bioconductor. *Nat Protoc*, *8*(9), 1765-1786. https://doi.org/10.1038/nprot.2013.099

Ando, H., Sato, T., Tomaru, U., Yoshida, M., Utsunomiya, A., Yamauchi, J., Araya, N., Yagishita, N., Coler-Reilly, A., Shimizu, Y., Yudoh, K., Hasegawa, Y., Nishioka, K., Nakajima, T., Jacobson, S., & Yamano, Y. (2013). Positive feedback loop via astrocytes causes chronic inflammation in virus-associated myelopathy. *Brain*, *136*(Pt 9), 2876-2887. https://doi.org/10.1093/brain/awt183

Andorfer, C., Acker, C. M., Kress, Y., Hof, P. R., Duff, K., & Davies, P. (2005). Cell-cycle reentry and cell death in transgenic mice expressing nonmutant human tau isoforms. *J Neurosci*, *25*(22), 5446-5454. https://doi.org/10.1523/jneurosci.4637-04.2005

Arreola, M. A., Soni, N., Crapser, J. D., Hohsfield, L. A., Elmore, M. R. P., Matheos, D. P., Wood, M. A., Swarup, V., Mortazavi, A., & Green, K. N. (2021). Microglial dyshomeostasis drives perineuronal net and synaptic loss in a CSF1R(+/-) mouse model of ALSP, which can be rescued via CSF1R inhibitors. *Sci Adv*, *7*(35). https://doi.org/10.1126/sciadv.abg1601

Asai, H., Ikezu, S., Tsunoda, S., Medalla, M., Luebke, J., Haydar, T., Wolozin, B., Butovsky, O., Kugler, S., & Ikezu, T. (2015). Depletion of microglia and inhibition of exosome synthesis halt tau propagation. *Nat Neurosci*, *18*(11), 1584-1593. https://doi.org/10.1038/nn.4132

Aschner, M. (1998). Immune and inflammatory responses in the CNS: modulation by astrocytes. *Toxicol Lett*, *102-103*, 283-287. https://doi.org/10.1016/s0378-4274(98)00324-5

Ashbrook, D. G., Arends, D., Prins, P., Mulligan, M. K., Roy, S., Williams, E. G., Lutz, C. M., Valenzuela, A., Bohl, C. J., Ingels, J. F., McCarty, M. S., Centeno, A. G., Hager, R., Auwerx, J., Lu, L., & Williams, R. W. (2021). A platform for experimental precision medicine: The extended BXD mouse family. *Cell Syst*, *12*(3), 235-247 e239. https://doi.org/10.1016/j.cels.2020.12.002

Ashe, K. H., & Zahs, K. R. (2010). Probing the biology of Alzheimer's disease in mice. *Neuron*, *66*(5), 631-645. https://doi.org/10.1016/j.neuron.2010.04.031

Au, K. F., Sebastiano, V., Afshar, P. T., Durruthy, J. D., Lee, L., Williams, B. A., van Bakel, H., Schadt, E. E., Reijo-Pera, R. A., Underwood, J. G., & Wong, W. H. (2013). Characterization of the human ESC transcriptome by hybrid sequencing. *Proc Natl Acad Sci U S A*, *110*(50), E4821-4830. https://doi.org/10.1073/pnas.1320101110

Auer, P. L., & Doerge, R. W. (2010). Statistical design and analysis of RNA sequencing data. *Genetics*, *185*(2), 405-416. https://doi.org/10.1534/genetics.110.114983

Aziz, N. A., van Belzen, M. J., Coops, I. D., Belfroid, R. D., & Roos, R. A. (2011). Parent-of-origin differences of mutant HTT CAG repeat instability in Huntington's disease. *Eur J Med Genet*, *54*(4), e413-418. https://doi.org/10.1016/j.ejmg.2011.04.002

Bacioglu, M., Maia, L. F., Preische, O., Schelle, J., Apel, A., Kaeser, S. A., Schweighauser, M., Eninger, T., Lambert, M., Pilotto, A., Shimshek, D. R., Neumann, U., Kahle, P. J., Staufenbiel, M., Neumann, M., Maetzler, W., Kuhle, J., & Jucker, M. (2016). Neurofilament Light Chain in Blood and CSF as Marker of Disease Progression in Mouse Models and in Neurodegenerative Diseases. *Neuron*, *91*(1), 56-66. https://doi.org/10.1016/j.neuron.2016.05.018

Baig, S., Wilcock, G. K., & Love, S. (2005). Loss of perineuronal net N-acetylgalactosamine in Alzheimer's disease. *Acta Neuropathol*, *110*(4), 393-401. https://doi.org/10.1007/s00401-005-1060-2

Baizabal-Carvallo, J. F., & Jankovic, J. (2016). Parkinsonism, movement disorders and genetics in frontotemporal dementia. *Nat Rev Neurol*, *12*(3), 175-185. https://doi.org/10.1038/nrneurol.2016.14

Baker, E., & Escott-Price, V. (2020). Polygenic Risk Scores in Alzheimer's Disease: Current Applications and Future Directions. *Front Digit Health*, *2*, 14. https://doi.org/10.3389/fdgth.2020.00014

Bales, K. R., Verina, T., Cummins, D. J., Du, Y., Dodel, R. C., Saura, J., Fishman, C. E., DeLong, C. A., Piccardo, P., Petegnief, V., Ghetti, B., & Paul, S. M. (1999). Apolipoprotein E is essential for amyloid deposition in the APP(V717F) transgenic mouse model of Alzheimer's disease. *Proc Natl Acad Sci U S A*, *96*(26), 15233-15238. https://doi.org/10.1073/pnas.96.26.15233

Banati, R. B., Gehrmann, J., Schubert, P., & Kreutzberg, G. W. (1993). Cytotoxicity of microglia. *Glia*, *7*(1), 111-118. https://doi.org/10.1002/glia.440070117

Bandyopadhyay, S. (2021). Role of Neuron and Glia in Alzheimer's Disease and Associated Vascular Dysfunction. *Front Aging Neurosci*, *13*, 653334. https://doi.org/10.3389/fnagi.2021.653334

Bar-Joseph, Z. (2004). Analyzing time series gene expression data. *Bioinformatics*, *20*(16), 2493-2503. https://doi.org/10.1093/bioinformatics/bth283

Bar-Joseph, Z., Gerber, G., Simon, I., Gifford, D. K., & Jaakkola, T. S. (2003). Comparing the continuous representation of time-series expression profiles to identify differentially

expressed genes. *Proc Natl Acad Sci U S A*, *100*(18), 10146-10151. https://doi.org/10.1073/pnas.1732547100

Barabasi, A. L., & Albert, R. (1999). Emergence of scaling in random networks. *Science*, *286*(5439), 509-512. https://doi.org/10.1126/science.286.5439.509

Barabasi, A. L., & Bonabeau, E. (2003). Scale-free networks. *Sci Am*, *288*(5), 60-69. https://doi.org/10.1038/scientificamerican0503-60

Battle, A., Mostafavi, S., Zhu, X., Potash, J. B., Weissman, M. M., McCormick, C., Haudenschild, C. D., Beckman, K. B., Shi, J., Mei, R., Urban, A. E., Montgomery, S. B., Levinson, D. F., & Koller, D. (2014). Characterizing the genetic basis of transcriptome diversity through RNA-sequencing of 922 individuals. *Genome Res*, *24*(1), 14-24. https://doi.org/10.1101/gr.155192.113

Bauer, S., Kerr, B. J., & Patterson, P. H. (2007). The neuropoietic cytokine family in development, plasticity, disease and injury. *Nat Rev Neurosci*, *8*(3), 221-232. https://doi.org/10.1038/nrn2054

Beecham, G. W., Hamilton, K., Naj, A. C., Martin, E. R., Huentelman, M., Myers, A. J., Corneveaux, J. J., Hardy, J., Vonsattel, J. P., Younkin, S. G., Bennett, D. A., De Jager, P. L., Larson, E. B., Crane, P. K., Kamboh, M. I., Kofler, J. K., Mash, D. C., Duque, L., Gilbert, J. R., . . . Montine, T. J. (2014). Genome-wide association meta-analysis of neuropathologic features of Alzheimer's disease and related dementias. *PLoS Genet*, *10*(9), e1004606. https://doi.org/10.1371/journal.pgen.1004606

Bélanger, M., & Magistretti, P. J. (2009). The role of astroglia in neuroprotection. *Dialogues Clin Neurosci*, *11*(3), 281-295. https://doi.org/10.31887/DCNS.2009.11.3/mbelanger

Bellenguez, C., Küçükali, F., Jansen, I. E., Kleineidam, L., Moreno-Grau, S., Amin, N., Naj, A. C., Campos-Martin, R., Grenier-Boley, B., Andrade, V., Holmans, P. A., Boland, A., Damotte, V., van der Lee, S. J., Costa, M. R., Kuulasmaa, T., Yang, Q., de Rojas, I., Bis, J. C., . . . Lambert, J. C. (2022). New insights into the genetic etiology of Alzheimer's disease and related dementias. *Nat Genet*, *54*(4), 412-436. https://doi.org/10.1038/s41588-022-01024-z

Bemiller, S. M., McCray, T. J., Allan, K., Formica, S. V., Xu, G., Wilson, G., Kokiko-Cochran, O. N., Crish, S. D., Lasagna-Reeves, C. A., Ransohoff, R. M., Landreth, G. E., & Lamb, B. T. (2017). TREM2 deficiency exacerbates tau pathology through dysregulated kinase signaling in a mouse model of tauopathy. *Mol Neurodegener*, *12*(1), 74. https://doi.org/10.1186/s13024-017-0216-6

Benedet, A. L., Ashton, N. J., Pascoal, T. A., Leuzy, A., Mathotaarachchi, S., Kang, M. S., Therriault, J., Savard, M., Chamoun, M., Scholl, M., Zimmer, E. R., Gauthier, S., Labbe, A., Zetterberg, H., Blennow, K., & Neto, P. R. (2019). Plasma neurofilament light associates with Alzheimer's disease metabolic decline in amyloid-positive individuals. *Alzheimers Dement (Amst)*, *11*, 679-689. https://doi.org/10.1016/j.dadm.2019.08.002

Bennett, B. J., Farber, C. R., Orozco, L., Kang, H. M., Ghazalpour, A., Siemers, N., Neubauer, M., Neuhaus, I., Yordanova, R., Guan, B., Truong, A., Yang, W. P., He, A., Kayne, P., Gargalovic, P., Kirchgessner, T., Pan, C., Castellani, L. W., Kostem, E., . . . Lusis, A. J. (2010). A high-resolution association mapping panel for the dissection of complex traits in mice. *Genome Res*, *20*(2), 281-290. https://doi.org/10.1101/gr.099234.109

Bennett, F. C., Bennett, M. L., Yaqoob, F., Mulinyawe, S. B., Grant, G. A., Hayden Gephart, M., Plowey, E. D., & Barres, B. A. (2018). A Combination of Ontogeny and CNS Environment Establishes Microglial Identity. *Neuron*, *98*(6), 1170-1183 e1178. https://doi.org/10.1016/j.neuron.2018.05.014

Benraiss, A., Wang, S., Herrlinger, S., Li, X., Chandler-Militello, D., Mauceri, J., Burm, H. B., Toner, M., Osipovitch, M., Jim Xu, Q., Ding, F., Wang, F., Kang, N., Kang, J., Curtin, P. C., Brunner, D., Windrem, M. S., Munoz-Sanjuan, I., Nedergaard, M., & Goldman, S. A. (2016). Human glia can both induce and rescue aspects of disease phenotype in Huntington disease. *Nat Commun*, *7*, 11758. https://doi.org/10.1038/ncomms11758

Bentley, D. R., Balasubramanian, S., Swerdlow, H. P., Smith, G. P., Milton, J., Brown, C. G., Hall, K. P., Evers, D. J., Barnes, C. L., Bignell, H. R., Boutell, J. M., Bryant, J., Carter, R. J., Keira Cheetham, R., Cox, A. J., Ellis, D. J., Flatbush, M. R., Gormley, N. A., Humphray, S. J., . . . Smith, A. J. (2008). Accurate whole human genome sequencing using reversible terminator chemistry. *Nature*, *456*(7218), 53-59. https://doi.org/10.1038/nature07517

Berard, J. L., Zarruk, J. G., Arbour, N., Prat, A., Yong, V. W., Jacques, F. H., Akira, S., & David, S. (2012). Lipocalin 2 is a novel immune mediator of experimental autoimmune encephalomyelitis pathogenesis and is modulated in multiple sclerosis. *Glia*, *60*(7), 1145-1159. https://doi.org/10.1002/glia.22342

Berry, J. D., Cudkowicz, M. E., & Shefner, J. M. (2014). Predicting success: optimizing phase II ALS trials for the transition to phase III. *Amyotroph Lateral Scler Frontotemporal Degener*, *15*(1-2), 1-8. https://doi.org/10.3109/21678421.2013.838969

Bezbradica, J. S., Coll, R. C., & Schroder, K. (2017). Sterile signals generate weaker and delayed macrophage NLRP3 inflammasome responses relative to microbial signals. *Cell Mol Immunol*, *14*(1), 118-126. https://doi.org/10.1038/cmi.2016.11

Bianco, F., Pravettoni, E., Colombo, A., Schenk, U., Möller, T., Matteoli, M., & Verderio, C. (2005). Astrocyte-derived ATP induces vesicle shedding and IL-1 beta release from microglia. *J Immunol*, *174*(11), 7268-7277. https://doi.org/10.4049/jimmunol.174.11.7268

Biber, K., Neumann, H., Inoue, K., & Boddeke, H. W. (2007). Neuronal 'On' and 'Off' signals control microglia. *Trends Neurosci*, *30*(11), 596-602. https://doi.org/10.1016/j.tins.2007.08.007

Black, R. A., Rauch, C. T., Kozlosky, C. J., Peschon, J. J., Slack, J. L., Wolfson, M. F., Castner, B. J., Stocking, K. L., Reddy, P., Srinivasan, S., Nelson, N., Boiani, N., Schooley, K. A., Gerhart, M., Davis, R., Fitzner, J. N., Johnson, R. S., Paxton, R. J., March, C. J., & Cerretti, D. P. (1997). A metalloproteinase disintegrin that releases tumour-necrosis factor-alpha from cells. *Nature*, *385*(6618), 729-733. https://doi.org/10.1038/385729a0

Blencowe, B. J., Ahmad, S., & Lee, L. J. (2009). Current-generation high-throughput sequencing: deepening insights into mammalian transcriptomes. *Genes Dev*, *23*(12), 1379-1386. https://doi.org/10.1101/gad.1788009

Blum, D., Chern, Y., Domenici, M. R., Buee, L., Lin, C. Y., Rea, W., Ferre, S., & Popoli, P. (2018). The Role of Adenosine Tone and Adenosine Receptors in Huntington's Disease. *J Caffeine Adenosine Res*, *8*(2), 43-58. https://doi.org/10.1089/caff.2018.0006

Bolger, A. M., Lohse, M., & Usadel, B. (2014). Trimmomatic: a flexible trimmer for Illumina sequence data. *Bioinformatics*, *30*(15), 2114-2120. https://doi.org/10.1093/bioinformatics/btu170

Bolmont, T., Clavaguera, F., Meyer-Luehmann, M., Herzig, M. C., Radde, R., Staufenbiel, M., Lewis, J., Hutton, M., Tolnay, M., & Jucker, M. (2007). Induction of tau pathology by intracerebral infusion of amyloid-beta -containing brain extract and by amyloid-beta deposition in APP x Tau transgenic mice. *Am J Pathol*, *171*(6), 2012-2020. https://doi.org/10.2353/ajpath.2007.070403

Bolmont, T., Haiss, F., Eicke, D., Radde, R., Mathis, C. A., Klunk, W. E., Kohsaka, S., Jucker, M., & Calhoun, M. E. (2008). Dynamics of the microglial/amyloid interaction indicate a role in plaque maintenance. *J Neurosci*, *28*(16), 4283-4292. https://doi.org/10.1523/jneurosci.4814-07.2008

Bouchareychas, L., & Raffai, R. L. (2018). Apolipoprotein E and Atherosclerosis: From Lipoprotein Metabolism to MicroRNA Control of Inflammation. *J Cardiovasc Dev Dis*, *5*(2). https://doi.org/10.3390/jcdd5020030

Boycott, K. M., Campeau, P. M., Howley, H. E., Pavlidis, P., Rogic, S., Oriel, C., Berman, J. N., Hamilton, R. M., Hicks, G. G., Lipshitz, H. D., Masson, J. Y., Shoubridge, E. A., Junker, A., Leroux, M. R., McMaster, C. R., Michaud, J. L., Turvey, S. E., Dyment, D., Innes, A. M., . . . Hieter, P. (2020). The Canadian Rare Diseases Models and Mechanisms (RDMM) Network: Connecting Understudied Genes to Model Organisms. *Am J Hum Genet*, *106*(2), 143-152. https://doi.org/10.1016/j.ajhg.2020.01.009

Brouwers, N., Van Cauwenberghe, C., Engelborghs, S., Lambert, J. C., Bettens, K., Le Bastard, N., Pasquier, F., Montoya, A. G., Peeters, K., Mattheijssens, M., Vandenberghe, R., Deyn, P. P., Cruts, M., Amouyel, P., Sleegers, K., & Van Broeckhoven, C. (2012). Alzheimer risk associated with a copy number variation in the complement receptor 1 increasing C3b/C4b binding sites. *Mol Psychiatry*, *17*(2), 223-233. https://doi.org/10.1038/mp.2011.24

Brumbaugh, C. D., Kim, H. J., Giovacchini, M., & Pourmand, N. (2011). NanoStriDE: normalization and differential expression analysis of NanoString nCounter data. *BMC Bioinformatics*, *12*, 479. https://doi.org/10.1186/1471-2105-12-479

Bruttger, J., Karram, K., Wörtge, S., Regen, T., Marini, F., Hoppmann, N., Klein, M., Blank, T., Yona, S., Wolf, Y., Mack, M., Pinteaux, E., Müller, W., Zipp, F., Binder, H., Bopp, T., Prinz, M., Jung, S., & Waisman, A. (2015). Genetic Cell Ablation Reveals Clusters of Local Self-Renewing Microglia in the Mammalian Central Nervous System. *Immunity*, *43*(1), 92-106. https://doi.org/10.1016/j.immuni.2015.06.012

Bsibsi, M., Persoon-Deen, C., Verwer, R. W., Meeuwsen, S., Ravid, R., & Van Noort, J. M. (2006). Toll-like receptor 3 on adult human astrocytes triggers production of neuroprotective mediators. *Glia*, *53*(7), 688-695. https://doi.org/10.1002/glia.20328

Bubela, T., & Cook-Deegan, R. (2015). Keeping score, strengthening policy and fighting bad actors over access to research tools. *Nat Biotechnol*, *33*(2), 143-147. https://doi.org/10.1038/nbt.3131

Bullard, J. H., Purdom, E., Hansen, K. D., & Dudoit, S. (2010). Evaluation of statistical methods for normalization and differential expression in mRNA-Seq experiments. *BMC Bioinformatics*, *11*, 94. https://doi.org/10.1186/1471-2105-11-94

Bushnell, B., Rood, J., & Singer, E. (2017). BBMerge - Accurate paired shotgun read merging via overlap. *PLOS ONE*, *12*(10), e0185056. https://doi.org/10.1371/journal.pone.0185056

Buskila, Y., Crowe, S. E., & Ellis-Davies, G. C. (2013). Synaptic deficits in layer 5 neurons precede overt structural decay in 5xFAD mice. *Neuroscience*, *254*, 152-159. https://doi.org/10.1016/j.neuroscience.2013.09.016

Butler, C. A., Popescu, A. S., Kitchener, E. J. A., Allendorf, D. H., Puigdellívol, M., & Brown, G. C. (2021). Microglial phagocytosis of neurons in neurodegeneration, and its regulation. *J Neurochem*, *158*(3), 621-639. https://doi.org/10.1111/jnc.15327

Cahoy, J. D., Emery, B., Kaushal, A., Foo, L. C., Zamanian, J. L., Christopherson, K. S., Xing, Y., Lubischer, J. L., Krieg, P. A., Krupenko, S. A., Thompson, W. J., & Barres, B. A. (2008). A transcriptome database for astrocytes, neurons, and oligodendrocytes: a new resource for understanding brain development and function. *J Neurosci*, *28*(1), 264-278. https://doi.org/10.1523/jneurosci.4178-07.2008

Canevari, L., Abramov, A. Y., & Duchen, M. R. (2004). Toxicity of amyloid beta peptide: tales of calcium, mitochondria, and oxidative stress. *Neurochem Res*, *29*(3), 637-650. https://doi.org/10.1023/b:nere.0000014834.06405.af

Cannarile, M. A., Weisser, M., Jacob, W., Jegg, A. M., Ries, C. H., & Ruttinger, D. (2017). Colony-stimulating factor 1 receptor (CSF1R) inhibitors in cancer therapy. *J Immunother Cancer*, *5*(1), 53. https://doi.org/10.1186/s40425-017-0257-y

Canouil, M., Bouland, G. A., Bonnefond, A., Froguel, P., t Hart, L. M., & Slieker, R. C. (2020). NACHO: an R package for quality control of NanoString nCounter data. *Bioinformatics*, *36*(3), 970-971. https://doi.org/10.1093/bioinformatics/btz647

Carlson, M. R., Zhang, B., Fang, Z., Mischel, P. S., Horvath, S., & Nelson, S. F. (2006). Gene connectivity, function, and sequence conservation: predictions from modular yeast co-expression networks. *BMC Genomics*, *7*, 40. https://doi.org/10.1186/1471-2164-7-40

Carmona, S., Hardy, J., & Guerreiro, R. (2018). The genetic landscape of Alzheimer disease. *Handb Clin Neurol*, *148*, 395-408. https://doi.org/10.1016/B978-0-444-64076-5.00026-0

Carneiro, M. O., Russ, C., Ross, M. G., Gabriel, S. B., Nusbaum, C., & DePristo, M. A. (2012). Pacific biosciences sequencing technology for genotyping and variation discovery in human data. *BMC Genomics*, *13*, 375. https://doi.org/10.1186/1471-2164-13-375

Carter, R. J., Lione, L. A., Humby, T., Mangiarini, L., Mahal, A., Bates, G. P., Dunnett, S. B., & Morton, A. J. (1999). Characterization of progressive motor deficits in mice transgenic for the human Huntington's disease mutation. *J Neurosci*, *19*(8), 3248-3257. https://doi.org/10.1523/JNEUROSCI.19-08-03248.1999

Carulli, D., Broersen, R., de Winter, F., Muir, E. M., Meskovic, M., de Waal, M., de Vries, S., Boele, H. J., Canto, C. B., De Zeeuw, C. I., & Verhaagen, J. (2020). Cerebellar plasticity and associative memories are controlled by perineuronal nets. *Proc Natl Acad Sci U S A*, *117*(12), 6855-6865. https://doi.org/10.1073/pnas.1916163117

Casali, B. T., MacPherson, K. P., Reed-Geaghan, E. G., & Landreth, G. E. (2020). Microglia depletion rapidly and reversibly alters amyloid pathology by modification of plaque compaction and morphologies. *Neurobiol Dis*, *142*, 104956. https://doi.org/10.1016/j.nbd.2020.104956

Cedazo-Mínguez, A., & Cowburn, R. F. (2001). Apolipoprotein E: a major piece in the Alzheimer's disease puzzle. *J Cell Mol Med*, *5*(3), 254-266. https://doi.org/10.1111/j.1582-4934.2001.tb00159.x

Chen, S. C., Abe, Y., Fang, P. T., Hsieh, Y. J., Yang, Y. I., Lu, T. Y., Oda, S., Mitani, H., Lian, S. L., Tyan, Y. C., Huang, C. J., & Hisatsune, T. (2017). Prognosis of Hippocampal Function after Sub-lethal Irradiation Brain Injury in Patients with Nasopharyngeal Carcinoma. *Sci Rep*, *7*(1), 14697. https://doi.org/10.1038/s41598-017-13972-2

Chen, S. F., Dias, R., Evans, D., Salfati, E. L., Liu, S., Wineinger, N. E., & Torkamani, A. (2020). Genotype imputation and variability in polygenic risk score estimation. *Genome Med*, *12*(1), 100. https://doi.org/10.1186/s13073-020-00801-x

Chen, Y., Zhu, J., Lum, P. Y., Yang, X., Pinto, S., MacNeil, D. J., Zhang, C., Lamb, J., Edwards, S., Sieberts, S. K., Leonardson, A., Castellini, L. W., Wang, S., Champy, M. F., Zhang, B., Emilsson, V., Doss, S., Ghazalpour, A., Horvath, S., . . . Schadt, E. E. (2008). Variations in DNA elucidate molecular networks that cause disease. *Nature*, *452*(7186), 429-435. https://doi.org/10.1038/nature06757

Chesler, E. J., Miller, D. R., Branstetter, L. R., Galloway, L. D., Jackson, B. L., Philip, V. M., Voy, B. H., Culiat, C. T., Threadgill, D. W., Williams, R. W., Churchill, G. A., Johnson, D. K., & Manly, K. F. (2008). The Collaborative Cross at Oak Ridge National Laboratory: developing a powerful resource for systems genetics. *Mamm Genome*, *19*(6), 382-389. https://doi.org/10.1007/s00335-008-9135-8

Chia, W. J., Dawe, G. S., & Ong, W. Y. (2011). Expression and localization of the iron-siderophore binding protein lipocalin 2 in the normal rat brain and after kainate-induced excitotoxicity. *Neurochem Int*, *59*(5), 591-599. https://doi.org/10.1016/j.neuint.2011.04.007

Chibnik, L. B., Yu, L., Eaton, M. L., Srivastava, G., Schneider, J. A., Kellis, M., Bennett, D. A., & De Jager, P. L. (2015). Alzheimer's loci: epigenetic associations and interaction with genetic factors. *Ann Clin Transl Neurol*, *2*(6), 636-647. https://doi.org/10.1002/acn3.201

Chitu, V., Biundo, F., Shlager, G. G. L., Park, E. S., Wang, P., Gulinello, M. E., Gokhan, S., Ketchum, H. C., Saha, K., DeTure, M. A., Dickson, D. W., Wszolek, Z. K., Zheng, D., Croxford, A. L., Becher, B., Sun, D., Mehler, M. F., & Stanley, E. R. (2020). Microglial Homeostasis Requires Balanced CSF-1/CSF-2 Receptor Signaling. *Cell Rep*, *30*(9), 3004-3019 e3005. https://doi.org/10.1016/j.celrep.2020.02.028

Chitu, V., Gokhan, S., Gulinello, M., Branch, C. A., Patil, M., Basu, R., Stoddart, C., Mehler, M. F., & Stanley, E. R. (2015). Phenotypic characterization of a Csf1r haploinsufficient mouse model of adult-onset leukodystrophy with axonal spheroids and pigmented glia (ALSP). *Neurobiol Dis*, *74*, 219-228. https://doi.org/10.1016/j.nbd.2014.12.001

Cho, K. (2019). Emerging Roles of Complement Protein C1q in Neurodegeneration. *Aging Dis*, *10*(3), 652-663. https://doi.org/10.14336/AD.2019.0118

Choi, S. S., Lee, H. J., Lim, I., Satoh, J., & Kim, S. U. (2014). Human astrocytes: secretome profiles of cytokines and chemokines. *PLOS ONE*, *9*(4), e92325. https://doi.org/10.1371/journal.pone.0092325

Chouraki, V., Reitz, C., Maury, F., Bis, J. C., Bellenguez, C., Yu, L., Jakobsdottir, J., Mukherjee, S., Adams, H. H., Choi, S. H., Larson, E. B., Fitzpatrick, A., Uitterlinden, A. G., de Jager, P. L., Hofman, A., Gudnason, V., Vardarajan, B., Ibrahim-Verbaas, C., van der Lee, S. J., . . . Seshadri, S. (2016). Evaluation of a Genetic Risk Score to Improve Risk Prediction for Alzheimer's Disease. *J Alzheimers Dis*, *53*(3), 921-932. https://doi.org/10.3233/jad-150749

Christodoulou, D. C., Gorham, J. M., Herman, D. S., & Seidman, J. G. (2011). Construction of normalized RNA-seq libraries for next-generation sequencing using the crab duplex-specific nuclease. *Curr Protoc Mol Biol*, *Chapter 4*, Unit4 12. https://doi.org/10.1002/0471142727.mb0412s94

Christopherson, K. S., Ullian, E. M., Stokes, C. C., Mullowney, C. E., Hell, J. W., Agah, A., Lawler, J., Mosher, D. F., Bornstein, P., & Barres, B. A. (2005). Thrombospondins are astrocyte-secreted proteins that promote CNS synaptogenesis. *Cell*, *120*(3), 421-433. https://doi.org/10.1016/j.cell.2004.12.020

Chung, W. S., & Barres, B. A. (2012). The role of glial cells in synapse elimination. *Curr Opin Neurobiol*, *22*(3), 438-445. https://doi.org/10.1016/j.conb.2011.10.003

Churchill, G. A., Airey, D. C., Allayee, H., Angel, J. M., Attie, A. D., Beatty, J., Beavis, W. D., Belknap, J. K., Bennett, B., Berrettini, W., Bleich, A., Bogue, M., Broman, K. W., Buck, K. J., Buckler, E., Burmeister, M., Chesler, E. J., Cheverud, J. M., Clapcote, S., . . . Complex Trait, C. (2004). The Collaborative Cross, a community resource for the genetic analysis of complex traits. *Nat Genet*, *36*(11), 1133-1137. https://doi.org/10.1038/ng1104-1133

Churchill, G. A., Gatti, D. M., Munger, S. C., & Svenson, K. L. (2012). The Diversity Outbred mouse population. *Mamm Genome*, *23*(9-10), 713-718. https://doi.org/10.1007/s00335-012-9414-2

Clark, K., Leung, Y. Y., Lee, W. P., Voight, B., & Wang, L. S. (2022). Polygenic Risk Scores in Alzheimer's Disease Genetics: Methodology, Applications, Inclusion, and Diversity. *J Alzheimers Dis*, *89*(1), 1-12. https://doi.org/10.3233/jad-220025

Colton, C. A., Mott, R. T., Sharpe, H., Xu, Q., Van Nostrand, W. E., & Vitek, M. P. (2006). Expression profiles for macrophage alternative activation genes in AD and in mouse models of AD. *J Neuroinflammation*, *3*, 27. https://doi.org/10.1186/1742-2094-3-27

Condello, C., Yuan, P., Schain, A., & Grutzendler, J. (2015). Microglia constitute a barrier that prevents neurotoxic protofibrillar Aβ42 hotspots around plaques. *Nat Commun*, *6*, 6176. https://doi.org/10.1038/ncomms7176

Consortium, E. P., Birney, E., Stamatoyannopoulos, J. A., Dutta, A., Guigo, R., Gingeras, T. R., Margulies, E. H., Weng, Z., Snyder, M., Dermitzakis, E. T., Thurman, R. E., Kuehn, M. S., Taylor, C. M., Neph, S., Koch, C. M., Asthana, S., Malhotra, A., Adzhubei, I., Greenbaum, J. A., . . . de Jong, P. J. (2007). Identification and analysis of functional elements in 1% of the human genome by the ENCODE pilot project. *Nature*, *447*(7146), 799-816. https://doi.org/10.1038/nature05874

Consortium, H. D. i. (2017). Developmental alterations in Huntington's disease neural cells and pharmacological rescue in cells and mice. *Nat Neurosci*, *20*(5), 648-660. https://doi.org/10.1038/nn.4532

Cornet, A., Bettelli, E., Oukka, M., Cambouris, C., Avellana-Adalid, V., Kosmatopoulos, K., & Liblau, R. S. (2000). Role of astrocytes in antigen presentation and naive T-cell activation. *J Neuroimmunol*, *106*(1-2), 69-77. https://doi.org/10.1016/s0165-5728(99)00215-5

Crapser, J. D., Ochaba, J., Soni, N., Reidling, J. C., Thompson, L. M., & Green, K. N. (2020). Microglial depletion prevents extracellular matrix changes and striatal volume reduction in a model of Huntington's disease. *Brain*, *143*(1), 266-288. https://doi.org/10.1093/brain/awz363

Crapser, J. D., Spangenberg, E. E., Barahona, R. A., Arreola, M. A., Hohsfield, L. A., & Green, K. N. (2020). Microglia facilitate loss of perineuronal nets in the Alzheimer's disease brain. *EBioMedicine*, *58*, 102919. https://doi.org/10.1016/j.ebiom.2020.102919

Crehan, H., Hardy, J., & Pocock, J. (2013). Blockage of CR1 prevents activation of rodent microglia. *Neurobiol Dis*, *54*, 139-149. https://doi.org/10.1016/j.nbd.2013.02.003

Cronk, J. C., Filiano, A. J., Louveau, A., Marin, I., Marsh, R., Ji, E., Goldman, D. H., Smirnov, I., Geraci, N., Acton, S., Overall, C. C., & Kipnis, J. (2018). Peripherally derived macrophages can engraft the brain independent of irradiation and maintain an identity distinct from microglia. *J Exp Med*, *215*(6), 1627-1647. https://doi.org/10.1084/jem.20180247

Crotti, A., & Glass, C. K. (2015). The choreography of neuroinflammation in Huntington's disease. *Trends Immunol*, *36*(6), 364-373. https://doi.org/10.1016/j.it.2015.04.007

Cui, X., & Churchill, G. A. (2003). Statistical tests for differential expression in cDNA microarray experiments. *Genome Biol*, *4*(4), 210. https://doi.org/10.1186/gb-2003-4-4-210

D'Cruz, P. M., Yasumura, D., Weir, J., Matthes, M. T., Abderrahim, H., LaVail, M. M., & Vollrath, D. (2000). Mutation of the receptor tyrosine kinase gene Mertk in the retinal dystrophic RCS rat. *Hum Mol Genet*, *9*(4), 645-651. https://doi.org/10.1093/hmg/9.4.645

Daborg, J., Andreasson, U., Pekna, M., Lautner, R., Hanse, E., Minthon, L., Blennow, K., Hansson, O., & Zetterberg, H. (2012). Cerebrospinal fluid levels of complement proteins C3, C4 and CR1 in Alzheimer's disease. *J Neural Transm (Vienna)*, *119*(7), 789-797. https://doi.org/10.1007/s00702-012-0797-8

Dagher, N. N., Najafi, A. R., Kayala, K. M., Elmore, M. R., White, T. E., Medeiros, R., West, B. L., & Green, K. N. (2015). Colony-stimulating factor 1 receptor inhibition prevents microglial plaque association and improves cognition in 3xTg-AD mice. *J Neuroinflammation*, *12*, 139. https://doi.org/10.1186/s12974-015-0366-9

Dawson, T. M., Golde, T. E., & Lagier-Tourenne, C. (2018). Animal models of neurodegenerative diseases. *Nat Neurosci*, *21*(10), 1370-1379. https://doi.org/10.1038/s41593-018-0236-8

de Calignon, A., Polydoro, M., Suárez-Calvet, M., William, C., Adamowicz, D. H., Kopeikina, K. J., Pitstick, R., Sahara, N., Ashe, K. H., Carlson, G. A., Spires-Jones, T. L., & Hyman, B. T. (2012). Propagation of tau pathology in a model of early Alzheimer's disease. *Neuron*, *73*(4), 685-697. https://doi.org/10.1016/j.neuron.2011.11.033

De Jager, P. L., Srivastava, G., Lunnon, K., Burgess, J., Schalkwyk, L. C., Yu, L., Eaton, M. L., Keenan, B. T., Ernst, J., McCabe, C., Tang, A., Raj, T., Replogle, J., Brodeur, W., Gabriel, S., Chai, H. S., Younkin, C., Younkin, S. G., Zou, F., . . . Bennett, D. A. (2014). Alzheimer's disease: early alterations in brain DNA methylation at ANK1, BIN1, RHBDF2 and other loci. *Nat Neurosci*, *17*(9), 1156-1163. https://doi.org/10.1038/nn.3786

De Strooper, B., & Karran, E. (2016). The Cellular Phase of Alzheimer's Disease. *Cell*, *164*(4), 603-615. https://doi.org/10.1016/j.cell.2015.12.056

de Wolf, F., Ghanbari, M., Licher, S., McRae-McKee, K., Gras, L., Weverling, G. J., Wermeling, P., Sedaghat, S., Ikram, M. K., Waziry, R., Koudstaal, W., Klap, J., Kostense, S., Hofman, A., Anderson, R., Goudsmit, J., & Ikram, M. A. (2020). Plasma tau, neurofilament light chain and amyloid-β levels and risk of dementia; a population-based cohort study. *Brain*, *143*(4), 1220-1232. https://doi.org/10.1093/brain/awaa054

Desikan, R. S., Fan, C. C., Wang, Y., Schork, A. J., Cabral, H. J., Cupples, L. A., Thompson, W. K., Besser, L., Kukull, W. A., Holland, D., Chen, C. H., Brewer, J. B., Karow, D. S., Kauppi, K., Witoelar, A., Karch, C. M., Bonham, L. W., Yokoyama, J. S., Rosen, H. J., . . . Dale, A. M. (2017). Genetic assessment of age-associated Alzheimer disease risk: Development and validation of a polygenic hazard score. *PLoS Med*, *14*(3), e1002258. https://doi.org/10.1371/journal.pmed.1002258

Deuss, M., Reiss, K., & Hartmann, D. (2008). Part-time alpha-secretases: the functional biology of ADAM 9, 10 and 17. *Curr Alzheimer Res*, *5*(2), 187-201. https://doi.org/10.2174/156720508783954686

Dickens, A. M., Tovar, Y. R. L. B., Yoo, S. W., Trout, A. L., Bae, M., Kanmogne, M., Megra, B., Williams, D. W., Witwer, K. W., Gacias, M., Tabatadze, N., Cole, R. N., Casaccia, P., Berman, J. W., Anthony, D. C., & Haughey, N. J. (2017). Astrocyte-shed extracellular vesicles regulate the peripheral leukocyte response to inflammatory brain lesions. *Sci Signal*, *10*(473). https://doi.org/10.1126/scisignal.aai7696

Dickson, D. W. (1997). The pathogenesis of senile plaques. *J Neuropathol Exp Neurol*, *56*(4), 321-339. https://doi.org/10.1097/00005072-199704000-00001

Dietrich, J., Baryawno, N., Nayyar, N., Valtis, Y. K., Yang, B., Ly, I., Besnard, A., Severe, N., Gustafsson, K. U., Andronesi, O. C., Batchelor, T. T., Sahay, A., & Scadden, D. T. (2018). Bone marrow drives central nervous system regeneration after radiation injury. *J Clin Invest*, *128*(1), 281-293. https://doi.org/10.1172/jci90647

Dobin, A., Davis, C. A., Schlesinger, F., Drenkow, J., Zaleski, C., Jha, S., Batut, P., Chaisson, M., & Gingeras, T. R. (2013). STAR: ultrafast universal RNA-seq aligner. *Bioinformatics*, *29*(1), 15-21. https://doi.org/10.1093/bioinformatics/bts635

Dong, J., & Horvath, S. (2007). Understanding network concepts in modules. *BMC Syst Biol*, *1*, 24. https://doi.org/10.1186/1752-0509-1-24

Dong, Y., Yu, T., Ding, L., Laurini, E., Huang, Y., Zhang, M., Weng, Y., Lin, S., Chen, P., Marson, D., Jiang, Y., Giorgio, S., Pricl, S., Liu, X., Rocchi, P., & Peng, L. (2018). A Dual Targeting Dendrimer-Mediated siRNA Delivery System for Effective Gene Silencing in Cancer Therapy. *J Am Chem Soc*, *140*(47), 16264-16274. https://doi.org/10.1021/jacs.8b10021

Dourlen, P., Kilinc, D., Malmanche, N., Chapuis, J., & Lambert, J. C. (2019). The new genetic landscape of Alzheimer's disease: from amyloid cascade to genetically driven synaptic failure hypothesis? *Acta Neuropathol*, *138*(2), 221-236. https://doi.org/10.1007/s00401-019-02004-0

Drummond, E., & Wisniewski, T. (2017). Alzheimer's disease: experimental models and reality. *Acta Neuropathol*, *133*(2), 155-175. https://doi.org/10.1007/s00401-016-1662-x

Dugger, B. N., Adler, C. H., Shill, H. A., Caviness, J., Jacobson, S., Driver-Dunckley, E., & Beach, T. G. (2014). Concomitant pathologies among a spectrum of parkinsonian disorders. *Parkinsonism Relat Disord*, *20*(5), 525-529. https://doi.org/10.1016/j.parkreldis.2014.02.012

Dunn, A. R., O'Connell, K. M. S., & Kaczorowski, C. C. (2019). Gene-by-environment interactions in Alzheimer's disease and Parkinson's disease. *Neurosci Biobehav Rev*, *103*, 73-80. https://doi.org/10.1016/j.neubiorev.2019.06.018

Duyao, M., Ambrose, C., Myers, R., Novelletto, A., Persichetti, F., Frontali, M., Folstein, S., Ross, C., Franz, M., Abbott, M., & et al. (1993). Trinucleotide repeat length instability and age of onset in Huntington's disease. *Nat Genet*, *4*(4), 387-392. https://doi.org/10.1038/ng0893-387

Dzamba, D., Harantova, L., Butenko, O., & Anderova, M. (2016). Glial Cells - The Key Elements of Alzheimer´s Disease. *Curr Alzheimer Res*, *13*(8), 894-911. https://doi.org/10.2174/1567205013666160129095924

Easley-Neal, C., Foreman, O., Sharma, N., Zarrin, A. A., & Weimer, R. M. (2019). CSF1R Ligands IL-34 and CSF1 Are Differentially Required for Microglia Development and Maintenance in White and Gray Matter Brain Regions. *Front Immunol*, *10*, 2199. https://doi.org/10.3389/fimmu.2019.02199

Eid, J., Fehr, A., Gray, J., Luong, K., Lyle, J., Otto, G., Peluso, P., Rank, D., Baybayan, P., Bettman, B., Bibillo, A., Bjornson, K., Chaudhuri, B., Christians, F., Cicero, R., Clark, S., Dalal, R., Dewinter, A., Dixon, J., . . . Turner, S. (2009). Real-time DNA sequencing from single polymerase molecules. *Science*, *323*(5910), 133-138. https://doi.org/10.1126/science.1162986

Elmore, M. R., Najafi, A. R., Koike, M. A., Dagher, N. N., Spangenberg, E. E., Rice, R. A., Kitazawa, M., Matusow, B., Nguyen, H., West, B. L., & Green, K. N. (2014). Colony-stimulating factor 1 receptor signaling is necessary for microglia viability, unmasking a microglia progenitor cell in the adult brain. *Neuron*, *82*(2), 380-397. https://doi.org/10.1016/j.neuron.2014.02.040

Elmore, M. R. P., Hohsfield, L. A., Kramár, E. A., Soreq, L., Lee, R. J., Pham, S. T., Najafi, A. R., Spangenberg, E. E., Wood, M. A., West, B. L., & Green, K. N. (2018). Replacement of microglia in the aged brain reverses cognitive, synaptic, and neuronal deficits in mice. *Aging Cell*, *17*(6), e12832. https://doi.org/10.1111/acel.12832

Elshatory, Y., & Gan, L. (2008). The LIM-homeobox gene Islet-1 is required for the development of restricted forebrain cholinergic neurons. *J Neurosci*, *28*(13), 3291-3297. https://doi.org/10.1523/JNEUROSCI.5730-07.2008

Engstrom, P. G., Steijger, T., Sipos, B., Grant, G. R., Kahles, A., Ratsch, G., Goldman, N., Hubbard, T. J., Harrow, J., Guigo, R., Bertone, P., & Consortium, R. (2013). Systematic evaluation of spliced alignment programs for RNA-seq data. *Nat Methods*, *10*(12), 1185-1191. https://doi.org/10.1038/nmeth.2722

Eratne, D., Loi, S. M., Farrand, S., Kelso, W., Velakoulis, D., & Looi, J. C. (2018). Alzheimer's disease: clinical update on epidemiology, pathophysiology and diagnosis. *Australas Psychiatry*, *26*(4), 347-357. https://doi.org/10.1177/1039856218762308

Erblich, B., Zhu, L., Etgen, A. M., Dobrenis, K., & Pollard, J. W. (2011). Absence of colony stimulation factor-1 receptor results in loss of microglia, disrupted brain development and olfactory deficits. *PLOS ONE*, *6*(10), e26317. https://doi.org/10.1371/journal.pone.0026317

Eroglu, C., Allen, N. J., Susman, M. W., O'Rourke, N. A., Park, C. Y., Ozkan, E., Chakraborty, C., Mulinyawe, S. B., Annis, D. S., Huberman, A. D., Green, E. M., Lawler, J., Dolmetsch, R., Garcia, K. C., Smith, S. J., Luo, Z. D., Rosenthal, A., Mosher, D. F., & Barres, B. A. (2009). Gabapentin receptor alpha2delta-1 is a neuronal thrombospondin receptor responsible for excitatory CNS synaptogenesis. *Cell*, *139*(2), 380-392. https://doi.org/10.1016/j.cell.2009.09.025

Escartin, C., Galea, E., Lakatos, A., O'Callaghan, J. P., Petzold, G. C., Serrano-Pozo, A., Steinhäuser, C., Volterra, A., Carmignoto, G., Agarwal, A., Allen, N. J., Araque, A., Barbeito, L., Barzilai, A., Bergles, D. E., Bonvento, G., Butt, A. M., Chen, W. T., Cohen-Salmon, M., . . . Verkhratsky, A. (2021). Reactive astrocyte nomenclature, definitions, and future directions. *Nat Neurosci*, *24*(3), 312-325. https://doi.org/10.1038/s41593-020-00783-4

Escott-Price, V., Myers, A. J., Huentelman, M., & Hardy, J. (2017). Polygenic risk score analysis of pathologically confirmed Alzheimer disease. *Ann Neurol*, *82*(2), 311-314. https://doi.org/10.1002/ana.24999

Escott-Price, V., Sims, R., Bannister, C., Harold, D., Vronskaya, M., Majounie, E., Badarinarayan, N., Morgan, K., Passmore, P., Holmes, C., Powell, J., Brayne, C., Gill, M., Mead, S., Goate, A., Cruchaga, C., Lambert, J. C., van Duijn, C., Maier, W., . . . Williams, J. (2015). Common polygenic variation enhances risk prediction for Alzheimer's disease. *Brain*, *138*(Pt 12), 3673-3684. https://doi.org/10.1093/brain/awv268

Fakhoury, M. (2018). Microglia and Astrocytes in Alzheimer's Disease: Implications for Therapy. *Curr Neuropharmacol*, *16*(5), 508-518. https://doi.org/10.2174/1570159x15666170720095240

Farhy-Tselnicker, I., & Allen, N. J. (2018). Astrocytes, neurons, synapses: a tripartite view on cortical circuit development. *Neural Dev*, *13*(1), 7. https://doi.org/10.1186/s13064-018-0104-y

Fawcett, J. W., Oohashi, T., & Pizzorusso, T. (2019). The roles of perineuronal nets and the perinodal extracellular matrix in neuronal function. *Nat Rev Neurosci*, *20*(8), 451-465. https://doi.org/10.1038/s41583-019-0196-3

Feng, T., Lacrampe, A., & Hu, F. (2021). Physiological and pathological functions of TMEM106B: a gene associated with brain aging and multiple brain disorders. *Acta Neuropathol*, *141*(3), 327-339. https://doi.org/10.1007/s00401-020-02246-3

Feng, X., Jopson, T. D., Paladini, M. S., Liu, S., West, B. L., Gupta, N., & Rosi, S. (2016). Colony-stimulating factor 1 receptor blockade prevents fractionated whole-brain irradiation-induced memory deficits. *J Neuroinflammation*, *13*(1), 215. https://doi.org/10.1186/s12974-016-0671-y

Fernandez-Castaneda, A., & Gaultier, A. (2016). Adult oligodendrocyte progenitor cells - Multifaceted regulators of the CNS in health and disease. *Brain Behav Immun*, *57*, 1-7. https://doi.org/10.1016/j.bbi.2016.01.005

Fernandez, A. M., Fernandez, S., Carrero, P., Garcia-Garcia, M., & Torres-Aleman, I. (2007). Calcineurin in reactive astrocytes plays a key role in the interplay between proinflammatory and anti-inflammatory signals. *J Neurosci*, *27*(33), 8745-8756. https://doi.org/10.1523/jneurosci.1002-07.2007

Fernandez, A. M., Jimenez, S., Mecha, M., Dávila, D., Guaza, C., Vitorica, J., & Torres-Aleman, I. (2012). Regulation of the phosphatase calcineurin by insulin-like growth factor I unveils a key role of astrocytes in Alzheimer's pathology. *Mol Psychiatry*, *17*(7), 705-718. https://doi.org/10.1038/mp.2011.128

Ferreira, A., & Paganoni, S. (2002). The formation of synapses in the central nervous system. *Mol Neurobiol*, *26*(1), 69-79. https://doi.org/10.1385/MN:26:1:069

Ferrero, E., Dunham, I., & Sanseau, P. (2017). In silico prediction of novel therapeutic targets using gene-disease association data. *J Transl Med*, *15*(1), 182. https://doi.org/10.1186/s12967-017-1285-6

Forner, S., Kawauchi, S., Balderrama-Gutierrez, G., Kramar, E. A., Matheos, D. P., Phan, J., Javonillo, D. I., Tran, K. M., Hingco, E., da Cunha, C., Rezaie, N., Alcantara, J. A., Baglietto-Vargas, D., Jansen, C., Neumann, J., Wood, M. A., MacGregor, G. R., Mortazavi, A., Tenner, A. J., . . . Green, K. N. (2021). Systematic phenotyping and characterization of the 5xFAD mouse model of Alzheimer's disease. *Sci Data*, *8*(1), 270. https://doi.org/10.1038/s41597-021-01054-y

Friese, M. A., Schattling, B., & Fugger, L. (2014). Mechanisms of neurodegeneration and axonal dysfunction in multiple sclerosis. *Nat Rev Neurol*, *10*(4), 225-238. https://doi.org/10.1038/nrneurol.2014.37

Fu, G. K., Xu, W., Wilhelmy, J., Mindrinos, M. N., Davis, R. W., Xiao, W., & Fodor, S. P. (2014). Molecular indexing enables quantitative targeted RNA sequencing and reveals poor efficiencies in standard library preparations. *Proc Natl Acad Sci U S A*, *111*(5), 1891-1896. https://doi.org/10.1073/pnas.1323732111

Fu, H., Rodriguez, G. A., Herman, M., Emrani, S., Nahmani, E., Barrett, G., Figueroa, H. Y., Goldberg, E., Hussaini, S. A., & Duff, K. E. (2017). Tau Pathology Induces Excitatory Neuron Loss, Grid Cell Dysfunction, and Spatial Memory Deficits Reminiscent of Early Alzheimer's Disease. *Neuron*, *93*(3), 533-541.e535. https://doi.org/10.1016/j.neuron.2016.12.023

Fuhrmann, M., Bittner, T., Jung, C. K., Burgold, S., Page, R. M., Mitteregger, G., Haass, C., LaFerla, F. M., Kretzschmar, H., & Herms, J. (2010). Microglial Cx3cr1 knockout prevents neuron loss in a mouse model of Alzheimer's disease. *Nat Neurosci*, *13*(4), 411-413. https://doi.org/10.1038/nn.2511

Fukada, Y., Yasui, K., Kitayama, M., Doi, K., Nakano, T., Watanabe, Y., & Nakashima, K. (2007). Gene expression analysis of the murine model of amyotrophic lateral sclerosis: studies of the Leu126delTT mutation in SOD1. *Brain Res*, *1160*, 1-10. https://doi.org/10.1016/j.brainres.2007.05.044

Fukumoto, H., Asami-Odaka, A., Suzuki, N., & Iwatsubo, T. (1996). Association of A beta 40-positive senile plaques with microglial cells in the brains of patients with Alzheimer's disease and in non-demented aged individuals. *Neurodegeneration*, *5*(1), 13-17. https://doi.org/10.1006/neur.1996.0002

Gabbita, S. P., Srivastava, M. K., Eslami, P., Johnson, M. F., Kobritz, N. K., Tweedie, D., Greig, N. H., Zemlan, F. P., Sharma, S. P., & Harris-White, M. E. (2012). Early intervention with a small molecule inhibitor for tumor necrosis factor-alpha prevents cognitive deficits in a triple transgenic mouse model of Alzheimer's disease. *J Neuroinflammation*, *9*, 99. https://doi.org/10.1186/1742-2094-9-99

Galatro, T. F., Holtman, I. R., Lerario, A. M., Vainchtein, I. D., Brouwer, N., Sola, P. R., Veras, M. M., Pereira, T. F., Leite, R. E. P., Moller, T., Wes, P. D., Sogayar, M. C., Laman, J. D., den Dunnen, W., Pasqualucci, C. A., Oba-Shinjo, S. M., Boddeke, E., Marie, S. K. N., & Eggen, B. J. L. (2017). Transcriptomic analysis of purified human cortical microglia reveals age-associated changes. *Nat Neurosci*, *20*(8), 1162-1171. https://doi.org/10.1038/nn.4597

Gall, T., Valkanas, E., Bello, C., Markello, T., Adams, C., Bone, W. P., Brandt, A. J., Brazill, J. M., Carmichael, L., Davids, M., Davis, J., Diaz-Perez, Z., Draper, D., Elson, J., Flynn, E. D., Godfrey, R., Groden, C., Hsieh, C. K., Fischer, R., . . . Boerkoel, C. F. (2017). Defining Disease, Diagnosis, and Translational Medicine within a Homeostatic Perturbation Paradigm: The National Institutes of Health Undiagnosed Diseases Program Experience. *Front Med (Lausanne)*, *4*, 62. https://doi.org/10.3389/fmed.2017.00062

Gao, S., Hendrie, H. C., Hall, K. S., & Hui, S. (1998). The relationships between age, sex, and the incidence of dementia and Alzheimer disease: a meta-analysis. *Arch Gen Psychiatry*, *55*(9), 809-815. https://doi.org/10.1001/archpsyc.55.9.809

Garcia-Estrada, J., Garcia-Segura, L. M., & Torres-Aleman, I. (1992). Expression of insulin-like growth factor I by astrocytes in response to injury. *Brain Res*, *592*(1-2), 343-347. https://doi.org/10.1016/0006-8993(92)91695-b

Gargalovic, P. S., Imura, M., Zhang, B., Gharavi, N. M., Clark, M. J., Pagnon, J., Yang, W. P., He, A., Truong, A., Patel, S., Nelson, S. F., Horvath, S., Berliner, J. A., Kirchgessner, T. G., & Lusis, A. J. (2006). Identification of inflammatory gene modules based on variations of human endothelial cell responses to oxidized lipids. *Proc Natl Acad Sci U S A*, *103*(34), 12741-12746. https://doi.org/10.1073/pnas.0605457103

Gatz, M., Pedersen, N. L., Berg, S., Johansson, B., Johansson, K., Mortimer, J. A., Posner, S. F., Viitanen, M., Winblad, B., & Ahlbom, A. (1997). Heritability for Alzheimer's disease: the study of dementia in Swedish twins. *J Gerontol A Biol Sci Med Sci*, *52*(2), M117-125. https://doi.org/10.1093/gerona/52a.2.m117

Gatz, M., Reynolds, C. A., Fratiglioni, L., Johansson, B., Mortimer, J. A., Berg, S., Fiske, A., & Pedersen, N. L. (2006). Role of genes and environments for explaining Alzheimer disease. *Arch Gen Psychiatry*, *63*(2), 168-174. https://doi.org/10.1001/archpsyc.63.2.168

Geisler, S., Schopf, C. L., & Obermair, G. J. (2015). Emerging evidence for specific neuronal functions of auxiliary calcium channel alpha(2)delta subunits. *Gen Physiol Biophys*, *34*(2), 105-118. https://doi.org/10.4149/gpb_2014037

Geiss, G. K., Bumgarner, R. E., Birditt, B., Dahl, T., Dowidar, N., Dunaway, D. L., Fell, H. P., Ferree, S., George, R. D., Grogan, T., James, J. J., Maysuria, M., Mitton, J. D., Oliveri, P., Osborn, J. L., Peng, T., Ratcliffe, A. L., Webster, P. J., Davidson, E. H., . . . Dimitrov, K. (2008). Direct multiplexed measurement of gene expression with color-coded probe pairs. *Nat Biotechnol*, *26*(3), 317-325. https://doi.org/10.1038/nbt1385

Gerrish, A., Russo, G., Richards, A., Moskvina, V., Ivanov, D., Harold, D., Sims, R., Abraham, R., Hollingworth, P., Chapman, J., Hamshere, M., Pahwa, J. S., Dowzell, K., Williams, A., Jones, N., Thomas, C., Stretton, A., Morgan, A. R., Lovestone, S., . . . Williams, J. (2012). The role of variation at AβPP, PSEN1, PSEN2, and MAPT in late onset Alzheimer's disease. *J Alzheimers Dis*, *28*(2), 377-387. https://doi.org/10.3233/jad-2011-110824

Gesase, A. P., & Kiyama, H. (2007). Peripheral nerve injury induced expression of mRNA for serine protease inhibitor 3 in the rat facial and hypoglossal nuclei but not in the spinal cord. *Ital J Anat Embryol*, *112*(3), 157-168.

Ghasemi, M., & Brown, R. H., Jr. (2018). Genetics of Amyotrophic Lateral Sclerosis. *Cold Spring Harb Perspect Med*, *8*(5). https://doi.org/10.1101/cshperspect.a024125

Gibb, W. R., & Lees, A. J. (1988). The relevance of the Lewy body to the pathogenesis of idiopathic Parkinson's disease. *J Neurol Neurosurg Psychiatry*, *51*(6), 745-752. https://doi.org/10.1136/jnnp.51.6.745

Ginhoux, F., Greter, M., Leboeuf, M., Nandi, S., See, P., Gokhan, S., Mehler, M. F., Conway, S. J., Ng, L. G., Stanley, E. R., Samokhvalov, I. M., & Merad, M. (2010). Fate mapping analysis reveals that adult microglia derive from primitive macrophages. *Science*, *330*(6005), 841-845. https://doi.org/10.1126/science.1194637

Ginhoux, F., Lim, S., Hoeffel, G., Low, D., & Huber, T. (2013). Origin and differentiation of microglia. *Front Cell Neurosci*, *7*, 45. https://doi.org/10.3389/fncel.2013.00045

Ginhoux, F., & Prinz, M. (2015). Origin of microglia: current concepts and past controversies. *Cold Spring Harb Perspect Biol*, *7*(8), a020537. https://doi.org/10.1101/cshperspect.a020537

Goedert, M., Eisenberg, D. S., & Crowther, R. A. (2017). Propagation of Tau Aggregates and Neurodegeneration. *Annu Rev Neurosci*, *40*, 189-210. https://doi.org/10.1146/annurev-neuro-072116-031153

Goetzl, E. J., Schwartz, J. B., Abner, E. L., Jicha, G. A., & Kapogiannis, D. (2018). High complement levels in astrocyte-derived exosomes of Alzheimer disease. *Ann Neurol*, *83*(3), 544-552. https://doi.org/10.1002/ana.25172

Golde, T. E., Schneider, L. S., & Koo, E. H. (2011). Anti-aβ therapeutics in Alzheimer's disease: the need for a paradigm shift. *Neuron*, *69*(2), 203-213. https://doi.org/10.1016/j.neuron.2011.01.002

Goldmann, T., Zeller, N., Raasch, J., Kierdorf, K., Frenzel, K., Ketscher, L., Basters, A., Staszewski, O., Brendecke, S. M., Spiess, A., Tay, T. L., Kreutz, C., Timmer, J., Mancini, G. M., Blank, T., Fritz, G., Biber, K., Lang, R., Malo, D., . . . Prinz, M. (2015). USP18 lack in microglia causes destructive interferonopathy of the mouse brain. *EMBO J*, *34*(12), 1612-1629. https://doi.org/10.15252/embj.201490791

Gomez-Nicola, D., & Perry, V. H. (2015). Microglial dynamics and role in the healthy and diseased brain: a paradigm of functional plasticity. *Neuroscientist*, *21*(2), 169-184. https://doi.org/10.1177/1073858414530512

Gong, K., Guo, G., Gerber, D. E., Gao, B., Peyton, M., Huang, C., Minna, J. D., Hatanpaa, K. J., Kernstine, K., Cai, L., Xie, Y., Zhu, H., Fattah, F. J., Zhang, S., Takahashi, M., Mukherjee, B., Burma, S., Dowell, J., Dao, K., . . . Habib, A. A. (2018). TNF-driven adaptive response mediates resistance to EGFR inhibition in lung cancer. *J Clin Invest*, *128*(6), 2500-2518. https://doi.org/10.1172/jci96148

Gottschling, C., Wegrzyn, D., Denecke, B., & Faissner, A. (2019). Elimination of the four extracellular matrix molecules tenascin-C, tenascin-R, brevican and neurocan alters the ratio of excitatory and inhibitory synapses. *Sci Rep*, *9*(1), 13939. https://doi.org/10.1038/s41598-019-50404-9

Götz, J., Chen, F., van Dorpe, J., & Nitsch, R. M. (2001). Formation of neurofibrillary tangles in P301l tau transgenic mice induced by Abeta 42 fibrils. *Science*, *293*(5534), 1491-1495. https://doi.org/10.1126/science.1062097

Grabherr, M. G., Haas, B. J., Yassour, M., Levin, J. Z., Thompson, D. A., Amit, I., Adiconis, X., Fan, L., Raychowdhury, R., Zeng, Q., Chen, Z., Mauceli, E., Hacohen, N., Gnirke, A., Rhind, N., di Palma, F., Birren, B. W., Nusbaum, C., Lindblad-Toh, K., . . . Regev, A. (2011). Full-length transcriptome assembly from RNA-Seq data without a reference genome. *Nat Biotechnol*, *29*(7), 644-652. https://doi.org/10.1038/nbt.1883

Grant, G. R., Farkas, M. H., Pizarro, A. D., Lahens, N. F., Schug, J., Brunk, B. P., Stoeckert, C. J., Hogenesch, J. B., & Pierce, E. A. (2011). Comparative analysis of RNA-Seq alignment algorithms and the RNA-Seq unified mapper (RUM). *Bioinformatics*, *27*(18), 2518-2528. https://doi.org/10.1093/bioinformatics/btr427

Grant, G. R., Liu, J., & Stoeckert, C. J., Jr. (2005). A practical false discovery rate approach to identifying patterns of differential expression in microarray data. *Bioinformatics*, *21*(11), 2684-2690. https://doi.org/10.1093/bioinformatics/bti407

Gratuze, M., Chen, Y., Parhizkar, S., Jain, N., Strickland, M. R., Serrano, J. R., Colonna, M., Ulrich, J. D., & Holtzman, D. M. (2021). Activated microglia mitigate Aβ-associated tau seeding and spreading. *J Exp Med*, *218*(8). https://doi.org/10.1084/jem.20210542

Gratuze, M., & Holtzman, D. M. (2021). Targeting pre-synaptic tau accumulation: a new strategy to counteract tau-mediated synaptic loss and memory deficits. *Neuron*, *109*(5), 741-743. https://doi.org/10.1016/j.neuron.2021.02.014

Gratuze, M., Leyns, C. E. G., & Holtzman, D. M. (2018). New insights into the role of TREM2 in Alzheimer's disease. *Mol Neurodegener*, *13*(1), 66. https://doi.org/10.1186/s13024-018-0298-9

Greter, M., Helft, J., Chow, A., Hashimoto, D., Mortha, A., Agudo-Cantero, J., Bogunovic, M., Gautier, E. L., Miller, J., Leboeuf, M., Lu, G., Aloman, C., Brown, B. D., Pollard, J. W., Xiong, H., Randolph, G. J., Chipuk, J. E., Frenette, P. S., & Merad, M. (2012). GM-CSF controls nonlymphoid tissue dendritic cell homeostasis but is dispensable for the differentiation of inflammatory dendritic cells. *Immunity*, *36*(6), 1031-1046. https://doi.org/10.1016/j.immuni.2012.03.027

Griciuc, A., Serrano-Pozo, A., Parrado, A. R., Lesinski, A. N., Asselin, C. N., Mullin, K., Hooli, B., Choi, S. H., Hyman, B. T., & Tanzi, R. E. (2013). Alzheimer's disease risk gene CD33 inhibits microglial uptake of amyloid beta. *Neuron*, *78*(4), 631-643. https://doi.org/10.1016/j.neuron.2013.04.014

Griebel, T., Zacher, B., Ribeca, P., Raineri, E., Lacroix, V., Guigo, R., & Sammeth, M. (2012). Modelling and simulating generic RNA-Seq experiments with the flux simulator. *Nucleic Acids Res*, *40*(20), 10073-10083. https://doi.org/10.1093/nar/gks666

Griffith, M., Griffith, O. L., Mwenifumbo, J., Goya, R., Morrissy, A. S., Morin, R. D., Corbett, R., Tang, M. J., Hou, Y. C., Pugh, T. J., Robertson, G., Chittaranjan, S., Ally, A., Asano, J. K., Chan, S. Y., Li, H. I., McDonald, H., Teague, K., Zhao, Y., . . . Marra, M. A. (2010). Alternative expression analysis by RNA sequencing. *Nat Methods*, *7*(10), 843-847. https://doi.org/10.1038/nmeth.1503

Guerreiro, R. J., Lohmann, E., Bras, J. M., Gibbs, J. R., Rohrer, J. D., Gurunlian, N., Dursun, B., Bilgic, B., Hanagasi, H., Gurvit, H., Emre, M., Singleton, A., & Hardy, J. (2013). Using exome sequencing to reveal mutations in TREM2 presenting as a frontotemporal dementia-like syndrome without bone involvement. *JAMA Neurol*, *70*(1), 78-84. https://doi.org/10.1001/jamaneurol.2013.579

Guo, M. F., Meng, J., Li, Y. H., Yu, J. Z., Liu, C. Y., Feng, L., Yang, W. F., Li, J. L., Feng, Q. J., Xiao, B. G., & Ma, C. G. (2014). The inhibition of Rho kinase blocks cell migration and accumulation possibly by challenging inflammatory cytokines and chemokines on astrocytes. *J Neurol Sci*, *343*(1-2), 69-75. https://doi.org/10.1016/j.jns.2014.05.034

Gustavsson, A., Norton, N., Fast, T., Frölich, L., Georges, J., Holzapfel, D., Kirabali, T., Krolak-Salmon, P., Rossini, P. M., Ferretti, M. T., Lanman, L., Chadha, A. S., & van der Flier, W. M. (2023). Global estimates on the number of persons across the Alzheimer's disease continuum. *Alzheimers Dement*, *19*(2), 658-670. https://doi.org/10.1002/alz.12694

Haass, C., & De Strooper, B. (1999). The presenilins in Alzheimer's disease--proteolysis holds the key. *Science*, *286*(5441), 916-919. https://doi.org/10.1126/science.286.5441.916

Hagemeyer, N., Hanft, K. M., Akriditou, M. A., Unger, N., Park, E. S., Stanley, E. R., Staszewski, O., Dimou, L., & Prinz, M. (2017). Microglia contribute to normal myelinogenesis and to oligodendrocyte progenitor maintenance during adulthood. *Acta Neuropathol*, *134*(3), 441-458. https://doi.org/10.1007/s00401-017-1747-1

Hamerman, J. A., Ni, M., Killebrew, J. R., Chu, C. L., & Lowell, C. A. (2009). The expanding roles of ITAM adapters FcRgamma and DAP12 in myeloid cells. *Immunol Rev*, *232*(1), 42-58. https://doi.org/10.1111/j.1600-065X.2009.00841.x

Hammond, T. R., Dufort, C., Dissing-Olesen, L., Giera, S., Young, A., Wysoker, A., Walker, A. J., Gergits, F., Segel, M., Nemesh, J., Marsh, S. E., Saunders, A., Macosko, E., Ginhoux, F., Chen, J., Franklin, R. J. M., Piao, X., McCarroll, S. A., & Stevens, B. (2019). Single-Cell RNA Sequencing of Microglia throughout the Mouse Lifespan and in the Injured Brain Reveals

Complex Cell-State Changes. *Immunity*, *50*(1), 253-271 e256. https://doi.org/10.1016/j.immuni.2018.11.004
Hardcastle, T. J., & Kelly, K. A. (2010). baySeq: empirical Bayesian methods for identifying differential expression in sequence count data. *BMC Bioinformatics*, *11*, 422. https://doi.org/10.1186/1471-2105-11-422
Hardy, J. A., & Higgins, G. A. (1992). Alzheimer's disease: the amyloid cascade hypothesis. *Science*, *256*(5054), 184-185. https://doi.org/10.1126/science.1566067
Harold, D., Abraham, R., Hollingworth, P., Sims, R., Gerrish, A., Hamshere, M. L., Pahwa, J. S., Moskvina, V., Dowzell, K., Williams, A., Jones, N., Thomas, C., Stretton, A., Morgan, A. R., Lovestone, S., Powell, J., Proitsi, P., Lupton, M. K., Brayne, C., . . . Williams, J. (2009). Genome-wide association study identifies variants at CLU and PICALM associated with Alzheimer's disease. *Nat Genet*, *41*(10), 1088-1093. https://doi.org/10.1038/ng.440
Harrell, F. E., Jr., Lee, K. L., Califf, R. M., Pryor, D. B., & Rosati, R. A. (1984). Regression modelling strategies for improved prognostic prediction. *Stat Med*, *3*(2), 143-152. https://doi.org/10.1002/sim.4780030207
Harry, G. J., & Kraft, A. D. (2008). Neuroinflammation and microglia: considerations and approaches for neurotoxicity assessment. *Expert Opin Drug Metab Toxicol*, *4*(10), 1265-1277. https://doi.org/10.1517/17425255.4.10.1265
He, P., Zhong, Z., Lindholm, K., Berning, L., Lee, W., Lemere, C., Staufenbiel, M., Li, R., & Shen, Y. (2007). Deletion of tumor necrosis factor death receptor inhibits amyloid beta generation and prevents learning and memory deficits in Alzheimer's mice. *J Cell Biol*, *178*(5), 829-841. https://doi.org/10.1083/jcb.200705042
Heidarzadeh, M., Gürsoy-Özdemir, Y., Kaya, M., Eslami Abriz, A., Zarebkohan, A., Rahbarghazi, R., & Sokullu, E. (2021). Exosomal delivery of therapeutic modulators through the blood-brain barrier; promise and pitfalls. *Cell Biosci*, *11*(1), 142. https://doi.org/10.1186/s13578-021-00650-0
Henningfield, C. M., Arreola, M. A., Soni, N., Spangenberg, E. E., & Green, K. N. (2022). Microglia-specific ApoE knock-out does not alter Alzheimer's disease plaque pathogenesis or gene expression. *Glia*, *70*(2), 287-302. https://doi.org/10.1002/glia.24105
Hickman, S. E., Kingery, N. D., Ohsumi, T. K., Borowsky, M. L., Wang, L. C., Means, T. K., & El Khoury, J. (2013). The microglial sensome revealed by direct RNA sequencing. *Nat Neurosci*, *16*(12), 1896-1905. https://doi.org/10.1038/nn.3554
Hinz, F. I., & Geschwind, D. H. (2017). Molecular Genetics of Neurodegenerative Dementias. *Cold Spring Harb Perspect Biol*, *9*(4). https://doi.org/10.1101/cshperspect.a023705
Hodges, A., Strand, A. D., Aragaki, A. K., Kuhn, A., Sengstag, T., Hughes, G., Elliston, L. A., Hartog, C., Goldstein, D. R., Thu, D., Hollingsworth, Z. R., Collin, F., Synek, B., Holmans, P. A., Young, A. B., Wexler, N. S., Delorenzi, M., Kooperberg, C., Augood, S. J., . . . Luthi-Carter, R. (2006). Regional and cellular gene expression changes in human Huntington's disease brain. *Hum Mol Genet*, *15*(6), 965-977. https://doi.org/10.1093/hmg/ddl013
Hoffmann, S., Murrell, J., Harms, L., Miller, K., Meisel, A., Brosch, T., Scheel, M., Ghetti, B., Goebel, H. H., & Stenzel, W. (2014). Enlarging the nosological spectrum of hereditary diffuse leukoencephalopathy with axonal spheroids (HDLS). *Brain Pathol*, *24*(5), 452-458. https://doi.org/10.1111/bpa.12120
Hohsfield, L. A., Najafi, A. R., Ghorbanian, Y., Soni, N., Crapser, J., Figueroa Velez, D. X., Jiang, S., Royer, S. E., Kim, S. J., Henningfield, C. M., Anderson, A., Gandhi, S. P., Mortazavi, A., Inlay, M. A., & Green, K. N. (2021). Subventricular zone/white matter microglia reconstitute the empty adult microglial niche in a dynamic wave. *eLife*, *10*. https://doi.org/10.7554/eLife.66738
Hohsfield, L. A., Najafi, A. R., Ghorbanian, Y., Soni, N., Hingco, E. E., Kim, S. J., Jue, A. D., Swarup, V., Inlay, M. A., & Green, K. N. (2020). Effects of long-term and brain-wide colonization of

peripheral bone marrow-derived myeloid cells in the CNS. *J Neuroinflammation*, *17*(1), 279. https://doi.org/10.1186/s12974-020-01931-0

Holstege, H., Hulsman, M., Charbonnier, C., Grenier-Boley, B., Quenez, O., Grozeva, D., Rooij, J. G. J. v., Sims, R., Ahmad, S., Amin, N., Norsworthy, P. J., Dols-Icardo, O., Hummerich, H., Kawalia, A., Amouyel, P., Beecham, G. W., Berr, C., Bis, J. C., Boland, A., . . . Lambert, J.-C. (2020). Exome sequencing identifies novel AD-associated genes. *medRxiv*, 2020.2007.2022.20159251. https://doi.org/10.1101/2020.07.22.20159251

Holtzman, D. M., Carrillo, M. C., Hendrix, J. A., Bain, L. J., Catafau, A. M., Gault, L. M., Goedert, M., Mandelkow, E., Mandelkow, E. M., Miller, D. S., Ostrowitzki, S., Polydoro, M., Smith, S., Wittmann, M., & Hutton, M. (2016). Tau: From research to clinical development. *Alzheimers Dement*, *12*(10), 1033-1039. https://doi.org/10.1016/j.jalz.2016.03.018

Holtzman, D. M., Fagan, A. M., Mackey, B., Tenkova, T., Sartorius, L., Paul, S. M., Bales, K., Ashe, K. H., Irizarry, M. C., & Hyman, B. T. (2000). Apolipoprotein E facilitates neuritic and cerebrovascular plaque formation in an Alzheimer's disease model. *Ann Neurol*, *47*(6), 739-747.

Holtzman, D. M., Morris, J. C., & Goate, A. M. (2011). Alzheimer's disease: the challenge of the second century. *Sci Transl Med*, *3*(77), 77sr71. https://doi.org/10.1126/scitranslmed.3002369

Horvath, S., & Dong, J. (2008). Geometric interpretation of gene coexpression network analysis. *PLoS Comput Biol*, *4*(8), e1000117. https://doi.org/10.1371/journal.pcbi.1000117

Horvath, S., Zhang, B., Carlson, M., Lu, K. V., Zhu, S., Felciano, R. M., Laurance, M. F., Zhao, W., Qi, S., Chen, Z., Lee, Y., Scheck, A. C., Liau, L. M., Wu, H., Geschwind, D. H., Febbo, P. G., Kornblum, H. I., Cloughesy, T. F., Nelson, S. F., & Mischel, P. S. (2006). Analysis of oncogenic signaling networks in glioblastoma identifies ASPM as a molecular target. *Proc Natl Acad Sci U S A*, *103*(46), 17402-17407. https://doi.org/10.1073/pnas.0608396103

Howell, G. R., Macalinao, D. G., Sousa, G. L., Walden, M., Soto, I., Kneeland, S. C., Barbay, J. M., King, B. L., Marchant, J. K., Hibbs, M., Stevens, B., Barres, B. A., Clark, A. F., Libby, R. T., & John, S. W. (2011). Molecular clustering identifies complement and endothelin induction as early events in a mouse model of glaucoma. *J Clin Invest*, *121*(4), 1429-1444. https://doi.org/10.1172/jci44646

Hsu, J. Y., Bourguignon, L. Y., Adams, C. M., Peyrollier, K., Zhang, H., Fandel, T., Cun, C. L., Werb, Z., & Noble-Haeusslein, L. J. (2008). Matrix metalloproteinase-9 facilitates glial scar formation in the injured spinal cord. *J Neurosci*, *28*(50), 13467-13477. https://doi.org/10.1523/JNEUROSCI.2287-08.2008

Hu, M. H., Zheng, Q. F., Jia, X. Z., Li, Y., Dong, Y. C., Wang, C. Y., Lin, Q. Y., Zhang, F. Y., Zhao, R. B., Xu, H. W., Zhou, J. H., Yuan, H. P., Zhang, W. H., & Ren, H. (2014). Neuroprotection effect of interleukin (IL)-17 secreted by reactive astrocytes is emerged from a high-level IL-17-containing environment during acute neuroinflammation. *Clin Exp Immunol*, *175*(2), 268-284. https://doi.org/10.1111/cei.12219

Huynh, T. V., Liao, F., Francis, C. M., Robinson, G. O., Serrano, J. R., Jiang, H., Roh, J., Finn, M. B., Sullivan, P. M., Esparza, T. J., Stewart, F. R., Mahan, T. E., Ulrich, J. D., Cole, T., & Holtzman, D. M. (2017). Age-Dependent Effects of apoE Reduction Using Antisense Oligonucleotides in a Model of β-amyloidosis. *Neuron*, *96*(5), 1013-1023.e1014. https://doi.org/10.1016/j.neuron.2017.11.014

Hyman, B. T., & Trojanowski, J. Q. (1997). Consensus recommendations for the postmortem diagnosis of Alzheimer disease from the National Institute on Aging and the Reagan Institute Working Group on diagnostic criteria for the neuropathological assessment of Alzheimer disease. *J Neuropathol Exp Neurol*, *56*(10), 1095-1097. https://doi.org/10.1097/00005072-199710000-00002

Illouz, T., Madar, R., Griffioen, K., & Okun, E. (2017). A protocol for quantitative analysis of murine and human amyloid-β(1-40) and (1-42). *J Neurosci Methods*, *291*, 28-35. https://doi.org/10.1016/j.jneumeth.2017.07.022

Ising, C., Venegas, C., Zhang, S., Scheiblich, H., Schmidt, S. V., Vieira-Saecker, A., Schwartz, S., Albasset, S., McManus, R. M., Tejera, D., Griep, A., Santarelli, F., Brosseron, F., Opitz, S., Stunden, J., Merten, M., Kayed, R., Golenbock, D. T., Blum, D., . . . Heneka, M. T. (2019). NLRP3 inflammasome activation drives tau pathology. *Nature*, *575*(7784), 669-673. https://doi.org/10.1038/s41586-019-1769-z

Iwai, K. (2021). LUBAC-mediated linear ubiquitination: a crucial regulator of immune signaling. *Proc Jpn Acad Ser B Phys Biol Sci*, *97*(3), 120-133. https://doi.org/10.2183/pjab.97.007

Jack, C. R., Jr., Bennett, D. A., Blennow, K., Carrillo, M. C., Feldman, H. H., Frisoni, G. B., Hampel, H., Jagust, W. J., Johnson, K. A., Knopman, D. S., Petersen, R. C., Scheltens, P., Sperling, R. A., & Dubois, B. (2016). A/T/N: An unbiased descriptive classification scheme for Alzheimer disease biomarkers. *Neurology*, *87*(5), 539-547. https://doi.org/10.1212/wnl.0000000000002923

Jackson, H. M., Onos, K. D., Pepper, K. W., Graham, L. C., Akeson, E. C., Byers, C., Reinholdt, L. G., Frankel, W. N., & Howell, G. R. (2015). DBA/2J genetic background exacerbates spontaneous lethal seizures but lessens amyloid deposition in a mouse model of Alzheimer's disease. *PLOS ONE*, *10*(5), e0125897. https://doi.org/10.1371/journal.pone.0125897

Jansen, A. H., van Hal, M., Op den Kelder, I. C., Meier, R. T., de Ruiter, A. A., Schut, M. H., Smith, D. L., Grit, C., Brouwer, N., Kamphuis, W., Boddeke, H. W., den Dunnen, W. F., van Roon, W. M., Bates, G. P., Hol, E. M., & Reits, E. A. (2017). Frequency of nuclear mutant huntingtin inclusion formation in neurons and glia is cell-type-specific. *Glia*, *65*(1), 50-61. https://doi.org/10.1002/glia.23050

Jansen, I. E., Savage, J. E., Watanabe, K., Bryois, J., Williams, D. M., Steinberg, S., Sealock, J., Karlsson, I. K., Hägg, S., Athanasiu, L., Voyle, N., Proitsi, P., Witoelar, A., Stringer, S., Aarsland, D., Almdahl, I. S., Andersen, F., Bergh, S., Bettella, F., . . . Posthuma, D. (2019). Genome-wide meta-analysis identifies new loci and functional pathways influencing Alzheimer's disease risk. *Nat Genet*, *51*(3), 404-413. https://doi.org/10.1038/s41588-018-0311-9

Jawhar, S., Trawicka, A., Jenneckens, C., Bayer, T. A., & Wirths, O. (2012). Motor deficits, neuron loss, and reduced anxiety coinciding with axonal degeneration and intraneuronal Aβ aggregation in the 5XFAD mouse model of Alzheimer's disease. *Neurobiol Aging*, *33*(1), 196.e129-140. https://doi.org/10.1016/j.neurobiolaging.2010.05.027

Jay, T. R., Hirsch, A. M., Broihier, M. L., Miller, C. M., Neilson, L. E., Ransohoff, R. M., Lamb, B. T., & Landreth, G. E. (2017). Disease Progression-Dependent Effects of TREM2 Deficiency in a Mouse Model of Alzheimer's Disease. *J Neurosci*, *37*(3), 637-647. https://doi.org/10.1523/jneurosci.2110-16.2016

Jay, T. R., Miller, C. M., Cheng, P. J., Graham, L. C., Bemiller, S., Broihier, M. L., Xu, G., Margevicius, D., Karlo, J. C., Sousa, G. L., Cotleur, A. C., Butovsky, O., Bekris, L., Staugaitis, S. M., Leverenz, J. B., Pimplikar, S. W., Landreth, G. E., Howell, G. R., Ransohoff, R. M., & Lamb, B. T. (2015). TREM2 deficiency eliminates TREM2+ inflammatory macrophages and ameliorates pathology in Alzheimer's disease mouse models. *J Exp Med*, *212*(3), 287-295. https://doi.org/10.1084/jem.20142322

Jiang, T., Yu, J. T., Hu, N., Tan, M. S., Zhu, X. C., & Tan, L. (2014). CD33 in Alzheimer's disease. *Mol Neurobiol*, *49*(1), 529-535. https://doi.org/10.1007/s12035-013-8536-1

Johnstone, M., Gearing, A. J., & Miller, K. M. (1999). A central role for astrocytes in the inflammatory response to beta-amyloid; chemokines, cytokines and reactive oxygen species are produced. *J Neuroimmunol*, *93*(1-2), 182-193. https://doi.org/10.1016/s0165-5728(98)00226-4

Justice, M. J., & Dhillon, P. (2016). Using the mouse to model human disease: increasing validity and reproducibility. *Dis Model Mech*, *9*(2), 101-103. https://doi.org/10.1242/dmm.024547

Karch, C. M., Jeng, A. T., Nowotny, P., Cady, J., Cruchaga, C., & Goate, A. M. (2012). Expression of novel Alzheimer's disease risk genes in control and Alzheimer's disease brains. *PLOS ONE*, *7*(11), e50976. https://doi.org/10.1371/journal.pone.0050976

Katz, Y., Wang, E. T., Airoldi, E. M., & Burge, C. B. (2010). Analysis and design of RNA sequencing experiments for identifying isoform regulation. *Nat Methods*, *7*(12), 1009-1015. https://doi.org/10.1038/nmeth.1528

Kempthorne, L., Yoon, H., Madore, C., Smith, S., Wszolek, Z. K., Rademakers, R., Kim, J., Butovsky, O., & Dickson, D. W. (2020a). Correction to: Loss of homeostatic microglial phenotype in CSF1R-related Leukoencephalopathy. *Acta Neuropathol Commun*, *8*(1), 90. https://doi.org/10.1186/s40478-020-00970-1

Kempthorne, L., Yoon, H., Madore, C., Smith, S., Wszolek, Z. K., Rademakers, R., Kim, J., Butovsky, O., & Dickson, D. W. (2020b). Loss of homeostatic microglial phenotype in CSF1R-related Leukoencephalopathy. *Acta Neuropathol Commun*, *8*(1), 72. https://doi.org/10.1186/s40478-020-00947-0

Keren-Shaul, H., Spinrad, A., Weiner, A., Matcovitch-Natan, O., Dvir-Szternfeld, R., Ulland, T. K., David, E., Baruch, K., Lara-Astaiso, D., Toth, B., Itzkovitz, S., Colonna, M., Schwartz, M., & Amit, I. (2017). A Unique Microglia Type Associated with Restricting Development of Alzheimer's Disease. *Cell*, *169*(7), 1276-1290 e1217. https://doi.org/10.1016/j.cell.2017.05.018

Kettenmann, H., Hanisch, U. K., Noda, M., & Verkhratsky, A. (2011). Physiology of microglia. *Physiol Rev*, *91*(2), 461-553. https://doi.org/10.1152/physrev.00011.2010

Kierdorf, K., & Prinz, M. (2017). Microglia in steady state. *J Clin Invest*, *127*(9), 3201-3209. https://doi.org/10.1172/JCI90602

Kim, J., Chakrabarty, P., Hanna, A., March, A., Dickson, D. W., Borchelt, D. R., Golde, T., & Janus, C. (2013). Normal cognition in transgenic BRI2-Aβ mice. *Mol Neurodegener*, *8*, 15. https://doi.org/10.1186/1750-1326-8-15

Kim, J. H. (2018). Genetics of Alzheimer's Disease. *Dement Neurocogn Disord*, *17*(4), 131-136. https://doi.org/10.12779/dnd.2018.17.4.131

Kim, S. K., Hayashi, H., Ishikawa, T., Shibata, K., Shigetomi, E., Shinozaki, Y., Inada, H., Roh, S. E., Kim, S. J., Lee, G., Bae, H., Moorhouse, A. J., Mikoshiba, K., Fukazawa, Y., Koizumi, S., & Nabekura, J. (2016). Cortical astrocytes rewire somatosensory cortical circuits for peripheral neuropathic pain. *J Clin Invest*, *126*(5), 1983-1997. https://doi.org/10.1172/jci82859

Kim, T., Vidal, G. S., Djurisic, M., William, C. M., Birnbaum, M. E., Garcia, K. C., Hyman, B. T., & Shatz, C. J. (2013). Human LilrB2 is a β-amyloid receptor and its murine homolog PirB regulates synaptic plasticity in an Alzheimer's model. *Science*, *341*(6152), 1399-1404. https://doi.org/10.1126/science.1242077

Kim, Y. S., & Joh, T. H. (2006). Microglia, major player in the brain inflammation: their roles in the pathogenesis of Parkinson's disease. *Exp Mol Med*, *38*(4), 333-347. https://doi.org/10.1038/emm.2006.40

Kinchen, J. M., Cabello, J., Klingele, D., Wong, K., Feichtinger, R., Schnabel, H., Schnabel, R., & Hengartner, M. O. (2005). Two pathways converge at CED-10 to mediate actin rearrangement and corpse removal in C. elegans. *Nature*, *434*(7029), 93-99. https://doi.org/10.1038/nature03263

Kiyota, T., Okuyama, S., Swan, R. J., Jacobsen, M. T., Gendelman, H. E., & Ikezu, T. (2010). CNS expression of anti-inflammatory cytokine interleukin-4 attenuates Alzheimer's disease-like pathogenesis in APP+PS1 bigenic mice. *FASEB J*, *24*(8), 3093-3102. https://doi.org/10.1096/fj.10-155317

Kleinman, C. L., & Majewski, J. (2012). Comment on "Widespread RNA and DNA sequence differences in the human transcriptome". *Science*, *335*(6074), 1302; author reply 1302. https://doi.org/10.1126/science.1209658

Koistinaho, M., Lin, S., Wu, X., Esterman, M., Koger, D., Hanson, J., Higgs, R., Liu, F., Malkani, S., Bales, K. R., & Paul, S. M. (2004). Apolipoprotein E promotes astrocyte colocalization and degradation of deposited amyloid-beta peptides. *Nat Med*, *10*(7), 719-726. https://doi.org/10.1038/nm1058

Kondo, Y., Matsushima, A., Nagasaki, S., Nakamura, K., Sekijima, Y., & Yoshida, K. (2020). Factors predictive of the presence of a CSF1R mutation in patients with leukoencephalopathy. *Eur J Neurol*, *27*(2), 369-375. https://doi.org/10.1111/ene.14086

Konnecke, H., & Bechmann, I. (2013). The role of microglia and matrix metalloproteinases involvement in neuroinflammation and gliomas. *Clin Dev Immunol*, *2013*, 914104. https://doi.org/10.1155/2013/914104

Konno, T., Miura, T., Harriott, A. M., Mezaki, N., Edwards, E. S., Rademakers, R., Ross, O. A., Meschia, J. F., Ikeuchi, T., & Wszolek, Z. K. (2018). Partial loss of function of colony-stimulating factor 1 receptor in a patient with white matter abnormalities. *Eur J Neurol*, *25*(6), 875-881. https://doi.org/10.1111/ene.13611

Konno, T., Tada, M., Tada, M., Koyama, A., Nozaki, H., Harigaya, Y., Nishimiya, J., Matsunaga, A., Yoshikura, N., Ishihara, K., Arakawa, M., Isami, A., Okazaki, K., Yokoo, H., Itoh, K., Yoneda, M., Kawamura, M., Inuzuka, T., Takahashi, H., . . . Ikeuchi, T. (2014). Haploinsufficiency of CSF-1R and clinicopathologic characterization in patients with HDLS. *Neurology*, *82*(2), 139-148. https://doi.org/10.1212/WNL.0000000000000046

Kopylova, E., Noe, L., & Touzet, H. (2012). SortMeRNA: fast and accurate filtering of ribosomal RNAs in metatranscriptomic data. *Bioinformatics*, *28*(24), 3211-3217. https://doi.org/10.1093/bioinformatics/bts611

Krasemann, S., Madore, C., Cialic, R., Baufeld, C., Calcagno, N., El Fatimy, R., Beckers, L., O'Loughlin, E., Xu, Y., Fanek, Z., Greco, D. J., Smith, S. T., Tweet, G., Humulock, Z., Zrzavy, T., Conde-Sanroman, P., Gacias, M., Weng, Z., Chen, H., . . . Butovsky, O. (2017). The TREM2-APOE Pathway Drives the Transcriptional Phenotype of Dysfunctional Microglia in Neurodegenerative Diseases. *Immunity*, *47*(3), 566-581 e569. https://doi.org/10.1016/j.immuni.2017.08.008

Kreutzberg, G. W. (1996). Microglia: a sensor for pathological events in the CNS. *Trends Neurosci*, *19*(8), 312-318. https://doi.org/10.1016/0166-2236(96)10049-7

Kunkle, B. W., Grenier-Boley, B., Sims, R., Bis, J. C., Damotte, V., Naj, A. C., Boland, A., Vronskaya, M., van der Lee, S. J., Amlie-Wolf, A., Bellenguez, C., Frizatti, A., Chouraki, V., Martin, E. R., Sleegers, K., Badarinarayan, N., Jakobsdottir, J., Hamilton-Nelson, K. L., Moreno-Grau, S., . . . Pericak-Vance, M. A. (2019). Genetic meta-analysis of diagnosed Alzheimer's disease identifies new risk loci and implicates Aβ, tau, immunity and lipid processing. *Nat Genet*, *51*(3), 414-430. https://doi.org/10.1038/s41588-019-0358-2

Kurosawa, M., Matsumoto, G., Kino, Y., Okuno, M., Kurosawa-Yamada, M., Washizu, C., Taniguchi, H., Nakaso, K., Yanagawa, T., Warabi, E., Shimogori, T., Sakurai, T., Hattori, N., & Nukina, N. (2015). Depletion of p62 reduces nuclear inclusions and paradoxically ameliorates disease phenotypes in Huntington's model mice. *Hum Mol Genet*, *24*(4), 1092-1105. https://doi.org/10.1093/hmg/ddu522

Labandeira-Garcia, J. L., Costa-Besada, M. A., Labandeira, C. M., Villar-Cheda, B., & Rodriguez-Perez, A. I. (2017). Insulin-Like Growth Factor-1 and Neuroinflammation. *Front Aging Neurosci*, *9*, 365. https://doi.org/10.3389/fnagi.2017.00365

Labbadia, J., & Morimoto, R. I. (2013). Huntington's disease: underlying molecular mechanisms and emerging concepts. *Trends Biochem Sci*, *38*(8), 378-385. https://doi.org/10.1016/j.tibs.2013.05.003

LaFerla, F. M., & Green, K. N. (2012). Animal models of Alzheimer disease. *Cold Spring Harb Perspect Med*, *2*(11). https://doi.org/10.1101/cshperspect.a006320

Lam, D., Enright, H. A., Cadena, J., Peters, S. K. G., Sales, A. P., Osburn, J. J., Soscia, D. A., Kulp, K. S., Wheeler, E. K., & Fischer, N. O. (2019). Tissue-specific extracellular matrix accelerates the

formation of neural networks and communities in a neuron-glia co-culture on a multi-electrode array. *Sci Rep*, *9*(1), 4159. https://doi.org/10.1038/s41598-019-40128-1

Lambert, J. C., Ibrahim-Verbaas, C. A., Harold, D., Naj, A. C., Sims, R., Bellenguez, C., DeStafano, A. L., Bis, J. C., Beecham, G. W., Grenier-Boley, B., Russo, G., Thorton-Wells, T. A., Jones, N., Smith, A. V., Chouraki, V., Thomas, C., Ikram, M. A., Zelenika, D., Vardarajan, B. N., . . . Amouyel, P. (2013). Meta-analysis of 74,046 individuals identifies 11 new susceptibility loci for Alzheimer's disease. *Nat Genet*, *45*(12), 1452-1458. https://doi.org/10.1038/ng.2802

Lane-Donovan, C., Wong, W. M., Durakoglugil, M. S., Wasser, C. R., Jiang, S., Xian, X., & Herz, J. (2016). Genetic Restoration of Plasma ApoE Improves Cognition and Partially Restores Synaptic Defects in ApoE-Deficient Mice. *J Neurosci*, *36*(39), 10141-10150. https://doi.org/10.1523/jneurosci.1054-16.2016

Langfelder, P., & Horvath, S. (2007). Eigengene networks for studying the relationships between co-expression modules. *BMC Syst Biol*, *1*, 54. https://doi.org/10.1186/1752-0509-1-54

Langfelder, P., & Horvath, S. (2008). WGCNA: an R package for weighted correlation network analysis. *BMC Bioinformatics*, *9*, 559. https://doi.org/10.1186/1471-2105-9-559

Langmead, B., Hansen, K. D., & Leek, J. T. (2010). Cloud-scale RNA-sequencing differential expression analysis with Myrna. *Genome Biol*, *11*(8), R83. https://doi.org/10.1186/gb-2010-11-8-r83

Langmead, B., Trapnell, C., Pop, M., & Salzberg, S. L. (2009). Ultrafast and memory-efficient alignment of short DNA sequences to the human genome. *Genome Biol*, *10*(3), R25. https://doi.org/10.1186/gb-2009-10-3-r25

Lanoiselée, H. M., Nicolas, G., Wallon, D., Rovelet-Lecrux, A., Lacour, M., Rousseau, S., Richard, A. C., Pasquier, F., Rollin-Sillaire, A., Martinaud, O., Quillard-Muraine, M., de la Sayette, V., Boutoleau-Bretonniere, C., Etcharry-Bouyx, F., Chauviré, V., Sarazin, M., le Ber, I., Epelbaum, S., Jonveaux, T., . . . Campion, D. (2017). APP, PSEN1, and PSEN2 mutations in early-onset Alzheimer disease: A genetic screening study of familial and sporadic cases. *PLoS Med*, *14*(3), e1002270. https://doi.org/10.1371/journal.pmed.1002270

Lappalainen, T., Sammeth, M., Friedlander, M. R., t Hoen, P. A., Monlong, J., Rivas, M. A., Gonzalez-Porta, M., Kurbatova, N., Griebel, T., Ferreira, P. G., Barann, M., Wieland, T., Greger, L., van Iterson, M., Almlof, J., Ribeca, P., Pulyakhina, I., Esser, D., Giger, T., . . . Dermitzakis, E. T. (2013). Transcriptome and genome sequencing uncovers functional variation in humans. *Nature*, *501*(7468), 506-511. https://doi.org/10.1038/nature12531

Lavin, Y., Winter, D., Blecher-Gonen, R., David, E., Keren-Shaul, H., Merad, M., Jung, S., & Amit, I. (2014). Tissue-resident macrophage enhancer landscapes are shaped by the local microenvironment. *Cell*, *159*(6), 1312-1326. https://doi.org/10.1016/j.cell.2014.11.018

Ledeboer, A., Brevé, J. J., Wierinckx, A., van der Jagt, S., Bristow, A. F., Leysen, J. E., Tilders, F. J., & Van Dam, A. M. (2002). Expression and regulation of interleukin-10 and interleukin-10 receptor in rat astroglial and microglial cells. *Eur J Neurosci*, *16*(7), 1175-1185. https://doi.org/10.1046/j.1460-9568.2002.02200.x

Lee, C. Y. D., Daggett, A., Gu, X., Jiang, L. L., Langfelder, P., Li, X., Wang, N., Zhao, Y., Park, C. S., Cooper, Y., Ferando, I., Mody, I., Coppola, G., Xu, H., & Yang, X. W. (2018). Elevated TREM2 Gene Dosage Reprograms Microglia Responsivity and Ameliorates Pathological Phenotypes in Alzheimer's Disease Models. *Neuron*, *97*(5), 1032-1048.e1035. https://doi.org/10.1016/j.neuron.2018.02.002

Lee, E. H., Kwon, H. S., Koh, S. H., Choi, S. H., Jin, J. H., Jeong, J. H., Jang, J. W., Park, K. W., Kim, E. J., Kim, H. J., Hong, J. Y., Yoon, S. J., Yoon, B., Kang, J. H., Lee, J. M., Park, H. H., & Ha, J. (2022). Serum neurofilament light chain level as a predictor of cognitive stage transition. *Alzheimers Res Ther*, *14*(1), 6. https://doi.org/10.1186/s13195-021-00953-x

Lee, S., Plavina, T., Singh, C. M., Xiong, K., Qiu, X., Rudick, R. A., Calabresi, P. A., Stevenson, L., Graham, D., Raitcheva, D., Green, C., Matias, M., & Uzgiris, A. J. (2022). Development of a Highly Sensitive Neurofilament Light Chain Assay on an Automated Immunoassay Platform. *Front Neurol*, *13*, 935382. https://doi.org/10.3389/fneur.2022.935382

Lee, S. H., Meilandt, W. J., Xie, L., Gandham, V. D., Ngu, H., Barck, K. H., Rezzonico, M. G., Imperio, J., Lalehzadeh, G., Huntley, M. A., Stark, K. L., Foreman, O., Carano, R. A. D., Friedman, B. A., Sheng, M., Easton, A., Bohlen, C. J., & Hansen, D. V. (2021). Trem2 restrains the enhancement of tau accumulation and neurodegeneration by β-amyloid pathology. *Neuron*, *109*(8), 1283-1301.e1286. https://doi.org/10.1016/j.neuron.2021.02.010

Lee, S. H., Turpin, W., Espin-Garcia, O., Raygoza Garay, J. A., Smith, M. I., Leibovitzh, H., Goethel, A., Turner, D., Mack, D., Deslandres, C., Cino, M., Aumais, G., Panaccione, R., Jacobson, K., Bitton, A., Steinhart, A. H., Huynh, H. Q., Princen, F., Moayyedi, P., . . . Colitis Canada Genetics Environment Microbial Project Research, C. (2021). Anti-Microbial Antibody Response is Associated With Future Onset of Crohn's Disease Independent of Biomarkers of Altered Gut Barrier Function, Subclinical Inflammation, and Genetic Risk. *Gastroenterology*, *161*(5), 1540-1551. https://doi.org/10.1053/j.gastro.2021.07.009

Lee, S. W., Park, H. J., Im, W., Kim, M., & Hong, S. (2018). Repeated immune activation with low-dose lipopolysaccharide attenuates the severity of Huntington's disease in R6/2 transgenic mice. *Anim Cells Syst (Seoul)*, *22*(4), 219-226. https://doi.org/10.1080/19768354.2018.1473291

Lee, Y., Aono, M., Laskowitz, D., Warner, D. S., & Pearlstein, R. D. (2004). Apolipoprotein E protects against oxidative stress in mixed neuronal-glial cell cultures by reducing glutamate toxicity. *Neurochem Int*, *44*(2), 107-118. https://doi.org/10.1016/s0197-0186(03)00112-8

Lewis, J., Dickson, D. W., Lin, W. L., Chisholm, L., Corral, A., Jones, G., Yen, S. H., Sahara, N., Skipper, L., Yager, D., Eckman, C., Hardy, J., Hutton, M., & McGowan, E. (2001). Enhanced neurofibrillary degeneration in transgenic mice expressing mutant tau and APP. *Science*, *293*(5534), 1487-1491. https://doi.org/10.1126/science.1058189

Lewis, J., McGowan, E., Rockwood, J., Melrose, H., Nacharaju, P., Van Slegtenhorst, M., Gwinn-Hardy, K., Paul Murphy, M., Baker, M., Yu, X., Duff, K., Hardy, J., Corral, A., Lin, W. L., Yen, S. H., Dickson, D. W., Davies, P., & Hutton, M. (2000). Neurofibrillary tangles, amyotrophy and progressive motor disturbance in mice expressing mutant (P301L) tau protein. *Nat Genet*, *25*(4), 402-405. https://doi.org/10.1038/78078

Li, A., & Horvath, S. (2007). Network neighborhood analysis with the multi-node topological overlap measure. *Bioinformatics*, *23*(2), 222-231. https://doi.org/10.1093/bioinformatics/btl581

Li, H., & Auwerx, J. (2020). Mouse Systems Genetics as a Prelude to Precision Medicine. *Trends Genet*, *36*(4), 259-272. https://doi.org/10.1016/j.tig.2020.01.004

Li, H., & Durbin, R. (2009). Fast and accurate short read alignment with Burrows-Wheeler transform. *Bioinformatics*, *25*(14), 1754-1760. https://doi.org/10.1093/bioinformatics/btp324

Li, J. J., Jiang, C. R., Brown, J. B., Huang, H., & Bickel, P. J. (2011). Sparse linear modeling of next-generation mRNA sequencing (RNA-Seq) data for isoform discovery and abundance estimation. *Proc Natl Acad Sci U S A*, *108*(50), 19867-19872. https://doi.org/10.1073/pnas.1113972108

Li, M., Li, Z., Ren, H., Jin, W. N., Wood, K., Liu, Q., Sheth, K. N., & Shi, F. D. (2017). Colony stimulating factor 1 receptor inhibition eliminates microglia and attenuates brain injury after intracerebral hemorrhage. *J Cereb Blood Flow Metab*, *37*(7), 2383-2395. https://doi.org/10.1177/0271678X16666551

Li, Q., & Barres, B. A. (2018). Microglia and macrophages in brain homeostasis and disease. *Nat Rev Immunol*, *18*(4), 225-242. https://doi.org/10.1038/nri.2017.125

Li, Q., Cheng, Z., Zhou, L., Darmanis, S., Neff, N. F., Okamoto, J., Gulati, G., Bennett, M. L., Sun, L. O., Clarke, L. E., Marschallinger, J., Yu, G., Quake, S. R., Wyss-Coray, T., & Barres, B. A. (2019). Developmental Heterogeneity of Microglia and Brain Myeloid Cells Revealed by Deep Single-Cell RNA Sequencing. *Neuron*, *101*(2), 207-223 e210. https://doi.org/10.1016/j.neuron.2018.12.006

Li, Z., Farias, F. H. G., Dube, U., Del-Aguila, J. L., Mihindukulasuriya, K. A., Fernandez, M. V., Ibanez, L., Budde, J. P., Wang, F., Lake, A. M., Deming, Y., Perez, J., Yang, C., Bahena, J. A., Qin, W., Bradley, J. L., Davenport, R., Bergmann, K., Morris, J. C., . . . Cruchaga, C. (2020). The

TMEM106B FTLD-protective variant, rs1990621, is also associated with increased neuronal proportion. *Acta Neuropathol*, *139*(1), 45-61. https://doi.org/10.1007/s00401-019-02066-0

Liang, X., Song, M. R., Xu, Z., Lanuza, G. M., Liu, Y., Zhuang, T., Chen, Y., Pfaff, S. L., Evans, S. M., & Sun, Y. (2011). Isl1 is required for multiple aspects of motor neuron development. *Mol Cell Neurosci*, *47*(3), 215-222. https://doi.org/10.1016/j.mcn.2011.04.007

Liddelow, S. A., Guttenplan, K. A., Clarke, L. E., Bennett, F. C., Bohlen, C. J., Schirmer, L., Bennett, M. L., Münch, A. E., Chung, W. S., Peterson, T. C., Wilton, D. K., Frouin, A., Napier, B. A., Panicker, N., Kumar, M., Buckwalter, M. S., Rowitch, D. H., Dawson, V. L., Dawson, T. M., . . . Barres, B. A. (2017). Neurotoxic reactive astrocytes are induced by activated microglia. *Nature*, *541*(7638), 481-487. https://doi.org/10.1038/nature21029

Lin, W., Piskol, R., Tan, M. H., & Li, J. B. (2012). Comment on "Widespread RNA and DNA sequence differences in the human transcriptome". *Science*, *335*(6074), 1302; author reply 1302. https://doi.org/10.1126/science.1210419

Linton, M. F., Moslehi, J. J., & Babaev, V. R. (2019). Akt Signaling in Macrophage Polarization, Survival, and Atherosclerosis. *Int J Mol Sci*, *20*(11). https://doi.org/10.3390/ijms20112703

Liraz, O., Boehm-Cagan, A., & Michaelson, D. M. (2013). ApoE4 induces Aβ42, tau, and neuronal pathology in the hippocampus of young targeted replacement apoE4 mice. *Mol Neurodegener*, *8*, 16. https://doi.org/10.1186/1750-1326-8-16

Lister, R., O'Malley, R. C., Tonti-Filippini, J., Gregory, B. D., Berry, C. C., Millar, A. H., & Ecker, J. R. (2008). Highly integrated single-base resolution maps of the epigenome in Arabidopsis. *Cell*, *133*(3), 523-536. https://doi.org/10.1016/j.cell.2008.03.029

Liu, Y., Zhou, J., & White, K. P. (2014). RNA-seq differential expression studies: more sequence or more replication? *Bioinformatics*, *30*(3), 301-304. https://doi.org/10.1093/bioinformatics/btt688

Livingston, G., Sommerlad, A., Orgeta, V., Costafreda, S. G., Huntley, J., Ames, D., Ballard, C., Banerjee, S., Burns, A., Cohen-Mansfield, J., Cooper, C., Fox, N., Gitlin, L. N., Howard, R., Kales, H. C., Larson, E. B., Ritchie, K., Rockwood, K., Sampson, E. L., . . . Mukadam, N. (2017). Dementia prevention, intervention, and care. *Lancet*, *390*(10113), 2673-2734. https://doi.org/10.1016/s0140-6736(17)31363-6

Lloyd, K. C. K., Adams, D. J., Baynam, G., Beaudet, A. L., Bosch, F., Boycott, K. M., Braun, R. E., Caulfield, M., Cohn, R., Dickinson, M. E., Dobbie, M. S., Flenniken, A. M., Flicek, P., Galande, S., Gao, X., Grobler, A., Heaney, J. D., Herault, Y., de Angelis, M. H., . . . Brown, S. D. M. (2020). The Deep Genome Project. *Genome Biol*, *21*(1), 18. https://doi.org/10.1186/s13059-020-1931-9

Lobanov, S. V., McAllister, B., McDade-Kumar, M., Landwehrmeyer, G. B., Orth, M., Rosser, A. E., network, R. I. o. t. E. H. s. d., Paulsen, J. S., Group, P.-H. I. o. t. H. S., Lee, J. M., MacDonald, M. E., Gusella, J. F., Long, J. D., Ryten, M., Williams, N. M., Holmans, P., Massey, T. H., & Jones, L. (2022). Huntington's disease age at motor onset is modified by the tandem hexamer repeat in TCERG1. *NPJ Genom Med*, *7*(1), 53. https://doi.org/10.1038/s41525-022-00317-w

Lohse, M., Bolger, A. M., Nagel, A., Fernie, A. R., Lunn, J. E., Stitt, M., & Usadel, B. (2012). RobiNA: a user-friendly, integrated software solution for RNA-Seq-based transcriptomics. *Nucleic Acids Res*, *40*(Web Server issue), W622-627. https://doi.org/10.1093/nar/gks540

Love, S., Siew, L. K., Dawbarn, D., Wilcock, G. K., Ben-Shlomo, Y., & Allen, S. J. (2006). Premorbid effects of APOE on synaptic proteins in human temporal neocortex. *Neurobiol Aging*, *27*(6), 797-803. https://doi.org/10.1016/j.neurobiolaging.2005.04.008

Luesse, H. G., Schiefer, J., Spruenken, A., Puls, C., Block, F., & Kosinski, C. M. (2001). Evaluation of R6/2 HD transgenic mice for therapeutic studies in Huntington's disease: behavioral testing and impact of diabetes mellitus. *Behav Brain Res*, *126*(1-2), 185-195. https://doi.org/10.1016/s0166-4328(01)00261-3

Lund, H., Pieber, M., Parsa, R., Han, J., Grommisch, D., Ewing, E., Kular, L., Needhamsen, M., Espinosa, A., Nilsson, E., Överby, A. K., Butovsky, O., Jagodic, M., Zhang, X. M., & Harris, R. A. (2018). Competitive repopulation of an empty microglial niche yields functionally distinct subsets of microglia-like cells. *Nat Commun*, *9*(1), 4845. https://doi.org/10.1038/s41467-018-07295-7

Luquez, T., Gaur, P., Kosater, I. M., Lam, M., Lee, D. I., Mares, J., Paryani, F., Yadav, A., & Menon, V. (2022). Cell type-specific changes identified by single-cell transcriptomics in Alzheimer's disease. *Genome Med*, *14*(1), 136. https://doi.org/10.1186/s13073-022-01136-5

MacDonald, K. P., Rowe, V., Bofinger, H. M., Thomas, R., Sasmono, T., Hume, D. A., & Hill, G. R. (2005). The colony-stimulating factor 1 receptor is expressed on dendritic cells during differentiation and regulates their expansion. *J Immunol*, *175*(3), 1399-1405. https://doi.org/10.4049/jimmunol.175.3.1399

Mallat, M., Marín-Teva, J. L., & Chéret, C. (2005). Phagocytosis in the developing CNS: more than clearing the corpses. *Curr Opin Neurobiol*, *15*(1), 101-107. https://doi.org/10.1016/j.conb.2005.01.006

Mandrekar-Colucci, S., & Landreth, G. E. (2010). Microglia and inflammation in Alzheimer's disease. *CNS Neurol Disord Drug Targets*, *9*(2), 156-167. https://doi.org/10.2174/187152710791012071

Marioni, J. C., Mason, C. E., Mane, S. M., Stephens, M., & Gilad, Y. (2008). RNA-seq: an assessment of technical reproducibility and comparison with gene expression arrays. *Genome Res*, *18*(9), 1509-1517. https://doi.org/10.1101/gr.079558.108

Marioni, R. E., Harris, S. E., Zhang, Q., McRae, A. F., Hagenaars, S. P., Hill, W. D., Davies, G., Ritchie, C. W., Gale, C. R., Starr, J. M., Goate, A. M., Porteous, D. J., Yang, J., Evans, K. L., Deary, I. J., Wray, N. R., & Visscher, P. M. (2018). GWAS on family history of Alzheimer's disease. *Transl Psychiatry*, *8*(1), 99. https://doi.org/10.1038/s41398-018-0150-6

Masuda, T., Nishimoto, N., Tomiyama, D., Matsuda, T., Tozaki-Saitoh, H., Tamura, T., Kohsaka, S., Tsuda, M., & Inoue, K. (2014). IRF8 is a transcriptional determinant for microglial motility. *Purinergic Signal*, *10*(3), 515-521. https://doi.org/10.1007/s11302-014-9413-8

Matarredona, E. R., Talaveron, R., & Pastor, A. M. (2018). Interactions Between Neural Progenitor Cells and Microglia in the Subventricular Zone: Physiological Implications in the Neurogenic Niche and After Implantation in the Injured Brain. *Front Cell Neurosci*, *12*, 268. https://doi.org/10.3389/fncel.2018.00268

Mathys, H., Adaikkan, C., Gao, F., Young, J. Z., Manet, E., Hemberg, M., De Jager, P. L., Ransohoff, R. M., Regev, A., & Tsai, L. H. (2017). Temporal Tracking of Microglia Activation in Neurodegeneration at Single-Cell Resolution. *Cell Rep*, *21*(2), 366-380. https://doi.org/10.1016/j.celrep.2017.09.039

Matos, M., Augusto, E., Oliveira, C. R., & Agostinho, P. (2008). Amyloid-beta peptide decreases glutamate uptake in cultured astrocytes: involvement of oxidative stress and mitogen-activated protein kinase cascades. *Neuroscience*, *156*(4), 898-910. https://doi.org/10.1016/j.neuroscience.2008.08.022

Matsunaga, W., Shirokawa, T., & Isobe, K. (2003). Specific uptake of Abeta1-40 in rat brain occurs in astrocyte, but not in microglia. *Neurosci Lett*, *342*(1-2), 129-131. https://doi.org/10.1016/s0304-3940(03)00240-4

Mayo, L., Trauger, S. A., Blain, M., Nadeau, M., Patel, B., Alvarez, J. I., Mascanfroni, I. D., Yeste, A., Kivisäkk, P., Kallas, K., Ellezam, B., Bakshi, R., Prat, A., Antel, J. P., Weiner, H. L., & Quintana, F. J. (2014). Regulation of astrocyte activation by glycolipids drives chronic CNS inflammation. *Nat Med*, *20*(10), 1147-1156. https://doi.org/10.1038/nm.3681

McCarthy, D. J., Chen, Y., & Smyth, G. K. (2012). Differential expression analysis of multifactor RNA-Seq experiments with respect to biological variation. *Nucleic Acids Res*, *40*(10), 4288-4297. https://doi.org/10.1093/nar/gks042

McGowan, E., Eriksen, J., & Hutton, M. (2006). A decade of modeling Alzheimer's disease in transgenic mice. *Trends Genet*, *22*(5), 281-289. https://doi.org/10.1016/j.tig.2006.03.007

McGowan, E., Pickford, F., Kim, J., Onstead, L., Eriksen, J., Yu, C., Skipper, L., Murphy, M. P., Beard, J., Das, P., Jansen, K., DeLucia, M., Lin, W. L., Dolios, G., Wang, R., Eckman, C. B., Dickson, D. W., Hutton, M., Hardy, J., & Golde, T. (2005). Abeta42 is essential for parenchymal and vascular amyloid deposition in mice. *Neuron*, *47*(2), 191-199. https://doi.org/10.1016/j.neuron.2005.06.030

Meilandt, W. J., Ngu, H., Gogineni, A., Lalehzadeh, G., Lee, S. H., Srinivasan, K., Imperio, J., Wu, T., Weber, M., Kruse, A. J., Stark, K. L., Chan, P., Kwong, M., Modrusan, Z., Friedman, B. A., Elstrott, J., Foreman, O., Easton, A., Sheng, M., & Hansen, D. V. (2020). Trem2 Deletion Reduces Late-Stage Amyloid Plaque Accumulation, Elevates the Aβ42:Aβ40 Ratio, and Exacerbates Axonal Dystrophy and Dendritic Spine Loss in the PS2APP Alzheimer's Mouse Model. *J Neurosci*, *40*(9), 1956-1974. https://doi.org/10.1523/jneurosci.1871-19.2019

Mendsaikhan, A., Tooyama, I., & Walker, D. G. (2019). Microglial Progranulin: Involvement in Alzheimer's Disease and Neurodegenerative Diseases. *Cells*, *8*(3). https://doi.org/10.3390/cells8030230

Metzker, M. L. (2010). Sequencing technologies - the next generation. *Nat Rev Genet*, *11*(1), 31-46. https://doi.org/10.1038/nrg2626

Meucci, O., Fatatis, A., Simen, A. A., & Miller, R. J. (2000). Expression of CX3CR1 chemokine receptors on neurons and their role in neuronal survival. *Proc Natl Acad Sci U S A*, *97*(14), 8075-8080. https://doi.org/10.1073/pnas.090017497

Meuwissen, M. E., Schot, R., Buta, S., Oudesluijs, G., Tinschert, S., Speer, S. D., Li, Z., van Unen, L., Heijsman, D., Goldmann, T., Lequin, M. H., Kros, J. M., Stam, W., Hermann, M., Willemsen, R., Brouwer, R. W., Van, I. W. F., Martin-Fernandez, M., de Coo, I., . . . Mancini, G. M. (2016). Human USP18 deficiency underlies type 1 interferonopathy leading to severe pseudo-TORCH syndrome. *J Exp Med*, *213*(7), 1163-1174. https://doi.org/10.1084/jem.20151529

Mezlini, A. M., Smith, E. J., Fiume, M., Buske, O., Savich, G. L., Shah, S., Aparicio, S., Chiang, D. Y., Goldenberg, A., & Brudno, M. (2013). iReckon: simultaneous isoform discovery and abundance estimation from RNA-seq data. *Genome Res*, *23*(3), 519-529. https://doi.org/10.1101/gr.142232.112

Michailidou, I., Willems, J. G., Kooi, E. J., van Eden, C., Gold, S. M., Geurts, J. J., Baas, F., Huitinga, I., & Ramaglia, V. (2015). Complement C1q-C3-associated synaptic changes in multiple sclerosis hippocampus. *Ann Neurol*, *77*(6), 1007-1026. https://doi.org/10.1002/ana.24398

Milenkovic, I., & Kovacs, G. G. (2013). Incidental corticobasal degeneration in a 76-year-old woman. *Clin Neuropathol*, *32*(1), 69-72. https://doi.org/10.5414/np300515

Mills, J. D., Kawahara, Y., & Janitz, M. (2013). Strand-Specific RNA-Seq Provides Greater Resolution of Transcriptome Profiling. *Curr Genomics*, *14*(3), 173-181. https://doi.org/10.2174/1389202911314030003

Mirra, S. S., Heyman, A., McKeel, D., Sumi, S. M., Crain, B. J., Brownlee, L. M., Vogel, F. S., Hughes, J. P., van Belle, G., & Berg, L. (1991). The Consortium to Establish a Registry for Alzheimer's Disease (CERAD). Part II. Standardization of the neuropathologic assessment of Alzheimer's disease. *Neurology*, *41*(4), 479-486. https://doi.org/10.1212/wnl.41.4.479

Misra, A., Chakrabarti, S. S., & Gambhir, I. S. (2018). New genetic players in late-onset Alzheimer's disease: Findings of genome-wide association studies. *Indian J Med Res*, *148*(2), 135-144. https://doi.org/10.4103/ijmr.IJMR_473_17

Misra, U. K., Adlakha, C. L., Gawdi, G., McMillian, M. K., Pizzo, S. V., & Laskowitz, D. T. (2001). Apolipoprotein E and mimetic peptide initiate a calcium-dependent signaling response in macrophages. *J Leukoc Biol*, *70*(4), 677-683.

Miyata, S., Komatsu, Y., Yoshimura, Y., Taya, C., & Kitagawa, H. (2012). Persistent cortical plasticity by upregulation of chondroitin 6-sulfation. *Nat Neurosci*, *15*(3), 414-422, S411-412. https://doi.org/10.1038/nn.3023

Miyazaki, H., Oyama, F., Inoue, R., Aosaki, T., Abe, T., Kiyonari, H., Kino, Y., Kurosawa, M., Shimizu, J., Ogiwara, I., Yamakawa, K., Koshimizu, Y., Fujiyama, F., Kaneko, T., Shimizu, H., Nagatomo, K., Yamada, K., Shimogori, T., Hattori, N., . . . Nukina, N. (2014). Singular localization of sodium channel beta4 subunit in unmyelinated fibres and its role in the striatum. *Nat Commun*, *5*, 5525. https://doi.org/10.1038/ncomms6525

Monteiro, S., Roque, S., Marques, F., Correia-Neves, M., & Cerqueira, J. J. (2017). Brain interference: Revisiting the role of IFNgamma in the central nervous system. *Prog Neurobiol*, *156*, 149-163. https://doi.org/10.1016/j.pneurobio.2017.05.003

Montgomery, S. B., Sammeth, M., Gutierrez-Arcelus, M., Lach, R. P., Ingle, C., Nisbett, J., Guigo, R., & Dermitzakis, E. T. (2010). Transcriptome genetics using second generation sequencing in a Caucasian population. *Nature*, *464*(7289), 773-777. https://doi.org/10.1038/nature08903

Montine, T. J., Phelps, C. H., Beach, T. G., Bigio, E. H., Cairns, N. J., Dickson, D. W., Duyckaerts, C., Frosch, M. P., Masliah, E., Mirra, S. S., Nelson, P. T., Schneider, J. A., Thal, D. R., Trojanowski, J. Q., Vinters, H. V., & Hyman, B. T. (2012). National Institute on Aging-Alzheimer's Association guidelines for the neuropathologic assessment of Alzheimer's disease: a practical approach. *Acta Neuropathol*, *123*(1), 1-11. https://doi.org/10.1007/s00401-011-0910-3

Morawski, M., Brückner, G., Jäger, C., Seeger, G., Matthews, R. T., & Arendt, T. (2012). Involvement of perineuronal and perisynaptic extracellular matrix in Alzheimer's disease neuropathology. *Brain Pathol*, *22*(4), 547-561. https://doi.org/10.1111/j.1750-3639.2011.00557.x

Moreno, M., Bannerman, P., Ma, J., Guo, F., Miers, L., Soulika, A. M., & Pleasure, D. (2014). Conditional ablation of astroglial CCL2 suppresses CNS accumulation of M1 macrophages and preserves axons in mice with MOG peptide EAE. *J Neurosci*, *34*(24), 8175-8185. https://doi.org/10.1523/jneurosci.1137-14.2014

Morizawa, Y. M., Hirayama, Y., Ohno, N., Shibata, S., Shigetomi, E., Sui, Y., Nabekura, J., Sato, K., Okajima, F., Takebayashi, H., Okano, H., & Koizumi, S. (2017). Reactive astrocytes function as phagocytes after brain ischemia via ABCA1-mediated pathway. *Nat Commun*, *8*(1), 28. https://doi.org/10.1038/s41467-017-00037-1

Mortazavi, A., Williams, B. A., McCue, K., Schaeffer, L., & Wold, B. (2008). Mapping and quantifying mammalian transcriptomes by RNA-Seq. *Nat Methods*, *5*(7), 621-628. https://doi.org/10.1038/nmeth.1226

Mosher, K. I., Andres, R. H., Fukuhara, T., Bieri, G., Hasegawa-Moriyama, M., He, Y., Guzman, R., & Wyss-Coray, T. (2012). Neural progenitor cells regulate microglia functions and activity. *Nat Neurosci*, *15*(11), 1485-1487. https://doi.org/10.1038/nn.3233

Mrdjen, D., Pavlovic, A., Hartmann, F. J., Schreiner, B., Utz, S. G., Leung, B. P., Lelios, I., Heppner, F. L., Kipnis, J., Merkler, D., Greter, M., & Becher, B. (2018). High-Dimensional Single-Cell Mapping of Central Nervous System Immune Cells Reveals Distinct Myeloid Subsets in Health, Aging, and Disease. *Immunity*, *48*(2), 380-395 e386. https://doi.org/10.1016/j.immuni.2018.01.011

Nadeau, J. H., & Auwerx, J. (2019). The virtuous cycle of human genetics and mouse models in drug discovery. *Nat Rev Drug Discov*, *18*(4), 255-272. https://doi.org/10.1038/s41573-018-0009-9

Nagele, R. G., D'Andrea, M. R., Lee, H., Venkataraman, V., & Wang, H. Y. (2003). Astrocytes accumulate A beta 42 and give rise to astrocytic amyloid plaques in Alzheimer disease brains. *Brain Res*, *971*(2), 197-209. https://doi.org/10.1016/s0006-8993(03)02361-8

Najafi, A. R., Crapser, J., Jiang, S., Ng, W., Mortazavi, A., West, B. L., & Green, K. N. (2018). A limited capacity for microglial repopulation in the adult brain. *Glia*, *66*(11), 2385-2396. https://doi.org/10.1002/glia.23477

Nakayama, Y., Tsuji, K., Ayaki, T., Mori, M., Tokunaga, F., & Ito, H. (2020). Linear Polyubiquitin Chain Modification of TDP-43-Positive Neuronal Cytoplasmic Inclusions in Amyotrophic Lateral Sclerosis. *J Neuropathol Exp Neurol*, *79*(3), 256-265. https://doi.org/10.1093/jnen/nlz135

Nazarian, A., Yashin, A. I., & Kulminski, A. M. (2019). Genome-wide analysis of genetic predisposition to Alzheimer's disease and related sex disparities. *Alzheimers Res Ther*, *11*(1), 5. https://doi.org/10.1186/s13195-018-0458-8

Neuner, S. M., Heuer, S. E., Huentelman, M. J., O'Connell, K. M. S., & Kaczorowski, C. C. (2019). Harnessing Genetic Complexity to Enhance Translatability of Alzheimer's Disease Mouse Models: A Path toward Precision Medicine. *Neuron*, *101*(3), 399-411.e395. https://doi.org/10.1016/j.neuron.2018.11.040

Nguyen, P. T., Dorman, L. C., Pan, S., Vainchtein, I. D., Han, R. T., Nakao-Inoue, H., Taloma, S. E., Barron, J. J., Molofsky, A. B., Kheirbek, M. A., & Molofsky, A. V. (2020). Microglial Remodeling of the Extracellular Matrix Promotes Synapse Plasticity. *Cell*, *182*(2), 388-403 e315. https://doi.org/10.1016/j.cell.2020.05.050

Nicod, J., Davies, R. W., Cai, N., Hassett, C., Goodstadt, L., Cosgrove, C., Yee, B. K., Lionikaite, V., McIntyre, R. E., Remme, C. A., Lodder, E. M., Gregory, J. S., Hough, T., Joynson, R., Phelps, H., Nell, B., Rowe, C., Wood, J., Walling, A., . . . Flint, J. (2016). Genome-wide association of multiple complex traits in outbred mice by ultra-low-coverage sequencing. *Nat Genet*, *48*(8), 912-918. https://doi.org/10.1038/ng.3595

Nimmerjahn, A., Kirchhoff, F., & Helmchen, F. (2005). Resting microglial cells are highly dynamic surveillants of brain parenchyma in vivo. *Science*, *308*(5726), 1314-1318. https://doi.org/10.1126/science.1110647

Nistico, R., Salter, E., Nicolas, C., Feligioni, M., Mango, D., Bortolotto, Z. A., Gressens, P., Collingridge, G. L., & Peineau, S. (2017). Synaptoimmunology - roles in health and disease. *Mol Brain*, *10*(1), 26. https://doi.org/10.1186/s13041-017-0308-9

Norden, D. M., Fenn, A. M., Dugan, A., & Godbout, J. P. (2014). TGFbeta produced by IL-10 redirected astrocytes attenuates microglial activation. *Glia*, *62*(6), 881-895. https://doi.org/10.1002/glia.22647

Nordengen, K., Kirsebom, B. E., Henjum, K., Selnes, P., Gísladóttir, B., Wettergreen, M., Torsetnes, S. B., Grøntvedt, G. R., Waterloo, K. K., Aarsland, D., Nilsson, L. N. G., & Fladby, T. (2019). Glial activation and inflammation along the Alzheimer's disease continuum. *J Neuroinflammation*, *16*(1), 46. https://doi.org/10.1186/s12974-019-1399-2

A novel gene containing a trinucleotide repeat that is expanded and unstable on Huntington's disease chromosomes. The Huntington's Disease Collaborative Research Group. (1993). *Cell*, *72*(6), 971-983. https://doi.org/10.1016/0092-8674(93)90585-e

Oakley, H., Cole, S. L., Logan, S., Maus, E., Shao, P., Craft, J., Guillozet-Bongaarts, A., Ohno, M., Disterhoft, J., Van Eldik, L., Berry, R., & Vassar, R. (2006). Intraneuronal beta-amyloid aggregates, neurodegeneration, and neuron loss in transgenic mice with five familial Alzheimer's disease mutations: potential factors in amyloid plaque formation. *J Neurosci*, *26*(40), 10129-10140. https://doi.org/10.1523/JNEUROSCI.1202-06.2006

Ochaba, J., Monteys, A. M., O'Rourke, J. G., Reidling, J. C., Steffan, J. S., Davidson, B. L., & Thompson, L. M. (2016). PIAS1 Regulates Mutant Huntingtin Accumulation and Huntington's Disease-Associated Phenotypes In Vivo. *Neuron*, *90*(3), 507-520. https://doi.org/10.1016/j.neuron.2016.03.016

Oddo, S., Caccamo, A., Shepherd, J. D., Murphy, M. P., Golde, T. E., Kayed, R., Metherate, R., Mattson, M. P., Akbari, Y., & LaFerla, F. M. (2003). Triple-transgenic model of Alzheimer's disease with plaques and tangles: intracellular Abeta and synaptic dysfunction. *Neuron*, *39*(3), 409-421. https://doi.org/10.1016/s0896-6273(03)00434-3

Ohtake, Y., Wong, D., Abdul-Muneer, P. M., Selzer, M. E., & Li, S. (2016). Two PTP receptors mediate CSPG inhibition by convergent and divergent signaling pathways in neurons. *Sci Rep*, *6*, 37152. https://doi.org/10.1038/srep37152

Olabarria, M., Noristani, H. N., Verkhratsky, A., & Rodríguez, J. J. (2010). Concomitant astroglial atrophy and astrogliosis in a triple transgenic animal model of Alzheimer's disease. *Glia*, *58*(7), 831-838. https://doi.org/10.1002/glia.20967

Oldham, M. C., Horvath, S., & Geschwind, D. H. (2006). Conservation and evolution of gene coexpression networks in human and chimpanzee brains. *Proc Natl Acad Sci U S A*, *103*(47), 17973-17978. https://doi.org/10.1073/pnas.0605938103

Onos, K. D., Sukoff Rizzo, S. J., Howell, G. R., & Sasner, M. (2016). Toward more predictive genetic mouse models of Alzheimer's disease. *Brain Res Bull*, *122*, 1-11. https://doi.org/10.1016/j.brainresbull.2015.12.003

Onos, K. D., Uyar, A., Keezer, K. J., Jackson, H. M., Preuss, C., Acklin, C. J., O'Rourke, R., Buchanan, R., Cossette, T. L., Sukoff Rizzo, S. J., Soto, I., Carter, G. W., & Howell, G. R. (2019). Enhancing face validity of mouse models of Alzheimer's disease with natural genetic variation. *PLoS Genet*, *15*(5), e1008155. https://doi.org/10.1371/journal.pgen.1008155

Oshlack, A., & Wakefield, M. J. (2009). Transcript length bias in RNA-seq data confounds systems biology. *Biol Direct*, *4*, 14. https://doi.org/10.1186/1745-6150-4-14

Osipovitch, M., Asenjo Martinez, A., Mariani, J. N., Cornwell, A., Dhaliwal, S., Zou, L., Chandler-Militello, D., Wang, S., Li, X., Benraiss, S. J., Agate, R., Lampp, A., Benraiss, A., Windrem, M. S., & Goldman, S. A. (2019). Human ESC-Derived Chimeric Mouse Models of Huntington's Disease Reveal Cell-Intrinsic Defects in Glial Progenitor Cell Differentiation. *Cell Stem Cell*, *24*(1), 107-122 e107. https://doi.org/10.1016/j.stem.2018.11.010

Oyama, F., Miyazaki, H., Sakamoto, N., Becquet, C., Machida, Y., Kaneko, K., Uchikawa, C., Suzuki, T., Kurosawa, M., Ikeda, T., Tamaoka, A., Sakurai, T., & Nukina, N. (2006). Sodium channel beta4 subunit: down-regulation and possible involvement in neuritic degeneration in Huntington's disease transgenic mice. *J Neurochem*, *98*(2), 518-529. https://doi.org/10.1111/j.1471-4159.2006.03893.x

Ozsoy, Y., Gungor, S., & Cevher, E. (2009). Nasal delivery of high molecular weight drugs. *Molecules*, *14*(9), 3754-3779. https://doi.org/10.3390/molecules14093754

Palay, S. L. (1956). Synapses in the central nervous system. *J Biophys Biochem Cytol*, *2*(4 Suppl), 193-202. https://doi.org/10.1083/jcb.2.4.193

Palpagama, T. H., Waldvogel, H. J., Faull, R. L. M., & Kwakowsky, A. (2019). The Role of Microglia and Astrocytes in Huntington's Disease. *Front Mol Neurosci*, *12*, 258. https://doi.org/10.3389/fnmol.2019.00258

Pantazopoulos, H., & Berretta, S. (2016). In Sickness and in Health: Perineuronal Nets and Synaptic Plasticity in Psychiatric Disorders. *Neural Plast*, *2016*, 9847696. https://doi.org/10.1155/2016/9847696

Paolicelli, R. C., Bolasco, G., Pagani, F., Maggi, L., Scianni, M., Panzanelli, P., Giustetto, M., Ferreira, T. A., Guiducci, E., Dumas, L., Ragozzino, D., & Gross, C. T. (2011). Synaptic pruning by microglia is necessary for normal brain development. *Science*, *333*(6048), 1456-1458. https://doi.org/10.1126/science.1202529

Parachikova, A., Vasilevko, V., Cribbs, D. H., LaFerla, F. M., & Green, K. N. (2010). Reductions in amyloid-beta-derived neuroinflammation, with minocycline, restore cognition but do not significantly affect tau hyperphosphorylation. *J Alzheimers Dis*, *21*(2), 527-542. https://doi.org/10.3233/JAD-2010-100204

Pardridge, W. M. (2022). A Historical Review of Brain Drug Delivery. *Pharmaceutics*, *14*(6). https://doi.org/10.3390/pharmaceutics14061283

Park, D., Tosello-Trampont, A. C., Elliott, M. R., Lu, M., Haney, L. B., Ma, Z., Klibanov, A. L., Mandell, J. W., & Ravichandran, K. S. (2007). BAI1 is an engulfment receptor for apoptotic cells upstream of the ELMO/Dock180/Rac module. *Nature*, *450*(7168), 430-434. https://doi.org/10.1038/nature06329

Park, T., Yi, S. G., Lee, S., Lee, S. Y., Yoo, D. H., Ahn, J. I., & Lee, Y. S. (2003). Statistical tests for identifying differentially expressed genes in time-course microarray experiments. *Bioinformatics*, *19*(6), 694-703. https://doi.org/10.1093/bioinformatics/btg068

Parkhomchuk, D., Borodina, T., Amstislavskiy, V., Banaru, M., Hallen, L., Krobitsch, S., Lehrach, H., & Soldatov, A. (2009). Transcriptome analysis by strand-specific sequencing of complementary DNA. *Nucleic Acids Res*, *37*(18), e123. https://doi.org/10.1093/nar/gkp596

Patterson, M., Barske, L., Van Handel, B., Rau, C. D., Gan, P., Sharma, A., Parikh, S., Denholtz, M., Huang, Y., Yamaguchi, Y., Shen, H., Allayee, H., Crump, J. G., Force, T. I., Lien, C. L., Makita, T., Lusis, A. J., Kumar, S. R., & Sucov, H. M. (2017). Frequency of mononuclear diploid cardiomyocytes underlies natural variation in heart regeneration. *Nat Genet*, *49*(9), 1346-1353. https://doi.org/10.1038/ng.3929

Paushter, D. H., Du, H., Feng, T., & Hu, F. (2018). The lysosomal function of progranulin, a guardian against neurodegeneration. *Acta Neuropathol*, *136*(1), 1-17. https://doi.org/10.1007/s00401-018-1861-8

Pavese, N., Gerhard, A., Tai, Y. F., Ho, A. K., Turkheimer, F., Barker, R. A., Brooks, D. J., & Piccini, P. (2006). Microglial activation correlates with severity in Huntington disease: a clinical and PET study. *Neurology*, *66*(11), 1638-1643. https://doi.org/10.1212/01.wnl.0000222734.56412.17

Peirce, J. L., Lu, L., Gu, J., Silver, L. M., & Williams, R. W. (2004). A new set of BXD recombinant inbred lines from advanced intercross populations in mice. *BMC Genet*, *5*, 7. https://doi.org/10.1186/1471-2156-5-7

Perea, G., Navarrete, M., & Araque, A. (2009). Tripartite synapses: astrocytes process and control synaptic information. *Trends Neurosci*, *32*(8), 421-431. https://doi.org/10.1016/j.tins.2009.05.001

Perry, V. H., Nicoll, J. A., & Holmes, C. (2010). Microglia in neurodegenerative disease. *Nat Rev Neurol*, *6*(4), 193-201. https://doi.org/10.1038/nrneurol.2010.17

Perry, V. H., & O'Connor, V. (2008). C1q: the perfect complement for a synaptic feast? *Nat Rev Neurosci*, *9*(11), 807-811. https://doi.org/10.1038/nrn2394

Pickrell, J. K., Gilad, Y., & Pritchard, J. K. (2012). Comment on "Widespread RNA and DNA sequence differences in the human transcriptome". *Science*, *335*(6074), 1302; author reply 1302. https://doi.org/10.1126/science.1210484

Pickrell, J. K., Marioni, J. C., Pai, A. A., Degner, J. F., Engelhardt, B. E., Nkadori, E., Veyrieras, J. B., Stephens, M., Gilad, Y., & Pritchard, J. K. (2010). Understanding mechanisms underlying human gene expression variation with RNA sequencing. *Nature*, *464*(7289), 768-772. https://doi.org/10.1038/nature08872

Pippucci, T., Parmeggiani, A., Palombo, F., Maresca, A., Angius, A., Crisponi, L., Cucca, F., Liguori, R., Valentino, M. L., Seri, M., & Carelli, V. (2013). A novel null homozygous mutation confirms CACNA2D2 as a gene mutated in epileptic encephalopathy. *PLOS ONE*, *8*(12), e82154. https://doi.org/10.1371/journal.pone.0082154

Pistollato, F., Ohayon, E. L., Lam, A., Langley, G. R., Novak, T. J., Pamies, D., Perry, G., Trushina, E., Williams, R. S., Roher, A. E., Hartung, T., Harnad, S., Barnard, N., Morris, M. C., Lai, M. C., Merkley, R., & Chandrasekera, P. C. (2016). Alzheimer disease research in the 21st century: past and current failures, new perspectives and funding priorities. *Oncotarget*, *7*(26), 38999-39016. https://doi.org/10.18632/oncotarget.9175

Pixley, F. J., & Stanley, E. R. (2004). CSF-1 regulation of the wandering macrophage: complexity in action. *Trends Cell Biol*, *14*(11), 628-638. https://doi.org/10.1016/j.tcb.2004.09.016

Politis, M., Pavese, N., Tai, Y. F., Kiferle, L., Mason, S. L., Brooks, D. J., Tabrizi, S. J., Barker, R. A., & Piccini, P. (2011). Microglial activation in regions related to cognitive function predicts disease onset in Huntington's disease: a multimodal imaging study. *Hum Brain Mapp*, *32*(2), 258-270. https://doi.org/10.1002/hbm.21008

Ponath, G., Ramanan, S., Mubarak, M., Housley, W., Lee, S., Sahinkaya, F. R., Vortmeyer, A., Raine, C. S., & Pitt, D. (2017). Myelin phagocytosis by astrocytes after myelin damage promotes lesion pathology. *Brain*, *140*(2), 399-413. https://doi.org/10.1093/brain/aww298

Posfai, B., Cserep, C., Orsolits, B., & Denes, A. (2019). New Insights into Microglia-Neuron Interactions: A Neuron's Perspective. *Neuroscience*, *405*, 103-117. https://doi.org/10.1016/j.neuroscience.2018.04.046

Presumey, J., Bialas, A. R., & Carroll, M. C. (2017). Complement System in Neural Synapse Elimination in Development and Disease. *Adv Immunol*, *135*, 53-79. https://doi.org/10.1016/bs.ai.2017.06.004

Price, D. L., Tanzi, R. E., Borchelt, D. R., & Sisodia, S. S. (1998). Alzheimer's disease: genetic studies and transgenic models. *Annu Rev Genet*, *32*, 461-493. https://doi.org/10.1146/annurev.genet.32.1.461

Prince, M., Acosta, D., Ferri, C. P., Guerra, M., Huang, Y., Llibre Rodriguez, J. J., Salas, A., Sosa, A. L., Williams, J. D., Dewey, M. E., Acosta, I., Jotheeswaran, A. T., & Liu, Z. (2012). Dementia incidence and mortality in middle-income countries, and associations with indicators of cognitive reserve: a 10/66 Dementia Research Group population-based cohort study. *Lancet*, *380*(9836), 50-58. https://doi.org/10.1016/s0140-6736(12)60399-7

Proitsi, P., Lee, S. H., Lunnon, K., Keohane, A., Powell, J., Troakes, C., Al-Sarraj, S., Furney, S., Soininen, H., Kłoszewska, I., Mecocci, P., Tsolaki, M., Vellas, B., Lovestone, S., & Hodges, A. (2014). Alzheimer's disease susceptibility variants in the MS4A6A gene are associated with altered levels of MS4A6A expression in blood. *Neurobiol Aging*, *35*(2), 279-290. https://doi.org/10.1016/j.neurobiolaging.2013.08.002

Rademakers, R., Baker, M., Nicholson, A. M., Rutherford, N. J., Finch, N., Soto-Ortolaza, A., Lash, J., Wider, C., Wojtas, A., DeJesus-Hernandez, M., Adamson, J., Kouri, N., Sundal, C., Shuster, E. A., Aasly, J., MacKenzie, J., Roeber, S., Kretzschmar, H. A., Boeve, B. F., . . . Wszolek, Z. K. (2011). Mutations in the colony stimulating factor 1 receptor (CSF1R) gene cause hereditary diffuse leukoencephalopathy with spheroids. *Nat Genet*, *44*(2), 200-205. https://doi.org/10.1038/ng.1027

Raff, M. C., Whitmore, A. V., & Finn, J. T. (2002). Axonal self-destruction and neurodegeneration. *Science*, *296*(5569), 868-871. https://doi.org/10.1126/science.1068613

Raghupathy, N., Choi, K., Vincent, M. J., Beane, G. L., Sheppard, K. S., Munger, S. C., Korstanje, R., Pardo-Manual de Villena, F., & Churchill, G. A. (2018). Hierarchical analysis of RNA-seq reads improves the accuracy of allele-specific expression. *Bioinformatics*, *34*(13), 2177-2184. https://doi.org/10.1093/bioinformatics/bty078

Ramirez, L. M., Goukasian, N., Porat, S., Hwang, K. S., Eastman, J. A., Hurtz, S., Wang, B., Vang, N., Sears, R., Klein, E., Coppola, G., & Apostolova, L. G. (2016). Common variants in ABCA7 and MS4A6A are associated with cortical and hippocampal atrophy. *Neurobiol Aging*, *39*, 82-89. https://doi.org/10.1016/j.neurobiolaging.2015.10.037

Ramoni, R. B., Mulvihill, J. J., Adams, D. R., Allard, P., Ashley, E. A., Bernstein, J. A., Gahl, W. A., Hamid, R., Loscalzo, J., McCray, A. T., Shashi, V., Tifft, C. J., Undiagnosed Diseases, N., & Wise, A. L. (2017). The Undiagnosed Diseases Network: Accelerating Discovery about Health and Disease. *Am J Hum Genet*, *100*(2), 185-192. https://doi.org/10.1016/j.ajhg.2017.01.006

Ransom, C. B., & Sontheimer, H. (1995). Biophysical and pharmacological characterization of inwardly rectifying K+ currents in rat spinal cord astrocytes. *J Neurophysiol*, *73*(1), 333-346. https://doi.org/10.1152/jn.1995.73.1.333

Ravasz, E., Somera, A. L., Mongru, D. A., Oltvai, Z. N., & Barabasi, A. L. (2002). Hierarchical organization of modularity in metabolic networks. *Science*, *297*(5586), 1551-1555. https://doi.org/10.1126/science.1073374

Reichenbach, N., Delekate, A., Plescher, M., Schmitt, F., Krauss, S., Blank, N., Halle, A., & Petzold, G. C. (2019). Inhibition of Stat3-mediated astrogliosis ameliorates pathology in an Alzheimer's disease model. *EMBO Mol Med*, *11*(2). https://doi.org/10.15252/emmm.201809665

Reilly, J. F., Games, D., Rydel, R. E., Freedman, S., Schenk, D., Young, W. G., Morrison, J. H., & Bloom, F. E. (2003). Amyloid deposition in the hippocampus and entorhinal cortex: quantitative

analysis of a transgenic mouse model. *Proc Natl Acad Sci U S A*, *100*(8), 4837-4842. https://doi.org/10.1073/pnas.0330745100

Reiner, A., Shelby, E., Wang, H., Demarch, Z., Deng, Y., Guley, N. H., Hogg, V., Roxburgh, R., Tippett, L. J., Waldvogel, H. J., & Faull, R. L. (2013). Striatal parvalbuminergic neurons are lost in Huntington's disease: implications for dystonia. *Mov Disord*, *28*(12), 1691-1699. https://doi.org/10.1002/mds.25624

Reis, P. P., Waldron, L., Goswami, R. S., Xu, W., Xuan, Y., Perez-Ordonez, B., Gullane, P., Irish, J., Jurisica, I., & Kamel-Reid, S. (2011). mRNA transcript quantification in archival samples using multiplexed, color-coded probes. *BMC Biotechnol*, *11*, 46. https://doi.org/10.1186/1472-6750-11-46

Rhinn, H., & Abeliovich, A. (2017). Differential Aging Analysis in Human Cerebral Cortex Identifies Variants in TMEM106B and GRN that Regulate Aging Phenotypes. *Cell Syst*, *4*(4), 404-415.e405. https://doi.org/10.1016/j.cels.2017.02.009

Ribeiro Xavier, A. L., Kress, B. T., Goldman, S. A., Lacerda de Menezes, J. R., & Nedergaard, M. (2015). A Distinct Population of Microglia Supports Adult Neurogenesis in the Subventricular Zone. *J Neurosci*, *35*(34), 11848-11861. https://doi.org/10.1523/jneurosci.1217-15.2015

Rice, R. A., Spangenberg, E. E., Yamate-Morgan, H., Lee, R. J., Arora, R. P., Hernandez, M. X., Tenner, A. J., West, B. L., & Green, K. N. (2015). Elimination of Microglia Improves Functional Outcomes Following Extensive Neuronal Loss in the Hippocampus. *J Neurosci*, *35*(27), 9977-9989. https://doi.org/10.1523/JNEUROSCI.0336-15.2015

Richter, S. H., Garner, J. P., Auer, C., Kunert, J., & Würbel, H. (2010). Systematic variation improves reproducibility of animal experiments. *Nat Methods*, *7*(3), 167-168. https://doi.org/10.1038/nmeth0310-167

Ricklin, D., Hajishengallis, G., Yang, K., & Lambris, J. D. (2010). Complement: a key system for immune surveillance and homeostasis. *Nat Immunol*, *11*(9), 785-797. https://doi.org/10.1038/ni.1923

Ridge, P. G., Mukherjee, S., Crane, P. K., & Kauwe, J. S. (2013). Alzheimer's disease: analyzing the missing heritability. *PLOS ONE*, *8*(11), e79771. https://doi.org/10.1371/journal.pone.0079771

Robb, J. L., Hammad, N. A., Weightman Potter, P. G., Chilton, J. K., Beall, C., & Ellacott, K. L. J. (2020). The metabolic response to inflammation in astrocytes is regulated by nuclear factor-kappa B signaling. *Glia*, *68*(11), 2246-2263. https://doi.org/10.1002/glia.23835

Robel, S., Buckingham, S. C., Boni, J. L., Campbell, S. L., Danbolt, N. C., Riedemann, T., Sutor, B., & Sontheimer, H. (2015). Reactive astrogliosis causes the development of spontaneous seizures. *J Neurosci*, *35*(8), 3330-3345. https://doi.org/10.1523/jneurosci.1574-14.2015

Roberts, A., Pimentel, H., Trapnell, C., & Pachter, L. (2011). Identification of novel transcripts in annotated genomes using RNA-Seq. *Bioinformatics*, *27*(17), 2325-2329. https://doi.org/10.1093/bioinformatics/btr355

Roberts, A., Trapnell, C., Donaghey, J., Rinn, J. L., & Pachter, L. (2011). Improving RNA-Seq expression estimates by correcting for fragment bias. *Genome Biol*, *12*(3), R22. https://doi.org/10.1186/gb-2011-12-3-r22

Robertson, G., Schein, J., Chiu, R., Corbett, R., Field, M., Jackman, S. D., Mungall, K., Lee, S., Okada, H. M., Qian, J. Q., Griffith, M., Raymond, A., Thiessen, N., Cezard, T., Butterfield, Y. S., Newsome, R., Chan, S. K., She, R., Varhol, R., . . . Birol, I. (2010). De novo assembly and analysis of RNA-seq data. *Nat Methods*, *7*(11), 909-912. https://doi.org/10.1038/nmeth.1517

Robinson, M. D., McCarthy, D. J., & Smyth, G. K. (2010). edgeR: a Bioconductor package for differential expression analysis of digital gene expression data. *Bioinformatics*, *26*(1), 139-140. https://doi.org/10.1093/bioinformatics/btp616

Robinson, M. D., & Oshlack, A. (2010). A scaling normalization method for differential expression analysis of RNA-seq data. *Genome Biol*, *11*(3), R25. https://doi.org/10.1186/gb-2010-11-3-r25

Robinson, M. D., & Smyth, G. K. (2007). Moderated statistical tests for assessing differences in tag abundance. *Bioinformatics*, *23*(21), 2881-2887. https://doi.org/10.1093/bioinformatics/btm453

Robinson, M. D., & Smyth, G. K. (2008). Small-sample estimation of negative binomial dispersion, with applications to SAGE data. *Biostatistics*, *9*(2), 321-332. https://doi.org/10.1093/biostatistics/kxm030

Robinson, P. N., Kohler, S., Oellrich, A., Sanger Mouse Genetics, P., Wang, K., Mungall, C. J., Lewis, S. E., Washington, N., Bauer, S., Seelow, D., Krawitz, P., Gilissen, C., Haendel, M., & Smedley, D. (2014). Improved exome prioritization of disease genes through cross-species phenotype comparison. *Genome Res*, *24*(2), 340-348. https://doi.org/10.1101/gr.160325.113

Rocha, S. M., Cristovão, A. C., Campos, F. L., Fonseca, C. P., & Baltazar, G. (2012). Astrocyte-derived GDNF is a potent inhibitor of microglial activation. *Neurobiol Dis*, *47*(3), 407-415. https://doi.org/10.1016/j.nbd.2012.04.014

Rodgers, M. A., Bowman, J. W., Fujita, H., Orazio, N., Shi, M., Liang, Q., Amatya, R., Kelly, T. J., Iwai, K., Ting, J., & Jung, J. U. (2014). The linear ubiquitin assembly complex (LUBAC) is essential for NLRP3 inflammasome activation. *J Exp Med*, *211*(7), 1333-1347. https://doi.org/10.1084/jem.20132486

Rojas-Rueda, D., Morales-Zamora, E., Alsufyani, W. A., Herbst, C. H., AlBalawi, S. M., Alsukait, R., & Alomran, M. (2021). Environmental Risk Factors and Health: An Umbrella Review of Meta-Analyses. *Int J Environ Res Public Health*, *18*(2). https://doi.org/10.3390/ijerph18020704

Rojo, R., Raper, A., Ozdemir, D. D., Lefevre, L., Grabert, K., Wollscheid-Lengeling, E., Bradford, B., Caruso, M., Gazova, I., Sánchez, A., Lisowski, Z. M., Alves, J., Molina-Gonzalez, I., Davtyan, H., Lodge, R. J., Glover, J. D., Wallace, R., Munro, D. A. D., David, E., . . . Pridans, C. (2019). Deletion of a Csf1r enhancer selectively impacts CSF1R expression and development of tissue macrophage populations. *Nat Commun*, *10*(1), 3215. https://doi.org/10.1038/s41467-019-11053-8

Rosen, A. M., & Stevens, B. (2010). The role of the classical complement cascade in synapse loss during development and glaucoma. *Adv Exp Med Biol*, *703*, 75-93. https://doi.org/10.1007/978-1-4419-5635-4_6

Ross, C. A., & Tabrizi, S. J. (2011). Huntington's disease: from molecular pathogenesis to clinical treatment. *Lancet Neurol*, *10*(1), 83-98. https://doi.org/10.1016/S1474-4422(10)70245-3

Rossi, D., Brambilla, L., Valori, C. F., Crugnola, A., Giaccone, G., Capobianco, R., Mangieri, M., Kingston, A. E., Bloc, A., Bezzi, P., & Volterra, A. (2005). Defective tumor necrosis factor-alpha-dependent control of astrocyte glutamate release in a transgenic mouse model of Alzheimer disease. *J Biol Chem*, *280*(51), 42088-42096. https://doi.org/10.1074/jbc.M504124200

Rostami, J., Mothes, T., Kolahdouzan, M., Eriksson, O., Moslem, M., Bergström, J., Ingelsson, M., O'Callaghan, P., Healy, L. M., Falk, A., & Erlandsson, A. (2021). Crosstalk between astrocytes and microglia results in increased degradation of α-synuclein and amyloid-β aggregates. *J Neuroinflammation*, *18*(1), 124. https://doi.org/10.1186/s12974-021-02158-3

Rothhammer, V., Borucki, D. M., Tjon, E. C., Takenaka, M. C., Chao, C. C., Ardura-Fabregat, A., de Lima, K. A., Gutierrez-Vazquez, C., Hewson, P., Staszewski, O., Blain, M., Healy, L., Neziraj, T., Borio, M., Wheeler, M., Dragin, L. L., Laplaud, D. A., Antel, J., Alvarez, J. I., . . . Quintana, F. J. (2018). Microglial control of astrocytes in response to microbial metabolites. *Nature*, *557*(7707), 724-728. https://doi.org/10.1038/s41586-018-0119-x

Rothwell, N. J., & Luheshi, G. N. (2000). Interleukin 1 in the brain: biology, pathology and therapeutic target. *Trends Neurosci*, *23*(12), 618-625. https://doi.org/10.1016/s0166-2236(00)01661-1

Rudloff, U., Bhanot, U., Gerald, W., Klimstra, D. S., Jarnagin, W. R., Brennan, M. F., & Allen, P. J. (2010). Biobanking of human pancreas cancer tissue: impact of ex-vivo procurement times on RNA quality. *Ann Surg Oncol*, *17*(8), 2229-2236. https://doi.org/10.1245/s10434-010-0959-6

Ryman, D., Gao, Y., & Lamb, B. T. (2008). Genetic loci modulating amyloid-beta levels in a mouse model of Alzheimer's disease. *Neurobiol Aging*, *29*(8), 1190-1198. https://doi.org/10.1016/j.neurobiolaging.2007.02.017

Safaiyan, S., Besson-Girard, S., Kaya, T., Cantuti-Castelvetri, L., Liu, L., Ji, H., Schifferer, M., Gouna, G., Usifo, F., Kannaiyan, N., Fitzner, D., Xiang, X., Rossner, M. J., Brendel, M., Gokce, O., & Simons, M. (2021). White matter aging drives microglial diversity. *Neuron*, *109*(7), 1100-1117.e1110. https://doi.org/10.1016/j.neuron.2021.01.027

Saito, T., Matsuba, Y., Mihira, N., Takano, J., Nilsson, P., Itohara, S., Iwata, N., & Saido, T. C. (2014). Single App knock-in mouse models of Alzheimer's disease. *Nat Neurosci*, *17*(5), 661-663. https://doi.org/10.1038/nn.3697

Salminen, A., & Kaarniranta, K. (2009). Siglec receptors and hiding plaques in Alzheimer's disease. *J Mol Med (Berl)*, *87*(7), 697-701. https://doi.org/10.1007/s00109-009-0472-1

Santacruz, K., Lewis, J., Spires, T., Paulson, J., Kotilinek, L., Ingelsson, M., Guimaraes, A., DeTure, M., Ramsden, M., McGowan, E., Forster, C., Yue, M., Orne, J., Janus, C., Mariash, A., Kuskowski, M., Hyman, B., Hutton, M., & Ashe, K. H. (2005). Tau suppression in a neurodegenerative mouse model improves memory function. *Science*, *309*(5733), 476-481. https://doi.org/10.1126/science.1113694

Santos, S. D., Xavier, M., Leite, D. M., Moreira, D. A., Custódio, B., Torrado, M., Castro, R., Leiro, V., Rodrigues, J., Tomás, H., & Pêgo, A. P. (2018). PAMAM dendrimers: blood-brain barrier transport and neuronal uptake after focal brain ischemia. *J Control Release*, *291*, 65-79. https://doi.org/10.1016/j.jconrel.2018.10.006

Sapp, E., Kegel, K. B., Aronin, N., Hashikawa, T., Uchiyama, Y., Tohyama, K., Bhide, P. G., Vonsattel, J. P., & DiFiglia, M. (2001). Early and progressive accumulation of reactive microglia in the Huntington disease brain. *J Neuropathol Exp Neurol*, *60*(2), 161-172. https://doi.org/10.1093/jnen/60.2.161

Saraiva, C., Praça, C., Ferreira, R., Santos, T., Ferreira, L., & Bernardino, L. (2016). Nanoparticle-mediated brain drug delivery: Overcoming blood-brain barrier to treat neurodegenerative diseases. *J Control Release*, *235*, 34-47. https://doi.org/10.1016/j.jconrel.2016.05.044

Sasaguri, H., Nilsson, P., Hashimoto, S., Nagata, K., Saito, T., De Strooper, B., Hardy, J., Vassar, R., Winblad, B., & Saido, T. C. (2017). APP mouse models for Alzheimer's disease preclinical studies. *EMBO J*, *36*(17), 2473-2487. https://doi.org/10.15252/embj.201797397

Schadt, E. E., Lamb, J., Yang, X., Zhu, J., Edwards, S., Guhathakurta, D., Sieberts, S. K., Monks, S., Reitman, M., Zhang, C., Lum, P. Y., Leonardson, A., Thieringer, R., Metzger, J. M., Yang, L., Castle, J., Zhu, H., Kash, S. F., Drake, T. A., . . . Lusis, A. J. (2005). An integrative genomics approach to infer causal associations between gene expression and disease. *Nat Genet*, *37*(7), 710-717. https://doi.org/10.1038/ng1589

Schafer, D. P., Lehrman, E. K., Kautzman, A. G., Koyama, R., Mardinly, A. R., Yamasaki, R., Ransohoff, R. M., Greenberg, M. E., Barres, B. A., & Stevens, B. (2012). Microglia sculpt postnatal neural circuits in an activity and complement-dependent manner. *Neuron*, *74*(4), 691-705. https://doi.org/10.1016/j.neuron.2012.03.026

Schafer, D. P., & Stevens, B. (2015). Microglia Function in Central Nervous System Development and Plasticity. *Cold Spring Harb Perspect Biol*, *7*(10), a020545. https://doi.org/10.1101/cshperspect.a020545

Schmitt, F. A., Davis, D. G., Wekstein, D. R., Smith, C. D., Ashford, J. W., & Markesbery, W. R. (2000). "Preclinical" AD revisited: neuropathology of cognitively normal older adults. *Neurology*, *55*(3), 370-376. https://doi.org/10.1212/wnl.55.3.370

Schulz, M. H., Zerbino, D. R., Vingron, M., & Birney, E. (2012). Oases: robust de novo RNA-seq assembly across the dynamic range of expression levels. *Bioinformatics*, *28*(8), 1086-1092. https://doi.org/10.1093/bioinformatics/bts094

Sebastiani, G., Krzywkowski, P., Dudal, S., Yu, M., Paquette, J., Malo, D., Gervais, F., & Tremblay, P. (2006). Mapping genetic modulators of amyloid plaque deposition in TgCRND8 transgenic mice. *Hum Mol Genet*, *15*(15), 2313-2323. https://doi.org/10.1093/hmg/ddl157

Seeley, W. W. (2017). Mapping Neurodegenerative Disease Onset and Progression. *Cold Spring Harb Perspect Biol*, *9*(8). https://doi.org/10.1101/cshperspect.a023622

Selkoe, D. J. (1991). The molecular pathology of Alzheimer's disease. *Neuron*, *6*(4), 487-498. https://doi.org/10.1016/0896-6273(91)90052-2

Selkoe, D. J., & Hardy, J. (2016). The amyloid hypothesis of Alzheimer's disease at 25 years. *EMBO Mol Med*, *8*(6), 595-608. https://doi.org/10.15252/emmm.201606210

Seshadri, S., Fitzpatrick, A. L., Ikram, M. A., DeStefano, A. L., Gudnason, V., Boada, M., Bis, J. C., Smith, A. V., Carassquillo, M. M., Lambert, J. C., Harold, D., Schrijvers, E. M., Ramirez-Lorca, R., Debette, S., Longstreth, W. T., Jr., Janssens, A. C., Pankratz, V. S., Dartigues, J. F., Hollingworth, P., . . . Breteler, M. M. (2010). Genome-wide analysis of genetic loci associated with Alzheimer disease. *JAMA*, *303*(18), 1832-1840. https://doi.org/10.1001/jama.2010.574

Sevigny, J., Chiao, P., Bussière, T., Weinreb, P. H., Williams, L., Maier, M., Dunstan, R., Salloway, S., Chen, T., Ling, Y., O'Gorman, J., Qian, F., Arastu, M., Li, M., Chollate, S., Brennan, M. S., Quintero-Monzon, O., Scannevin, R. H., Arnold, H. M., . . . Sandrock, A. (2016). The antibody aducanumab reduces Aβ plaques in Alzheimer's disease. *Nature*, *537*(7618), 50-56. https://doi.org/10.1038/nature19323

Sharon, D., Tilgner, H., Grubert, F., & Snyder, M. (2013). A single-molecule long-read survey of the human transcriptome. *Nat Biotechnol*, *31*(11), 1009-1014. https://doi.org/10.1038/nbt.2705

Shemer, A., Grozovski, J., Tay, T. L., Tao, J., Volaski, A., Süß, P., Ardura-Fabregat, A., Gross-Vered, M., Kim, J. S., David, E., Chappell-Maor, L., Thielecke, L., Glass, C. K., Cornils, K., Prinz, M., & Jung, S. (2018). Engrafted parenchymal brain macrophages differ from microglia in transcriptome, chromatin landscape and response to challenge. *Nat Commun*, *9*(1), 5206. https://doi.org/10.1038/s41467-018-07548-5

Shi, J. Q., Shen, W., Chen, J., Wang, B. R., Zhong, L. L., Zhu, Y. W., Zhu, H. Q., Zhang, Q. Q., Zhang, Y. D., & Xu, J. (2011). Anti-TNF-α reduces amyloid plaques and tau phosphorylation and induces CD11c-positive dendritic-like cell in the APP/PS1 transgenic mouse brains. *Brain Res*, *1368*, 239-247. https://doi.org/10.1016/j.brainres.2010.10.053

Shi, Y., Manis, M., Long, J., Wang, K., Sullivan, P. M., Remolina Serrano, J., Hoyle, R., & Holtzman, D. M. (2019). Microglia drive APOE-dependent neurodegeneration in a tauopathy mouse model. *J Exp Med*, *216*(11), 2546-2561. https://doi.org/10.1084/jem.20190980

Shi, Y., Yamada, K., Liddelow, S. A., Smith, S. T., Zhao, L., Luo, W., Tsai, R. M., Spina, S., Grinberg, L. T., Rojas, J. C., Gallardo, G., Wang, K., Roh, J., Robinson, G., Finn, M. B., Jiang, H., Sullivan, P. M., Baufeld, C., Wood, M. W., . . . Holtzman, D. M. (2017). ApoE4 markedly exacerbates tau-mediated neurodegeneration in a mouse model of tauopathy. *Nature*, *549*(7673), 523-527. https://doi.org/10.1038/nature24016

Shulman, J. M., Chen, K., Keenan, B. T., Chibnik, L. B., Fleisher, A., Thiyyagura, P., Roontiva, A., McCabe, C., Patsopoulos, N. A., Corneveaux, J. J., Yu, L., Huentelman, M. J., Evans, D. A., Schneider, J. A., Reiman, E. M., De Jager, P. L., & Bennett, D. A. (2013). Genetic susceptibility for Alzheimer disease neuritic plaque pathology. *JAMA Neurol*, *70*(9), 1150-1157. https://doi.org/10.1001/jamaneurol.2013.2815

Shusterman, A., Salyma, Y., Nashef, A., Soller, M., Wilensky, A., Mott, R., Weiss, E. I., Houri-Haddad, Y., & Iraqi, F. A. (2013). Genotype is an important determinant factor of host susceptibility to periodontitis in the Collaborative Cross and inbred mouse populations. *BMC Genet*, *14*, 68. https://doi.org/10.1186/1471-2156-14-68

Simmons, D. A., Casale, M., Alcon, B., Pham, N., Narayan, N., & Lynch, G. (2007). Ferritin accumulation in dystrophic microglia is an early event in the development of Huntington's disease. *Glia*, *55*(10), 1074-1084. https://doi.org/10.1002/glia.20526

Sipe, J. D., Carreras, I., Gonnerman, W. A., Cathcart, E. S., de Beer, M. C., & de Beer, F. C. (1993). Characterization of the inbred CE/J mouse strain as amyloid resistant. *Am J Pathol*, *143*(5), 1480-1485.

Sirkis, D. W., Bonham, L. W., & Yokoyama, J. S. (2021). The Role of Microglia in Inherited White-Matter Disorders and Connections to Frontotemporal Dementia. *Appl Clin Genet*, *14*, 195-207. https://doi.org/10.2147/tacg.S245029

Smedley, D., & Robinson, P. N. (2015). Phenotype-driven strategies for exome prioritization of human Mendelian disease genes. *Genome Med*, *7*(1), 81. https://doi.org/10.1186/s13073-015-0199-2

Smith, A. M., Heisler, L. E., St Onge, R. P., Farias-Hesson, E., Wallace, I. M., Bodeau, J., Harris, A. N., Perry, K. M., Giaever, G., Pourmand, N., & Nislow, C. (2010). Highly-multiplexed barcode sequencing: an efficient method for parallel analysis of pooled samples. *Nucleic Acids Res*, *38*(13), e142. https://doi.org/10.1093/nar/gkq368

Smyth, G. K. (2004). Linear models and empirical bayes methods for assessing differential expression in microarray experiments. *Stat Appl Genet Mol Biol*, *3*, Article3. https://doi.org/10.2202/1544-6115.1027

Sofroniew, M. V. (2009). Molecular dissection of reactive astrogliosis and glial scar formation. *Trends Neurosci*, *32*(12), 638-647. https://doi.org/10.1016/j.tins.2009.08.002

Sofroniew, M. V., & Vinters, H. V. (2010). Astrocytes: biology and pathology. *Acta Neuropathol*, *119*(1), 7-35. https://doi.org/10.1007/s00401-009-0619-8

Solberg, L. C., Valdar, W., Gauguier, D., Nunez, G., Taylor, A., Burnett, S., Arboledas-Hita, C., Hernandez-Pliego, P., Davidson, S., Burns, P., Bhattacharya, S., Hough, T., Higgs, D., Klenerman, P., Cookson, W. O., Zhang, Y., Deacon, R. M., Rawlins, J. N., Mott, R., & Flint, J. (2006). A protocol for high-throughput phenotyping, suitable for quantitative trait analysis in mice. *Mamm Genome*, *17*(2), 129-146. https://doi.org/10.1007/s00335-005-0112-1

Son, Y., Jeong, Y. J., Shin, N. R., Oh, S. J., Nam, K. R., Choi, H. D., Choi, J. Y., & Lee, H. J. (2020). Inhibition of Colony-Stimulating Factor 1 Receptor by PLX3397 Prevents Amyloid Beta Pathology and Rescues Dopaminergic Signaling in Aging 5xFAD Mice. *Int J Mol Sci*, *21*(15). https://doi.org/10.3390/ijms21155553

Spangenberg, E., Severson, P. L., Hohsfield, L. A., Crapser, J., Zhang, J., Burton, E. A., Zhang, Y., Spevak, W., Lin, J., Phan, N. Y., Habets, G., Rymar, A., Tsang, G., Walters, J., Nespi, M., Singh, P., Broome, S., Ibrahim, P., Zhang, C., . . . Green, K. N. (2019). Sustained microglial depletion with CSF1R inhibitor impairs parenchymal plaque development in an Alzheimer's disease model. *Nat Commun*, *10*(1), 3758. https://doi.org/10.1038/s41467-019-11674-z

Spangenberg, E. E., Lee, R. J., Najafi, A. R., Rice, R. A., Elmore, M. R., Blurton-Jones, M., West, B. L., & Green, K. N. (2016). Eliminating microglia in Alzheimer's mice prevents neuronal loss without modulating amyloid-beta pathology. *Brain*, *139*(Pt 4), 1265-1281. https://doi.org/10.1093/brain/aww016

Spires, T. L., & Hyman, B. T. (2004). Neuronal structure is altered by amyloid plaques. *Rev Neurosci*, *15*(4), 267-278. https://doi.org/10.1515/revneuro.2004.15.4.267

Spit, M., Rieser, E., & Walczak, H. (2019). Linear ubiquitination at a glance. *J Cell Sci*, *132*(2). https://doi.org/10.1242/jcs.208512

Spitz, C., Schlosser, C., Guschtschin-Schmidt, N., Stelzer, W., Menig, S., Götz, A., Haug-Kröper, M., Scharnagl, C., Langosch, D., Muhle-Goll, C., & Fluhrer, R. (2020). Non-canonical Shedding of TNFα by SPPL2a Is Determined by the Conformational Flexibility of Its Transmembrane Helix. *iScience*, *23*(12), 101775. https://doi.org/10.1016/j.isci.2020.101775

Spooner, C. J., Cheng, J. X., Pujadas, E., Laslo, P., & Singh, H. (2009). A recurrent network involving the transcription factors PU.1 and Gfi1 orchestrates innate and adaptive immune cell fates. *Immunity*, *31*(4), 576-586. https://doi.org/10.1016/j.immuni.2009.07.011

Sredni-Kenigsbuch, D. (2002). TH1/TH2 cytokines in the central nervous system. *Int J Neurosci*, *112*(6), 665-703. https://doi.org/10.1080/00207450290025725

Srinivasan, K., Friedman, B. A., Etxeberria, A., Huntley, M. A., van der Brug, M. P., Foreman, O., Paw, J. S., Modrusan, Z., Beach, T. G., Serrano, G. E., & Hansen, D. V. (2020). Alzheimer's Patient Microglia Exhibit Enhanced Aging and Unique Transcriptional Activation. *Cell Rep*, *31*(13), 107843. https://doi.org/10.1016/j.celrep.2020.107843

Srivastava, S., & Chen, L. (2010). A two-parameter generalized Poisson model to improve the analysis of RNA-seq data. *Nucleic Acids Res*, *38*(17), e170. https://doi.org/10.1093/nar/gkq670

Stafford, J. H., Hirai, T., Deng, L., Chernikova, S. B., Urata, K., West, B. L., & Brown, J. M. (2016). Colony stimulating factor 1 receptor inhibition delays recurrence of glioblastoma after radiation by altering myeloid cell recruitment and polarization. *Neuro Oncol*, *18*(6), 797-806. https://doi.org/10.1093/neuonc/nov272

Stalder, M., Phinney, A., Probst, A., Sommer, B., Staufenbiel, M., & Jucker, M. (1999). Association of microglia with amyloid plaques in brains of APP23 transgenic mice. *Am J Pathol*, *154*(6), 1673-1684. https://doi.org/10.1016/s0002-9440(10)65423-5

Staszewski, O., & Hagemeyer, N. (2019). Unique microglia expression profile in developing white matter. *BMC Res Notes*, *12*(1), 367. https://doi.org/10.1186/s13104-019-4410-1

Steijger, T., Abril, J. F., Engstrom, P. G., Kokocinski, F., Consortium, R., Hubbard, T. J., Guigo, R., Harrow, J., & Bertone, P. (2013). Assessment of transcript reconstruction methods for RNA-seq. *Nat Methods*, *10*(12), 1177-1184. https://doi.org/10.1038/nmeth.2714

Stephan, A. H., Barres, B. A., & Stevens, B. (2012). The complement system: an unexpected role in synaptic pruning during development and disease. *Annu Rev Neurosci*, *35*, 369-389. https://doi.org/10.1146/annurev-neuro-061010-113810

Stephan, A. H., Madison, D. V., Mateos, J. M., Fraser, D. A., Lovelett, E. A., Coutellier, L., Kim, L., Tsai, H. H., Huang, E. J., Rowitch, D. H., Berns, D. S., Tenner, A. J., Shamloo, M., & Barres, B. A. (2013). A dramatic increase of C1q protein in the CNS during normal aging. *J Neurosci*, *33*(33), 13460-13474. https://doi.org/10.1523/jneurosci.1333-13.2013

Stephenson, J., Nutma, E., van der Valk, P., & Amor, S. (2018). Inflammation in CNS neurodegenerative diseases. *Immunology*, *154*(2), 204-219. https://doi.org/10.1111/imm.12922

Sterpka, A., & Chen, X. (2018). Neuronal and astrocytic primary cilia in the mature brain. *Pharmacol Res*, *137*, 114-121. https://doi.org/10.1016/j.phrs.2018.10.002

Stevens, B. (2008). Neuron-astrocyte signaling in the development and plasticity of neural circuits. *Neurosignals*, *16*(4), 278-288. https://doi.org/10.1159/000123038

Stevens, B., Allen, N. J., Vazquez, L. E., Howell, G. R., Christopherson, K. S., Nouri, N., Micheva, K. D., Mehalow, A. K., Huberman, A. D., Stafford, B., Sher, A., Litke, A. M., Lambris, J. D., Smith, S. J., John, S. W., & Barres, B. A. (2007). The classical complement cascade mediates CNS synapse elimination. *Cell*, *131*(6), 1164-1178. https://doi.org/10.1016/j.cell.2007.10.036

Strang, K. H., Croft, C. L., Sorrentino, Z. A., Chakrabarty, P., Golde, T. E., & Giasson, B. I. (2018). Distinct differences in prion-like seeding and aggregation between Tau protein variants provide mechanistic insights into tauopathies. *J Biol Chem*, *293*(7), 2408-2421. https://doi.org/10.1074/jbc.M117.815357

Stratoulias, V., Venero, J. L., Tremblay, M., & Joseph, B. (2019). Microglial subtypes: diversity within the microglial community. *EMBO J*, *38*(17), e101997. https://doi.org/10.15252/embj.2019101997

Strohmeyer, R., Ramirez, M., Cole, G. J., Mueller, K., & Rogers, J. (2002). Association of factor H of the alternative pathway of complement with agrin and complement receptor 3 in the

Alzheimer's disease brain. *J Neuroimmunol*, *131*(1-2), 135-146. https://doi.org/10.1016/s0165-5728(02)00272-2
Subhramanyam, C. S., Wang, C., Hu, Q., & Dheen, S. T. (2019). Microglia-mediated neuroinflammation in neurodegenerative diseases. *Semin Cell Dev Biol*, *94*, 112-120. https://doi.org/10.1016/j.semcdb.2019.05.004
Sundal, C., & Wszolek, Z. K. (1993). CSF1R-Related Adult-Onset Leukoencephalopathy with Axonal Spheroids and Pigmented Glia. In M. P. Adam, G. M. Mirzaa, R. A. Pagon, S. E. Wallace, L. J. H. Bean, K. W. Gripp, & A. Amemiya (Eds.), *GeneReviews((R))*. https://www.ncbi.nlm.nih.gov/pubmed/22934315
Svenson, K. L., Gatti, D. M., Valdar, W., Welsh, C. E., Cheng, R., Chesler, E. J., Palmer, A. A., McMillan, L., & Churchill, G. A. (2012). High-resolution genetic mapping using the Mouse Diversity outbred population. *Genetics*, *190*(2), 437-447. https://doi.org/10.1534/genetics.111.132597
Szalay, G., Martinecz, B., Lenart, N., Kornyei, Z., Orsolits, B., Judak, L., Csaszar, E., Fekete, R., West, B. L., Katona, G., Rozsa, B., & Denes, A. (2016). Microglia protect against brain injury and their selective elimination dysregulates neuronal network activity after stroke. *Nat Commun*, *7*, 11499. https://doi.org/10.1038/ncomms11499
Szepesi, Z., Manouchehrian, O., Bachiller, S., & Deierborg, T. (2018). Bidirectional Microglia-Neuron Communication in Health and Disease. *Front Cell Neurosci*, *12*, 323. https://doi.org/10.3389/fncel.2018.00323
t Hoen, P. A., Friedlander, M. R., Almlof, J., Sammeth, M., Pulyakhina, I., Anvar, S. Y., Laros, J. F., Buermans, H. P., Karlberg, O., Brannvall, M., Consortium, G., den Dunnen, J. T., van Ommen, G. J., Gut, I. G., Guigo, R., Estivill, X., Syvanen, A. C., Dermitzakis, E. T., & Lappalainen, T. (2013). Reproducibility of high-throughput mRNA and small RNA sequencing across laboratories. *Nat Biotechnol*, *31*(11), 1015-1022. https://doi.org/10.1038/nbt.2702
Tagliavini, F., Giaccone, G., Frangione, B., & Bugiani, O. (1988). Preamyloid deposits in the cerebral cortex of patients with Alzheimer's disease and nondemented individuals. *Neurosci Lett*, *93*(2-3), 191-196. https://doi.org/10.1016/0304-3940(88)90080-8
Tai, Y. F., Pavese, N., Gerhard, A., Tabrizi, S. J., Barker, R. A., Brooks, D. J., & Piccini, P. (2007). Microglial activation in presymptomatic Huntington's disease gene carriers. *Brain*, *130*(Pt 7), 1759-1766. https://doi.org/10.1093/brain/awm044
Tan, Y. L., Yuan, Y., & Tian, L. (2020). Microglial regional heterogeneity and its role in the brain. *Mol Psychiatry*, *25*(2), 351-367. https://doi.org/10.1038/s41380-019-0609-8
Tang, W., Lu, Y., Tian, Q. Y., Zhang, Y., Guo, F. J., Liu, G. Y., Syed, N. M., Lai, Y., Lin, E. A., Kong, L., Su, J., Yin, F., Ding, A. H., Zanin-Zhorov, A., Dustin, M. L., Tao, J., Craft, J., Yin, Z., Feng, J. Q., . . . Liu, C. J. (2011). The growth factor progranulin binds to TNF receptors and is therapeutic against inflammatory arthritis in mice. *Science*, *332*(6028), 478-484. https://doi.org/10.1126/science.1199214
Tansey, K. E., Cameron, D., & Hill, M. J. (2018). Genetic risk for Alzheimer's disease is concentrated in specific macrophage and microglial transcriptional networks. *Genome Med*, *10*(1), 14. https://doi.org/10.1186/s13073-018-0523-8
Tay, T. L., Sagar, Dautzenberg, J., Grun, D., & Prinz, M. (2018). Unique microglia recovery population revealed by single-cell RNAseq following neurodegeneration. *Acta Neuropathol Commun*, *6*(1), 87. https://doi.org/10.1186/s40478-018-0584-3
Tay, T. L., Savage, J. C., Hui, C. W., Bisht, K., & Tremblay, M. (2017). Microglia across the lifespan: from origin to function in brain development, plasticity and cognition. *J Physiol*, *595*(6), 1929-1945. https://doi.org/10.1113/jp272134
Taylor, B. A., Wnek, C., Kotlus, B. S., Roemer, N., MacTaggart, T., & Phillips, S. J. (1999). Genotyping new BXD recombinant inbred mouse strains and comparison of BXD and consensus maps. *Mamm Genome*, *10*(4), 335-348. https://doi.org/10.1007/s003359900998

Tcw, J., & Goate, A. M. (2017). Genetics of β-Amyloid Precursor Protein in Alzheimer's Disease. *Cold Spring Harb Perspect Med*, *7*(6). https://doi.org/10.1101/cshperspect.a024539
Terry, R. D., Masliah, E., Salmon, D. P., Butters, N., DeTeresa, R., Hill, R., Hansen, L. A., & Katzman, R. (1991). Physical basis of cognitive alterations in Alzheimer's disease: synapse loss is the major correlate of cognitive impairment. *Ann Neurol*, *30*(4), 572-580. https://doi.org/10.1002/ana.410300410
Thal, D. R., Rüb, U., Orantes, M., & Braak, H. (2002). Phases of A beta-deposition in the human brain and its relevance for the development of AD. *Neurology*, *58*(12), 1791-1800. https://doi.org/10.1212/wnl.58.12.1791
Tham, M., Ramasamy, S., Gan, H. T., Ramachandran, A., Poonepalli, A., Yu, Y. H., & Ahmed, S. (2010). CSPG is a secreted factor that stimulates neural stem cell survival possibly by enhanced EGFR signaling. *PLOS ONE*, *5*(12), e15341. https://doi.org/10.1371/journal.pone.0015341
Thompson, K. L., Pine, P. S., Rosenzweig, B. A., Turpaz, Y., & Retief, J. (2007). Characterization of the effect of sample quality on high density oligonucleotide microarray data using progressively degraded rat liver RNA. *BMC Biotechnol*, *7*, 57. https://doi.org/10.1186/1472-6750-7-57
Threadgill, D. W., Miller, D. R., Churchill, G. A., & de Villena, F. P. (2011). The collaborative cross: a recombinant inbred mouse population for the systems genetic era. *Ilar j*, *52*(1), 24-31. https://doi.org/10.1093/ilar.52.1.24
Tian, G., Kong, Q., Lai, L., Ray-Chaudhury, A., & Lin, C. L. (2010). Increased expression of cholesterol 24S-hydroxylase results in disruption of glial glutamate transporter EAAT2 association with lipid rafts: a potential role in Alzheimer's disease. *J Neurochem*, *113*(4), 978-989. https://doi.org/10.1111/j.1471-4159.2010.06661.x
Tomita, H., Vawter, M. P., Walsh, D. M., Evans, S. J., Choudary, P. V., Li, J., Overman, K. M., Atz, M. E., Myers, R. M., Jones, E. G., Watson, S. J., Akil, H., & Bunney, W. E., Jr. (2004). Effect of agonal and postmortem factors on gene expression profile: quality control in microarray analyses of postmortem human brain. *Biol Psychiatry*, *55*(4), 346-352. https://doi.org/10.1016/j.biopsych.2003.10.013
Trapnell, C., Hendrickson, D. G., Sauvageau, M., Goff, L., Rinn, J. L., & Pachter, L. (2013). Differential analysis of gene regulation at transcript resolution with RNA-seq. *Nat Biotechnol*, *31*(1), 46-53. https://doi.org/10.1038/nbt.2450
Trapnell, C., Pachter, L., & Salzberg, S. L. (2009). TopHat: discovering splice junctions with RNA-Seq. *Bioinformatics*, *25*(9), 1105-1111. https://doi.org/10.1093/bioinformatics/btp120
Trapnell, C., Roberts, A., Goff, L., Pertea, G., Kim, D., Kelley, D. R., Pimentel, H., Salzberg, S. L., Rinn, J. L., & Pachter, L. (2012). Differential gene and transcript expression analysis of RNA-seq experiments with TopHat and Cufflinks. *Nat Protoc*, *7*(3), 562-578. https://doi.org/10.1038/nprot.2012.016
Trapnell, C., Williams, B. A., Pertea, G., Mortazavi, A., Kwan, G., van Baren, M. J., Salzberg, S. L., Wold, B. J., & Pachter, L. (2010). Transcript assembly and quantification by RNA-Seq reveals unannotated transcripts and isoform switching during cell differentiation. *Nat Biotechnol*, *28*(5), 511-515. https://doi.org/10.1038/nbt.1621
Tropea, T. F., Mak, J., Guo, M. H., Xie, S. X., Suh, E., Rick, J., Siderowf, A., Weintraub, D., Grossman, M., Irwin, D., Wolk, D. A., Trojanowski, J. Q., Van Deerlin, V., & Chen-Plotkin, A. S. (2019). TMEM106B Effect on cognition in Parkinson disease and frontotemporal dementia. *Ann Neurol*, *85*(6), 801-811. https://doi.org/10.1002/ana.25486
Ueno, M., Fujita, Y., Tanaka, T., Nakamura, Y., Kikuta, J., Ishii, M., & Yamashita, T. (2013). Layer V cortical neurons require microglial support for survival during postnatal development. *Nat Neurosci*, *16*(5), 543-551. https://doi.org/10.1038/nn.3358
Ulrich, J. D., Ulland, T. K., Mahan, T. E., Nyström, S., Nilsson, K. P., Song, W. M., Zhou, Y., Reinartz, M., Choi, S., Jiang, H., Stewart, F. R., Anderson, E., Wang, Y., Colonna, M., & Holtzman, D. M. (2018). ApoE facilitates the microglial response to amyloid plaque pathology. *J Exp Med*, *215*(4), 1047-1058. https://doi.org/10.1084/jem.20171265

Valdar, W., Solberg, L. C., Gauguier, D., Burnett, S., Klenerman, P., Cookson, W. O., Taylor, M. S., Rawlins, J. N., Mott, R., & Flint, J. (2006). Genome-wide genetic association of complex traits in heterogeneous stock mice. *Nat Genet*, *38*(8), 879-887. https://doi.org/10.1038/ng1840

Vass, R., Ashbridge, E., Geser, F., Hu, W. T., Grossman, M., Clay-Falcone, D., Elman, L., McCluskey, L., Lee, V. M., Van Deerlin, V. M., Trojanowski, J. Q., & Chen-Plotkin, A. S. (2011). Risk genotypes at TMEM106B are associated with cognitive impairment in amyotrophic lateral sclerosis. *Acta Neuropathol*, *121*(3), 373-380. https://doi.org/10.1007/s00401-010-0782-y

Veldman-Jones, M. H., Brant, R., Rooney, C., Geh, C., Emery, H., Harbron, C. G., Wappett, M., Sharpe, A., Dymond, M., Barrett, J. C., Harrington, E. A., & Marshall, G. (2015). Evaluating Robustness and Sensitivity of the NanoString Technologies nCounter Platform to Enable Multiplexed Gene Expression Analysis of Clinical Samples. *Cancer Res*, *75*(13), 2587-2593. https://doi.org/10.1158/0008-5472.CAN-15-0262

Venegas, C., Kumar, S., Franklin, B. S., Dierkes, T., Brinkschulte, R., Tejera, D., Vieira-Saecker, A., Schwartz, S., Santarelli, F., Kummer, M. P., Griep, A., Gelpi, E., Beilharz, M., Riedel, D., Golenbock, D. T., Geyer, M., Walter, J., Latz, E., & Heneka, M. T. (2017). Microglia-derived ASC specks cross-seed amyloid-β in Alzheimer's disease. *Nature*, *552*(7685), 355-361. https://doi.org/10.1038/nature25158

Verney, C., Monier, A., Fallet-Bianco, C., & Gressens, P. (2010). Early microglial colonization of the human forebrain and possible involvement in periventricular white-matter injury of preterm infants. *J Anat*, *217*(4), 436-448. https://doi.org/10.1111/j.1469-7580.2010.01245.x

Verstrepen, L., Carpentier, I., Verhelst, K., & Beyaert, R. (2009). ABINs: A20 binding inhibitors of NF-kappa B and apoptosis signaling. *Biochem Pharmacol*, *78*(2), 105-114. https://doi.org/10.1016/j.bcp.2009.02.009

Virgintino, D., Perissinotto, D., Girolamo, F., Mucignat, M. T., Montanini, L., Errede, M., Kaneiwa, T., Yamada, S., Sugahara, K., Roncali, L., & Perris, R. (2009). Differential distribution of aggrecan isoforms in perineuronal nets of the human cerebral cortex. *J Cell Mol Med*, *13*(9b), 3151-3173. https://doi.org/10.1111/j.1582-4934.2009.00694.x

Vivancos, A. P., Guell, M., Dohm, J. C., Serrano, L., & Himmelbauer, H. (2010). Strand-specific deep sequencing of the transcriptome. *Genome Res*, *20*(7), 989-999. https://doi.org/10.1101/gr.094318.109

Voskobiynyk, Y., Roth, J. R., Cochran, J. N., Rush, T., Carullo, N. V., Mesina, J. S., Waqas, M., Vollmer, R. M., Day, J. J., McMahon, L. L., & Roberson, E. D. (2020). Alzheimer's disease risk gene BIN1 induces Tau-dependent network hyperexcitability. *eLife*, *9*. https://doi.org/10.7554/eLife.57354

Waggott, D., Chu, K., Yin, S., Wouters, B. G., Liu, F. F., & Boutros, P. C. (2012). NanoStringNorm: an extensible R package for the pre-processing of NanoString mRNA and miRNA data. *Bioinformatics*, *28*(11), 1546-1548. https://doi.org/10.1093/bioinformatics/bts188

Wang, H., Horbinski, C., Wu, H., Liu, Y., Sheng, S., Liu, J., Weiss, H., Stromberg, A. J., & Wang, C. (2016). NanoStringDiff: a novel statistical method for differential expression analysis based on NanoString nCounter data. *Nucleic Acids Res*, *44*(20), e151. https://doi.org/10.1093/nar/gkw677

Wang, K., Singh, D., Zeng, Z., Coleman, S. J., Huang, Y., Savich, G. L., He, X., Mieczkowski, P., Grimm, S. A., Perou, C. M., MacLeod, J. N., Chiang, D. Y., Prins, J. F., & Liu, J. (2010). MapSplice: accurate mapping of RNA-seq reads for splice junction discovery. *Nucleic Acids Res*, *38*(18), e178. https://doi.org/10.1093/nar/gkq622

Wang, L., Feng, Z., Wang, X., Wang, X., & Zhang, X. (2010). DEGseq: an R package for identifying differentially expressed genes from RNA-seq data. *Bioinformatics*, *26*(1), 136-138. https://doi.org/10.1093/bioinformatics/btp612

Wang, Y., Cella, M., Mallinson, K., Ulrich, J. D., Young, K. L., Robinette, M. L., Gilfillan, S., Krishnan, G. M., Sudhakar, S., Zinselmeyer, B. H., Holtzman, D. M., Cirrito, J. R., & Colonna, M. (2015).

TREM2 lipid sensing sustains the microglial response in an Alzheimer's disease model. *Cell*, *160*(6), 1061-1071. https://doi.org/10.1016/j.cell.2015.01.049

Wangler, M. F., Yamamoto, S., Chao, H. T., Posey, J. E., Westerfield, M., Postlethwait, J., Members of the Undiagnosed Diseases, N., Hieter, P., Boycott, K. M., Campeau, P. M., & Bellen, H. J. (2017). Model Organisms Facilitate Rare Disease Diagnosis and Therapeutic Research. *Genetics*, *207*(1), 9-27. https://doi.org/10.1534/genetics.117.203067

Waterston, R. H., Lindblad-Toh, K., Birney, E., Rogers, J., Abril, J. F., Agarwal, P., Agarwala, R., Ainscough, R., Alexandersson, M., An, P., Antonarakis, S. E., Attwood, J., Baertsch, R., Bailey, J., Barlow, K., Beck, S., Berry, E., Birren, B., Bloom, T., . . . Lander, E. S. (2002). Initial sequencing and comparative analysis of the mouse genome. *Nature*, *420*(6915), 520-562. https://doi.org/10.1038/nature01262

Wegiel, J., Wang, K. C., Tarnawski, M., & Lach, B. (2000). Microglia cells are the driving force in fibrillar plaque formation, whereas astrocytes are a leading factor in plague degradation. *Acta Neuropathol*, *100*(4), 356-364. https://doi.org/10.1007/s004010000199

Wen, T. H., Binder, D. K., Ethell, I. M., & Razak, K. A. (2018). The Perineuronal 'Safety' Net? Perineuronal Net Abnormalities in Neurological Disorders. *Front Mol Neurosci*, *11*, 270. https://doi.org/10.3389/fnmol.2018.00270

Wesolowski, R., Sharma, N., Reebel, L., Rodal, M. B., Peck, A., West, B. L., Marimuthu, A., Severson, P., Karlin, D. A., Dowlati, A., Le, M. H., Coussens, L. M., & Rugo, H. S. (2019). Phase Ib study of the combination of pexidartinib (PLX3397), a CSF-1R inhibitor, and paclitaxel in patients with advanced solid tumors. *Ther Adv Med Oncol*, *11*, 1758835919854238. https://doi.org/10.1177/1758835919854238

Wheeler, M. A., Clark, I. C., Tjon, E. C., Li, Z., Zandee, S. E. J., Couturier, C. P., Watson, B. R., Scalisi, G., Alkwai, S., Rothhammer, V., Rotem, A., Heyman, J. A., Thaploo, S., Sanmarco, L. M., Ragoussis, J., Weitz, D. A., Petrecca, K., Moffitt, J. R., Becher, B., . . . Quintana, F. J. (2020). MAFG-driven astrocytes promote CNS inflammation. *Nature*, *578*(7796), 593-599. https://doi.org/10.1038/s41586-020-1999-0

Wu, T. D., & Nacu, S. (2010). Fast and SNP-tolerant detection of complex variants and splicing in short reads. *Bioinformatics*, *26*(7), 873-881. https://doi.org/10.1093/bioinformatics/btq057

Wu, Y., Singh, S., Georgescu, M. M., & Birge, R. B. (2005). A role for Mer tyrosine kinase in alphavbeta5 integrin-mediated phagocytosis of apoptotic cells. *J Cell Sci*, *118*(Pt 3), 539-553. https://doi.org/10.1242/jcs.01632

Xu, X. L., Olson, J. M., & Zhao, L. P. (2002). A regression-based method to identify differentially expressed genes in microarray time course studies and its application in an inducible Huntington's disease transgenic model. *Hum Mol Genet*, *11*(17), 1977-1985. https://doi.org/10.1093/hmg/11.17.1977

Yamanaka, M., Ishikawa, T., Griep, A., Axt, D., Kummer, M. P., & Heneka, M. T. (2012). PPARgamma/RXRalpha-induced and CD36-mediated microglial amyloid-beta phagocytosis results in cognitive improvement in amyloid precursor protein/presenilin 1 mice. *J Neurosci*, *32*(48), 17321-17331. https://doi.org/10.1523/JNEUROSCI.1569-12.2012

Yamano, Y., & Coler-Reilly, A. (2017). HTLV-1 induces a Th1-like state in CD4(+)CCR4(+) T cells that produces an inflammatory positive feedback loop via astrocytes in HAM/TSP. *J Neuroimmunol*, *304*, 51-55. https://doi.org/10.1016/j.jneuroim.2016.08.012

Yang, H. M., Yang, S., Huang, S. S., Tang, B. S., & Guo, J. F. (2017). Microglial Activation in the Pathogenesis of Huntington's Disease. *Front Aging Neurosci*, *9*, 193. https://doi.org/10.3389/fnagi.2017.00193

Yang, H. S., Onos, K. D., Choi, K., Keezer, K. J., Skelly, D. A., Carter, G. W., & Howell, G. R. (2021). Natural genetic variation determines microglia heterogeneity in wild-derived mouse models of Alzheimer's disease. *Cell Rep*, *34*(6), 108739. https://doi.org/10.1016/j.celrep.2021.108739

Yang, H. S., White, C. C., Klein, H. U., Yu, L., Gaiteri, C., Ma, Y., Felsky, D., Mostafavi, S., Petyuk, V. A., Sperling, R. A., Ertekin-Taner, N., Schneider, J. A., Bennett, D. A., & De Jager, P. L. (2020). Genetics of Gene Expression in the Aging Human Brain Reveal TDP-43 Proteinopathy Pathophysiology. *Neuron*, *107*(3), 496-508.e496. https://doi.org/10.1016/j.neuron.2020.05.010

Yip, A. M., & Horvath, S. (2007). Gene network interconnectedness and the generalized topological overlap measure. *BMC Bioinformatics*, *8*, 22. https://doi.org/10.1186/1471-2105-8-22

Yong, S. M., Lim, M. L., Low, C. M., & Wong, B. S. (2014). Reduced neuronal signaling in the ageing apolipoprotein-E4 targeted replacement female mice. *Sci Rep*, *4*, 6580. https://doi.org/10.1038/srep06580

Youmans, K. L., Tai, L. M., Kanekiyo, T., Stine, W. B., Jr., Michon, S. C., Nwabuisi-Heath, E., Manelli, A. M., Fu, Y., Riordan, S., Eimer, W. A., Binder, L., Bu, G., Yu, C., Hartley, D. M., & LaDu, M. J. (2012). Intraneuronal Aβ detection in 5xFAD mice by a new Aβ-specific antibody. *Mol Neurodegener*, *7*, 8. https://doi.org/10.1186/1750-1326-7-8

Yshii, L., Pasciuto, E., Bielefeld, P., Mascali, L., Lemaitre, P., Marino, M., Dooley, J., Kouser, L., Verschoren, S., Lagou, V., Kemps, H., Gervois, P., de Boer, A., Burton, O. T., Wahis, J., Verhaert, J., Tareen, S. H. K., Roca, C. P., Singh, K., . . . Liston, A. (2022). Astrocyte-targeted gene delivery of interleukin 2 specifically increases brain-resident regulatory T cell numbers and protects against pathological neuroinflammation. *Nat Immunol*, *23*(6), 878-891. https://doi.org/10.1038/s41590-022-01208-z

Yu, J. S., & Cui, W. (2016). Proliferation, survival and metabolism: the role of PI3K/AKT/mTOR signalling in pluripotency and cell fate determination. *Development*, *143*(17), 3050-3060. https://doi.org/10.1242/dev.137075

Yu, L., Chibnik, L. B., Srivastava, G. P., Pochet, N., Yang, J., Xu, J., Kozubek, J., Obholzer, N., Leurgans, S. E., Schneider, J. A., Meissner, A., De Jager, P. L., & Bennett, D. A. (2015). Association of Brain DNA methylation in SORL1, ABCA7, HLA-DRB5, SLC24A4, and BIN1 with pathological diagnosis of Alzheimer disease. *JAMA Neurol*, *72*(1), 15-24. https://doi.org/10.1001/jamaneurol.2014.3049

Yu, X., Lu, N., & Zhou, Z. (2008). Phagocytic receptor CED-1 initiates a signaling pathway for degrading engulfed apoptotic cells. *PLoS Biol*, *6*(3), e61. https://doi.org/10.1371/journal.pbio.0060061

Yuan, S., & Sun, Z. (2013). Expanding horizons: ciliary proteins reach beyond cilia. *Annu Rev Genet*, *47*, 353-376. https://doi.org/10.1146/annurev-genet-111212-133243

Yutsudo, N., & Kitagawa, H. (2015). Involvement of chondroitin 6-sulfation in temporal lobe epilepsy. *Exp Neurol*, *274*(Pt B), 126-133. https://doi.org/10.1016/j.expneurol.2015.07.009

Zamanian, J. L., Xu, L., Foo, L. C., Nouri, N., Zhou, L., Giffard, R. G., & Barres, B. A. (2012). Genomic analysis of reactive astrogliosis. *J Neurosci*, *32*(18), 6391-6410. https://doi.org/10.1523/jneurosci.6221-11.2012

Zambrowicz, B. P., & Sands, A. T. (2003). Knockouts model the 100 best-selling drugs--will they model the next 100? *Nat Rev Drug Discov*, *2*(1), 38-51. https://doi.org/10.1038/nrd987

Zeiss, C. J. (2015). Improving the predictive value of interventional animal models data. *Drug Discov Today*, *20*(4), 475-482. https://doi.org/10.1016/j.drudis.2014.10.015

Zeng, W., & Mortazavi, A. (2012). Technical considerations for functional sequencing assays. *Nat Immunol*, *13*(9), 802-807. https://doi.org/10.1038/ni.2407

Zhan, L., Fan, L., Kodama, L., Sohn, P. D., Wong, M. Y., Mousa, G. A., Zhou, Y., Li, Y., & Gan, L. (2020). A MAC2-positive progenitor-like microglial population is resistant to CSF1R inhibition in adult mouse brain. *eLife*, *9*. https://doi.org/10.7554/eLife.51796

Zhan, L., Krabbe, G., Du, F., Jones, I., Reichert, M. C., Telpoukhovskaia, M., Kodama, L., Wang, C., Cho, S. H., Sayed, F., Li, Y., Le, D., Zhou, Y., Shen, Y., West, B., & Gan, L. (2019). Proximal recolonization by self-renewing microglia re-establishes microglial homeostasis in the adult mouse brain. *PLoS Biol*, *17*(2), e3000134. https://doi.org/10.1371/journal.pbio.3000134

Zhang, B., & Horvath, S. (2005). A general framework for weighted gene co-expression network analysis. *Stat Appl Genet Mol Biol*, *4*, Article17. https://doi.org/10.2202/1544-6115.1128

Zhang, J., Liu, Y., Liu, X., Li, S., Cheng, C., Chen, S., & Le, W. (2018). Dynamic changes of CX3CL1/CX3CR1 axis during microglial activation and motor neuron loss in the spinal cord of ALS mouse model. *Transl Neurodegener*, *7*, 35. https://doi.org/10.1186/s40035-018-0138-4

Zhang, P., Kishimoto, Y., Grammatikakis, I., Gottimukkala, K., Cutler, R. G., Zhang, S., Abdelmohsen, K., Bohr, V. A., Misra Sen, J., Gorospe, M., & Mattson, M. P. (2019). Senolytic therapy alleviates Abeta-associated oligodendrocyte progenitor cell senescence and cognitive deficits in an Alzheimer's disease model. *Nat Neurosci*, *22*(5), 719-728. https://doi.org/10.1038/s41593-019-0372-9

Zhang, Q., Sidorenko, J., Couvy-Duchesne, B., Marioni, R. E., Wright, M. J., Goate, A. M., Marcora, E., Huang, K. L., Porter, T., Laws, S. M., Sachdev, P. S., Mather, K. A., Armstrong, N. J., Thalamuthu, A., Brodaty, H., Yengo, L., Yang, J., Wray, N. R., McRae, A. F., & Visscher, P. M. (2020). Risk prediction of late-onset Alzheimer's disease implies an oligogenic architecture. *Nat Commun*, *11*(1), 4799. https://doi.org/10.1038/s41467-020-18534-1

Zhao, R., Hu, W., Tsai, J., Li, W., & Gan, W. B. (2017). Microglia limit the expansion of β-amyloid plaques in a mouse model of Alzheimer's disease. *Mol Neurodegener*, *12*(1), 47. https://doi.org/10.1186/s13024-017-0188-6

Zheng, H., Jia, L., Liu, C. C., Rong, Z., Zhong, L., Yang, L., Chen, X. F., Fryer, J. D., Wang, X., Zhang, Y. W., Xu, H., & Bu, G. (2017). TREM2 Promotes Microglial Survival by Activating Wnt/β-Catenin Pathway. *J Neurosci*, *37*(7), 1772-1784. https://doi.org/10.1523/jneurosci.2459-16.2017

Zhu, Y., Liu, C., & Pang, Z. (2019). Dendrimer-Based Drug Delivery Systems for Brain Targeting. *Biomolecules*, *9*(12). https://doi.org/10.3390/biom9120790

Ziemianska, K., Konopka, A., & Wilczynski, G. M. (2012). [The role of extracellular proteolysis in synaptic plasticity of the central nervous system]. *Postepy Hig Med Dosw (Online)*, *66*, 959-975. https://doi.org/10.5604/17322693.1021851 (Rola proteolizy zewnatrzkomorkowej w plastycznosci synaptycznej osrodkowego ukladu nerwowego.)